IMPROVED NUMERICAL TECHNIQUES FOR OCCUPATION-TIME DERIVATIVES AND OTHER COMPLEX FINANCIAL INSTRUMENTS

Johnson, Paul

2008

MIMS EPrint: **2009.92**

Manchester Institute for Mathematical Sciences
School of Mathematics

The University of Manchester

ISSN 1749-9097

IMPROVED NUMERICAL TECHNIQUES FOR OCCUPATION-TIME DERIVATIVES AND OTHER COMPLEX FINANCIAL INSTRUMENTS

A thesis submitted to the University of Manchester
for the degree of Doctor of Philosophy
in the Faculty of Engineering and Physical Sciences

2008

Paul Johnson
School of Mathematics

Contents

Word count 65316

List of Tables

List of Figures

Abstract

Occupation-time derivatives are complex barrier-type options where valuation depends on the time spent beyond the barrier by the underlying asset. This thesis presents a model for corporate bonds using an occupation-time derivative, the ParAsian option, the features of which can capture bankruptcy resolution and complex capital structure with violations of the absolute priority rule. It investigates the numerics of the problem, and proposes appropriate numerical techniques to enable accurate and rapid solutions. The model is extended to include bond conversion in a two-tier structure, which presents its own numerical problems. A new occupation-time derivative that takes into account the distance of deviations beyond the barrier is presented and solved.

Using existing knowledge on the asymptotic structure, new fast and efficient techniques are created for pricing American options. A second new occupation-time derivative is proposed, combining elements of early exercise with the ParAsian option to produce the American delayed-exercise option.

The numerical methods employed in this thesis are based on accurate finite-difference schemes, specifically developed and enhanced to treat the various classes of problem considered.

Declaration

No portion of the work referred to in this thesis has been submitted in support of an application for another degree or qualification of this or any other university or other institute of learning.

Copyright

Acknowledgements

Many thanks to my supervisors Peter Duck and David Newton who have given guidance and support throughout the PhD, especially when I fell ill for some time. Their thoughts and comments are always well appreciated, and always available.

I would like to thank my Mum. Special mentions go to my girlfriend Helen for her love and support and my sister Anna, who has provided me with free board and lodge at various stages of the PhD. Thanks also to Nick Sharp and Lingzhi Yu for useful discussions on the work presented in this Thesis.

Chapter 1

Introduction

1.1 Background

A derivative is a financial contract, whose value depends on some underlying asset. Even though derivatives had existed for some time, it was not until the early 1970's that derivative markets became fully established. Around the same time as the papers of Black and Scholes (1973) and Merton (1973) set a framework in which simple European options could be priced, the Chicago Board of Options Exchange was formed to trade OTC (over the counter) options. The trading in options has been increasing ever since with no sign of abating; recent growth shows the OTC derivatives market increase from 220 trillion in the first half of 2004 to 370 trillion in the first half of 2006[1].

The Black, Scholes and Merton model (BSM) is still the benchmark, and, although it is by no means perfect, the fundamental assumptions of no arbitrage and random walk will be hard to shake off for some time yet. From this model, we arrive at the celebrated Black-Scholes partial differential equation (PDE), which has excited mathematicians and physicists almost as much as it has the finance world. Driven by the markets, the need for ever more complex financial derivatives has led to interesting mathematical problems, many of which do not have closed form or analytical

[1]The notional amount outstanding taken from the regular OTC derivatives market statistics 17th November 2006. http://www.bis.org

solutions.

In this thesis we concentrate mainly on exotic options, for which there are no known closed form or analytical solutions. Early work in collaboration with Lingzhi Yu, in Yu (2004), developed a model for corporate bonds, where the corporate bond is seen as a contingent claim on a firm. In addition, new methods are proposed for solving the numerical problems involved in pricing such an option. The numerical methods must tackle multiple dimensions, barriers and early exercise when the bond is convertible. Along the way we also propose two new classes of barrier option, both extensions to current occupational time derivatives.

1.2 Options

First, let us introduce the concept of an option. In its simplest form, the holder of an option has the right to buy (with a call option) or sell (with a put option) the underlying asset for a given price at or before some maturity date. The asset may be traded, such as stock, currency, commodity, but also can be something measurable such as temperature, or the volatility of a stock; or even another derivative. With an option, the writer of the option (who sells it to another party), takes on all of the risk and as compensation, the holder must pay a premium for this. The insight impounded by the BSM framework was that the writer of the option can eliminate risk by replicating the option using a self-financing dynamic hedging strategy with an underlying asset and the option, one side bought, one side sold, so as to produce a portfolio that is locally riskless. If it is possible to construct such a portfolio in the market, then the market is said to be complete. An option on temperature is a classic example of incomplete markets, as the underlying asset, temperature, cannot be bought or sold. Therefore we cannot hedge the option and as a consequence the option is priced as the expected discounted value.

1.2.1 Arbitrage-free Pricing

When pricing derivatives one of the fundamental assumptions is that of **arbitrage**. Arbitrage is the practice of taking advantage of an opportunity presented by market prices to make an instantaneous profit. In the Black-Scholes framework we assume that the option prices reflect an arbitrage-free market, in that any mispricing will be 'arbitraged' away.

1.2.2 The Black, Scholes and Merton Framework

The BSM analysis starts by assuming that the asset price S follows a lognormal geometric Brownian motion process

$$\frac{dS}{S} = (\mu - d)dt + \sigma dW_t, \tag{1.1}$$

where μ, d and σ are constants, which represent the expected return, the continuous dividend rate and the volatility of the asset respectively. The process W is a Wiener process, capturing the uncertainty in the market. Equation (1.1) is the stochastic differential equation (SDE) for the asset price. In this thesis, we will assume that the asset price always follows that process. There is evidence to suggest that this is not strictly followed by stock prices: the distribution of returns exhibits sharper peaks and fatter tails than would be expected from the model. Notable attempts to address this problem are to include a jump process (Merton, 1976), stochastic volatility (Heston, 1993), and the local volatility model (Dupire, 1994). These solutions however, come with their own problems, and we are not yet at the stage where the lognormal process must be abandoned. Moreover, deviations from Brownian motion only become more significant under certain conditions, most especially longer time to maturity of an option, or for certain underlyings, such as oil prices or interest rates (in the long term). For the mass of options traded with maturities under a year, Brownian motion can remain a practical modelling assumption.

As well as the assumption of an arbitrage-free market, trading in the asset must

be unrestricted, i.e. no transaction costs, continuous trading and shortselling allowed, and assets are divisible. An investor may also invest at a risk-free rate r, which is commonly taken to be constant over time.

1.2.3 The Black-Scholes Equation

Assuming that a derivative V is a function of S and t, and is twice differentiable, then we may apply Itô's lemma to show that

$$dV = \left(\frac{\partial V}{\partial t} + (\mu - d)S\frac{\partial V}{\partial S} + \frac{1}{2}\sigma^2 S^2 \frac{\partial^2 V}{\partial S^2}\right) dt + \sigma S \frac{\partial V}{\partial S} dW. \tag{1.2}$$

Then by setting up a risk-free portfolio such that,

$$\Pi = V(S,t) - \frac{\partial V}{\partial S} S \tag{1.3}$$

we have that

$$d\Pi = \left(\frac{\partial V}{\partial t} + \frac{1}{2}\sigma^2 S^2 \frac{\partial^2 V}{\partial S^2}\right) dt. \tag{1.4}$$

The return on this portfolio is locally riskless. Because we could have invested the initial capital risklessly, to ensure the arbitrage-free market, the return on the portfolio must be equal to the risk-free rate. So then, the derivative's price must satisfy

$$\frac{\partial V}{\partial t} + \frac{1}{2}\sigma^2 S^2 \frac{\partial^2 V}{\partial S^2} + (r - d)S\frac{\partial V}{\partial S} - rV = 0. \tag{1.5}$$

This is the Black-Scholes equation. It is the fundamental equation for derivative pricing.

1.3 Numerical Techniques

In this section we give a brief overview of the numerical techniques commonly used to solve for different options.

1.3.1 Monte-Carlo methods

The Monte-Carlo method is the simplest of all approaches. As first suggested by Boyle (1977), the price is derived by simulating a large number of the random sample paths under the risk-neutral measure, calculating the value of said paths, and then discounting back and taking the average.

Let the process followed by the underlying asset value in a risk-neutral world be

$$dS = \hat{\mu} S dt + \sigma S dW \tag{1.6}$$

where dW is a Weiner process, σ is the volatility and $\hat{\mu}$ is the rate of return in a risk-neutral world. We can approximate (1.6) with greater accuracy if we non-dimensionalize the problem to be in terms of $\ln S$. From Itô's lemma we can write the process followed by $\ln S$ as

$$d \ln S = \left(\hat{\mu} - \tfrac{1}{2}\sigma^2\right) dt + \sigma dW. \tag{1.7}$$

Then to simulate paths, we can write (1.7) as

$$\delta \ln S = \left(\hat{\mu} - \tfrac{1}{2}\sigma^2\right) \delta t + \sigma \phi \sqrt{\delta t},$$

where ϕ is a random sample drawn from the normal distribution and δt may be any size required.

If S is a non-dividend paying stock then we may replace $\hat{\mu}$ by r, the risk-free interest rate. Consequently the value of the stock at time $t + \delta t$ is

$$S(t + \delta t) = S(t) \exp\left\{\left(r - \tfrac{1}{2}\sigma^2\right) \delta t + \sigma \phi \sqrt{\delta t}\right\}. \tag{1.8}$$

The value of the asset can be calculated at however many points in time are needed to calculate the value of the option. For a simple European option the only time we need to know the value of the asset is at maturity. The value of a vanilla European

call option with n sample paths can be expressed as

$$V(S_0, t=0) = \frac{1}{n}\sum_{i=1}^{n} e^{-rT} \max\left[S_0 \exp\left\{\left(r - \tfrac{1}{2}\sigma^2\right)T + \sigma\phi_i\sqrt{T}\right\} - E, 0\right]. \qquad (1.9)$$

More complex options will require the calculation of the asset value at multiple times. In terms of errors for a calculation such as (1.9), from simple statistics the standard error of the estimate is

$$\frac{\omega}{\sqrt{N}}$$

where ω is the standard deviation of the results. Then if μ is the mean price, we can construct a confidence interval so that the exact value V_e is given by

$$\mu - \psi\frac{\omega}{\sqrt{N}} < V_e < \mu + \psi\frac{\omega}{\sqrt{N}},$$

where ψ determines the percentage confidence. Then in order to reduce the errors by a factor of 2, we must quadruple the number of trials.

The main advantage of the approach is the ability to extend it to multiple dimensions with only a linear extension in calculations. The convergence of the method as shown above is $O(1/\sqrt{n})$ for a European option, and is independent of the number of dimensions. In terms of work done to generate a solution, the linear increase in calculations allied with $O(1/\sqrt{n})$ convergence makes the Monte-Carlo method comparable to the binomial method (see below) where calculations increase by a power of 2 and the convergence is $O(1/n)$. The forward path simulation makes solving for complicated path-dependent options simple, although optimal strategies can be harder to generate. The Monte-Carlo method also has a distinct advantage that the stochastic process may be arbitrary – even collected data may be used as input. The literature focuses on methods to improve the convergence of the method by reducing bias and variance, the pricing of derivatives with American features and also SDEs with nonlinear components.

In order to price American features, one must generate the optimal exercise strategy for the option. Perhaps the simplest method to understand is the regression-based

approach of Longstaff and Schwartz (2001). The crux of the method is to identify the conditional expected value of continuation. After generating a set of asset paths over a number of time steps, the method works backward from expiry. We generate the value of the 'option to continue' at the current time step for all possible asset values by using least-squares regression analysis on all the discounted future payments for each path. Then comparing the value of exercising at that point with the value of continuing to the next time step we can choose the optimal path.

1.3.2 Lattice Methods

A lattice method can be considered as a discrete time model of the varying price over time of the underlying asset. The first lattice method was the binomial model proposed by Cox et al. (1979). The trinomial model was studied by Parkinson (1977) and then again by Boyle (1986). The basic idea is the same for both methods, so we will just discuss the binomial method.

The binomial model uses a discrete-time framework, where the duration of the option from the start to expiry is divided into n time steps of equal length, δt. Starting with an asset price S at time $t = 0$, at the next period of time the asset price can either move up to Su, with probability p, or have moved down to Sd, with probability $(1 - p)$, where $u > 1$ and $d < 1$ are independent of the asset price. On a lattice, the position of the asset price at a particular time is described as a node.

In figure 1.1 a three step binomial tree is shown. In order to price an option, we will price a portfolio containing a long position in the option and short a quantity Δ in the asset. Then by arbitrage, we may calculate the value of Δ which forces the portfolio to be riskless. Take for instance the first step in figure 1.1, the value of the portfolio is initially $V - \Delta S$, and if there is an up movement in the stock price the value becomes

$$V_u - \Delta Su.$$

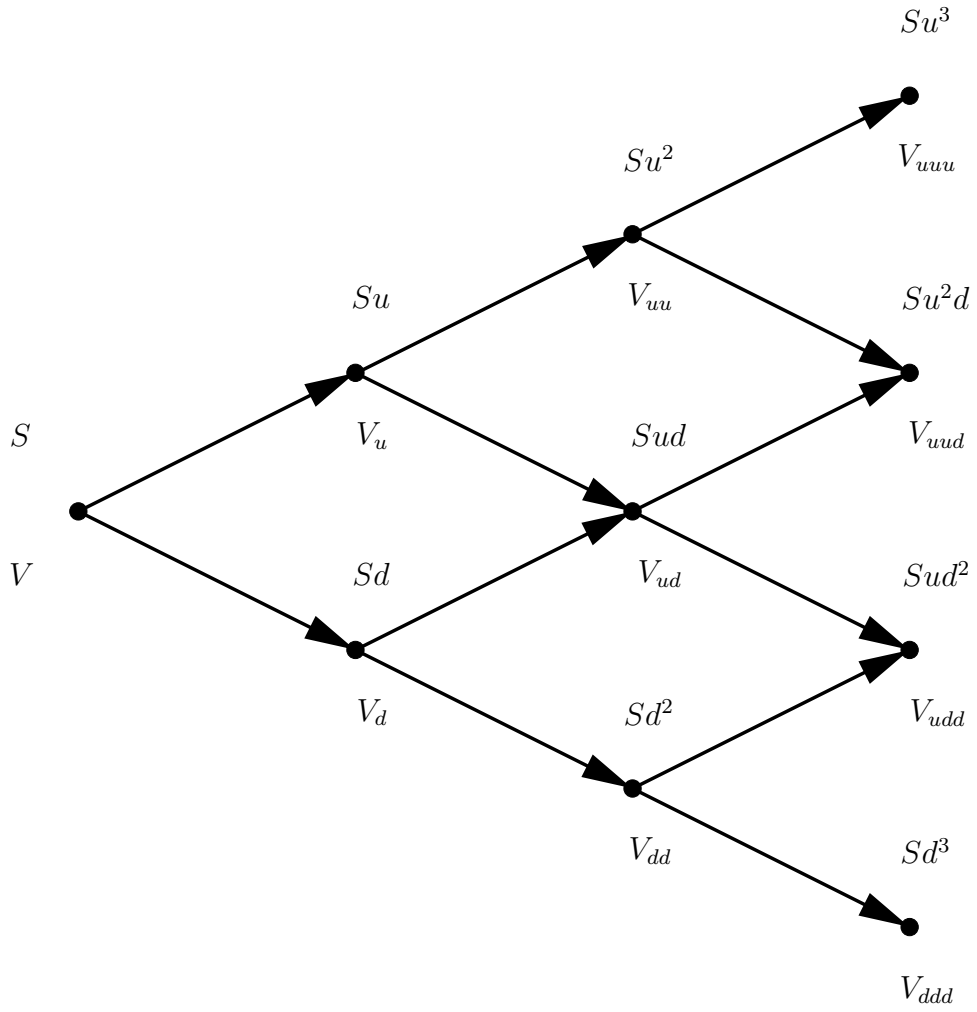

Figure 1.1
Stock and option value in a three-step binomial tree.

If there is a down movement then the price becomes

$$V_d - \Delta Sd.$$

Setting the value of an up movement to be equal to the value of a down movement gives the value of Δ to be

$$\Delta = \frac{V_u - V_d}{Su - Sd}, \tag{1.10}$$

and since the portfolio is invariant to movements in asset price the portfolio is locally riskless. Hence the present value of the portfolio is just the discounted value at the next timestep. Given the cost of setting up the portfolio, we can equate the two to obtain

$$V = \Delta S + (V_u - \Delta Su)e^{-r\delta t}.$$

Then after rearranging and using (1.10) we can express the value of the option as:

$$V = e^{-r\delta t}\{pV_u + (1-p)V_d\}, \tag{1.11}$$

where

$$p = \frac{e^{-r\delta t} - d}{u - d}. \tag{1.12}$$

Equations (1.11) and (1.12) allow us to price the option at $t = 0$ if the price is known at $t = \delta t$.

In the analysis above there is no specification of the probability of an up or a down movement above, even so it is intuitive to interpret the value p as the probability of an up movement in asset price, and $(1 - p)$ as the probability of a down movement in asset price. In fact, letting p for the asset price be defined by (1.12) is equivalent to setting the expected return on the asset price equal to the risk-free rate.

In practice we must match both the rate of return and volatility of the asset price to the parameters p, u and d in our model. We have shown above how p is used to match to the risk-free rate, so to match the binomial variance to the volatility we

have

$$pu^2 + (1-p)d^2 - (pu + (1-p)d)^2 = \sigma^2 \delta t, \tag{1.13}$$

and we have two equations in three unknowns, so there still exists a degree of freedom. This freedom allows for different parameter choices, which could be tailored to the problem. A simple choice is that of Cox et al. (1979), who set

$$ud = 1. \tag{1.14}$$

so that the distance moved up is the same as the distance moved down for the lognormal walk. After some algebra we find that $u = e^{\sigma\delta t}$ and $d = e^{-\sigma\delta t}$. Another popular choice is that of Amin (1991), who choose u and d so that $p = \frac{1}{2}$ and there is an equal chance of moving up or down.

In order to price an option using the full binomial tree, we must start at expiry, at which point we know the value of the option. Then for all nodes at $T - \delta t$, the value is given by (1.11). Then by working recursively through the tree we will eventually reach $t = 0$ and hence the value of the option at $t = 0$.

Applications and convergence

Lattice methods are easily applied to European, American (Bermudan) options. For the European option, the convergence is $1/n$ for binomial tree calculation, unmodified, as described above. However misplacing of nodes at expiry can lead to large errors. This has been addressed in the literature (Widdicks et al., 2002) and with careful Richardson extrapolation the rate of convergence can be improved to $1/n^2$.

Although the extension from European to Bermudan and American is simple to code, the reduction of the errors are not quite so simple here. As well as the errors at expiry due to the exercise price, the position of the free boundary at each time step also introduces some form of error. This means that the techniques introduced for the European option, although effective in increasing accuracy, cannot improve the convergence rate above $1/n$ (Broadie and Detemple, 1996; Figlewski and Gao, 1999; Leisen, 1998; Tian, 1999).

The method also struggles to price binary options; the large discontinuity at expiry exaggerates the errors. Using the basic method, the convergence is slow ($1/\sqrt{n}$) and the errors are large. Attempts have been made to address this problem (Heston and Zhou, 2000; Widdicks et al., 2002) with limited success.

When pricing barrier options, as with the pricing of American options, we introduce a second source of error through the position of the barrier. This can have a significant effect on the convergence of the scheme, reducing the rate to $1/\sqrt{n}$ (Boyle and Lau, 1994). Clever placing of nodes close or on the barrier can reduce these problems. The ability to place nodes on the barrier is much easier when using a trinomial scheme due to the two degrees of freedom inherent in the scheme (Ritchken, 1995), whilst moving barriers can be dealt with by a coordinate transformation (Rogers and Zane, 1997).

Other barrier options such as Parisian options (see chapter 4) require more work than the simple barrier option. In a Parisian option the option is knocked in or out only when the asset value has been consecutively over the barrier for a specified time. They contain an extra dimension, capturing the time spent over the barrier. Avellaneda and Wu (1999) detail a trinomial scheme to solve the Parisian option, which involves a complicated condition at the barrier to ensure continuity of the delta hedge.

1.3.3 Finite-Difference Methods

Commonly used in applied mathematics to solve complex PDEs, the finite-difference method already comes with a wealth of knowledge that can be used to solve the BSM PDE. As such there are a number of finite-difference methods at our disposal, such as explicit, implicit, semi-implicit (Crank-Nicolson), finite element and alternating direction implicit (ADI), for which the convergence rate and behaviour of the algorithms is well known. The finite-difference approach also offers flexibility in the choice of time and asset dimensions that can be exploited to increase the rate of convergence. Finite-difference methods are related to lattice methods; in fact the trinomial

lattice method can be viewed as the explicit finite-difference method.

Finite-difference methods require the discretisation of the problem. The grid is usually divided into an equally spaced grid in the spatial dimension, although it is possible to easily vary the size of the time steps. Let us describe a typical discretisation of the solution space with $n+1$ points in S and $m+1$ points in τ, where $\tau = T - t$ implying we are moving backward in time. We may then write

$$\begin{aligned} \Delta\tau &= \frac{T}{m} & \tau &= k\Delta\tau \\ \Delta S &= \frac{S_{max}}{n} & S &= i\Delta S \end{aligned}$$

and we write

$$V(\tau, S) = v_i^k.$$

Whereas in the explicit finite difference scheme, we discretise by taking the spatial derivative approximations at the known time τ, and for the implicit model, at the time step at which we are solving $\tau + \Delta\tau$, the Crank-Nicolson scheme takes the approximation to be halfway between the two time steps, and acts as the average of the two methods. In fact, a general semi-implicit scheme may be specified to be an approximation to a PDE at a fraction between the time steps θ, where $\theta = 0$ implies the explicit scheme, $\theta = 1$ implies the implicit scheme and $\theta = 1/2$ implies the Crank-Nicolson scheme. Then the Crank and Nicolson (1947) method uses approximations at $t + \frac{1}{2}\Delta t$ for the discretisation of the PDE. The result is a method that is not only unconditionally stable (for smooth payoffs) but also second order in both the spatial dimension and the time dimension. The method has a similar order of computational expense to the implicit method, taking all of its advantages but with an increased rate of convergence.

The follow gives some brief notes on three of the methods, but for a more detailed explanation of finite-difference methods see Smith (1985).

Explicit Method

The explicit finite difference method is popular within the finance literature (Brennan and Schwartz, 1978; Hull and White, 1990) possibly due more to the easy implementation rather than the efficiency or accuracy of the method. One problem with the method is the stability constraint which must be imposed. For the heat conduction equation, characterised by the heat conduction PDE

$$\frac{\partial u}{\partial t} = \frac{\partial^2 u}{\partial x^2}, \tag{1.15}$$

the constraint on an explicit method can be shown to be

$$\frac{\Delta t}{\Delta x^2} \leq \frac{1}{2}. \tag{1.16}$$

Since the Black-Scholes model can be transformed into the heat conduction via the change of variables

$$S \to Ee^x, \tag{1.17}$$

$$t \to T - \frac{1}{2}\sigma^2\tau, \tag{1.18}$$

we can construct the constraint in terms of the original variables to be

$$\Delta\tau \leq \frac{\Delta S^2}{\sigma^2 S^2}. \tag{1.19}$$

Since this condition must be met over the entire grid the condition is dependent on the maximum value of S. For this reason when solving using the explicit method it is best to transform to the grid to the non-dimensional form x so that the constraint is less restrictive (see Brennan and Schwartz, 1978), but this does result in a rather inefficient bunching of nodes for small S.

The accuracy of this explicit scheme can be shown to be $O(\Delta x^2, \Delta\tau)$. Although Δx convergence is second order, the coefficient is often very large meaning a reduction in Δx has a far larger effect than a reduction in $\Delta\tau$. However, to reduce Δx by a half,

the stability constraint implies that $\Delta\tau$ must reduce by a factor of four, consequently for four times the accuracy the computation cost increases eight-fold.

Implicit Method

The implicit method can be shown to be unconditionally stable. Although the accuracy of the scheme is of the same order as the explicit method ($O(\Delta x^2, \Delta\tau)$), the method has two advantages. First, the stability of the method means that there is no need to transform the problem to the non-dimensional space, avoiding any bunching of the nodes in S space. Second, there are no restrictions on the size of the time step. Although the order of convergence in time is only first order the coefficient is often small so similar accuracy to the explicit method can be achieved with fewer time steps, although there will be extra computational expense as the implicit scheme requires the solution of a tridiagonal system of equations.

Crank-Nicolson Method

Here we describe the Crank-Nicolson scheme in detail (since this technique will be used throughtout this thesis). The approximations for V and its derivatives are as follows:

$$V(\tau + \tfrac{1}{2}\Delta\tau, S) = \frac{v_i^k + v_i^{k+1}}{2} + O(\Delta\tau^2), \tag{1.20}$$

$$\frac{\partial V}{\partial \tau}(\tau + \tfrac{1}{2}\Delta\tau, S) = \frac{v_i^{k+1} - v_i^k}{\Delta\tau} + O(\Delta\tau^2), \tag{1.21}$$

$$\frac{\partial V}{\partial S}(\tau + \tfrac{1}{2}\Delta\tau, S) = \tfrac{1}{4\Delta S}(v_{i+1}^k - v_{i-1}^k + v_{i+1}^{k+1} - v_{i-1}^{k+1}) \tag{1.22}$$

$$+O(\Delta S^2, \Delta\tau^2), \tag{1.23}$$

$$\frac{\partial^2 V}{\partial S^2}(\tau + \tfrac{1}{2}\Delta\tau, S) = \tfrac{1}{2\Delta S^2}(v_{i+1}^k - 2v_i^k + v_{i-1}^k + v_{i+1}^{k+1} - 2v_i^{k+1} + v_{i-1}^{k+1})$$

$$+O(\Delta S^2, \Delta\tau^2), \tag{1.24}$$

After substitution into the Black-Scholes equation (1.5) and performing some algebra the equation may be written as

$$\alpha_i v_{i-1}^{k+1} + \left(\tfrac{1}{\Delta\tau} + \beta_i\right) v_i^{k+1} + \gamma_i v_{i+1}^{k+1} = Z_i \tag{1.25}$$

where

$$Z_i = -\alpha_i v_{i-1}^{k} + \left(\tfrac{1}{\Delta\tau} - \beta_i\right) v_i^{k} - \gamma_i v_{i+1}^{k}. \tag{1.26}$$

Here α_i, β_i, and γ_i are constants and Z_i can be explicitly calculated. The constants are given by

$$\alpha_i = -\frac{\sigma^2 S^2}{4\Delta S^2} + \frac{(r-d)S}{4\Delta S} \tag{1.27}$$

$$\beta_i = \frac{\sigma^2 S^2}{2\Delta S^2} + \frac{r}{2} \tag{1.28}$$

$$\gamma_i = -\frac{\sigma^2 S^2}{4\Delta S^2} - \frac{(r-d)S}{4\Delta S}. \tag{1.29}$$

Then we have a tridiagonal system to solve at each time step. This can be performed using LU decomposition or simple Gaussian elimination.

Applications

The flexibility offered by the finite-difference method makes it superior to the lattice method in almost every situation. The method is easily adapted to include barriers, early exercise, and stochastic interest rates or volatility, so long as appropriate boundary conditions can be provided. The flexibility of the method is exploited in this thesis, to increase the accuracy and convergence of American options (chapters 2 and 3), price credit risk (chapter 5), convertible bonds (chapter 6) and finally to price a new complex barrier option in chapter 7. The particular finite-difference methods used are discussed further in each chapter of the thesis.

1.3.4 Richardson Extrapolation

When convergence of a method is smooth and monotonic, and when the order of the convergence is known, it is possible to extrapolate using what is known as 'Richardson Extrapolation'. The basic idea is as follows.

Let V_E be the exact price of the option, and V_n be the value given by the numerical method with n steps. If the rate of convergence as $n \to \infty$ is known to be $1/(n^d)$, where d is the order of convergence, then V_n is assumed to take the following form:

$$V_n = V_E + \frac{f_1}{n^d} + \text{smaller terms}; \tag{1.30}$$

where f_1 is an unknown function that stays constant over different n. Using two different values of n (n_1 and n_2, giving values V_{n1} and V_{n2}) and ignoring the smaller terms in (1.30) we obtain:

$$f_1 = n_1 V_{n1} + n_1 V_E = n_2 V_{n2} + n_2 V_E, \tag{1.31}$$

which can be rearranged to give:

$$V_E = \frac{n_1 V_{n1} - n_2 V_{n2}}{n_1 - n_2}. \tag{1.32}$$

This simple idea can be extremely important in increasing accuracy of given numerical methods.

1.3.5 Overview

Finite-difference methods are generally superior to other methods when the dimension of the problem is one or two. The choice of whether to use the Crank-Nicolson or the explicit method depends on whether the extra work needed for computing the Crank-Nicolson scheme is balanced by the increased accuracy. We choose to use the Crank-Nicolson scheme throughout this thesis, investigating ways to exploit the method and get the best out of it. The second-order convergence and flexibility of

the method make it an attractive choice. One other factor to take into account when using a finite-difference method is that the final solution gives the values for a set of ratios of the asset price S to the exercise price E, so can be vastly superior if option prices over a range of underlying values need to be calculated.

Chapter 2

Advanced Numerical Techniques for Early Exercise Options

The pricing of the American option is a long standing problem in mathematical finance. With no fully analytical solution available, academics have sought to find analytical approximations or efficient numerical methods with which to solve the problem. Notably, the majority of analytical approximations require a fair amount of numerical work. One of the first investigations into the American put option was by McKean Jr (1965), who formulated the problem in terms of a free boundary, similar to those seen in melting ice or dam problems (a free boundary formulation is given below in section 2.2). This allows the option price to be written explicitly in terms of the free boundary, equivalent to the optimal stopping boundary. However, the hedging arguments for why the American option can be formulated in such a way were not laid down until Bensoussan (1984) and Karatzas (1988).

2.1 Introduction

In this chapter we develop improvements to existing numerical methods for solving an American option. The analytical solution for American options is mathematically severely limited by the presence of the free boundary. Merton (1990) has shown that the American call, in the absence of dividends (continuous or otherwise), will never

be exercised optimally, and hence the free boundary problem is circumvented and the value is equal to that of the European call. If dividends on an American call are paid discretely, then the solution may be found quasi-analytically (Roll, 1977; Geske, 1979; Whaley, 1981) by compounding the problem into an option on an option, since the only time at which the holder would exercise optimally is just after the dividend is paid. The method does however require the calculation of the critical stock price above which the holder would exercise, which must be calculated numerically. It can be easily extended to include any number of dividend payments, but Roll (1977) admits the algebra can easily become tiresome, and the numerical calculations can become excessive. Further, this analysis cannot be extended to either the American put, or the American call with continuous (known) dividends. When the holder may exercise continuously at any time, the exercise premium, which we define to be the difference in value between the American and the European option, is far more difficult to find. There also exist options for which the exercise policy is trivial, and the optimal exercise boundary is known *a priori*, such as the American digital call option, noted by Wilmott et al. (1995). For such an option, it is always optimal to exercise if the asset price is above the exercise price.

The closed form solution for the American option was found by Geske and Johnson (1984), although they were only able to express the option price as the sum of a series of compound options, or an infinite sum of integrals. This integral nature of the problem lends itself to numerical integration or quadrature methods. Pricing algorithms had been developed with varying degrees of success (Parkinson, 1977; Bunch and Johnson, 1992; Huang et al., 1996; Sullivan, 2000), until Andricopoulos et al. (2003) set the benchmark with the fast and efficient QUAD algorithm. Andricopoulos et al. (2007) have subsequently extended the method so it can be used on options including more than one underlying.

Barone-Adesi and Whaley (1987) improved on the quadratic approximation of MacMillan (1986) to arrive at an analytical approximation which is simple to calculate and may be programmed on a calculator. They achieved this by pricing the exercise premium, or the option to exercise, as defined above. Once the PDE and boundary

conditions are found for the exercise premium, the full problem is reduced (by ignoring smaller terms in the equation) to a simple ODE with an analytical solution. Earlier, Johnson (1983) had provided a crude approximation, although there was little rigour in the approach, simply attempting to fit parameters to the model from empirical values. The idea is to trap the price difference between the European value and a European with increasing strike price, subject to some 'simpler' function. Since there is no intuition to the form of the function, an estimate is all that can be made. Then with probably the most simplistic approach, Joubert and Rogers (1995) form a set of tables (by calculating the exact price numerically over a range of values) from which the American price may be read subject to the choice of four parameters. More recently, a more intuitive approach saw Widdicks et al. (2005) use singular perturbation theory to produce their look-up tables, and with just two variables; finding the price amounts to a simple interpolation of table values.

Brennan and Schwartz (1977b) were first to solve the Black-Scholes PDE with early exercise directly, using a numerical technique. The technique, including a simple search algorithm to find the optimal exercise boundary, is analogous to solving the variational inequality problem, explained later in section 2.4. Some justification for the algorithm is given by Jaillet et al. (1990), who note that the scheme only works because of the specific nature of the free boundary in American put or call problems. Brennan uses an implicit scheme, however the Crank-Nicolson scheme coupled with the PSOR scheme, explained later, is far superior.

In this chapter we detail two basic methods for solving free boundary problems: fixed grid and moving grid methods. We propose improvements to both schemes, that can be applied to problems in which there is some prior knowledge of the form of the free boundary. We formulate the problem in section 2.2, investigate the behaviour in the limit time tends to expiry in section 2.3, then examine some existing approaches and extensions in sections 2.4 and 2.5, and finally sample results are given in section 2.6 and some conclusions are drawn in section 2.7.

2.2 Formulation

To understand the free boundary imposed by the American option, arbitrage arguments must be used. In figure 2.1, the value of a typical European put is seen to be lower than that of the payoff function $(E - S)$ for some range of S. If this were to be the price of the American put option P, then $P(S,t) < E - S$ in this range. If the option is bought, one would simply exercise it making an instant risk-free profit of $E - S - P$ (since $P < E - S$). Then, by arbitrage, the option price would move so as an instantaneous profit could no longer be made. Consequently the following constraint must hold for the American put;

$$P(S,t) \geq \max(E - S, 0). \tag{2.1}$$

Now assume that there exists some point in S, say S_f, below which it is optimal to exercise, but not so above. For the American put, the holder will exercise in the region $S < S_f$. In this region, the return on a bank deposit is more than if the option is held. Clearly, the solution in the region $S < S_f$ does not need to be calculated since we know that the option is exercised and therefore $P = E - S$.

In the region $S > S_f$, the BSM equation must still hold, but another condition is needed in order to close the problem: the value of S_f must be chosen so as to maximise the value of the option. This is found by examining the gradient of P at the free boundary. We can show that $\partial P/\partial S = -1$, i.e. the function P runs smoothly into the payoff function (see figure 2.2). If $\partial P/\partial S < -1$ then $P < E - S$ for some region close to S_f and we have already discussed earlier how this would not be possible. For the case $\partial P/\partial S > -1$, consider the strategy taken by the holder on when to exercise. A holder would wish to allow the asset price drop as low as possible before exercising, so if $\partial P/\partial S > -1$ the value of the option near S_f can be increased if we take a smaller value of S_f. We conclude, therefore, that the only possibility is that $\partial P/\partial S = -1$.

Assuming that the option is priced under the BSM framework with continuous

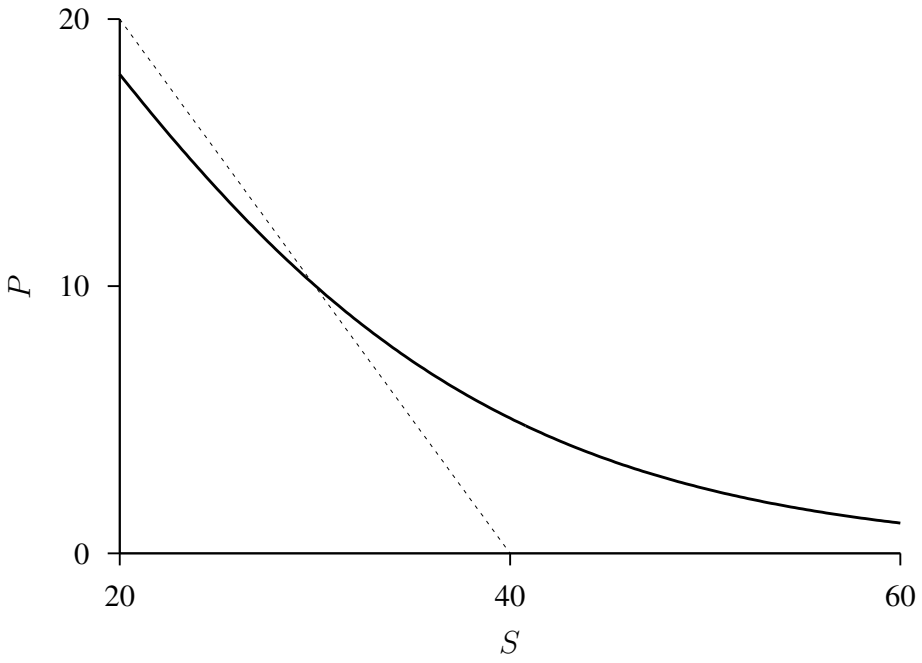

Figure 2.1
The European put option.
The exercise price (dotted) alongside the European put (solid bold line) with $\sigma = 0.4$, $E = 40$, $T = 1$, and $r = 0.06$.

dividends, in the region $0 \leq S \leq S_f$ we therefore have the following

$$P = E - S, \qquad \frac{\partial P}{\partial t} + \frac{1}{2}\sigma^2 S^2 \frac{\partial^2 P}{\partial S^2} + (r-d)S\frac{\partial P}{\partial S} - rP < 0, \tag{2.2}$$

where d is the continuous dividend. Even when the dividends are zero, it may still be optimal to exercise early for the American put, and since the maturity of these options are short it is possible that no dividends will be paid over the lifetime of the option. Therefore it would not be unreasonable to assume that dividends are zero for the American put, and this is often the case in the literature. In the other region $S > S_f$ we have

$$P > E - S, \qquad \frac{\partial P}{\partial t} + \frac{1}{2}\sigma^2 S^2 \frac{\partial^2 P}{\partial S^2} + (r-d)S\frac{\partial P}{\partial S} - rP = 0. \tag{2.3}$$

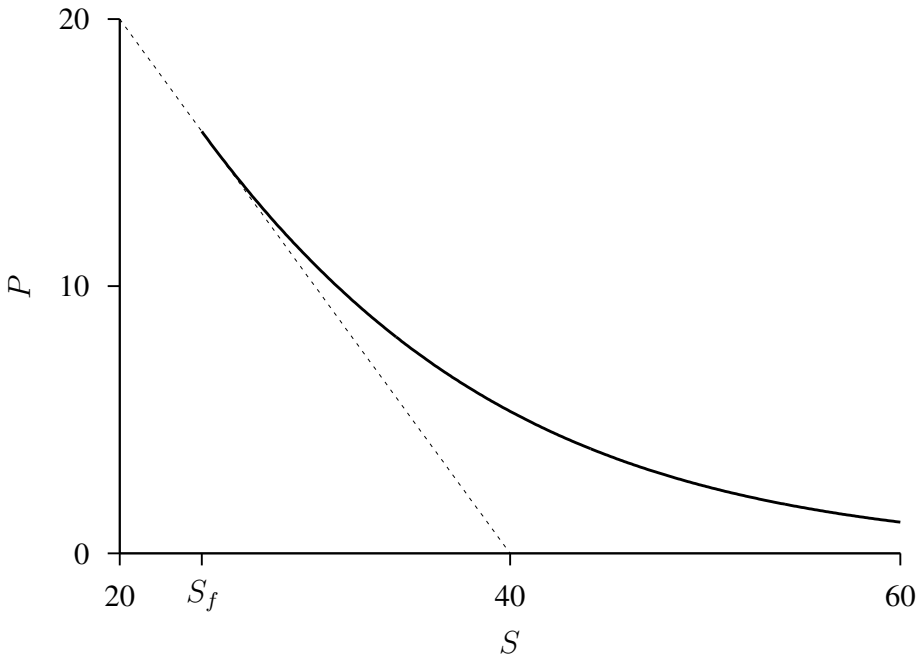

Figure 2.2
The American put option.
The exercise price (dotted) alongside the American put (solid bold line) with $\sigma = 0.4$, $E = 40$, $T = 1$, and $r = 0.06$. The American put option is exercised for $S < S_f$.

The boundary conditions at the free boundary are correspondingly

$$P(S_f(t), t) = E - S_f, \qquad \frac{\partial P}{\partial S}(S_f(t), t) = -1. \tag{2.4}$$

The final condition (location) for the free boundary must be found by asymptotic analysis of the problem in the limit as we approach maturity. For the American put, Kim (1990) finds the initial free boundary value to be

$$S_f(T) = \min\left[E, \frac{r}{d}E\right]. \tag{2.5}$$

Hence for the American put with no dividend, the final condition is simply $S_f(T) = E$.

Similar arguments lead to the following boundary conditions for an American

call C,

$$C(S,T) = \max[S-E,0] \tag{2.6}$$

$$C(S_f(t),t) = S_f - E \tag{2.7}$$

$$\frac{\partial C}{\partial S}(S_f(t),t) = 1 \tag{2.8}$$

$$S_f(T) = \max\left[E, \frac{r}{d}E\right]. \tag{2.9}$$

2.3 Asymptotic analysis of the American option near expiry

Following the paper by Kuske and Keller (1998) using integral equations, both Evans et al. (2002) and Widdicks et al. (2005) confirm the three tier structure to the solution of the American put option using matched asymptotic expansions in the limit as time tends to expiry. Furthermore, Evans et al. (2002) also includes analysis of both call and put options with dividends. They find that the ratio between the dividend and interest rate is important in determining the structure of both the solution and the free boundary in the limit as time tends to zero. For the call, there are three distinct cases dependent on this ratio. Firstly, when $d = 0$ the well known case arises where it is never optimal to exercise and hence the American call is exactly the same as the European call. Second, when $0 < d < r$, the solution can be captured with a simple structure, the boundary is $O(\tau^{\frac{1}{2}})$ around the limit of the free boundary (as time tends to expiry). Finally, when $d \geq r$ the situation becomes more complex, equivalent in fact to the structure of the American put option, the free boundary is $O\left(\left(\tau \ln \frac{1}{\tau}\right)^{\frac{1}{2}}\right)$ and the solution exhibits a three tier structure. Roles are reversed for the American put, with $0 \leq d \leq r$ the solution is the complex three tier structure, and with $d > r$ the solution is the simple structure.

In the next two subsections we will run through the equations detailing the structure for the two cases $0 < d < r$ and $d \geq r$ involving an American call. The analysis used for a call when $0 < d < r$ is later used in chapter 7 for the delayed-exercise

option.

2.3.1 The American call with $0 < d < r$

In order to use the asymptotic analysis we must convert the BSM PDE to non-dimensional form. Making the following substitutions

$$S = Ee^x, \quad t = T - \tau/\frac{1}{2}\sigma^2, \quad C(S,t) = S - E + Ee^{-\rho\tau}c(x,\tau),$$

with

$$\rho = \frac{r}{\frac{1}{2}\sigma^2} \qquad \nu = \frac{d}{\frac{1}{2}\sigma^2}$$

into (1.5) results in the following equation

$$\frac{\partial c}{\partial \tau} = \frac{\partial^2 c}{\partial x^2} + (\rho - \nu - 1)\frac{\partial c}{\partial x} + e^{\rho\tau}(\rho - \nu e^x), \tag{2.10}$$

for $x < x_f(\tau)$ where $S_f(t) = Ee^{x_f(\tau)}$. Then the boundary conditions may be expressed as:

$$c = \frac{\partial c}{\partial x} = 0 \quad \text{at} \quad x = x_f(\tau), \tag{2.11}$$

$$c \sim e^{\rho\tau}(1 - e^x) \quad \text{as} \quad x \to -\infty, \tag{2.12}$$

$$c = \max(1 - e^x, 0) \quad \text{at} \quad \tau = 0, \tag{2.13}$$

From equations (2.10) to (2.13) we may confirm Kim's (1990) limit of x_0, the free boundary as time tends to expiry. At expiry, we have that $\partial^2 c/\partial x^2 = \partial c/\partial x = 0$ for $x > 0$. Then (2.10) becomes

$$\frac{\partial c}{\partial \tau} = \rho - \nu e^x \quad \text{for} \quad x > 0. \tag{2.14}$$

Now in order to satisfy the constraint $c \geq \max(1 - e^x, 0)$, we require that $\partial c/\partial \tau > 0$. If we specify $x_0 = \log(\rho/\nu)$, then $\partial c/\partial \tau > 0$ for $0 \leq x \leq x_0$, and $\partial c/\partial \tau < 0$ for $x > x_0$. Clearly then we exercise in the region $x > x_0$, so then $x_f(0) = x_0$, or

$S_f(T) = \frac{rE}{d}$ in the original variables.

Both Wilmott et al. (1995) and Evans et al. (2002) show that the free boundary here is of parabolic form. Let us consider the limit of small time behaviour near expiry, letting $\tau = \epsilon\hat{T}$, with $\hat{T} = O(1)$ and ϵ a small parameter, we have the following expansion for $x < x_0$

$$c(x,\tau) = \max(1 - e^x, 0) + (\rho - \nu e^x)\tau + O(\epsilon^2). \tag{2.15}$$

This expansion can only satisfy one of the boundary ($c = 0$) conditions at $x = x_f$, hence we require a separate region close to the free boundary to satisfy the derivative condition, $\frac{\partial c}{\partial x} = 0$. Let us introduce the following scalings

$$x = x_0 + \epsilon^{\frac{1}{2}} X, \quad c = \epsilon^{\frac{3}{2}}\hat{C}, \quad x_f = x_0 + \epsilon^{\frac{1}{2}} L_0$$

Then substituting these into (2.10) to $O(\epsilon^{\frac{1}{2}})$ we get the following:

$$\frac{\partial \hat{C}}{\partial \hat{T}} = \frac{\partial^2 \hat{C}}{\partial X^2} - \rho X, \tag{2.16}$$

with the conditions

$$\hat{C} = \frac{\partial \hat{C}}{\partial X} = 0 \quad \text{at} \quad X = L_0(\hat{T}), \tag{2.17}$$

$$\hat{C}(X,0) = 0, \qquad L_0(0) = 0, \tag{2.18}$$

$$\hat{C} \to -\rho X\hat{T} \quad \text{as} \quad X \to -\infty, \tag{2.19}$$

where the third condition matches to the outer solution (2.15).

Then seeking a similarity solution of the form $\hat{V} = \tau^{\frac{3}{2}} g(\xi)$ where $\xi = X/\sqrt{\hat{T}}$, and $L_0 = \xi_0\sqrt{\hat{T}}$, we arrive at the following ODE;

$$g'' + \frac{1}{2}\xi g' - \frac{3}{2}g = \rho\xi, \tag{2.20}$$

with conditions

$$g(\xi_0) = g'(\xi_0) = 0, \tag{2.21}$$

$$g(\xi) \sim -\rho\xi \quad \text{as} \quad X \to -\infty. \tag{2.22}$$

where the ξ_0 is a constant. Then we see that the free boundary $x_f - x_0 \sim O(\tau^{\frac{1}{2}})$. Solving the ODE both Wilmott et al. (1995) and Evans et al. (2002) find the transcendental equation for the problem to be

$$\xi_0^3 e^{\frac{1}{4}\xi_0^2} \int_{-\infty}^{\xi_0} e^{-\frac{1}{4}s^2} ds = 2(2 - \xi_0^2), \tag{2.23}$$

and the constant ξ_0 can be found using numerical methods to be

$$\xi_0 = 0.9034\ldots \tag{2.24}$$

Then in original variables we have that as $t \to T$

$$S_f(t) \sim \frac{rE}{D_0}\left(1 + \xi_0\sqrt{\frac{1}{2}\sigma^2(T-t)} + \ldots\right). \tag{2.25}$$

We note that the derivation here is independent of dividend payments except for the location of the exercise boundary at expiry. Figure 2.3 diagrammatically illustrates the structure of the solution near expiry. The solution is approximately European to order $O(\tau^{1/2})$ around $x = 0$, with the American element of the option only coming into play in a smaller region also $O(\tau^{1/2})$ around x_0. Obviously, as time to expiry increases the region around $x = 0$ will begin to interact with the region around x_0 and a more complex structure will arise. In the case when $d \geq r$, $x_0 = 0$ so that a complex structure prevails even in the limit as time tends to expiry. In the next section we give a brief outline of the matched asymptotic expansions presented by Evans et al. (2002) to demonstrate the three tier structure of the solution.

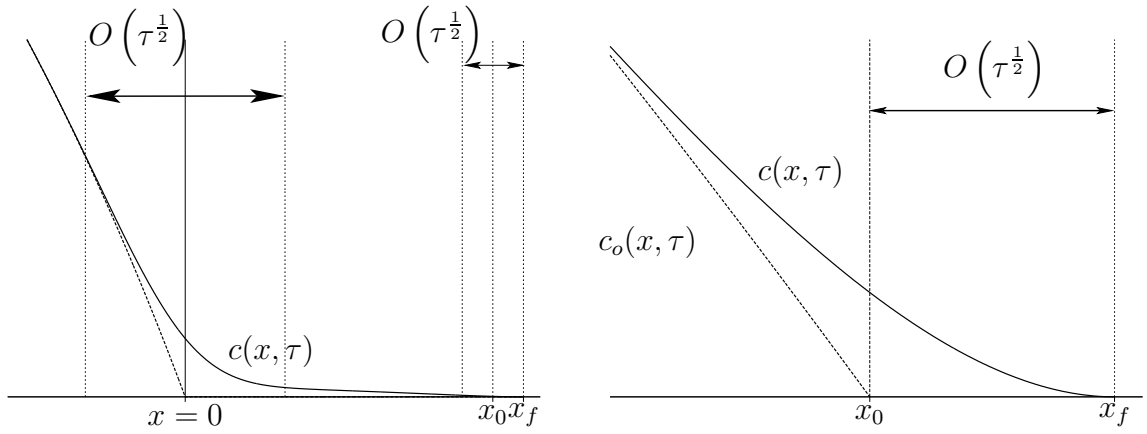

(a) Overview (b) Zoomed region

Figure 2.3
The simple structure for an American call with $0 < d < r$.
The solid line shows the numerical solution for the American call with dividends. We can see the solution has two parts, both order $O(\tau^{1/2})$, around $x = 0$ and $x = x_0$. (a) shows the entire solution space whilst (b) shows a zoomed region around x_0 with the outer solution c_o (dashed). Parameters here are $T = 0.1$, $E = 40$, $r = 0.06$, $\sigma = 0.2$, and $d = 0.03$, chosen so that $x_0 \gg \sqrt{\tau}$.

2.3.2 Asymptotic analysis for the case $d \geq r$

The free boundary in this case does not have a parabolic form, which can be verified by setting $x_f(\tau) \sim \xi_0\sqrt{\tau}$, and attempting to find a constant such that the boundary conditions are satisfied. Since no constant can be found ($\xi_0 \to \infty$), the solution is instead found to have a three tier structure.

If we look at the problem (2.10) with conditions (2.11) to (2.13) and look for a solution in the limit of small time where $\tau = \epsilon\hat{T}$, we get

$$\frac{\partial c}{\partial \hat{T}} = \epsilon\left[\frac{\partial^2 c}{\partial x^2} + (\rho - \nu - 1)\frac{\partial c}{\partial x} + e^{\epsilon\rho\hat{T}}(\rho - \nu e^x)\right]. \tag{2.26}$$

Then we look for a solution of the form

$$c(x,\tau) = C_0(x,\hat{T}) + \epsilon C_1(x,\hat{T}) + O(\epsilon^2).$$

Then for $x < 0$ we have the $O(1)$ problem

$$\frac{\partial C_0}{\partial \hat{T}} = 0, \tag{2.27}$$

with the condition

$$C_0(x,0) = 1 - e^x. \tag{2.28}$$

Then we have that

$$C_0(x,\hat{T}) = 1 - e^x. \tag{2.29}$$

At O(ϵ) we have

$$\frac{\partial C_1}{\partial \hat{T}} = \frac{\partial^2 C_0}{\partial x^2} + (\rho - \nu - 1)\frac{\partial C_0}{\partial x} + (\rho - \nu e^x), \tag{2.30}$$

so using the above form for C_0 we get

$$\frac{\partial C_1}{\partial \hat{T}} = \rho(1 - e^x), \tag{2.31}$$

with the conditions

$$C_1(x,\hat{T}) \sim \rho\hat{T}(1 - e^x) \quad \text{as} \quad x \to -\infty, \tag{2.32}$$

$$C_1(x,0) = 0, \tag{2.33}$$

so then we have the following expansion for c in the region $x < 0$

$$c(x,\tau) = 1 - e^x + \rho\tau(1 - e^x) + O(\epsilon^2). \tag{2.34}$$

We can now introduce a region around the free boundary of $O(\epsilon)$ to satisfy the boundary conditions, $x = x_f(\tau) + \epsilon z$ where $z = O(1)$. Then we have

$$\begin{aligned} \frac{\partial}{\partial \tau} &\to \frac{1}{\epsilon}\frac{\partial}{\partial \hat{T}} - \frac{1}{\epsilon^2}\frac{\mathrm{d}x_f(\hat{T})}{\mathrm{d}\hat{T}}\frac{\partial}{\partial z}, \\ \frac{\partial}{\partial x} &\to \frac{1}{\epsilon}\frac{\partial}{\partial z}. \end{aligned}$$

So from (2.10) and (2.11) - (2.13) we obtain

$$\begin{aligned}\frac{1}{\epsilon}\frac{\partial c}{\partial \hat{T}} - \frac{1}{\epsilon^2}\frac{\mathrm{d}x_f(\hat{T})}{\mathrm{d}\hat{T}}\frac{\partial c}{\partial z} &= \frac{1}{\epsilon^2}\frac{\partial^2 c}{\partial z^2} + \frac{1}{\epsilon}(\rho-\nu-1)\frac{\partial c}{\partial z} + \\ &\quad e^{\epsilon\rho T}(\rho - \nu e^{(x_f+\epsilon z)}), \qquad (2.35)\\ c(x_f,\hat{T}) &= \frac{\partial}{\partial z}c(x_f,\hat{T}) = 0, \qquad (2.36)\end{aligned}$$

then clearly $c = O(\epsilon^2)$.

We now need an inner expansion to bridge between the outer expansion and the region near x_f. The outer expansion breaks down when $x = O(\epsilon^{1/2})$, so we let $x = \epsilon^{1/2}X$ and write

$$c(x,\tau) = \epsilon^{1/2}C_0(X,\hat{T}) + \epsilon C_1(X,\hat{T}) + \epsilon^{3/2}C_2(X,\hat{T}) + O(\epsilon^2).$$

Then we have the following problem

$$\frac{\partial c}{\partial T} = \frac{\partial^2 c}{\partial X^2} + \epsilon^{1/2}(\rho-\nu-1)\frac{\partial c}{\partial X} + \epsilon(\rho-\nu) - \epsilon^{3/2}\nu X + O(\epsilon^2), \qquad (2.37)$$

$$c = \frac{\partial c}{\partial X} = 0 \quad \text{as} \quad X \to \infty, \qquad (2.38)$$

$$c = -\epsilon^{1/2}X - \frac{1}{2}\epsilon X^2 - \epsilon^{3/2}(\frac{1}{6}X^3 + \rho\hat{T}X) + O(\epsilon^2) \quad \text{as} \quad X \to -\infty, \qquad (2.39)$$

$$c(X,0) = \max(-\epsilon^{1/2}X - \frac{1}{2}\epsilon X^2 - \epsilon^{3/2}\frac{1}{6}X^3 + O(\epsilon^2), 0). \qquad (2.40)$$

Now to $O(\epsilon^{1/2})$ we have the following problem

$$\begin{aligned}\frac{\partial C_0}{\partial T} &= \frac{\partial^2 C_0}{\partial X^2}, \qquad (2.41)\\ C_0 \to 0 \quad &\text{as} \quad X \to \infty, \qquad (2.42)\\ C_0 \sim -X \quad &\text{as} \quad X \to -\infty, \qquad (2.43)\\ C_0(X,0) &= \max(-X,0). \qquad (2.44)\end{aligned}$$

We seek a similarity solution of the form $C_0 = \hat{T}^{1/2}h_0(\xi)$ where $\xi = \frac{X}{2\hat{T}^{1/2}}$ we have the

following problem

$$h_0'' + 2\xi h_0' - 2h_0 = 0, \tag{2.45}$$

$$h_0 \sim - - 2\xi \quad \text{as} \quad X \to -\infty, \tag{2.46}$$

$$h_0 \to 0 \quad \text{as} \quad X \to +\infty. \tag{2.47}$$

which has the solution

$$h_0 = \frac{1}{\sqrt{\pi}} e^{-\xi^2} - \xi \text{erfc}(\xi). \tag{2.48}$$

Next, to order $O(\epsilon)$ we have

$$\frac{\partial C_1}{\partial \hat{T}} = \frac{\partial^2 C_1}{\partial X^2} + (\rho - \nu - 1)\frac{\partial C_0}{\partial X} + (\rho - \nu), \tag{2.49}$$

$$\frac{\partial C_1}{\partial X} = 0 \quad \text{as} \quad X \to \infty, \tag{2.50}$$

$$C_1 \sim -\frac{1}{2}X^2 \quad \text{as} \quad X \to -\infty, \tag{2.51}$$

$$C_1(X, 0) = \begin{cases} -\frac{1}{2}X^2 & X \leq 0 \\ 0 & X > 0 \end{cases}. \tag{2.52}$$

Then we seek a solution of the form $C_1 = \hat{T} h_1(\xi)$ where again $\xi = \frac{X}{2\hat{T}^{1/2}}$. Then we obtain

$$h_1'' + 2\xi h_1' - 4h_1 = 2(1 + \nu - \rho)h_0' + 4(\nu - \rho), \tag{2.53}$$

$$h_1 \sim -2\xi^2 \quad \text{as} \quad X \to -\infty, \tag{2.54}$$

$$h_1' \to 0 \quad \text{as} \quad X \to \infty, \tag{2.55}$$

which has the asymptotic form

$$h_1 \sim \rho - \nu + \frac{1}{2\sqrt{\pi}}(1 + \nu - \rho)\frac{e^{-\xi^2}}{\xi} \quad \text{as} \quad X \to \infty. \tag{2.56}$$

Next, to order $O(\epsilon^{3/2})$ we have

$$\frac{\partial C_2}{\partial \hat{T}} = \frac{\partial^2 C_2}{\partial X^2} + (\rho - \nu - 1)\frac{\partial C_1}{\partial X} - \nu X, \tag{2.57}$$

$$\frac{\partial C_2}{\partial X} = 0 \quad \text{as} \quad X \to \infty, \tag{2.58}$$

$$C_2 \sim -\frac{1}{6}X^3 - \rho X\hat{T} \quad \text{as} \quad X \to -\infty, \tag{2.59}$$

$$C_2(X,0) = \begin{cases} -\frac{1}{6}X^3 & X \leq 0 \\ 0 & X > 0 \end{cases}. \tag{2.60}$$

Then we seek a solution of the form $C_2 = \hat{T}^{3/2}h_2(\xi)$ where again $\xi = \frac{X}{2\hat{T}^{1/2}}$. Then we obtain

$$h_2'' + 2\frac{1}{2}\xi h_2' - 6h_2 = 2(1 + \nu - \rho)h_1' + 8\nu\xi, \tag{2.61}$$

$$h_2 \sim -\frac{4}{3}\xi^3 - 2\rho\xi \quad \text{as} \quad X \to -\infty, \tag{2.62}$$

$$h_2' \to 0 \quad \text{as} \quad X \to \infty, \tag{2.63}$$

which has the asymptotic form

$$h_2 \sim -2\nu\xi + \frac{1}{4\sqrt{\pi}}(1 + \nu - \rho)^2 e^{-\xi^2} \quad \text{as} \quad X \to \infty. \tag{2.64}$$

The solution in this region is

$$c(x,\tau) = \tau^{1/2}h_0\left(\frac{x}{2\sqrt{\tau}}\right) + \tau h_1\left(\frac{x}{2\sqrt{\tau}}\right) + \tau^{3/2}h_2\left(\frac{x}{2\sqrt{\tau}}\right) + \ldots. \tag{2.65}$$

with the asymptotic behaviour as $\xi \to \infty$:

$$h_0 \sim \frac{1}{2\sqrt{\pi}}\frac{e^{-\xi^2}}{\xi^2} + \ldots, \tag{2.66}$$

$$h_1 \sim (\rho - \nu) + \ldots \tag{2.67}$$

$$h_2 \sim -2\nu\xi + \ldots \tag{2.68}$$

Then matching in the region of $O(\tau)$ around the free boundary using (2.65) and

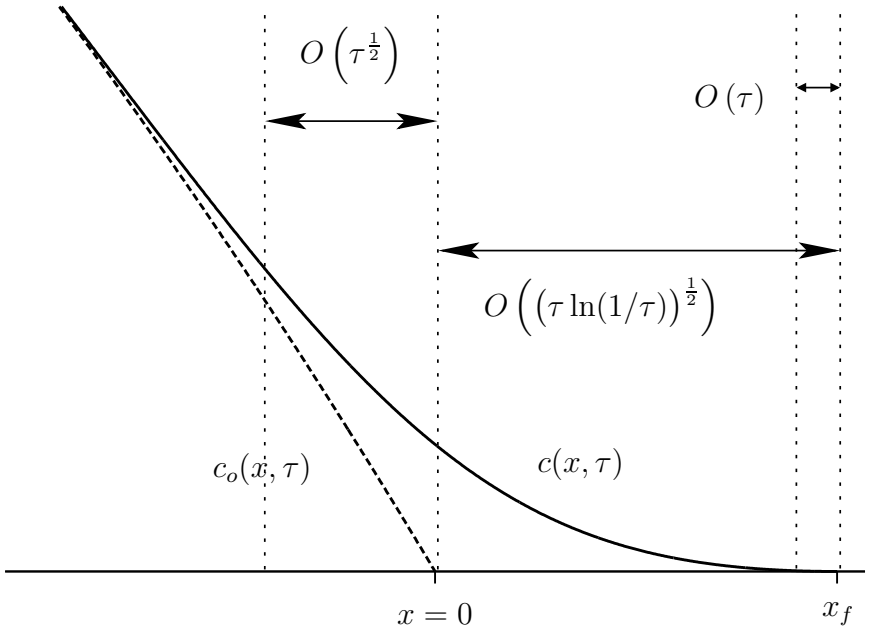

Figure 2.4
The simple structure for an American call with $d \geq r$.
The solid line shows the numerical solution for the American call with dividends, the dashed line shows the asymptotic outer solution. We can see the solution has three interacting regions, around $x = 0$, $x = x_f$ and in between. Parameters here are $T = 0.1$, $E = 40$, $r = 0.06$, $\sigma = 0.2$, and $d = 0.06$.

(2.68), we obtain the two following transcendental equations

$$\begin{aligned} \frac{1}{2\sqrt{\pi\tau}} e^{-x_f^2/4\tau} + \rho - \nu \sim 0, \quad \rho < \nu, \\ \frac{1}{4\sqrt{\pi\tau}} e^{-x_f^2/4\tau} - \nu \sim 0, \quad \nu = \rho. \end{aligned} \tag{2.69}$$

Then in the original variables we have the following formula for the free boundary as $\tau \to 0$

$$\begin{aligned} S_f(t) \sim E + E\sigma\sqrt{(T-t)\ln[\sigma^2/(8\pi(T-t)(r-d)^2)]}, \quad r < d \\ S_f(t) \sim E + E\sigma\sqrt{2(T-t)\ln[1/(4\sqrt{\pi}d(T-t))]}, \quad r = d. \end{aligned} \tag{2.70}$$

2.3.3 The American put with dividends

For the American put option, Evans et al. (2002) find that the free boundary has a parabolic solution for $r > d$, and the parabolic logarithmic solution for $r \leq d$. In the limit as time tends to expiry we have that

$$\begin{aligned} S_f(t) &\sim E - E\sigma\sqrt{(T-t)\ln[\sigma^2/(8\pi(T-t)(r-d)^2)]}, \quad r > d \\ S_f(t) &\sim E - E\sigma\sqrt{2(T-t)\ln[1/(4\sqrt{\pi}d(T-t))]}, \quad r = d, \\ S_f(t) &\sim \frac{dE}{r}\left(1 - \xi_0\sqrt{\frac{1}{2}\sigma^2(T-t)} + \ldots\right), \quad r < d. \end{aligned} \tag{2.71}$$

2.4 Numerical Techniques and extensions

It is not normally the case that an analytical solution can be found for free boundary problems (which are inherently nonlinear) and so we generally require a numerical method in order to solve them. One method is to write the free boundary problem in terms of a body-fitted coordinate system, in which we simultaneously solve for the free boundary, explained later in section 2.4.3. This results in a relatively simple, albeit non-linear PDE in the single asset case, but is much more difficult to implement with an increase in the number of assets. The method also relies on the free boundary being a smooth continuous function that does not disappear at any stage. For instance, to price a Bermudan option (relatively simple by other methods) the free boundary is only defined at the exercise dates. A body-fitted coordinate system is not appropriate in this instance, so a more robust method (over a fixed domain) in which the boundary conditions are implicitly satisfied in the new set of equations is then necessary. Crank (1984) describes two such formulations that can be applied to the heat equation; the enthalpy method and variational inequalities (see Elliot and Ockendon, 1982 for a detailed description). The variational inequality formulation is the most appealing for finance problems (since there is no obvious equivalent condition in financial terms to the overall conservation of heat). Wilmott et al. (1993) have used the methods described by Crank (1984) to formulate the American option

as a variational inequality.

The American Option as a Variational Inequality

We have already formulated the American option earlier in this section. It is now simple to formulate this as a parabolic variational inequality, and then after discretisation, a linear complementary problem. If we let $\mathcal{L}_{BSM}$ be the standard BSM operator, and $G(S,t)$ be the constraint applied to the problem, the value of early exercise, then we can write (2.1)–(2.4) as

$$\mathcal{L}_{BSM}\big\{V(S,t)\big\}\cdot\big(V(S,t)-G(S,t)\big)=0,\quad \mathcal{L}_{BSM}\big\{V(S,t)\big\}\leq 0,\quad V(S,t)-G(S,t)\geq 0, \tag{2.72}$$

such that V and $\partial V/\partial S$ are continuous. Note here that for the American put, $G(S,t)=\max(E-S,0)$, and consequently its derivative is discontinuous at $S=E$. However, it can be shown that $V(S=E,t)>G(S=E,t)$ for any time before expiry so the constraint will never be applied there. This is not always the case, as for example in the case of the cash-or-nothing American option, there is a discontinuous constraint, implying that the free boundary is known *a priori*, since it is always optimal to exercise at the strike price. The smooth-pasting condition therefore does not apply, since $G(S_f,t)$ and $\partial G(S_f,t)/\partial S$ are not continuous at the strike price.

Elliot and Ockendon (1982), Friedman (1988) and Kinderlehrer and Stampacchia (1980) give detailed accounts of the existence and uniqueness proof for variational inequalities of this form, which involves knowledge of abstract functional analysis; the problem is basically reduced to minimising a convex set of functions.

2.4.1 The PSOR Method

First the problem is discretised according to the Crank-Nicolson method. Since the problem is backwards parabolic, for convenience we make the substitution $\tau = T-t$ so that the problem is now forward in τ. Now discretise the problem so that

$$\Delta S=\frac{S_{max}}{n},\quad \Delta\tau=\frac{T}{m},\quad V(i\cdot\Delta S,k\cdot\Delta\tau)=u_i^k,$$

then we can write an approximation to the BSM operator as

$$\alpha_i u_{i-1}^{k+1} + (1/\Delta t + \beta_i) u_i^{k+1} + \gamma_i u_{i+1}^{k+1} = -\alpha_i u_{i-1}^{k} + (1/\Delta t - \beta_i) u_i^{k} - \gamma_i u_{i+1}^{k}, \quad (2.73)$$

where u^k is known and u^{k+1} must be found. The errors in this scheme are of the order $O(\Delta S^2, \Delta\tau^2)$. The coefficients α, β and γ are defined in the introduction section 1.3.3. Next, let $G(i \cdot \Delta S, k \cdot \Delta t) = g_i^k$, then the early exercise constraint can be written as

$$u_i^k \geq g_i^k, \quad \text{for } k \geq 1 \text{ and } \forall i, \quad (2.74)$$

and so the discretised problem is

$$\left(\alpha_i u_{i-1}^{k+1} + (1/\Delta t + \beta_i) u_i^{k+1} + \gamma_i u_{i+1}^{k+1} - Z_i^k\right) \cdot \left(u_i^{k+1} - g_i^{k+1}\right) = 0, \quad (2.75)$$

where we have defined

$$Z_i^k = -\alpha_i u_{i-1}^{k} + (1/\Delta t - \beta_i) u_i^{k} - \gamma_i u_{i+1}^{k}.$$

The boundary conditions can be determined explicitly so that

$$\begin{aligned} u_0^k &= Z_0^k, \\ u_n^k &= Z_n^k, \end{aligned} \qquad \forall k. \quad (2.76)$$

For example, the boundary conditions on the American put give $Z_0^k = E$ and $Z_n^k = 0$.

Hence, discretisation leads to a succession of elliptic variational inequalities to be solved at each time step. Such inequalities can be expressed in the general linear complementarity (vector) form

$$\mathcal{A}\mathcal{B} = 0, \qquad \mathcal{A} \geq 0, \qquad \mathcal{B} \geq 0. \quad (2.77)$$

where the product here implies that at least one element in $\mathcal{A}$ and $\mathcal{B}$ must be zero at every position.

Many methods have been proposed to solve such a problem when

$$\mathcal{A} = \mathbf{A}\mathbf{x} - \mathbf{b},$$

and

$$\mathcal{B} = \mathbf{x},$$

where $\mathbf{x}$ is the n-vector to be determined, $\mathbf{b}$ is a known n-vector and $\mathbf{A}$ is an $n \times n$ matrix. Generic methods for solving such a system of equations are not geared toward finite-difference formulation, so by adapting the SOR method Cryer (1971) was able to exploit the sparseness of matrix $\mathbf{A}$.

Now, let $\boldsymbol{u}^k$ and $\boldsymbol{g}$ denote the vectors as follows

$$\boldsymbol{u}^k = \begin{pmatrix} x_1^k \\ \vdots \\ x_{n-1}^k \end{pmatrix}, \qquad \boldsymbol{g}^k = \begin{pmatrix} g_1^k \\ \vdots \\ g_{n-1}^k \end{pmatrix}. \tag{2.78}$$

The values at the boundary are not included, since we do not need to iterate over them. We can then construct a matrix $\mathbf{A}$ and a vector $\boldsymbol{b^k}$ such that we can rewrite (2.75), as the linear complementarity problem

$$\left(\mathbf{A}\boldsymbol{u}^{k+1} - \boldsymbol{b}^k\right) \cdot \left(\boldsymbol{u}^{k+1} - \boldsymbol{g}^{k+1}\right) = 0, \tag{2.79}$$

where the product represents the set of equations such that either the first bracket or the second bracket is zero.

We now define the Projected Successive Over Relaxation algorithm, or PSOR. It is basically an extension of the SOR method, modified to solve the linear complementary problem. Crank (1984) notes that although the PSOR method has been used heuristically as far back as Christopherson and Southwell (1938), convergence was not proved rigorously until Cryer (1971).

In the SOR method we have

$$y_i^{k+1,q+1} = \frac{1}{1/\Delta t+\beta_i}\left(Z_i^k - \alpha_i u_{i-1}^{k+1,q+1} - \gamma_i u_{i+1}^{k+1,q}\right), \tag{2.80}$$

$$u_i^{k+1,q+1} = u_i^{k-1,q} + \omega(y_i^{k+1,q+1} - u_i^{k+1,q}), \tag{2.81}$$

where q represents the qth iteration. If we iterate using equations (2.80) and (2.81) over the domain until successive iterates are sufficiently close to one another, then u will satisfy the first constraint of the problem $\mathbf{A}\boldsymbol{u}^{k+1} = \boldsymbol{b}^k$. Then we must modify the algorithm to satisfy the constraint that $\boldsymbol{u}^{k+1} \geq \boldsymbol{g}^{k+1}$. This is undertaken by modifying the second step in the SOR algorithm (2.81) to obtain the projected SOR algorithm:

$$y_i^{k+1,q+1} = \frac{1}{1/\Delta t+\beta_i}\left(Z_i^k - \alpha_i u_{i-1}^{k+1,q+1} - \gamma_i u_{i+1}^{k+1,q}\right), \tag{2.82}$$

$$u_i^{k+1,q+1} = \max\left[u_i^{k+1,q} + \omega(y_i^{k+1,q+1} - u_i^{k+1,q}), g_i^{k+1}\right]. \tag{2.83}$$

We then iterate over these two equations until the difference between successive iterations is sufficiently small.

The problem is reduced to maximising the vector $\boldsymbol{u}^{k+1}$ over the solution space. This can be interpreted in finance terms as choosing the free boundary in order to maximise the value of the option.

2.4.2 Modifying PSOR - A Novel Approach

We define Block SOR to be a modified SOR method in which the vectors $\boldsymbol{u}^{k+1}$, $\mathbf{A}$ and $\boldsymbol{b}^k$ are partitioned into smaller subsets, over which we solve (with a direct method) while all other points are constant. This method is well known and is particularly efficient when solving multi-dimensional problems.

If timesteps are large, and parameter σ is large, the rate of convergence for the PSOR scheme can be very slow, especially when extended to the multi-asset problem. We can take advantage of some of the properties of the free boundary in order to make the PSOR solver converge much quicker. We know that for the American put,

the value of the free boundary is monotonically decreasing. Consequently, at step $k+1$, let us partition $\boldsymbol{u}^{k+1}$ into the subsets

$$\boldsymbol{u}_1^{k+1} = \begin{pmatrix} x_1^k \\ \vdots \\ x_{a^k-1}^k \end{pmatrix}, \qquad \boldsymbol{u}_2^{k+1} = \begin{pmatrix} x_{a^k}^k \\ \vdots \\ x_{n-1}^k \end{pmatrix}, \tag{2.84}$$

where $a^k \cdot \Delta S$ is the position of the free boundary at time k on the grid. We can also construct the corresponding subsets $\mathbf{A}_1$, $\mathbf{A}_2$, $\boldsymbol{b}_1^k$, and $\boldsymbol{b}_2^k$. Due to the monotonicity of the free boundary we know that for a put

$$a^{k+1} \leq a^k,$$

whilst for a call

$$a^{k+1} \geq a^k.$$

Thus, when pricing a put, we know with certainty that $\boldsymbol{u}_2^{k+1}$ is not exercised, implying that we may solve this subset using a direct method, since no projection is required, but for the other subset $\boldsymbol{u}_1^{k+1}$, point PSOR is still used. We define this new algorithm to be the Advanced PSOR scheme, or APSOR. If there were a large number of iterations at each time step then iterating with the direct solver would become slow and inefficient. However, due to the fact that the boundary rarely moves more than one or two nodes in any one time step, and often stays at the same node, the number of necessary iterations is small (there is no need to iterate at all if the free boundary does not move).

Figures 2.5 and 2.6 give a brief description of the algorithms needed to generate the APSOR. The function 'TridiagonalSolver' (an adaptation of the Thomas algorithm) is a modified tridiagonal solver for the region $[a+1, n]$. The result can then be over relaxed (if optimal to do so) and an error over the region calculated. Then function 'PointSolverDown' is called, which solves over the region $[1, a]$. The solver moves downward, starting at a, because once the option is exercised at i_f, we know

```
AdvancedPsorSolver(freeBoundary, u, g)
1  ComputeScheme(alpha, beta, gamma, z)
2  while error > tol
3  do
4      a ← freeBoundary
5      TridiagonalSolver(a, alpha, beta, gamma, z, u, error)
6      freeBoundary ← PointSolverDown(a, error, alpha, beta, gamma, z, u, g)
7  return loops
```

Figure 2.5
Advanced PSOR solver – pseudo code
The algorithm performed at each time step. Values of 'alpha', 'beta', 'gamma' and 'z' come from (2.73), and TridiagonalSolver uses Gaussian elimination. 'loops' is returned for optimisation.

```
PointSolverDown(a, error, alpha, beta, gamma, z, u, g)
 1  for i ← a to 1
 2  do
 3      y ← SOR(alpha, beta, gamma, z, u)
 4      if y ≤ g_i
 5        then
 6              u_i ← g_i
 7              break
 8        else
 9              error ← error + (y − u_i) ∗ (y − u_i)
10              u_i ← y
11  return i
```

Figure 2.6
Point Solver Down – pseudo code
The "search" type algorithm (that also updates the solution) to find the next approximation to the free boundary.

that it will be exercised for all $i < i_f$ (we are assuming here that the option is the American put for these conditions to hold). This implies that once the condition is satisfied we can break the 'for' loop as the solution will not change in the remainder of the region. If the free boundary is stationary (with respect to the nodes) then the condition is satisfied at a and the solution has already been found, and no more iteration is required.

It is trivial to modify the algorithm to solve a problem where the free boundary is strictly increasing, but it can also be modified to solve problems where the movement of the boundary is unknown, or changes direction, so long as we know an approximate

start point and that the boundary is a single point. For example, in figure 2.6, if the algorithm breaks when $i = a$, it may be possible that the free boundary is in the region $[a + 1, n]$. So when a break occurs at a we must then move upward through the solution space, using PSOR, checking for the first point at which the condition is *not* satisfied. The last point at which it has been satisfied is passed out as the free boundary.

2.4.3 The Boundary-fitted Coordinate Formulation

The body-fitted coordinate (BFC) method is an alternative means to solve the American option problem. As mentioned earlier, it is relatively simple to formulate with a single underlying asset, however the complexity increases dramatically each time we increase the number of assets. For the single asset case, we may usefully use the BFC to test the accuracy of our PSOR method.

The BFC uses a transformation in order to solve the moving boundary problem over a fixed coordinate system. While Landau (1950) was the first to propose such a transformation, Crank (1957) was the first to apply it to a finite-difference scheme to solve diffusion equations, then more recently Widdicks (2002) adapted the scheme to solve the American option problem. Smooth convergence of the method in both S and t, enabled Widdicks (2002) to use Richardson extrapolation of the results to improve accuracy, resulting in a highly accurate method.

The advantage of the BFC method is this: the position of the free boundary is solved accurately at each time step, which is important in finance since the holder of the option will need to know precisely when it is optimal to exercise. The PSOR scheme will calculate the position of the free boundary to $O(\Delta S)$, whereas we would expect the BFC to position the boundary to $O((\Delta S)^2)$. Although we have accuracy at the free boundary, when we wish to calculate the solution at some prescribed point in S space, then we will almost certainly not have a grid point located at this position, although the value can then be found easily using interpolation. This is a minor drawback as an inaccurate location of the boundary can easily lead to larger

errors.

Widdicks (2002) notes that BFC has difficulty tracking the free boundary when the time to expiry is small (as do many of the numerical methods for solving American options). For the scheme to converge, the timesteps may be altered so that they are smaller when the time to expiry is small, and larger when the time to expiry is large. The rate at which they are scaled is chosen to be $\tau^{\frac{1}{2}}$ so as to mimic (approximately) the behaviour of the free boundary near expiry (c.f. section 2.3). For this reason, section 2.5 outlines a new procedure that combines the 'curtailed range' analysis used by Andricopoulos et al. (2004) on lattice methods, with the BFC, to arrive at a scheme which is both accurate and does not have restrictions on the size of the time steps.

Here the method as used by Widdicks (2002) is first explained. In the BFC, the coordinate system is allowed to move with the free boundary. Again we use the transformation $\tau = T - t$, and in the case of the American put, we use the following transformation for S,

$$\hat{S} = S - S_f(\tau), \tag{2.85}$$

where $\hat{S} \in [0, \infty]$ and $S = S_f(t) \Rightarrow \hat{S} = 0$. The Black-Scholes equation under this transformation then becomes

$$\frac{\partial V}{\partial \tau} - \frac{dS_f}{d\tau}\frac{\partial V}{\partial \hat{S}} = \frac{1}{2}\sigma^2(\hat{S} + S_f)^2\frac{\partial^2 V}{\partial \hat{S}^2} + r(\hat{S} + S_f)\frac{\partial V}{\partial \hat{S}} - rV. \tag{2.86}$$

The PDE (2.86) is clearly non-linear, but we can use Newton iteration in order to linearise the PDE; this involves making a guess at the solution, and assuming the correction to the guess is small, say $O(\delta)$, then we can write

$$\begin{aligned} V_i^{k+1,(q+1)} &= V_i^{k+1,(q)} + \delta V_i, \\ S_f^{k+1,(q+1)} &= S_f^{k+1,(q)} + \delta S_f. \end{aligned} \tag{2.87}$$

Then using a Crank-Nicolson scheme, we have (for example) the following approximations,

$$\frac{\partial V}{\partial \tau}(\hat{S}, \tau + \frac{1}{2}\Delta\tau) \approx \frac{1}{\Delta t}(V_i^{k+1} + \delta V_i - V_i^k),$$
$$S_f(\tau + \frac{1}{2}\Delta\tau) \approx \frac{1}{2}(S_f^{k+1} + \delta S_f - S_f^k). \tag{2.88}$$

Then substituting (2.88) along with other terms into (2.86) we have a collection of $O(\delta)$ and $O(1)$ terms. Then collecting the $O(\delta)$ terms on the left hand side and the $O(1)$ terms on the right we arrive at an equation of the form,

$$\delta V_{i-1}\alpha_i + \delta V_i\beta_i + \delta V_{i+1}\gamma_i + \delta S_f\theta_i = \epsilon_i. \tag{2.89}$$

This represents a tri-diagonal system but it also includes an extra column corresponding to δS_f. This can be readily solved using Gaussian elimination to find the correction terms. We may iterate at each time level until the maximum correction term is less than some prescribed tolerance,

$$\max|\delta V_i, \delta S_f| \leq \text{tol}, \qquad \text{tol} > 0.$$

2.5 An Improved Numerical Technique

As stated previously in section 2.4.3, the BFC method struggles to cope with the free boundary as time tends toward expiry. However, Johnson (2003) finds that in a problem with two free boundaries that converge to the same point at expiry, the BFC on such a problem can track both of the boundaries even in this limit. If there exists some way of defining an upper (lower) boundary on the solution for a put (call) the problem can be formulated with one free boundary and one *known* boundary. If the two boundaries converge to the same point, then any difficulties experienced with tracking the boundary near expiry will be overcome, although the nodes are equally spaced in the transformed space, the distance between nodes in real space will tend

become increasingly small (a very positive feature) near expiry.

Andricopoulos et al. (2004) suggest that the 'curtailed range' technique can be applied to both lattice and finite-difference grid methods. However, this suggestion involves discounting nodes over which the solution is obtained, rather than fitting the coordinate system around the curtailed range. The range suggested by Andricopoulos et al. (2004) is

$$S_{min} = \min\left[S_0 e^{r\tau - \xi\sigma\sqrt{\tau}}, Ee^{-r\tau - \xi\sigma\sqrt{\tau}}, 0\right], \tag{2.90}$$

$$S_{max} = \max\left[S_0 e^{r\tau + \xi\sigma\sqrt{\tau}}, Ee^{-r\tau + \xi\sigma\sqrt{\tau}}\right], \tag{2.91}$$

where ξ is a parameter that the user defines and will effect the accuracy of the scheme. Such a region can be thought of as follows: for a put, given $S_t \in [S_{max}, \infty]$, the probability that a random walk followed by the asset will finish at time T in a position to be exercised is set to be so small that it is not even worth calculating. The parameter ξ measures how many standard deviations in the normal distribution it will be from the mean, and hence increasing ξ will make the probability ever smaller and accuracy will be increased. This is corroborated by the asymptotic analysis by Evans et al. (2002) (for the singular perturbation analysis see also Widdicks et al., 2005), in which the solution is found to have three distinct regions, and above the upper most region, approximately of order $\tau^{\frac{1}{2}}$, the American put option price is approximately zero.

The upper-bound, $S_{max} = U(\tau)$ is specified for the American put option, and is

$$U(\tau) = \min\left[Ee^{\xi\sigma\sqrt{\tau}}, \lambda E\right]. \tag{2.92}$$

The $-r\tau$ term is dropped from (2.91) so that $U(\tau) > E$, and λ is some constant that defines the maximum value of the grid required. The constant ξ is taken to be 10, somewhat larger than the value suggested by Andricopoulos et al. (2002) in order to

make sure the domain is of sufficient extent. For the American call, we set

$$L(\tau) = \max\left[Ee^{-\xi\sigma\sqrt{\tau}}, 0\right], \tag{2.93}$$

where L here is a lower bound.

Now, if we define $F(\tau) = L(\tau)$ to be the lower boundary, and the function $G(\tau) = U(\tau) - F(\tau)$ to be the difference between the upper and lower boundaries. Then the mapping $[S_{min}, S_{max}] \to [0, 1]$ is defined as follows

$$\hat{S} = \frac{S - F(\tau)}{G(\tau)}. \tag{2.94}$$

Here the initial transformation is independent of the type of option. We must now specify F and G subject to the option for which we are solving. For the American put, U is known and given by (2.92), $F(\tau) = S_f(\tau)$ is the free boundary, and therefore $G(\tau) = U(\tau) - S_f(\tau)$. For a call, $F(\tau) = L(\tau)$ is the known boundary, $U(\tau) = S_f(\tau)$ corresponds to the free boundary, and so $G(\tau) = S_f(\tau) - L(\tau)$. It can be now seen why using this transformation will be accurate. Other methods struggle as time tends to expiry, because ΔS cannot be set small enough to fully capture the solution in this limit. Here, however, as time tends to expiry, $G(\tau) \to 0$, and so $\Delta S = G\Delta\hat{S} \to 0$ as well. Since we are discretising over $\Delta\hat{S}$, and the scheme is $O(\Delta\hat{S}^2, \Delta\tau^2)$, as we approach expiry the scheme becomes very accurate in ΔS, no matter how small the time to expiry is, as the corresponding ΔS is also reduced.

Now using (2.94) on the Black-Scholes equation we obtain;

$$V_\tau - \frac{1}{G}(\hat{S}G_\tau + F_\tau)V_{\hat{S}} = \frac{1}{2}\sigma^2\left(\hat{S} + \frac{F}{G}\right)^2 V_{\hat{S}\hat{S}} + r\left(\hat{S} + \frac{F}{G}\right)V_{\hat{S}} - rV. \tag{2.95}$$

This equation is solved over $\hat{S} \in [0, 1]$. Note here that when solving for a put, both F and G are unknown functions (G is a known plus an unknown function), so both must be solved, thus making the problem slightly more complicated than the previous BFC formulation. For the call, however, F is a known function and we need only solve for G.

The boundary conditions for the put are as follows

$$\begin{aligned} F(0) &= \min\left[E, \frac{rE}{d}\right], \\ V(\hat{S},0) &= \max[E-S,0], \\ V(0,\tau) = E - F(\tau), &\qquad \frac{\partial V}{\partial \hat{S}}(1,\tau) = -G(\tau), \\ V(1,\tau) = 0, &\qquad F(\tau) + G(\tau) = U(\tau), \end{aligned} \tag{2.96}$$

and similarly for the call we have

$$\begin{aligned} U(0) &= \max\left[E, \frac{rE}{d}\right], \\ V(\hat{S},0) &= \max[S-E,0], \\ V(0,\tau) &= 0, \\ V(1,\tau) = G(\tau) + F(\tau) - E, &\qquad \frac{\partial V}{\partial \hat{S}}(1,\tau) = G(\tau). \end{aligned} \tag{2.97}$$

2.5.1 The Advanced Body-Fitted Coordinated Method (ABFC)

To price a put, we must solve equation (2.95) subject to the boundary conditions (2.96). This is a non-linear PDE, and so we use the Newton method as described in section 2.4.3 to linearise the problem. This is slightly different to the BFC formulation, since there is an extra equation that determines the value of G. Using a guess such as that in (2.87) and discretising according to the Crank-Nicolson method, we obtain a scheme of the form,

$$\delta V_{i-1}\alpha_i + \delta V_i\beta_i + \delta V_{i+1}\gamma_i + \delta F\theta_i + \delta G\phi_i = \epsilon_i, \tag{2.98}$$

where ϵ_i contains the $O(1)$ terms. If there are n nodes in $\hat{S}$ space over which to solve, along with F and G, we have $n+2$ unknowns, and correspondingly there are $n+2$ equations. From (2.96), there are four boundary conditions which will result in a problem with $n+2$ equations as required. The form of the system which must be solved is of a tridiagonal format with two extra columns. This too can be solved

simply by Gaussian elimination.

For the call, the scheme is of a similar form to that of the BFC,

$$\delta V_{i-1}\alpha_i + \delta V_i\beta_i + \delta V_{i+1}\gamma_i + \delta G\phi_i = \epsilon_i. \tag{2.99}$$

In fact, the format of the matrix is identical to when the problem is posed in the BFC formulation, the coefficients for the BFC and ABFC are given in Appendix A.1.

2.6 Results

One of the reasons Widdicks (2002) cites for the use of the BFC method is the smooth convergence obtained. Figure 2.7 shows the rate of convergence using both the PSOR and the BFC methods. The PSOR method, has two sources of non-linear error, both from the position of the free-boundary, and from the position of the discontinuity at expiry. The discontinuity error at expiry is the larger component, and causes the (magnified) oscillations shown in figure 2.7(b). If we choose n correctly (such as placing a node at the strike price), we can avoid this error. Widdicks et al. (2002) show that when pricing using lattice methods the oscillations are in fact a function of the distance between the (nearest) node and the discontinuity at expiry. This assumes that we know the position of the discontinuity and that it is constant over the duration of the option. Widdicks (2002) also shows that this is the case for finite-difference grids. However, the true positioning of the free boundary is not constant with respect to grid position over time, so the PSOR method over or under estimates the position of the free boundary. Since we cannot expect to know the extent to which the PSOR method over or under estimates the position of the free boundary, a clever extrapolation of the PSOR results is not possible.

Table 2.1 shows relative RMS errors for the four methods described in this chapter. The RMS errors are calculated over 8 put options, with different exercise prices, volatilities and expiry times. First compare the fixed grid methods to the boundary-tracking grids methods. Both sets of results have been improved using Richardson

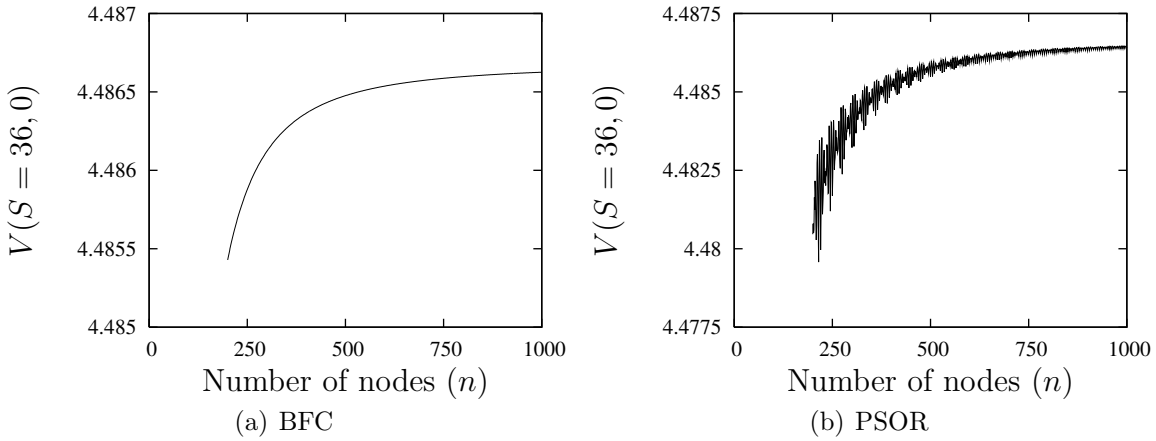

(a) BFC (b) PSOR

Figure 2.7
Convergence
Convergence for the BFC method and the PSOR method. Here $T = 1$, $S_0 = 36$, $\sigma = 0.2$, $r = 0.06$ and $E = 40$.

extrapolation. The values of n are chosen for the fixed grid methods so that a node is placed at the strike price, hence non-linearity error at expiry is not present. The results for the PSOR method are poor, and do not work optimally with Richardson extrapolation, since the convergence is not monotonic, unlike that for BFC method. To gain comparable accuracy to the BFC method, 4 or 5 times as many points need to be used in the PSOR method.

The PSOR method also suffers from a slow rate of iterative convergence, so slow in fact that it can sometimes appear not to converge. If the volatility σ is large, and ΔS is small, then the number of iterations required to gain a sufficient level of accuracy can run into the hundreds. The method seems to struggle when the free boundary is $O(\sqrt{\tau \log(\frac{1}{\tau})})$ rather than $O(\tau^{1/2})$. When solving for an American call with dividends (the boundary is $O(\tau^{1/2})$ when $0 < d \leq r$, see section 2.3), the solver converges far quicker than for the put, which has the $O(\sqrt{\tau \log(\frac{1}{\tau})})$ boundary. When the size of the timestep is reduced, the rate at which the number of iterations required falls linearly. Using the APSOR reduces the computation time by taking advantage of the monotonically decreasing (increasing) nature of the free boundary for the American put (call). The Newton method is a fast converging method, typically only taking less than 10 iterations to gain the required accuracy. This then explains why the computation time for the PSOR increases faster than the BFC when ΔS is reduced,

Table 2.1
Relative RMS errors for American Put Options

n	PSOR (time)	APSOR (time)	BFC (time)	ABFC (time)
500	0.0001845	0.000184503	0.000029571	0.000000897
	(0.09)	(0.02)	(0.12)	(0.17)
1000	0.00019475	0.000194750	0.000004905	0.000000077
	(0.51)	(0.07)	(0.47)	(0.63)
1500	0.000013906	0.000013906	0.000001713	0.000000012
	(1.46)	(0.16)	(1.02)	(1.35)
2000	0.000015668	0.000015668	0.000000782	0.000000005
	(3.15)	(0.30)	(1.79)	(2.35)
2500	0.000008150	0.000008150	0.000000426	0.000000002
	(5.81)	(0.47)	(2.70)	(3.57)

The relative errors for each of the four methods described in this chapter. PSOR is the standard fixed grid method, with APSOR the extended fixed grid method (section 2.4.2). Boundary fitted coordinate (BFC) is the standard moving grid method, and Advanced boundary fitted coordinate (ABFC) the extended moving grid method (section 2.5) . The relative RMS errors are calculated against exact values over 8 different put options with $T = 0.5/1$, $X = 35/45$, and $\sigma = 0.2/0.4$. For all options $r = 0.06$ and $S_0 = 40$. The exact values are calculated by allowing $n \to \infty$ until successive solutions are sufficiently close to one another (1.E-10). We set there to be 4 times as many times points in asset space, as there are in time, where n gives the number of nodes in $\hat{S}$. Richardson extrapolation is carried out on $n/2$ and n points. All processes are run on an AMD Athlon(tm) 64 Processor 3400+ with 512Kb of cache.

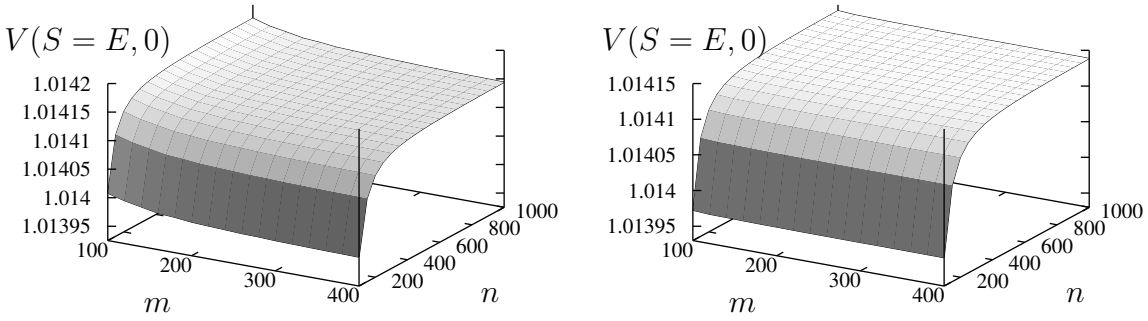

(a) $\Delta\tau = (T-t)/n$ (b) $\Delta\tau \sim (T-t)^{1/2}/n$

Figure 2.8
Convergence for different time steps
Convergence for an at-the-money American put option w.r.t. m number of nodes in τ space and n number of nodes in $\hat{S}$. Parameters are chosen to exaggerate the effects: $\sigma = 0.4$, $r = 0.05$, $E = 10$, and $T = 1$.

even though the PDE we solve is more complicated than that for the PSOR method.

The ABFC method is stable even for large timesteps. Figure 2.8 shows the rate of convergence for various combinations of nodes in $\hat{S}$ and τ for the ABFC method. Figure 2.8(a) shows results obtained by discretising in the usual manner, with constant timesteps across time. Figure 2.8(b) has results obtained using scaled timesteps such as those employed to improve stability in the BFC method. Clearly, bunching the timesteps near expiry improves accuracy, and unlike the the PSOR method (reducing the timesteps has little effect on the computation time due to the increase in iterations required) using a small number of timesteps will greatly improve efficiency of the scheme.

Figure 2.9 gives a graphical representation of how much more accurate the ABFC is compared to the PSOR and even BFC methods at tracking the free boundary. The value of ΔS in the PSOR is the same as that of $\Delta\hat{S}$ in the BFC, suggesting that the BFC can only track the boundary to $O(\Delta\hat{S})$ as we approach expiry. The ABFC however is at the value that has been predicted by the asymptotic analysis carried out by Kuske and Keller (1998).

Tables 2.1 and 2.2 show the high accuracy of the ABFC method. In table 2.1 we see that for only a small increase in computation time, accuracy is increased (w.r.t.

Table 2.2
Relative RMS and ABS errors for American Call Options

n	Cpu time	RMS error	ABS error
40	0.0000	0.05066467	0.29738690
80	0.0037	0.00405497	0.02373406
120	0.0050	0.00118193	0.00738587
160	0.0100	0.00029856	0.00185306
200	0.0150	0.00011227	0.00069487
240	0.0225	0.00005183	0.00032030
280	0.0288	0.00002755	0.00017023
320	0.0375	0.00001607	0.00009929
360	0.0475	0.00000990	0.00006110
400	0.0575	0.00000655	0.00004044
440	0.0700	0.00000445	0.00002748
480	0.0825	0.00000314	0.00001940
520	0.0963	0.00000230	0.00001420
560	0.1100	0.00000170	0.00001047
600	0.1275	0.00000130	0.00000802
640	0.1438	0.00000100	0.00000620
680	0.1625	0.00000079	0.00000485
720	0.1800	0.00000063	0.00000390
760	0.2013	0.00000051	0.00000312
800	0.2212	0.00000041	0.00000256
840	0.2437	0.00000034	0.00000211
880	0.2675	0.00000028	0.00000175
920	0.2912	0.00000024	0.00000148
960	0.3163	0.00000020	0.00000124
1000	0.3413	0.00000017	0.00000106

Errors are calculated against 40 different American call options. The relative RMS errors are calculated against exact values over 8 different put options with $T = 0.5/1$, $X = 35/45$, and $\sigma = 0.2/0.4$. For all options $r = 0.06$ and $S_0 = 40$. The exact values are calculated by allowing $n \to \infty$ until successive solutions are sufficiently close to one another (1.E-10). The solutions has been extrapolated once using Richardson extrapolation, with n and $n/2$. The number of time points is a quarter of the number used in $\hat{S}$. All processes are run on an AMD Athlon(tm) 64 Processor 3400+ with 512Kb of cache.

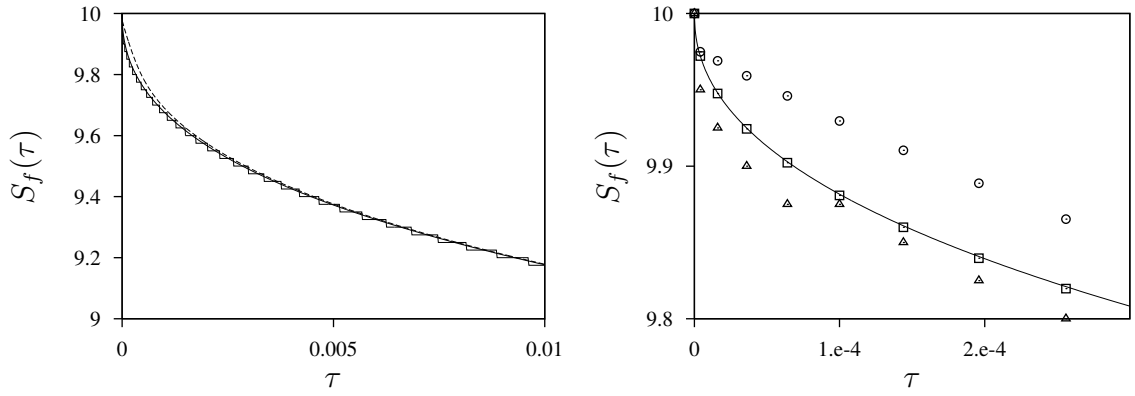

(a) Large time to expiry (b) Small time to expiry

Figure 2.9
The free boundary - BFC vs. PSOR vs. ABFC
The free boundary for the three different methods. (a) The BFC (dashed), the PSOR (solid step-like) and the ABFC (solid) shown together. (b) The free boundary for PSOR (triangle), BFC (circle), and ABFC (square). The asymptotic value is shown by the solid line.

RMS errors) by a factor of 100 on the (already very accurate) BFC solver. In table 2.2 the RMS and ABS relative errors are shown for a range of 40 call options. The results are comparable to those tabled by Broadie and Detemple (1996). The exact solution has been calculated by setting $n = 15000$, and is correct to the accuracy shown by Broadie (1996). The number of time points is set to be a quarter of the number of the points in $\hat{S}$ since the errors proportional to $\Delta\hat{S}$ are larger (c.f. figure 2.8). We can see that to obtain an ABS error of less than 0.1% we need just 200 points in $\hat{S}$ with 50 time steps.

2.7 Conclusions

The contribution of this chapter has been two-fold. First, the monotonicity of the free boundary has been exploited to improve the efficiency of the PSOR method. This is important in the next chapter when the number of underlying assets is increased, the use of finite-difference methods on 3 or 4 assets is highly dependent on the efficiency of the algorithm. With some intuition regarding the whereabouts of the free boundary, computation times can be reduced ten-fold. Secondly, the body-fitted coordinate solver, fitted to an appropriate upper and lower bound, has impressive

accuracy and efficiency. If it were possible to extend the method to the multi-asset case, the reduction in nodes needed for high accuracy will help to maintain efficiency. However the complex topology of the problem renders this extremely difficult if not impossible.

Chapter 3

Multi-Asset American Options

A natural development in option pricing theory has been to extend the number of assets on which options depend. There are numerous types of options on multiple assets that have been proposed, some of which are listed below to set the scene for discussion in the rest of the chapter. Most are bracketed under the umbrella term **rainbow options**, the only exception listed below being the basket option.

Min-max options

The **maximum** option allows the holder to choose to exercise the best performing of two or more vanilla options, depending on different assets, each of which may be a call or a put, with independent strike prices. The **minimum** version forces the holder to take the vanilla option of least value at expiry. These options usually have the same expiry date; if the strike prices are different, the option is called a dual-strike option.

Alternative options

The alternative option is based on a bundle of forward contracts, all with different underlying assets. At expiry the holder may either choose the best performing contract, a **best-of** option, or be forced to take the least valuable, a **worst-of** option.

Two asset correlation

The two-asset correlation option, or correlation digital option, has been priced analytically by Zhang (1995). The payoff of the European call version can be expressed as follows;

$$C(S_1, S_2, T; X_1, X_2) = \begin{cases} 0 & \text{if} \quad S_1 < X_1 \\ \max[S_2 - X_2, 0] & \text{if} \quad S_1 > X_1 \end{cases}, \tag{3.1}$$

and similarly for the European put we have

$$P(S_1, S_2, T; X_1, X_2) = \begin{cases} \max[X_2 - S_2, 0] & \text{if} \quad S_1 < X_1 \\ 0 & \text{if} \quad S_1 > X_1 \end{cases}. \tag{3.2}$$

Early exercise features are also possible here.

Exchange options

The exchange option is the right to exchange one asset for another, in some predetermined ratio. The payoff at expiry is given by

$$V(S_1, S_2, T) = \max[q_1 S_1 - q_2 S_2, 0], \tag{3.3}$$

where q_1 and q_2 are constants. Margrabe (1978) was the first to present a solution to this problem.

Compound exchange options

Carr (1988) suggests situations in which the option to exchange may only come alive after a previous option to exchange, such as the conversion of bond to stock, and then from this stock to another acquiring firms' stock. The pricing formula is derived by combining the work of Geske (1977) with that of Margrabe (1978).

Portfolio options

A portfolio option is an American (or European) style option and has a fixed strike price. The payoff at expiry for the call is given by

$$\max[(S_1 + S_2) - X, 0],$$

and for the put option it is

$$\max[X - (S_1 + S_2), 0].$$

Basket options

The basket options have their values linked to the weighted sum over a number of assets. They are very popular when hedging foreign exchange risk, since the value of a basket is less than buying up individual options; they can typically be on a large number of assets. Methods such as lattice or finite difference are not readily able to handle a large number of dimensions, so the vast majority of the literature on these options has focused on simulation. However, even simulation can struggle when the dimensions is increased considerably, so the average price is often treated as a stochastic process itself and priced using standard methods, with some error term to account for the multi-dimensionality.

3.1 Literature

The exchange option was one of the first multi-dimensional options to be studied. Although options involving two underlyings, such as the convertible bond with stochastic interest rates, had also been investigated, they do not have payoffs that depend on both of the underlying factors. In his paper, Margrabe (1978) develops the pricing equation for the European exchange option, as well as the American exchange option. The price is derived by setting up a hedged portfolio with zero return, reducing the order of the problem to a single transformed asset BSM PDE, where

the single transformed asset is the ratio of the two assets. From the multi-asset BSM PDE, similarity solutions can derive the same pricing formula, as shown by Wilmott (2001). Margrabe further shows that it is never optimal to exercise such an option early.

Stulz (1982) studies the valuation of min-max options on two assets when the strike prices on each of the assets are equal. This allows for some simplification and the construction of an analytical formula for European options of this form, involving the bivariate cumulative standard normal distribution. Johnson (1987) considers the formula when the number of assets increases, again taking the ratio between assets to be new transformed assets, so as to reduce the order of the problem; he obtains relatively simple formula for the n-asset case, involving a multi-variate cumulative standard normal distribution. Again however, the assumption of equal strike prices is important in delivering these results. The solution for a dual strike option is much harder to obtain. Boyle and Tse (1990) use an approach developed by Clark (1961) to generate the first four moments of the maximum (minimum) of n jointly normal random variables, to value calls or puts on the maximum or minimum of the n assets. The results are compared to those of Johnson (1987) and give a reasonable approximation. Broadie and Detemple (1997) investigate the early exercise region on the American version of the maximum option, as well as some other options such as the exchange option and capped exchange option. Villeneuve (1999) also presents results on the existence and shape of the exercise region for options on two assets, concentrating mainly on min/max options with a single strike price, and is able to describe the shape of the exercise region in both the limit as maturity tends to infinity (perpetual case), and in the limit as time tends to expiry. For the perpetual case, Villeneuve (1999) shows that for the maximum of two puts (which he describes as a put on the minimum of two assets), the optimal exercise boundary tends to the critical value for the single asset, as the value of the other asset(s) tend to infinity. In the limit as time tends to expiry, he presents results which complement those of Broadie and Detemple (1997).

There have been numerous attempts to extend the binomial or trinomial tree

to treat options including multiple assets. Boyle (1988) suggests an algorithm for a lattice with two underlying assets, which Boyle et al. (1989) extend to the n-asset case. In the algorithm suggested by Boyle (1988), the multi-factor model is an extension of the trinomial tree, which, for a two-factor model, results in five possible states at the next timestep, which leads to four equations in five unknowns, implying that there is extra parameter that must be chosen carefully. The model used by Boyle et al. (1989) circumvents this by abandoning the trinomial tree and allowing only four possible states at the next time step, and hence is more easily extended to the n-asset case. Kamrad and Ritchken (1991) improves the efficienccy of the multi-asset lattice method, while Ho et al. (1995) extend the model to include a time-varying variance-covariance structure.

An alternative method to pricing options on multiple assets was suggested by Stapleton and Subrahmanyam (1984) when continuous trading in the relevant assets is not possible. They generate the risk neutral valuation relationships under different risk aversion preferences. Ho et al. (1997) extend the Geske and Johnson (1984) approach to options on stocks with stochastic interest rates. The authors use a multivariate binomial approximation of the underlying stock and zero-coupon prices to price put options using up to three equally spaced exercise dates and Richardson extrapolation. The effect of stochastic rates was significant for long- term options with low asset volatility and high interest rates.

As noted earlier, the vast majority of the literature focuses on simulation to solve multi-asset problems. Broadie and Glasserman (1997) obtain American option values by Monte Carlo simulation, generating two algorithms, one with a high bias, which takes advantage of future knowledge to calculate the optimal exercise boundary, and one with a low bias, which does not, so both converge to the true price independently, which creates a confidence interval. The computation time is linear in the number of assets; however it is exponential in the number of exercise dates. Longstaff and Schwartz (2001) propose a Monte-Carlo method, that is both linear in state variables and linear in the number of exercise dates. The least-squares regression method, or LSM, is just one method to use regression to calculate the value of early exercise.

It is based on finding the value of the continuation function, or the expected future payoff, at each time step. Such regression methods have been shown to give a upper bound to the option value. Duck et al. (2005) exploit the manner in which the option value converges to the true value in the LSM method to improve efficiency through extrapolation. Andersen and Broadie (2004) use the work of Haugh and Kogan (2004) to create an upper bound, and regression type analysis for the lower bound to improve on the confidence intervals of Broadie and Glasserman (1997).

Another possible method is that of quadrature. Andricopoulos et al. (2007) have extended their previous work on the single-asset quadrature (Andricopoulos et al., 2003) to encompass multi-assets. Although the method suffers from the same exponential increases in storage and calculations as do lattice methods (both trees and finite-difference), the high speed of calculation enables reasonable results can be obtained for several underlying assets.

In this chapter we attempt to improve on existing finite-difference methods for pricing multi-asset options with a limited number of state variables (less than four). Many of the options of interest on the market contain just two or three assets, while many of the others can be reduced to a lower number of assets if the correlation between some of the assets is high. Here we choose to solve the problem by modifying the PSOR algorithm (see chapter 2), since this is easily extended to two or more assets. There is little literature in finance on the efficiency of the PSOR algorithm, however Reisinger and Wittum (2004) apply multigrid methods to the American option problem, and investigate the most efficient block solving and projection to use. They find that using blocks (see chapter 2 for a description of the block solver) of one dimension less than the problem, i.e. point on a one-dimensional problem, one-dimensional on a two-dimensional problem, or two-dimensional on a three-dimensional problem is the most efficient. Villeneuve and Zanette (2002) adapt the alternating direction implicit method (or ADI) to solve variational equalities, resulting in a computational scheme that is around five times faster than a corresponding PSOR scheme. The PSOR algorithm, with a fixed grid, will be able to price options with any number of payoffs, such as those described above. However, with some knowledge about the solution

topology, the algorithms can be modified for a specific problem for much improved efficiency, for at least as much speed up as that found by Villeneuve and Zanette for the ADI method.

In section 3.2, we introduce the multi-asset BSM framework, defining the PDE and boundary conditions for the maximum of two vanilla options. We then discuss numerical methods for European options in section 3.3, before moving on to American options in section 3.4. After some results are presented in section 3.5, we discuss some new and improved numerical techniques implemented by the author in section 3.6. Finally, a number of conclusions are drawn in section 3.7.

3.2 The Multi-Asset BSM Equation

Many of the options described above will have stock prices as underlyings. Consequently, it is not unreasonable to assume that all of the underlyings follow a log-normal random walk. If we have two assets, each with a constant drift parameter μ_i, and a constant volatility σ_i $(i = 1, 2)$, we can express their distributions as

$$\frac{dS_1}{S_1} = \mu_1 \, dt + \sigma_1 \, dW_1$$
$$\frac{dS_2}{S_2} = \mu_2 \, dt + \sigma_2 \, dW_2,$$

such that the two distributions are correlated as follows

$$E[dW_1 dW_2] \to \rho dt,$$

where E is the expectation.

Then we construct a portfolio, Π, long an option, and short a number Δ_1 of asset S_1, and short a number Δ_2 of asset S_2, as follows

$$\Pi = V(S_1, S_2, t) - \Delta_1 S_1 - \Delta_2 S_2. \tag{3.4}$$

Now, by using Itô's lemma, we can express a small change in V as $dt \to 0$

$$\begin{aligned} dV &= \left[\frac{\partial V}{\partial t} + \mu_1 S_1 . \frac{\partial V}{\partial S_1} + \mu_2 S_2 . \frac{\partial V}{\partial S_2} \right. \\ &\quad \left. + \frac{1}{2}\sigma_1^2 S_1^2 . \frac{\partial^2 V}{\partial S_1^2} + \frac{1}{2}\sigma_2^2 S_2^2 . \frac{\partial^2 V}{\partial S_2^2} + \rho\sigma_1\sigma_2 S_1 S_2 . \frac{\partial^2 V}{\partial S_1 \partial S_2}\right] . \, dt \\ &\quad + \sigma_1 S_1 dW_1 . \frac{\partial V}{\partial S_1} + \sigma_2 S_2 dW_2 . \frac{\partial V}{\partial S_2} . \end{aligned}$$

Hence, we can write a small change in Π, holding Δ_1 and Δ_2 constant over dt, as

$$\begin{aligned} d\Pi &= \left[\frac{\partial V}{\partial t} + \mu_1 S_1 \left\{\frac{\partial V}{\partial S_1} - \Delta_1\right\} + \mu_2 S_2 \left\{\frac{\partial V}{\partial S_2} - \Delta_2\right\} \right. \\ &\quad \left. + \frac{1}{2}\sigma_1^2 S_1^2 \frac{\partial^2 V}{\partial S_1^2} + \frac{1}{2}\sigma_2^2 S_2^2 . \frac{\partial^2 V}{\partial S_2^2} + \rho\sigma_1\sigma_2 S_1 S_2 \frac{\partial^2 V}{\partial S_1 \partial S_2}\right] . \, dt \\ &\quad + \sigma_1 S_1 dW_1 \left\{\frac{\partial V}{\partial S_1} - \Delta_1\right\} + \sigma_2 S_2 dW_2 \left\{\frac{\partial V}{\partial S_2} - \Delta_2\right\} . \end{aligned}$$

Then, following standard BSM methodology, if we take $\Delta_1 = \partial V/\partial S_1$ and $\Delta_2 = \partial V/\partial S_2$, then we can eliminate risk from our portfolio. Since this is a risk-free portfolio, it can only grow at a risk free rate, hence

$$d\Pi = r \ \Pi \ dt,$$

and we can construct the two-asset BSM PDE:

$$\begin{aligned} \frac{\partial V}{\partial t} + \frac{1}{2}\sigma_1^2 S_1^2 \frac{\partial^2 V}{\partial S_1^2} + \frac{1}{2}\sigma_2^2 S_2^2 \frac{\partial^2 V}{\partial S_2^2} + \rho\sigma_1\sigma_2 S_1 S_2 \frac{\partial^2 V}{\partial S_1 \partial S_2} \\ + r S_1 \frac{\partial V}{\partial S_1} + r S_2 \frac{\partial V}{\partial S_2} - rV = 0. \end{aligned} \tag{3.5}$$

If the two assets S_1 and S_2 pay a constant dividend rate d_1 and d_2 respectively then (3.5) becomes

$$\begin{aligned} \frac{\partial V}{\partial t} + \frac{1}{2}\sigma_1^2 S_1^2 \frac{\partial^2 V}{\partial S_1^2} + \frac{1}{2}\sigma_2^2 S_2^2 \frac{\partial^2 V}{\partial S_2^2} + \rho\sigma_1\sigma_2 S_1 S_2 \frac{\partial^2 V}{\partial S_1 \partial S_2} \\ + (r - d_1) S_1 \frac{\partial V}{\partial S_1} + (r - d_2) S_2 \frac{\partial V}{\partial S_2} - rV = 0. \end{aligned} \tag{3.6}$$

By similar arguments, we can construct a general multi-asset BSM PDE, for n-assets, S_i, each paying a constant dividend rate d_i:

$$\frac{\partial V}{\partial t} + \sum_i^n \sum_j^n \frac{1}{2}\rho_{i,j}\sigma_i\sigma_j S_i S_j \frac{\partial^2 V}{\partial S_i \partial S_j} + \sum_i^n (r - d_i) S_i \frac{\partial V}{\partial S_i} - rV = 0. \tag{3.7}$$

3.2.1 Maximum Options

Final conditions

The final condition for the maximum of two calls or puts is simple; at expiry $t = T$, we can choose to either sell or buy either of the assets, at their respective strike price. Then for the dual strike put at expiry we obtain

$$P(S_1, S_2, T) = \max[E_1 - S_1, E_2 - S_2, 0]. \tag{3.8}$$

Similarly, for a dual strike call, we have

$$C(S_1, S_2, T) = \max[S_1 - E_1, S_2 - E_2, 0]. \tag{3.9}$$

Boundary Conditions

The boundary conditions have to be imposed along lines rather than points (as in the one-dimensional case), although sometimes the problem can be reduced to a one-dimensional PDE on the boundary.

The conditions for the put are simple, so we will consider these first. Now, on $S_1 = S_2 = 0$, then the option holder will receive $\max[E_1, E_2]$ at expiry, and so for $t < T$

$$P(0, 0, t) = \max[E_1 e^{-r(T-t)}, E_2 e^{-r(T-t)}]. \tag{3.10}$$

On the $S_1 = 0$ boundary, we now have an option depending on the S_2 asset and t only. If we set $S_1 = 0$ into (3.6), then it will reduce the problem to the one-dimensional

BSM equation in S_2,

$$\frac{\partial P}{\partial t} + \frac{1}{2}\sigma_2^2 S_2^2 \frac{\partial^2 P}{\partial S_2^2} + (r - d_2) S_2 \frac{\partial P}{\partial S_2} - rP = 0, \tag{3.11}$$

with the following conditions at expiry

$$P(0, S_2, T) = \max[E_2 - S_2, E_1]. \tag{3.12}$$

Note here that if $E_1 \geq E_2$ then $P(0, S_2, T) = E_1$ and the boundary condition reduces to

$$P(0, S_2, t) = E_1 e^{-r(T-t)}. \tag{3.13}$$

We can follow a similar argument for the $S_2 = 0$ boundary.

We still require boundary conditions as each of the asset values become large. This is straightforward when *both* assets are large, as the probability of the option to exercise in either asset is small, so we have

$$P \to 0 \qquad \text{as} \quad \text{both} \qquad S_1, S_2 \to \infty. \tag{3.14}$$

However, what if $S_1 \to \infty$, but S_2 remains close to E_2? Then, the probability of ever exercising the option in S_1 is practically zero, so a move up or down in S_1 will not affect the price of P. A similar argument follows in S_2; from this we can set the boundary condition to be

$$\frac{\partial P(S_1, S_2, t)}{\partial S_1} \to 0 \qquad \text{as} \qquad S_1 \to \infty, \tag{3.15}$$

$$\frac{\partial P(S_1, S_2, t)}{\partial S_2} \to 0 \qquad \text{as} \qquad S_2 \to \infty. \tag{3.16}$$

Now we consider the corresponding conditions for a call. Almost identical to the arguments presented for the put, the conditions at $S_1 = 0$ and $S_2 = 0$ are the solutions

to the single-asset BSM equation. Therefore we arrive at the following conditions

$$C(S_1 = 0, S_2, t; E_1, E_2) = C^*(S_2, t; E_2, r, d_2, \sigma_2), \tag{3.17}$$

$$C(S_1, S_2 = 0, t; E_1, E_2) = C^*(S_1, t; E_1, r, d_1, \sigma_1), \tag{3.18}$$

where C^* is the solution to the single asset BSM equation for a call option with final conditions

$$C(S_1 = 0, S_2, t = T; E_1, E_2) = \max[0, S_2 - E_2], \tag{3.19}$$

$$C(S_1, S_2 = 0, t = T; E_1, E_2) = \max[0, S_1 - E_1]. \tag{3.20}$$

However, when we study the solution as S_1 and S_2 both become large, it is not as easy to determine conditions as it was in the case for a put. A Neumann condition in either direction will not be sufficient, since, in the region close to the line $S_1 - E_1 = S_2 - E_2$, there is a discontinuity at payoff on the line $S_1 - E_1 = S_2 - E_2$ as S_1 and S_2 tend to infinity, which persists for $t < T$ in these limits.

Nevertheless, if we investigate the solution as $S_1 \to \infty$ such that $S_1 >> S_2$, then we can argue that any change in the price of asset S_1, must lead to a corresponding change in the option value, directly proportional to the change in S_1, hence

$$\frac{\partial V}{\partial S_1} = 1. \tag{3.21}$$

If we seek a solution of the form $V(S_1, S_2, t) = S_1 - A(S_2, t)$, as $S_1 \to \infty$, substituting into the BSM PDE (3.6), we have the following,

$$\frac{\partial A}{\partial t} + \frac{1}{2}\sigma_2^2 S_2^2 . \frac{\partial^2 A}{\partial S_2^2} + (r - d_2) S_2 \frac{\partial A}{\partial S_2} - rA \;\; = \;\; 0, \tag{3.22}$$

which is just the one asset BSM equation. A similar argument can be used for $S_2 \to \infty$ such that $S_2 >> S_1$. This does not help us define a condition as $S_1 \to \infty$ and $S_2 \to \infty$ at the same rate, and we will attempt to reformulate this later in this section. Next we show how it is possible to formulate a boundary condition for the

simple single strike maximum of two calls.

Similarity Solution with $E_1 = E_2$

We need to employ a different method in order to obtain conditions for the call as $S_1, S_2 \to \infty$ (simultaneously, at the same rate). The complexity of the problem is reduced somewhat when we study the single strike option, with $E_1 = E_2 = E$. Now, in the limit $S_1, S_2 \to \infty$ the discontinuity around $S_1 = E$ and $S_2 = E$ becomes less important[1], so let us reduce the terminal condition to the simpler form,

$$V(S_1, S_2, T) = \max[S_1 - E, S_2 - E] \ .$$

The difference here is that the holder must exercise one of the two assets even if the payout is negative. This option is close to the exchange option priced by Margrabe (1978) and others. By using a similarity solution, note that we can solve exactly for the simplified option over the entire domain with out the need to set S_1 and S_2 to be large. This is not the case in the next subsection when we seek a solution where $E_1 \neq E_2$, a solution can only be found in the limit as the assets tend to infinity even for the equivalent simplified option.

In order to solve the BSM equation with this terminal condition, we set

$$\xi = \frac{S_2}{S_1}.$$

and $\hat{S} = S_1$, then write,

$$V(\hat{S}, \xi, t) = \hat{S} \ H(\xi, t) - E, \tag{3.23}$$

with $H(\xi, T) = \max(1, \xi)$. Wilmott (2001) outlines a similar method for exchange options, but this is slightly different because of the inclusion of the exercise price.

[1]When S_1 and S_2 are large, the holder of the maximum option will almost certainly receive a positive payoff, so the value of the option *not* to exercise will become insignificant.

For the first derivatives we obtain

$$\begin{aligned} \frac{\partial}{\partial S_1} &\rightarrow -\frac{\xi}{\hat{S}}\frac{\partial}{\partial \xi} + \frac{\partial}{\partial \hat{S}} \\ \frac{\partial}{\partial S_2} &\rightarrow \frac{1}{\hat{S}}\frac{\partial}{\partial \xi} \end{aligned} \tag{3.24}$$

and for the second derivatives we obtain

$$\begin{aligned} \frac{\partial^2}{\partial S_1^2} &\rightarrow \frac{\partial^2}{\partial \hat{S}^2} - \frac{2\xi}{\hat{S}}\frac{\partial^2}{\partial \hat{S}\partial \xi} + \frac{2\xi}{\hat{S}^2}\frac{\partial}{\partial \xi} + \frac{\xi^2}{\hat{S}^2}\frac{\partial^2}{\partial \xi^2}, \\ \frac{\partial^2}{\partial S_1 \partial S_2} &\rightarrow \frac{1}{\hat{S}}\frac{\partial^2}{\partial \xi \partial \hat{S}} - \frac{1}{\hat{S}^2}\frac{\partial}{\partial \xi} - \frac{\xi}{\hat{S}^2}\frac{\partial^2}{\partial \xi^2}, \\ \frac{\partial^2}{\partial \hat{S}^2} &\rightarrow \frac{1}{\hat{S}^2}\frac{\partial^2}{\partial \xi^2}. \end{aligned} \tag{3.25}$$

Substituting the above into the BSM equation, we can express $\mathcal{L}_{2-BSM}$, the BSM operator on two underlying assets, as

$$\begin{aligned} \mathcal{L}_{2-BS} &= \frac{\partial}{\partial t} + \frac{1}{2}\sigma_1^2\hat{S}^2\left\{\frac{\partial^2}{\partial \hat{S}^2} - \frac{2\xi}{\hat{S}}\frac{\partial^2}{\partial \hat{S}\partial \xi} + \frac{2\xi}{\hat{S}^2}\frac{\partial}{\partial \xi} + \frac{\xi^2}{\hat{S}^2}\frac{\partial^2}{\partial \xi^2}\right\} \\ &\quad + \frac{1}{2}\sigma_2^2 S_2^2\left\{\frac{1}{\hat{S}^2}\frac{\partial^2}{\partial \xi^2}\right\} + \rho\sigma_1\sigma_2\hat{S}S_2\left\{\frac{1}{\hat{S}}\frac{\partial^2}{\partial \xi \partial \hat{S}} - \frac{1}{\hat{S}^2}\frac{\partial}{\partial \xi} - \frac{\xi}{\hat{S}^2}\frac{\partial^2}{\partial \xi^2}\right\} \\ &\quad + (r-d_1)\hat{S}\left\{-\frac{\xi}{\hat{S}}\frac{\partial}{\partial \xi} + \frac{\partial}{\partial \hat{S}}\right\} + (r-d_2)S_2\left\{\frac{1}{\hat{S}}\frac{\partial}{\partial \xi}\right\} - r. \end{aligned} \tag{3.26}$$

Therefore we must calculate $\mathcal{L}_{2-BS}\{V\} = 0$, from which we obtain the following equation for H,

$$\begin{aligned} &\frac{\partial H}{\partial t} + \frac{1}{2}\sigma_1^2\left\{\xi^2\frac{\partial^2 H}{\partial \xi^2}\right\} + \frac{1}{2}\sigma_2^2\xi^2\left\{\frac{\partial^2 H}{\partial \xi^2}\right\} + \rho\sigma_1\sigma_2\xi\left\{-\xi\frac{\partial^2 H}{\partial \xi^2}\right\} \\ &\quad + (r-d_1)\left\{-\xi\frac{\partial H}{\partial \xi} + H\right\} + (r-d_2)\xi\left\{\frac{\partial H}{\partial \xi}\right\} - r(H - \frac{E}{\hat{S}}) = 0. \end{aligned}$$

On rearrangement this gives

$$\frac{\partial H}{\partial t} + [\frac{1}{2}\sigma_1^2 - \rho\sigma_1\sigma_2 + \frac{1}{2}\sigma_2^2]\xi^2\frac{\partial^2 H}{\partial \xi^2} + [d_1 - d_2]\xi\frac{\partial H}{\partial \xi} - d_1 H = -r\frac{E}{\hat{S}}. \tag{3.27}$$

We notice that on the left hand side, the equation in H is in fact just the BSM

equation with ξ as the underlying asset, and $-rE/\hat{S}$ forming a constant coupon-like term on the right-hand-side. As stated earlier, apart from justification to form the final conditions, we have made no assumptions that S_1 and S_2 are large. Then we can express (3.27) as

$$\frac{\partial H}{\partial t} + \frac{1}{2}\bar{\sigma}^2\xi^2\frac{\partial^2 H}{\partial \xi^2} + (\bar{r} - \bar{d})\xi\frac{\partial H}{\partial \xi} - \bar{r}H \quad = \quad K(\hat{S}).$$

We have a function of ξ and t on the left hand side, and $\hat{S}$ on the right hand side, hence a separable solution is appropriate. We can set each side of the equation equal to a constant and then solve the resulting two equations independently, thus

$$\mathcal{L}_{BS}\left\{H(\xi, t; \bar{\sigma}, \bar{r}, \bar{d})\right\} = c \tag{3.28}$$

$$K(\hat{S}) = c \ , \tag{3.29}$$

with $\bar{\sigma} = \sqrt{\sigma_1^2 - 2\rho\sigma_1\sigma_2 + \sigma_2^2}$, $\bar{r} = d_1$, $\bar{d} = d_2$ and c the separation constant. Then for a particular value of S_1, we can find c, and then we need only solve a simple BSM equation to find the value at the boundary. We can easily interchange S_1 for S_2 to obtain the same equation for a particular value of S_2, with $\xi = S_1/S_2$.

General boundary condition with $E_1 \neq E_2$

In the previous section the boundary condition for the single strike call option is found relatively easily by a similarity solution, however for the dual strike option the terms do not drop out so easily, and we must take an asymptotic approximation in order to accurately find the boundary condition. Again, set the final condition on the option be

$$V(S_1, S_2, T) = \max[S_1 - E_1, S_2 - E_2] \ ,$$

as we look for a solution for large S_1 and S_2. Then the appropriate substitutions will be

$$\xi = \frac{S_2 - E_2}{S_1 - E_1} \quad , \qquad \hat{S} = S_1 - E_1 \quad .$$

and the option value can be written in the transformed coordinates as

$$V(\hat{S},\xi,t) = \hat{S}\ H(\xi,t) \quad ,$$

where $H(\xi,T) = \max(1,\xi)$. Then under this transformation the derivatives will remain the same as that calculated in the previous section (3.24) and (3.25), so after substitution into the BSM operator, we obtain

$$\begin{aligned}\mathcal{L}_{2-BS} &= \frac{\partial}{\partial t} + \frac{1}{2}\sigma_1^2(\hat{S}+E_1)^2\left\{\frac{\partial^2}{\partial\hat{S}^2} - \frac{2\xi}{\hat{S}}\frac{\partial^2}{\partial\hat{S}\partial\xi} + \frac{2\xi}{\hat{S}^2}\frac{\partial}{\partial\xi} + \frac{\xi^2}{\hat{S}^2}\frac{\partial^2}{\partial\xi^2}\right\} \\ &\quad + \frac{1}{2}\sigma_2^2 S_2^2\left\{\frac{1}{\hat{S}^2}\frac{\partial^2}{\partial\xi^2}\right\} + \rho\sigma_1\sigma_2(\hat{S}+E_1)S_2\left\{\frac{1}{\hat{S}}\frac{\partial^2}{\partial\xi\partial\hat{S}} - \frac{1}{\hat{S}^2}\frac{\partial}{\partial\xi} - \frac{\xi}{\hat{S}^2}\frac{\partial^2}{\partial\xi^2}\right\} \\ &\quad + (r-d_1)(\hat{S}+E_1)\left\{-\frac{\xi}{\hat{S}}\frac{\partial}{\partial\xi} + \frac{\partial}{\partial\hat{S}}\right\} + (r-d_2)S_2\left\{\frac{1}{\hat{S}}\frac{\partial}{\partial\xi}\right\} - r. \quad (3.30)\end{aligned}$$

Next we apply the transformed BSM operator to $V(\hat{S},\xi,t)$ to obtain

$$\begin{aligned}&\frac{\partial H}{\partial t} + \frac{1}{2}\sigma_1^2\left\{1 + \frac{2E_1}{\hat{S}} + \frac{E_1^2}{\hat{S}^2}\right\}\xi^2\frac{\partial^2 H}{\partial\xi^2} + \frac{1}{2}\sigma_2^2\left\{\xi^2 + \frac{2E_2}{\hat{S}} - \frac{E_2^2}{\hat{S}^2}\right\}\frac{\partial^2 H}{\partial\xi^2} \\ &\qquad - \rho\sigma_1\sigma_2\xi\left\{\xi + \xi\frac{E_1}{\hat{S}} + \frac{E_2}{\hat{S}} + \frac{E_1E_2}{\hat{S}}\right\}\frac{\partial^2 H}{\partial\xi^2} \\ &+ (r-d_1)\left\{1+\frac{E_1}{\hat{S}}\right\}\left\{-\xi\frac{\partial H}{\partial\xi} + H\right\} + (r-d_2)\left\{\xi + \frac{E_2}{\hat{S}}\right\}\frac{\partial H}{\partial\xi} - rH = 0.\end{aligned}$$

It is clear here that the solution is not separable, and we cannot solve the reduced problem. Instead, let $\hat{S}\to\infty$, and so to first order in $\hat{S}$ we have

$$\frac{\partial H}{\partial t} + \left[\frac{1}{2}\sigma_1^2 - \rho\sigma_1\sigma_2 + \frac{1}{2}\sigma_2^2\right]\xi^2\frac{\partial^2 H}{\partial\xi^2} + (d_1-d_2)\xi\frac{\partial H}{\partial\xi} + (r-d_2)\xi = 0 \qquad (3.31)$$

3.3 Numerical methods for the European Option

After discretisation we have a choice between using a direct solver or SOR solvers. In one dimension the direct solver is always better than iterative methods, with inversion of the matrix very simple using LU decomposition or Gaussian elimination.

In two or more dimensions, the direct solver is advantageous when the rate of convergence for the iterative solvers is sufficiently slow. However, the direct solver is now much more difficult to code (it involves inverting a large matrix), although the sparseness of the matrix may be exploited in some way, such as using a Big-Banded Solver (BBS) or other sparse solvers from the NAG (or other) libraries (the sparse solvers do involve iteration, so strictly should be classed as iterative solvers). There are many situations, however, when the rate of convergence is very slow for the iterative solvers, such as if the volatility is high and the timesteps are large. Using the Crank-Nicolson scheme allows the use of large timesteps due to the unconditional stability imposed by the scheme.

The SOR method has long been known to perform better in higher dimensions when the solution space is partitioned into blocks, which can be solved directly. These blocks are typically a set of nodes encompassing a single line, plane or cube, depending on the dimensionality of the problem. The errors can be bounded over the solution space much more efficiently than when point SOR is used. For a two-dimensional problem, we compare the direct solver with line or point SOR iteration in table 3.1.

Let us consider the two-asset case first. According to the Crank-Nicolson scheme (Smith, 1985), the discretised equations may be written as

$$\begin{aligned}\alpha_{i,j}u^{k+1}_{i-1,j} + (1/\Delta\tau + \beta_{i,j})u^{k+1}_{i,j} + \gamma_{i,j}u^{k+1}_{i+1,j} + \delta_{i,j}u^{k+1}_{i,j-1} + \epsilon_{i,j}u^{k+1}_{i,j+1} & \\ +\mu_{i,j}(u^{k+1}_{i-1,j-1} - u^{k+1}_{i+1,j-1} - u^{k+1}_{i-1,j+1} + u^{k+1}_{i+1,j+1}) &= Z^k_{i,j}, \quad (3.32)\end{aligned}$$

where $u^k_{i,j} = V(i\Delta S_1, j\Delta S_2, k\Delta\tau)$. Then in matrix form, this set of equations can be expressed as

$$\mathbf{A}\boldsymbol{u}^{k+1} = \boldsymbol{b}^k, \quad (3.33)$$

where $\boldsymbol{u}^{k+1}$ is the solution vector. The matrix $\mathbf{A}$ is sparse, typically only containing less than 15 nonzero diagonal rows, depending on the boundary conditions. The diagonal rows are grouped into three bands, separated by either n or m zero diagonal rows, where n and m are the number of nodes in each direction. The way in which

we express the solution vector $\boldsymbol{u}^{k+1}$ determines whether it is n or m zero rows. If the number of nodes required in one direction is significantly less than the other, such as when the volatility is small in one direction, then the distance between the three bands can be kept relatively small, effectively not unlike one large band. This is exploited by the BBS which is a direct solver for matrices with large bands; however, if the band is too large, the solver is slow and cumbersome. There are routines available that exploit diagonal sparse matrices, but it is unlikely that they will perform better than a block SOR scheme tailored to the problem.

The point SOR scheme is easy to generate and is just

$$u_n^{k+1,q+1} = \frac{1}{A_{nn}} \left(b_n^k - \sum_{m<n} A_{nm} u_m^{k+1,q+1} - \sum_{m>n} A_{nm} u_m^{k+1,q} \right), \tag{3.34}$$

where the array $u_{i,j}$ is expressed as the one dimensional vector u_n, and n and m are now counters. Alternatively in terms of the original array

$$\begin{aligned} u_{i,j}^{k+1,q+1} \;=\; & \frac{1}{1/\Delta t + \beta_{i,j}} \Big(Z_{i,j}^k - \alpha_{i,j} u_{i-1,j}^{k+1,q+1} - \gamma_{i,j} u_{i+1,j}^{k+1,q} - \delta_{i,j} u_{i,j-1}^{k+1,q+1} - \epsilon_{i,j} u_{i,j+1}^{k+1,q} \\ & - \mu_{i,j} \big(u_{i-1,j-1}^{k+1,q+1} - u_{i+1,j-1}^{k+1,q+1} - u_{i-1,j+1}^{k+1,q} + u_{i+1,j+1}^{k+1,q} \big) \Big) \end{aligned} \tag{3.35}$$

Then the block SOR algorithm is also easy to generate and is

$$\boldsymbol{u}_n^{k+1,q+1} = \mathbf{A}_{nn}^{-1} \left(\boldsymbol{b}_n^k - \sum_{m<n} \mathbf{A}_{nm} \boldsymbol{u}_m^{k+1,q+1} - \sum_{m>n} \mathbf{A}_{nm} \boldsymbol{u}_m^{k+1,q} \right) \tag{3.36}$$

where the vectors $\boldsymbol{u}$, $\boldsymbol{b}$ and the matrix $\mathbf{A}$ have been partitioned into appropriate subsets $\boldsymbol{u}_n$, $\boldsymbol{b_n}$, and $\mathbf{A}_{nm}$ (n and m are counters). Now consider the line SOR on a two asset problem; we must solve

$$\alpha_{i,j} u_{i-1,j}^{k+1,q+1} + (1/\Delta\tau + \beta_{i,j}) u_{i,j}^{k+1,q+1} + \gamma_{i,j} u_{i+1,j}^{k+1,q+1} = b_{i,j} \quad , \tag{3.37}$$

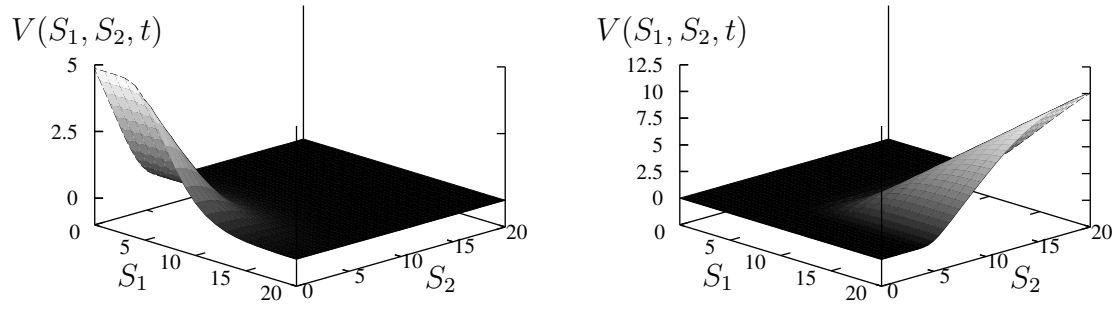

(a) Put (b) Call

Figure 3.1
The minimum of two vanilla options.

over $0 \leq i \leq N$ where

$$\begin{aligned} b_{i,j} &= Z^k_{i,j} - \delta_{i,j} u^{k+1,q+1}_{i,j-1} - \epsilon_{i,j} u^{k+1,q}_{i,j+1} \\ &\quad -\mu_{i,j}(u^{k+1,q+1}_{i-1,j-1} - u^{k+1,q+1}_{i+1,j-1} - u^{k+1,q}_{i-1,j+1} + u^{k+1,q}_{i+1,j+1}). \end{aligned} \tag{3.38}$$

The value of j is held constant until all nodes in i have been found, using a direct solver such as LU decomposition. Then we can move through all values of j to solve over the entire space. The constant value can be interchanged in i and j so that the errors may be bounded.

3.3.1 Results

Figures 3.1-3.4 show the values of various different European options on two assets. All four figures correspond to $E_1 = 10$, $E_2 = 5$, $d_1 = d_2 = \rho = 0$, $\sigma_1 = \sigma_2 = 0.2$, and $T = 0.5$. Later, we will consider the solution to American options, but these graphs, along with the schematics of the terminal exercise regions, can give an indication of the positioning of the free boundary for the corresponding American option. This may be exploited later in order to improve the PSOR algorithm. If we plot the payoff function along with the European option value, we can find the regions in which the European option is less than the exercise value. We may then assume that the free boundary will be approximately of the same topology as the intersection of

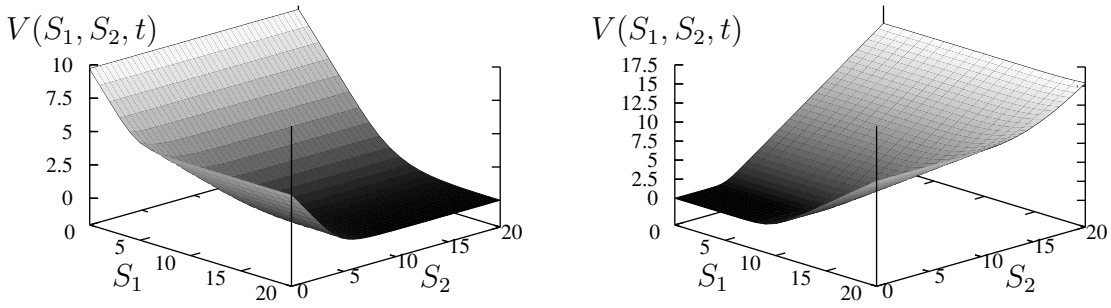

(a) Put (b) Call

Figure 3.2
The maximum of two vanilla options

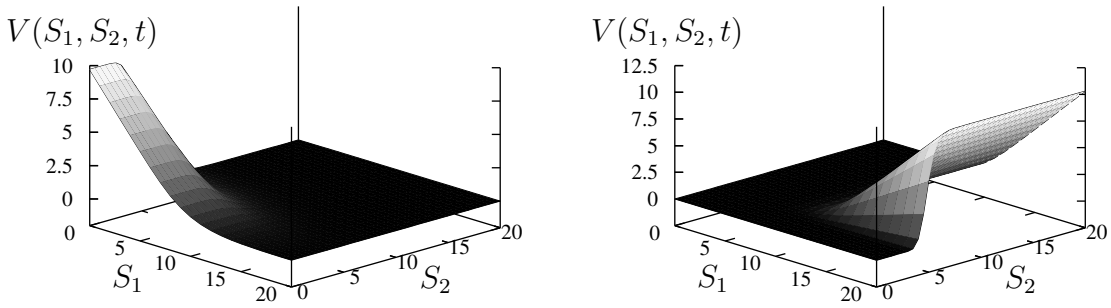

(a) Put (b) Call

Figure 3.3
The 2-asset correlation option.

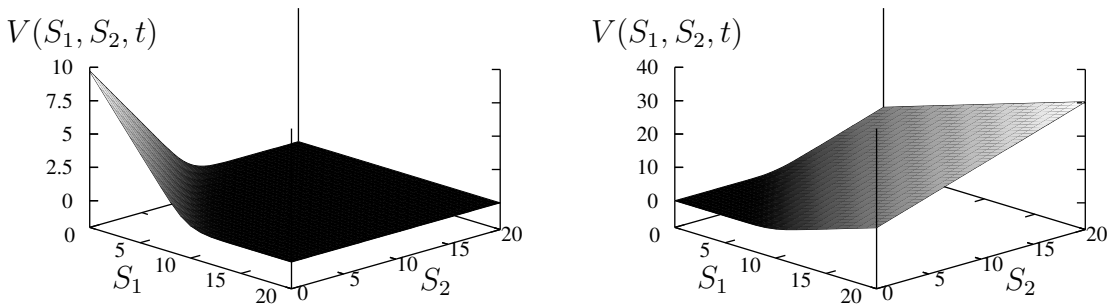

(a) Put (b) Call

Figure 3.4
The portfolio option.

the two graphs. For instance, consider the portfolio put option in figure 3.4(a), the intersection would be a single line approximately of the form $S_1 = c - S_2$ for some constant c. In section 3.5 we may determine whether this assertion is correct. The point to note is that inspecting the European solution can give us information about the resulting American solution.

In this section we also present table 3.1, that compares the standard point SOR method with the block method and the direct solver. The RMS errors are calculated over nearly 4000 European dual strike put options, and calculations are carried out on an Intel(R) Xeon(TM) CPU 3.40GHz with 8Gb of RAM. Standard ifort compile is used with the *-fast* flag on the SOR and block solver, and *-O3* on the direct solver. Solving block-wise is far more efficient than solving either point-wise or directly. It must be noted however that the SOR and block solver times are sensitive to the ratio $-2r/\sigma^2$ whereas the direct solver is not, so although on average the block solver is better for specific cases when σ is large the direct solver may be faster. The direct method produces similar speeds to those those of the point SOR solver. Both the point SOR scheme and the block solver (with increased programming complexity) may be adapted in the curtailed range fashion detailed later in this chapter. However, the increase in programming difficulty compared to that of the scheme described here will not be offset by the increased efficiency of the scheme, mainly due to the fast convergence of the block scheme without the need to project, as is required for the American options.

3.4 American Options

For a two-asset American option, we can choose to exercise an option on either of the assets. So not only do we have the option to exercise early, but also the option to choose either asset. Even for the simple single-strike call or put option, the topology of the problem is complex, with two exercise regions to contend with. The free boundary now forms a line between the exercise/continuation regions in $[S_1, S_2]$ space, and a surface through time. The difficulty in accurately positioning the free

Table 3.1
Relative RMS errors for European dual strike put options

n	SOR (time)	BB (time)	Block SOR (time)
50	0.0221087	0.0220935	0.0221087
	(0.06)	(0.07)	(0.05)
100	0.0029058	0.0029065	0.0029058
	(0.73)	(1.12)	(0.39)
150	0.0007834	0.0007843	0.0007834
	(3.13)	(5.41)	(1.33)
200	0.0002200	0.0002207	0.0002200
	(11.27)	(16.60)	(3.63)
250	0.0000893	0.0000895	0.0000892
	(29.43)	(39.59)	(7.70)
300	0.0000354	0.0000356	0.0000354
	(59.97)	(79.82)	(13.83)
350	0.0000195	0.0000196	0.0000195
	(106.74)	(145.00)	(23.04)
400	0.0000116	0.0000117	0.0000116
	(179.42)	(245.84)	(37.02)
450	0.0000074	0.0000074	0.0000074
	(284.82)	(390.40)	(55.27)
500	0.0000039	0.0000039	0.0000039
	(430.76)	(592.11)	(83.14)

The relative errors for each of the three methods described in this chapter. The relative RMS errors are calculated against exact values of close to 4000 different put options with $T = 0.5/1$, $S_1 \in [0.9E_1, 1.1E_1]$, $S_2 \in [0.9E_2, 1.1E_2]$, $E_2 = E_1/0.5E_1$, $\sigma_1 = 0.4/0.2$, $\sigma_2 = 0.2/0.1$ and $\rho = 0/0.5$. For all options $r = 0.06$ and $E_1 = 10$. The exact values are calculated by allowing $n \to \infty$ until successive solutions are sufficiently close to one another (1.E-10). We use n nodes in both spacial directions, with $S_1^{max} = 5E_1$ and $S_2^{max} = 5E_2$, and results are extrapolated once using n and $n/2$, and the number of timesteps is $n/5$ and $n/10$ respectively.

boundary is greatly increased each time we add another dimension and, therefore, so is difficulty in computing the solution. In this section we investigate some variants of the multi-asset American option, concentrating on the dual-strike American put for the most part, which, although one of the simplest to express, is also the one most difficult to compute.

3.4.1 Multi-Asset American Option

The holder of the dual strike maximum American put can choose to exercise either asset, whenever it is optimal to do so. As a consequence, the value of the option is greater than both $E_1 - S_1$ and $E_2 - S_2$, which gives

$$V(S_1, S_2, t) \geq \max[E_1 - S_1, E_2 - S_2]. \tag{3.39}$$

Let $G(S_1, S_2) = \max[E_1 - S_1, E_2 - S_2]$ denote the constraint applied to the system. The value of the option must also satisfy the BSM equation (in the region in which it has not been exercised), so (3.7) is valid in this region, i.e.

$$\frac{\partial V}{\partial t} + \frac{1}{2}\sigma_1^2 S_1^2 . \frac{\partial^2 V}{\partial S_1^2} + \frac{1}{2}\sigma_2^2 S_2^2 . \frac{\partial^2 V}{\partial S_2^2} + \rho\sigma_1\sigma_2 S_1 S_2 . \frac{\partial^2 V}{\partial S_1 \partial S_2} + rS_1\frac{\partial V}{\partial S_1} + rS_2\frac{\partial V}{\partial S_2} - rV = 0.$$

It can be shown that for the dual-strike American put, there are two free boundary lines, one in the region where $S_1 - E_1 < S_2 - E_2$ and the other in the region $S_1 - E_1 > S_2 - E_2$; we show a schematic of the regions in figure 3.5. It is logical that we define the free boundary, S_f^A, in region A to be a function of S_1, and similarly that the free boundary, S_f^B, in region B to be a function of S_2. Then we can write

$$V\big(S_1, S_f^A(S_1, t), t\big) = E_2 - S_2, \tag{3.40}$$

$$V\big(S_f^B(S_2, t), S_2, t\big) = E_1 - S_1. \tag{3.41}$$

Now, for the single asset case, optimal exercise and arbitrage arguments lead to

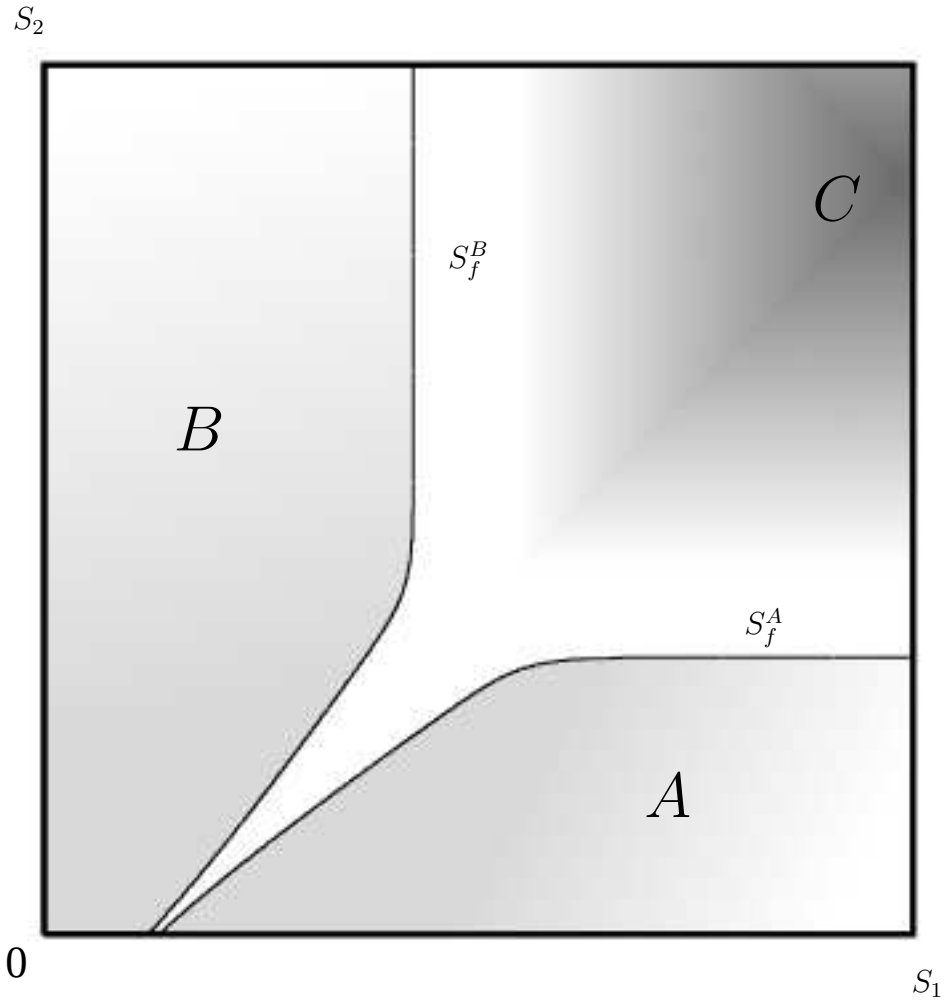

Figure 3.5
The early exercise regions for the maximum of two puts option.

the smooth pasting condition for the American put at the optimal exercise boundary. With similar arguments, the maximum American put option also has a smooth pasting condition, although we must enforce the continuity of Δ in both of the assets. This gives us four more constraints on the free boundary, namely

$$\begin{aligned}
\frac{\partial V}{\partial S_1}\big(S_1, S_f^A(S_1,t), t\big) &= 0, \\
\frac{\partial V}{\partial S_2}\big(S_1, S_f^A(S_1,t), t\big) &= -1, \\
\frac{\partial V}{\partial S_1}\big(S_f^B(S_2,t), S_2, t\big) &= -1, \\
\frac{\partial V}{\partial S_2}\big(S_f^B(S_2,t), S_2, t\big) &= 0.
\end{aligned} \tag{3.42}$$

These four constraints equate to two tangential derivative conditions. We can see here that adding one more dimension has made it impractical to use a boundary-fitted coordinate system such as that used to solve for the one-dimensional case in chapter 2. It is possible to specify a mapping from the region in (S_1, S_2) space to the unit square $(\hat{S}_1, \hat{S}_2)$ using similar transformations to those used for the single asset American put or call, although to implement such a scheme would rely on the topology of the problem to be of appropriate form. Even then, the increased complexity of the problem may reduce any possible benefits.

If we solve for a multi-strike option, with more than two assets, the complexity of even the free boundary formulation will become tedious. It is sufficient to say that the smooth pasting condition ensures that at each point on the free boundary, all partial derivatives in S_i must be equal to the corresponding derivative of the constraint G at that point. This leads to the conclusion that the most appropriate (finite-difference) methods to solve for an American option in multi-dimensions are variational techniques, of which the PSOR scheme is one implementation. The PSOR scheme applied to multi-asset option is described in the next section.

3.4.2 PSOR on Multi-Asset Options

The PSOR method is easily extended to multi-asset options and because the method is a fixed grid method, a solution can be obtained without detailed prior knowledge of the number of distinct regions in solution space in which it is optimal to exercise or not to exercise. We study the two asset problem in detail, which can be generalised to the multi-asset case.

The problem is discretised in the usual manner

$$V(i \cdot \Delta S_1, j \cdot \Delta S_2, k \cdot \Delta t) = u_{i,j}^k \quad ,$$
$$G(i \cdot \Delta S_1, j \cdot \Delta S_2, k \cdot \Delta t) = g_{i,j}^k \quad ,$$

then we refer to (3.32) for the discrete approximation to the BSM PDE. Now let us express (3.32) in matrix form. Let $\boldsymbol{u}^k$ and $\boldsymbol{g}^k$ denote the vectors

$$\boldsymbol{u}^k = \begin{pmatrix} x_{0,0}^k \\ \vdots \\ x_{n,0}^k \\ x_{0,1}^k \\ \vdots \\ x_{n,m}^k \end{pmatrix}, \qquad \boldsymbol{g}^k = \begin{pmatrix} g_{0,0}^k \\ \vdots \\ g_{n,0}^k \\ g_{0,1}^k \\ \vdots \\ g_{n,m}^k \end{pmatrix}.$$

We can then construct a matrix $\mathbf{A}$ and a vector $\boldsymbol{b^k}$ such that we can rewrite (3.32) as

$$\mathbf{A}\boldsymbol{u}^{k+1} = \boldsymbol{b}^k.$$

We can then express the problem in linear complementary form:

$$\left(\mathbf{A}\boldsymbol{u}^{k+1} - \boldsymbol{b}^k\right) \cdot \left(\boldsymbol{u}^{k+1} - \boldsymbol{g}^{k+1}\right) = 0. \tag{3.43}$$

Now (3.43) is identical to (2.79), so we can adapt the SOR algorithm to obtain

the projected SOR solver:

$$y_{i,j}^{k+1,q+1} = \frac{1}{1/\Delta t + \beta_{i,j}}\Bigg(Z_{i,j}^{k} - \alpha_{i,j} u_{i-1,j}^{k+1,q+1} - \gamma_{i,j} u_{i+1,j}^{k+1,q} - \delta_{i,j} u_{i,j-1}^{k+1,q+1} - \epsilon_{i,j} u_{i,j+1}^{k+1,q} - \mu_{i,j}\big(u_{i-1,j-1}^{k+1,q+1} - u_{i+1,j-1}^{k+1,q+1} - u_{i-1,j+1}^{k+1,q} + u_{i+1,j+1}^{k+1,q}\big)\Bigg), \tag{3.44}$$

$$u_{i,j}^{k+1,q+1} = \max\left[u_{i,j}^{k+1,q} + \omega(y_{i,j}^{k+1,q+1} - u_{i,j}^{k+1,q}), g_{i,j}^{k+1}\right]. \tag{3.45}$$

As we iterate over these two equations we will have a consistent solution that satisfies either $\mathbf{A}\boldsymbol{u}^{k+1} = \boldsymbol{b}^{k}$ or $\boldsymbol{u}^{k+1} = \boldsymbol{g}^{k+1}$.

In the single-asset case (chapter 2), the boundary conditions were explicitly defined. In the two-asset case however, we must solve a PDE along the boundary lines using the PSOR scheme in order to satisfy the appropriate constraints. We use the boundary conditions defined by equations (3.11), (3.15), and (3.16) to form $\mathbf{A}\boldsymbol{u}^{k+1} = \boldsymbol{b}^{k}$ for a put, and (3.17), (3.18), (3.28) and (3.29) for the call.

3.5 Results

In the following section we discuss solutions to the American problem, and the specific properties which allow us to enhance the numerical techniques used to solve the problem. The results are represented in both graphical and tabular form.

3.5.1 The Early Exercise Region

The early exercise regions for various different options are shown in figures 3.6-3.8. The free boundary is found as a result of the algorithm used to solve the option (cf section 3.6.3) defined as the outer-most node at which the option is exercised. Figure 3.6 shows the most common class of put to be investigated, the maximum of two options on a single strike price, or a put/call on the minimum of two assets. The shape and magnitude of the results agree with those detailed by Broadie and Detemple (1997). We note the terminal condition of the free boundary, either by inspection, or by asymptotic analysis. For the put (figure 3.6(a)), the condition is

given by;

$$S_f^A(S_1, T) = \max\left[0, \min\left[S_1, E, \frac{r\ E}{d_2}\right]\right] \tag{3.46}$$

$$S_f^B(S_2, T) = \max\left[0, \min\left[S_2, E, \frac{r\ E}{d_1}\right]\right], \tag{3.47}$$

and for the call (figure 3.6(b)) it is

$$S_f^B(S_1, T) = \max\left[S_1, E, \frac{r\ E}{d_2}\right] \tag{3.48}$$

$$S_f^A(S_2, T) = \max\left[S_2, E, \frac{r\ E}{d_1}\right]. \tag{3.49}$$

Both of these conditions are fairly straightforward to derive, by discarding the second order derivatives and looking at the first order solutions. Here we have defined the line $S_1 = S_2$ to be a free boundary line at expiry, when clearly the option should be exercised on this line. However, we define the free boundary at expiry to be the value in the limit as time tends to expiry. The argument as to why the holder never exercises when $S_1 = S_2$ until expiry is simple. Suppose that $S_1 = S_2$, and the holder exercises asset S_2, and then there is movement up or down in S_1, the holder would be better off to have waited to see if it was beneficial to exercise asset S_1. Then it is the option to choose which asset to exercise which causes the limit at expiry of the free boundary to be $S_1 = S_2$.

The early exercise region is shown over a range of times, and we can see how the region develops. For the maximum put, we can see that when S_1 is large, and the likelihood of the option being exercised in the S_1 asset is therefore small, the free boundary S_f^A behaves as that for the single asset case. In figure 3.6(a), the chosen values of σ_1 and σ_2, 0.4 and 0.2 respectively, are significantly different, as $S_f^A(S_1 = 20) \approx 8.25$ and $S_f^B(S_2 = 20) \approx 6.4$ shows. However, for $S_1 < 10$ and $S_2 < 10$ the free boundary appears to be approximately symmetric around the line $S_1 = S_2$, suggesting that it is the combination of the two volatilities and their correlation that drives the pricing in this region. The rate at which the free boundary moves in this region ($S_1 \approx S_2$) with time is also far faster than the boundary moves for large S_1 or

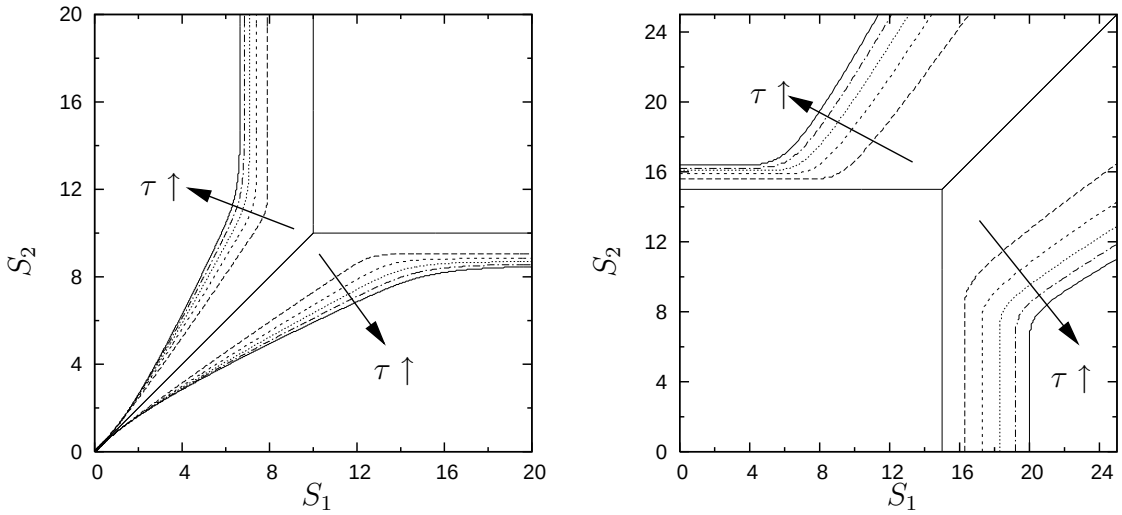

(a) Put (b) Call

Figure 3.6
American single strike option
An illustration of the early exercise region for single strike option, with time t ranging from 0 (solid) to 0.5 (solid) with increments of 0.1. The free boundary moves outward from the angular lines as time to expiry increases. Parameters are $E = 10$, $\sigma_1 = 0.4$, $\sigma_2 = 0.2$, $\rho = -0.5$, $r = 0.06$ (a) $d_1 = d_2 = 0$ (b) $d_1 = d_2 = 0.04$.

S_2 when the option price is effectively driven by a single asset. This again appears to confirm that it is the combination of volatilities driving the option price around $S_1 = S_2$.

For figure 3.6(b), parameters are the same as that for the put in figure 3.6(a), except that we have now included dividends $d_1 = d_2 = 0.04$ (so that the solution is not just trivially the European). In the limit as S_1 tends to infinity, we know that the solution for the single strike option has the similarity solution defined by equations (3.28) and (3.29), and so the solution is essentially one dimensional for large S_1, S_2, and is characterised by the parameters $\bar{\sigma}$, $\bar{d}$ and $\bar{r}$ as given in equations (3.28) and (3.29). Since we have chosen d_1 and d_2 to be equal, the solution is symmetric around $S_1 = S_2$ which may explain why the similar situation arises for the put.

The portfolio option has the most simple free boundary of the three options shown here. In figure 3.7 the portfolio option free boundary is shown. The free boundary is just a single line, and in the limit as time tends to expiry its form can be found by studying the solution without the second order terms. Expressing the free boundary

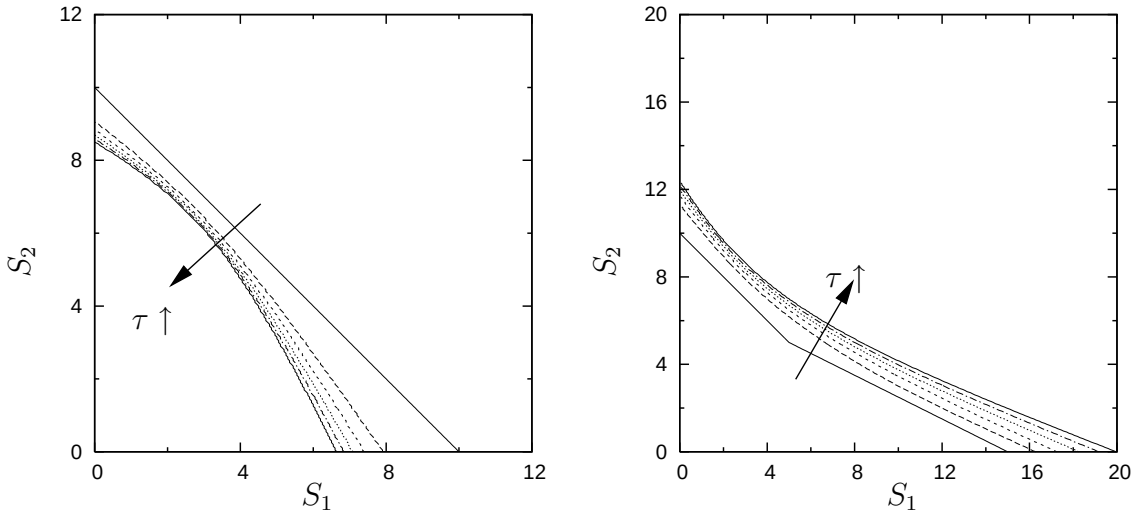

(a) Put (b) Call

Figure 3.7
American portfolio option
An illustration of the early exercise region for a portfolio option, with time t ranging from 0 (solid) to 0.5 (solid) with increments of 0.1. The free boundary moves to the right (left) as time increases for the put (call). Parameters are $E = 10$, $\sigma_1 = 0.4$, $\sigma_2 = 0.2$, $\rho = -0.5$, $r = 0.06$ (a) $d_1 = d_2 = 0$ (b) $d_1 = 0.04$, $d_2 = 0.08$.

as a function of S_1 we find that the put has the limit at expiry of

$$S_f(S_1, T) = \min[E - S_1, \frac{r\ E}{d_2} - \frac{r\ d_1\ E}{d_2} S_1], \tag{3.50}$$

and the limit for the call is

$$S_f(S_1, T) = \max[E - S_1, \frac{r\ E}{d_2} - \frac{r\ d_1\ E}{d_2} S_1]. \tag{3.51}$$

In figure 3.7(b) we see that the initial position of the free boundary is the maximum of two lines. This can be interpreted by considering the boundary at $S_1 = 0$, where the problem reduces to the single asset BSM equation. On this boundary, from (2.5) the limit for a put is $S_f(0, T) = \min[E, \frac{rE}{d_2}]$, and similarly, the boundary $S_2 = 0$ implies that $S_f(\min[E, \frac{rE}{d_1}], T) = 0$.

The free boundary of the dual strike option, as shown in figure 3.8 has a far more intricate free boundary than either of the two previous cases. We now have a more complicated interaction due to the different strike prices. The limit of the free

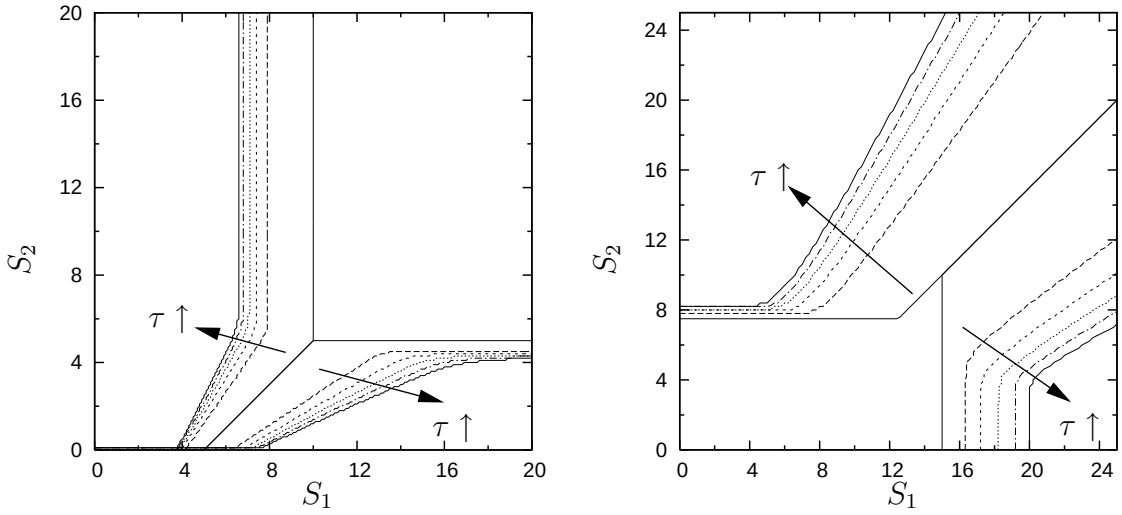

(a) Put (b) Call

Figure 3.8
American dual strike option
An illustration of the early exercise region for dual strike option, with time t ranging from 0 (solid) to 0.5 (solid) with increments of 0.1. The free boundary moves outward from the angular lines as time to expiry increases. Parameters are $E_1 = 10$, $E_2 = 5$, $\sigma_1 = 0.4$, $\sigma_2 = 0.2$, $\rho = -0.5$, $r = 0.06$ (a) $d_1 = d_2 = 0$ (b) $d_1 = 0.04$, $d_2 = 0.04$.

boundary as time tends to expiry is found to be

$$S_f^A(S_1, T) = \max\left[0, \min\left[S_1 - E_1 + E_2, E_2, \frac{r\ E_2}{d_2}\right]\right] \tag{3.52}$$

$$S_f^B(S_2, T) = \max\left[0, \min\left[S_2 - E_2 + E_2, E_1, \frac{r\ E_1}{d_1}\right]\right], \tag{3.53}$$

for the put (figure 3.8(a)) and for the call (figure 3.8(b)) it is

$$S_f^B(S_1, T) = \max\left[S_1 - E_1 + E_2, E_2, \frac{r\ E_2}{d_2}\right] \tag{3.54}$$

$$S_f^A(S_2, T) = \max\left[S_2 - E_2 + E_2, E_1, \frac{r\ E_1}{d_1}\right]. \tag{3.55}$$

Although the shape of the boundaries is similar to the single strike option (figure 3.6), the boundary is no longer symmetric around the line $S_1 = S_2 - E_2 + E_1$, and is skewed to one side.

3.6 Enhanced Numerical Techniques

Even with the rapid growth of computer power, the numerical solution to PDEs with multi dimensions can still be a problem. In order to maintain accuracy as we increase the number of dimensions, the number of nodes over which we must solve grows exponentially. The numerical techniques developed for the single-dimension case are not as robust/efficient in multiple dimensions.

3.6.1 Optimising the relaxation parameter ω

Work on optimising the over-relaxation parameter ω has been carried out by Cryer (1971), who has shown that the optimum value of ω for the linear complementarity PSOR scheme is always slightly less than that for the corresponding linear SOR scheme. For the one-dimensional case, by running an optimising algorithm with the solver, the optimum value of ω was found to be between 1.6 and 1.8. When the scheme was modified to involve a block solver, in the APSOR (see later section 3.6.3), the optimum value was also found to be around 1.6 to 1.8. The value is highly dependent on the value of σ_1 and σ_2 and also the size of the time-steps.

3.6.2 Simple Banding

Andricopoulos et al. (2004) show that when solving using trees, the number of nodes over which you must solve can be reduced according to the probability of exercising at a particular node, and the probability of reaching that node, starting from the initial node. Inspection of the solution for the American put, shown diagrammatically in figure 3.5, indicates that there are significant regions in state space over which it is unnecessary solve. In regions A and B the option is exercised, and in region C the option is worthless since the probability of it ever being exercised is so small.

If we are to solve the PDE, discarding regions where the option is exercised or worthless, then we must fully understand the topology of the problem, ensuring that these discarded regions play no role at any time. Region C is calculated following

Andricopolous et al. (2002),

$$S_1^{max} = E_1 \cdot e^{-r(T-t)+\xi\sigma_1\sqrt{T-t}} \tag{3.56}$$

$$S_2^{max} = E_2 \cdot e^{-r(T-t)+\xi\sigma_1\sqrt{T-t}}. \tag{3.57}$$

Now let us consider regions A and B for the two-asset American put. For a single asset put, it is simple to find a minimum for the free boundary. We simply look at the perpetual option for which we have an analytical solution. Now, we know

$$P(S, T-t_1) > P(S, T-t_2) \qquad \text{for } t_1 < t_2, \tag{3.58}$$

where $P(S,t)$ is the single asset American put option. This statement says that the option price is monotonically increasing as we move backwards in time, a detailed description as to why this is so can be found later in chapter 7, where other such rational pricing criteria are discussed. Since the option price is always increasing as we move backwards in time, then the free boundary must be monotonically decreasing, or

$$S_f(T-t_1) < S_f(T-t_2) \qquad \text{for } t_1 < t_2, \tag{3.59}$$

where $S_f(t)$ is the free boundary. In the limit as time to maturity becomes large we can write

$$\lim_{(T-t)\to\infty} P(S,t) = P^*(S),$$
$$\lim_{(T-t)\to\infty} S_f(t) = S_f^*,$$

where P^*, S_f^* is the perpetual option and the corresponding free boundary respectively, since S_f^* is a minimum for $S_f(t)$. Now, if $V(S_1, S_2, t)$ is the price of the dual strike American option, as $S_1 \to \infty$ the boundary condition that $\frac{\partial}{\partial S_1} = 0$ implies that

$$V(S_1, S_2, t) \to P(S_2, t; E_2, \sigma_2, r, d_2), \tag{3.60}$$

where $P(S_2, t)$ is the solution to the single asset BSM equation with the given parameters. From our reasoning above it is clear that

$$\lim_{S_1 \to \infty} S_f^A(S_1, t) = S_f(t) \tag{3.61}$$

where $S_f(t)$ is the free boundary for $P(S_2, t)$.

Let the region for which we will discard, inside A, (cf figure 3.5) have the boundary $\mathcal{C}_A(S_1)$. Then we require

$$\mathcal{C}_A(S_1) \leq \lim_{(T-t) \to \infty} S_f^A(S_1). \tag{3.62}$$

If we could solve the perpetual case for two-assets, then

$$\mathcal{C}_A(S_1) = \lim_{(T-t) \to \infty} S_f^A(S_1),$$
$$\mathcal{C}_B(S_2) = \lim_{(T-t) \to \infty} S_f^B(S_2),$$

and our two regions are well defined. The author is unaware of any analytical solution for the two-asset problem, however, there is an analytical solution to the single-asset perpetual American option with two free boundaries. The next section describes how, in a somewhat heuristic approach, the solution to such a problem can be exploited to estimate the perpetual location of the free boundary.

A perpetual option with two free boundaries

In order to reduce the complexity of the problem, we consider a slice (with constant S_2) of the solution in the region $S_2 < E_2$. Let such a slice be defined where $\hat{E} = E_2 - S_2$ is a constant, where V is now just a function of S_1, then the final condition of this option is

$$V(S_1, t = T) = \max[\hat{E}, E_1 - S_1]. \tag{3.63}$$

Then since we ignore the effects of variations in S_2, the problem will reduce to the one-dimensional case, now with two free boundaries, and a smooth pasting condition on each. The motivation for investigating such an option is to give an estimation of

the lower bound for the free boundary, and so we are only interested in the limit as time tends to infinity, i.e. the perpetual option, as this is the when the free boundary is expected to reach its minimum. To compensate for not considering derivatives in the S_2 direction, let us introduce a new volatility, that takes into account the volatility in both directions,

$$\bar{\sigma} = \sqrt{\sigma_1 - 2\rho\sigma_1\sigma_2 + \sigma_2}.$$

This volatility is similar to (3.27) derived earlier when a similarity solution is used to solve in the limit as $S_1 \to \infty$. For this option, an analytical solution exists for the steady state solution, or the perpetual option, which we will now derive.

By seeking a solution of the Euler type

$$V(S) = AS^{\alpha}, \tag{3.64}$$

we can insert this into the one dimensional BSM (less the time derivative) with our modified volatility

$$\frac{1}{2}\bar{\sigma}^2 S_1^2 \frac{\partial V}{\partial S_1^2} + (r - d_1) S_1 \frac{\partial V}{\partial S_1} - rV = 0, \tag{3.65}$$

we arrive at a solution of the form

$$V(S) = AS^{\alpha_-} + BS^{\alpha_+}, \tag{3.66}$$

where α_+ and α_- denote the positive and negative roots respectively of the quadratic equation

$$\frac{1}{2}\bar{\sigma}^2\alpha(\alpha - 1) + (r - d_1)\alpha + r = 0. \tag{3.67}$$

We now require the boundary conditions at $S_1 = S_l$, the lower boundary, and $S_1 = S_u$, the upper boundary. Since we exercise at the free boundary, we have

$$V(S_1 = S_l) = E_1 - S_1, \tag{3.68}$$

$$V(S_1 = S_u) = \hat{E}. \tag{3.69}$$

From the smooth pasting conditions we obtain

$$\frac{\partial V}{\partial S_1}(S_1 = S_l) = -1, \tag{3.70}$$

$$\frac{\partial V}{\partial S_1}(S_1 = S_u) = 0. \tag{3.71}$$

Now, (3.69) implies that

$$AS_u^{\alpha_-} + BS_u^{\alpha_+} = \hat{E},$$

$$B = (\hat{E} - A \cdot S_u^{\alpha_-})S_u^{-\alpha_+}. \tag{3.72}$$

and so

$$A = \frac{\hat{E}\alpha_+}{\alpha_+ S_u^{\alpha_-} - \alpha_- S_u^{\alpha_-}}. \tag{3.73}$$

So if we substitute (3.72) and (3.73) into (3.68) and (3.70) we obtain

$$\frac{\hat{E}\alpha_+}{\alpha_+ S_u^{\alpha_-} - \alpha_- S_u^{\alpha_-}} S_l^{\alpha_-} + \left(\hat{E} - \frac{\hat{E}\alpha_+}{\alpha_+ S_u^{\alpha_-} - \alpha_- S_u^{\alpha_-}} S_u^{\alpha_-} \right) S_u^{-\alpha_+} S_l^{\alpha_+}$$

$$= E_1 - S_l, \tag{3.74}$$

$$\frac{\hat{E}\alpha_+}{\alpha_+ S_u^{\alpha_-} - \alpha_- S_u^{\alpha_-}} \alpha_- S_l^{\alpha_- - 1} + \left(\hat{E} - \frac{\hat{E}\alpha_+}{\alpha_+ S_u^{\alpha_-} - \alpha_- S_u^{\alpha_-}} S_u^{\alpha_-} \right) S_u^{-\alpha_+} \alpha_+ S_l^{\alpha_+ - 1}$$

$$= -1. \tag{3.75}$$

After some algebra on (3.74) and (3.75) we find

$$\frac{\hat{E} \cdot \alpha_+}{\alpha_+ - \alpha_-} \cdot \frac{S_l^{\alpha_-}}{S_u^{\alpha_-}} - \frac{\hat{E} \cdot \alpha_-}{\alpha_+ - \alpha_-} \cdot \frac{S_l^{\alpha_+}}{S_u^{\alpha_+}} = E_1 - S_l, \tag{3.76}$$

$$\frac{\hat{E} \cdot \alpha_+ \alpha_-}{\alpha_+ - \alpha_-} \cdot \frac{S_l^{\alpha_-}}{S_u^{\alpha_-}} - \frac{\hat{E} \cdot \alpha_- \alpha_+}{\alpha_+ - \alpha_-} \cdot \frac{S_l^{\alpha_+}}{S_u^{\alpha_+}} = -S_l. \tag{3.77}$$

These equations lead to the conclusion that

$$(\alpha_+ - \alpha_+\alpha_-)\frac{\hat{E}}{\alpha_+ - \alpha_-} \cdot \frac{S_l^{\alpha_-}}{S_u^{\alpha_-}} - (\alpha_- - \alpha_+\alpha_-)\frac{\hat{E}}{\alpha_+ - \alpha_-} \cdot \frac{S_l^{\alpha_+}}{S_u^{\alpha_+}} = E_1,$$
$$\frac{S_l^{\alpha_-}}{S_u^{\alpha_-}} - \frac{\alpha_- - \alpha_+\alpha_-}{\alpha_+ - \alpha_+\alpha_-} \cdot \frac{S_l^{\alpha_+}}{S_u^{\alpha_+}} = \frac{E_1(\alpha_+ - \alpha_-)}{\hat{E}(\alpha_+ - \alpha_+\alpha_-)}. \tag{3.78}$$

If we assume that dividends d_1 are zero, then $\alpha_+ = 1$ and $\alpha_- = \frac{2r}{\sigma^2}$, the equation may be solved explicitly

$$\frac{S_l}{S_u} = \left(\frac{E_1}{\hat{E}}\right)^{\frac{1}{\alpha_-}}, \tag{3.79}$$

and therefore

$$S_l = \frac{\alpha_-\hat{E}}{1-\alpha_-}\left\{\left(\frac{E_1}{\hat{E}}\right)^{\frac{1}{\alpha_-}} - \frac{E_1}{\hat{E}}\right\} \tag{3.80}$$

$$S_u = \frac{\alpha_- E_1}{1-\alpha_-}\left\{\frac{\hat{E}}{E_1} - \left(\frac{\hat{E}}{E_1}\right)^{\frac{1}{\alpha_-}}\right\}. \tag{3.81}$$

and as a consequence the solution to the problem (without dividends) is

$$V(S_1) = \frac{\hat{E}}{S_u^{\alpha_-} - \alpha_- S_u^{\alpha_-}} \cdot S_1^{\alpha_-} - \frac{\alpha_-\hat{E}}{S_u - \alpha_- S_u} \cdot S_1 . \tag{3.82}$$

In figure 3.9 we plot the perpetual free boundary, along with our estimate, gleaned using the analysis above. The estimate is made by using the appropriate value for $\hat{E}$, given the value of S_2. We note here that the analysis assumed the dividend value to be zero, in order to gain an analytical boundary. Even with dividends included, an appropriate increase or decrease in the value of $\bar{\sigma}$ and r should be able to take any increase (decrease) in the free boundary into account. The estimate appears to follow closely the path of the actual barrier, and importantly is always inside the region of exercise where required. Using this boundary, the computation time can be decreased by a large factor, as shown in table 3.2, especially when the values of σ_1 and σ_2 are small.

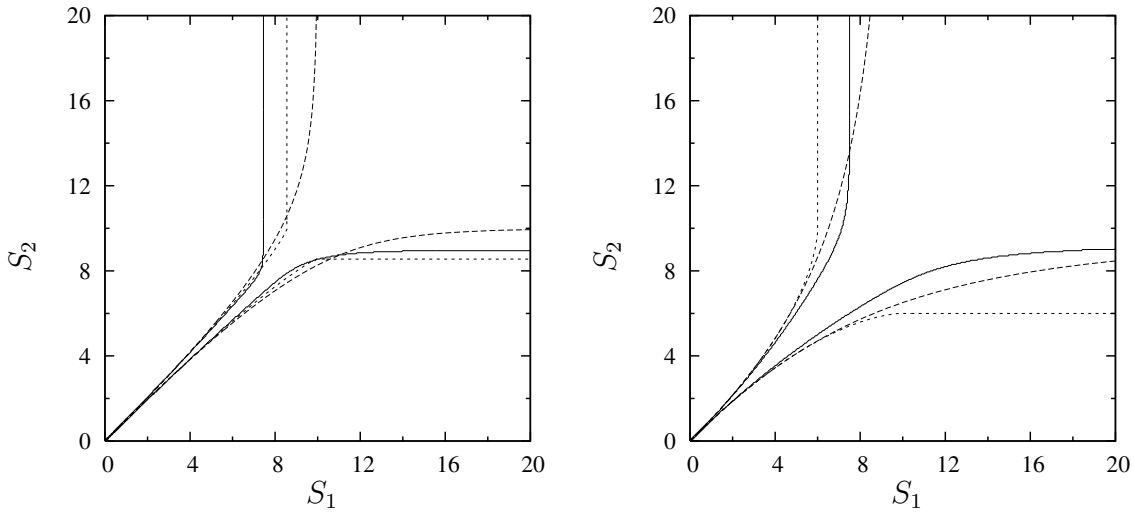

(a) $\rho = 0.75$ (b) $\rho = -0.75$

Figure 3.9
Simple banded estimate
An illustration of the early exercise region for single-strike perpetual put option (solid) along with our estimates S_l (dotted) and S_u (dashed) plotted on both axis.

3.6.3 Boundary Updating Solver

One of the biggest problems with estimating regions A and B (c.f. figure 3.5) is that we have to make the estimate large enough so that the region is never crossed for any possible time. If σ_1 and/or σ_2 are large, then the estimate for $\mathcal{C}_A(S_1)$ and $\mathcal{C}_B(S_2)$ may be significantly larger than could possibly be reached in the finite time we solve over. One possible way to overcome this is to check the position of the free boundary at each time step, and then update the scheme so as to only solve in the regions where we are not exercising. Such a scheme has already been implemented for the one-dimensional case as described earlier in section 2.4.2, however the extension to multiple dimensions requires complex programming.

When solving with the PSOR scheme, since the free boundary is not explicitly calculated, we can only estimate its position by noting whether or not the constraint $(g \geq u)$ has been enforced at a particular node. In figure 3.10 the pseudo code to determine the barrier is shown; note that the max function that would normally used in the PSOR scheme is replaced by an IF statement, which will prevent calculating for any more nodes when the constraint is applied, and return the position at which

```
PointSolverDown(alpha, beta, gamma, delta, eps, mu, z, u)
 1  for i ← nDown to 1
 2  do
 3      y ← SOR(alpha, beta, gamma, delta, eps, mu, z, u)
 4      if y < g_{i,j}
 5        then
 6                u_{i,j} ← g_{i,j}
 7                break
 8        else
 9                u_{i,j} ← y
10  return i
```

Figure 3.10
Point solver down – pseudo code
The algorithm used to 'search' for the free boundary, updating the solution u as it does.

```
PointSolverUp(alpha, beta, gamma, delta, eps, mu, z, u)
 1  for i ← nUp to n
 2  do
 3      y ← SOR(alpha, beta, gamma, delta, eps, mu, z, u)
 4      if y < g_{i,j}
 5        then
 6                u_{i,j} ← g_{i,j}
 7                break
 8        else
 9                u_{i,j} ← y
10  return NIL
```

Figure 3.11
PointSolverUp – pseudo code
The algorithm to update the solution u, breaking if a free boundary has been reached, but not returning any value.

it is first applied. Essentially we search for the barrier at the same time as we solve, *killing two birds with one stone.*

The pseudo codes shown in figures 3.10 - 3.12 are geared toward the maximum of two puts option, both single- and dual-strike, and take advantage of the special form of the free boundary, specifically that we can express the two boundaries as functions of S_1 and S_2 respectively. This allows us to specify the region over which we need to consider by two points in either S_1 or S_2 depending on which way the blocks are formed (c.f. section 3.3) by holding either i or j constant and solving for a line of nodes in j or i. The position of the boundary is found by searching downward, because

```
AdvancedPsorSolver(boundaryS1, boundaryS2, u)
 1  ComputeScheme(alpha, beta, gamma, delta, eps, mu, z)
 2  while error < tol
 3  do
 4      nDown ← MinRegion(boundaryS1, boundaryS2)
 5      nUp ← MaxRegion(boundaryS1, boundaryS2)
 6      for j ← 1 to m
 7      do
 8          for i ← nUp to nDown
 9          do
10              zstar_i ← AdjustForTri(delta_{i,j}, eps_{i,j}, mu_{i,j}, u, z_{i,j})
11          TridiagonalSolver(alpha, beta, gamma, zstar, u, nDown, nUp)
12          PointSolverUp(alpha, beta, gamma, delta, eps, mu, z, u)
13          boundaryS2 ← PointSolverDown(alpha, beta, gamma, delta, eps, mu, z, u)
14  return loops
```

Figure 3.12
The advanced PSOR algorithm – pseudo code
'alpha', 'beta', 'gamma', 'delta', 'eps', 'mu' and 'z' are $n \times m$ arrays defined by (3.32)

of the topology of the problem. If we refer to the function 'AdvancedPsorSolver' in figure 3.12, then we solve blocks in constant j (S_2), the free boundary '$boundaryS2$ ($S_f^B(S_2)$)' represents the minimum value in i (S_1), and so it is straightforward to return the minimum value of i to '$boundaryS2$'. The other free boundary is a function of S_1, and cannot be assigned in this way. If we were solving for the maximum of two calls option, then the boundaries would be found as the maximum by searching upward. For other options, even finding the location of the boundary can become difficult if it is not a smooth/monotonic function of S_1 or S_2.

The algorithm shown in figure 3.12 is not the full algorithm, rather it is only partitioned into blocks in j, while the full algorithm will partition in i also, allowing $boundaryS1$ to be found. The functions 'MinRegion' and 'MaxRegion' can also include the upper bounds discussed in section 3.6.2 to reflect the banded nature of the solution, further reducing the computation time.

3.6.4 Comparison of methods

In table 3.2 we show computation times for each of the three methods described previously. We note from columns 1 and 3, comparing unextrapolated results with

Table 3.2
Relative RMS errors for American dual strike put options

n	APSOR (time)	PSOR(x) (time)	APSOR(x) (time)	Simple band(x) (time)
50	0.06756	0.02886	0.02886	0.02886
	(0.03)	(0.10)	(0.05)	(0.07)
100	0.01584	0.00438	0.00438	0.00438
	(0.26)	(1.35)	(0.30)	(0.68)
150	0.00707	0.00145	0.00145	0.00145
	(0.95)	(6.96)	(1.04)	(2.68)
200	0.00398	0.00045	0.00045	0.00046
	(2.75)	(26.80)	(2.97)	(8.19)
250	0.00255	0.00028	0.00028	0.00028
	(6.27)	(74.98)	(6.82)	(21.26)
300	0.00178	0.00014	0.00014	0.00015
	(11.81)	(160.62)	(12.49)	(47.17)
350	0.00130	0.00009	0.00009	0.00010
	(20.12)	(304.24)	(28.60)	(85.59)
400	0.00100	0.00007	0.00007	0.00008
	(32.02)	(520.88)	(34.82)	(145.29)
450	0.00087	0.00005	0.00005	0.00007
	(49.54)	(827.47)	(53.60)	(220.71)
500	0.00064	0.00002	0.00002	0.00006
	(72.51)	(1132.98)	(80.74)	(325.25)

The relative RMS errors are calculated against exact values for approximately 4000 different put options. Here $S_1 \in [0.9E_1, 1.1E_1]$, $S_2 \in [0.9E_2, 1.1E_2]$, $E_2 = E_1/\frac{1}{2}E_1$, $T = 0.5/1$, $\rho = 0/0.5$, $\sigma_1 = 0.4/0.2$, and $\sigma_2 = 0.2/0.1$. We have that $r = 0.06$ and $E_1 = 10$. We use n nodes in both spacial directions, with $S_1^{max} = 5E_1$ and $S_2^{max} = 5E_2$, and $k = n/5$ timesteps. The relaxation parameter ω initially set to 1.6, is optimised step by step. Results marked with x are extrapolated using Richardson extrapolation, with n and $n/2$.

extrapolated results, that although the convergence may not be exactly of order $O(\Delta S^2, \Delta\tau^2)$ (due to non-linear errors), the results are dramatically improved by extrapolation, though not to the same extent as for the European prices (table 3.1). The APSOR method, with boundary updating, is clearly far superior to both the base method PSOR and also the simple banded solver. Notably, the APSOR method is even faster at calculating American prices than the block solver was in solving for the corresponding European price (table 3.1), mainly due to the fact we are only solving in the important regions. Consequently the extra computational effort in locating the free boundary (while simultaneously updating the solution) is offset by the enhanced convergence of the scheme. We note here that for large n, the simple banded solver does slightly worse than the other two methods. This may be because there may be some regions over which we are not solving but should be. This is major drawback in the method, namely that the position of the free boundary can only be guessed *a priori*. If it is not guessed correctly, which is particularly difficult when volatility is large, then errors may contaminate the entire solution.

3.7 Conclusions

The APSOR method proposed in this chapter is both fast and efficient as compared to the standard PSOR method (around 15 times faster). For the continuously exercised option the method is comparative to other methods in 2 and possibly 3 dimensions, although above this both the coding and calculation would become increasingly difficult. However, the method is robust enough to handle a stochastic interest rate as the second underlying, which will have applications, for instance, in convertible bonds (chapter 6). As a result in low multi-dimensional problems the method is fast and robust, with the added bonus that the optimal exercise barrier is calculated at each time step for free.

Chapter 4

Time Dependent Barrier Options

The vanilla barrier option is a path-dependent option. Snyder (1969) describes options of this type in detail, as well as the reasons why they may be traded. There are four main types, 'up-and-in', 'up-and-out', 'down-and-in' and 'down-and-out'. The barrier is defined as the level in the asset space so that when the underlying asset value crosses this point from above (down) or from below (up) the holder of the option either receives (in) or has taken away (out) the rights to a European option of the same maturity. While closed-form solutions have been found for simple vanilla barrier options (Merton, 1990 shows that with a transform of variables the European 'down-and-out' call option problem can be solved by using either separation of variables or Fourier transform), the options can be extended to include early exercise or rebate, resulting in a more complex problem which may require numerical solutions (Merton also gives a solution for a 'down-and-out' call with rebate). The rebate takes the form of a cash payment when the option is knocked out, or fails to knock in. When early exercise is allowed, e.g. American-type barrier options, they can present an interesting problem quite different from the standard American option if the location of the optimal exercise boundary is close to the location of the barrier, since there may be an interaction between the two. This results in different problems for numerical solution, since there exist two locations for non-linearity errors. For instance, the highly accurate scheme described in chapter 2 will not be as accurate here since the grid may not be aligned with both the barrier and the optimal exercise boundary.

The assumption of instant knock-out or knock-in may also be relaxed, allowing the asset price to be above or below the barrier for a specified time before the option is knocked in or out. Options where the barrier can be crossed for a predetermined time are discussed next in section 4.1.

4.1 Occupation-Time Derivatives

Occupation-time derivatives are highly path-dependent options for which the time spent above or below a barrier affects the payout of the option. Options of this form include: Parisian and ParAsian (delayed barrier) options, switch and step options (double barrier), and the α-quantile option (delayed look-back option).

The Parisian option is a barrier option for which the knock-in/out feature is only realised when the stock has been above/below the barrier consecutively for a predetermined time. This class of option came to prominence for a number of reasons. Straight barrier options are difficult to hedge ($\Delta = \frac{\partial V}{\partial S}$ is discontinuous near the barrier) and open to price manipulation. Also, when companies issue convertible bonds, if they wish to embed an option to force conversion, this is normally undertaken with reference to the stock price being above the call price for a certain amount of time, i.e. a Parisian option.

Several papers have attempted to use occupation-time derivatives to model real world occurrences. Gauthier (2000) uses the delayed nature of the Parisian option in the analysis of real options. When valuing a real option in a project, there is sometimes a delay between an investment decision and its implementation. The delay is defined as the time the underlying asset spends above the threshold at which it is optimal to invest. In another application, Francois and Morellec (2004) and Moraux (2003) use down-and-out Parisian options to model Chapter 11 bankruptcy and hence the default risk for bonds.

An obvious extension to the Parisian option is to count the time spent *cumulatively* beyond the barrier. This has been dubbed the ParAsian option due to the Asian style counting over the life of the option. Work performed by the author in collaboration

with Yu (2004) argues that the cumulative nature of ParAsian options is better suited to model Chapter 11, as the Parisian option barrier can be crossed and recrossed numerous times without the option ever being knocked-out. Creditors may grow weary of such a situation and decide to liquidate the bond. Model parameters and the numerical scheme used to solve for such a bond are discussed in detail later in chapter 5.

An even better model may be one that gives greater weight to the knockout time when the asset value is further beneath the barrier. Creditors are likely to be far more worried if the firm value drops to a very low level, even if it is just for a short period of time; such an "Integral Time" model is proposed in this chapter.

The Parisian option can be simulated using the Monte-Carlo method, by simply recording the length of time each path has spent beyond the barrier. There is, however, a possible bias linked to the discretisation of the problem, and the computation time is slow. Due to this slow and cumbersome approach to pricing the option, the options only caught the imagination of the finance community when Chesney et al. (1997) priced them in a rigorous fashion. By using the theory of Brownian excursions, they derive the price of a European Parisian option in terms of a Laplace transform, that must then be inverted numerically. Others have since extended the approach to the ParAsian option, which are found to be slightly easier to price than their Parisian counterparts; Hugonnier (1999) presents an quasi-analytical pricing formula, as well as numerous numerical results. However, Moraux (2002) notes that the results represented are not from the pricing formula itself, and, following the framework of Chesney et al. (1997) and Hugonnier (1999) derives the proper closed-form solutions. Strangely, though, no results are shown to back up these claims. Bernard et al. (2005) develop a new inverse Laplace transform that improves on the method of Chesney et al. (1997) to gain a fast solution to the Parisian problem. The most difficult part of finding the solution via the method of Chesney et al. (1997) is to calculate the inverse Laplace transform. They improve on this by approximating the function as the sum of functions that have explicit inverse transforms. This allows the computation time to be reduced significantly with minimal loss in accuracy.

It is not immediately obvious as to how one would go about solving for the Parisian option using lattice or finite-difference methods. Avellaneda and Wu (1999) make three observations about the Parisian option in order to use a lattice method. Firstly, when beyond the barrier, the option looks (and therefore hedges) like a knock-in option, with maturity equal to time to knock-out, and a 'rebate' that equals the value of the option at the barrier. Secondly, when the asset price has not crossed the barrier, the option can be viewed as a knock-out option with the same maturity and a rebate that equals the option value at the barrier. Thirdly, the option value at the barrier is determined by imposing a smooth pasting condition, namely that the derivative of the option value is continuous across the barrier; this can be justified by no-arbitrage arguments. From these observations, they conclude that the problem may be split into two coupled options, one which must be solved above the barrier, and one to be solved below the barrier. They use a trinomial tree approach but conclude that in the continuous time limit, the problem is in fact two coupled PDEs, and a Crank-Nicolson scheme could also be applied without loss of generality. They also express the approach in the limit of continuous time as an integral, suggesting that quadrature methods may be applied, possibly more successfully than lattice or finite-difference methods. However, the smooth pasting condition at the barrier becomes very complicated when expressed in integral form. Costabile (2002) uses the framework of Cox et al. (1979) to construct a binomial tree method which is fast, but as with all lattice methods, the method is not flexible enough to include cumulative time spent under the barrier or other modifications to time under the barrier. Kwok and Lau (2001) use a forward shooting algorithm, pioneered by Hull and White (1993) and others. This is an extension to the usual binomial or trinomial trees, where an extra auxiliary state vector is used at each node to capture the path dependency of the option. This has the advantage that it can handle situations where the governing PDE is not simple and the asset value is not monitored continuously. Haber et al. (1999) derive the PDE for the occupation-time derivative, and propose an explicit finite-difference scheme with which to solve the problem. The finite-difference method is flexible and is easily modified to include features such as early

exercise, rebates and cumulative time spent under the barrier. Zhu and Stokes (1999) develop a finite-element approach to the problem of Parisian options using the PDE approach. This has the advantage that the elements can be refined in areas where it is needed to improve the accuracy of the solution. Whether or not the method is easily extended to include early exercise is unclear, though Crank (1984) states that the Projected SOR algorithm can be used just as easily on finite-element as finite-difference schemes.

Studying practitioners' procedure, Anderluh and van der Weide (2004) seek an *implied* barrier. Most practitioners hedge and price Parisian options as straight barrier options with barriers slightly above or below that stated in the contract. They use Brownian excursion theory (Revuz and Yor, 1999) to model what this difference should be. The errors with this scheme are highly dependent on the barrier time, which is reasonable since Parisian options tend to the straight/fixed barrier as the barrier time is reduced. They do find a close match to the Δ hedge though, which is probably explained by the observations made by Avellaneda et al. (1999) (that the option out of the barrier is like a knock-out option with rebate).

Chesney and Gauthier (2006) note that the vast majority of previous literature focuses on European options, with only a brief mention of American options in Haber et al. (1999). They study the similarities between American barrier options, which have closed form solutions in the perpetual case (Russian options) and the American Parisians. They show that American Parisians also have a closed-form solution in the perpetual case. Using a probabilistic approach they reformulate the non-perpetual case into a function of the exercise boundary. A corresponding equation for the exercise boundary is also therefore required to solve for the option value.

To summarise, there are four possible methods with which to solve time-dependent derivatives: simulation, lattice, Laplace transform and PDE. The major disadvantage of the Laplace method is its inflexibility, while the simulation and lattice methods are very slow. For its flexibility, we choose to extend the finite-difference method as proposed by Haber et al. (1999). Using a Crank-Nicolson discretisation with relatively large time steps, the solution time can be significantly reduced so as to

allay the fears of Bernard et al. (2005) and others.

4.2 Parisian Options

Let us define a variable to represent the time spent above (below) the barrier, $\bar{t}$ (the barrier-clock). Now let H be the barrier level for which the asset value must spend time above or below. When the asset value is beyond the barrier, and if the barrier-clock moves at the same rate as real time t, then $d\bar{t} = dt$. When the asset value has not crossed the barrier, then the barrier-clock does not advance in time and $d\bar{t} = 0$. When the asset price hits the barrier after it has gone beyond the barrier, the barrier-clock is reset to zero again. For an up option, we can write

$$d\bar{t} = \begin{cases} 0 & \text{if} \quad S(t) < H \\ dt & \text{if} \quad S(t) > H \end{cases}, \tag{4.1}$$

where the counter resets to zero when $S(t) = H$. The knock-in/out effects will be triggered when the barrier-clock reaches some pre-specified level, say $\bar{t} = \bar{T}$, where $\bar{T}$ is sometimes referred to as the length of the window.

The option value V, is now a function of three state variables, S, t and $\bar{t}$, so we have $V = V(S, t, \bar{t}\,)$. Let us assume a BSM framework with constant drift, volatility and interest rate. Then S follows a log-normal geometric Brownian motion and the small change in asset price is given by

$$\frac{dS}{S} = \mu dt + \sigma dX \tag{4.2}$$

From Itô calculus, it follows that the small change in option price is given by

$$dV = \sigma S \frac{\partial V}{\partial S} dX + \left(\mu S \frac{\partial V}{\partial S} + \frac{1}{2}\sigma^2 S^2 \frac{\partial^2 V}{\partial S^2} + \frac{\partial V}{\partial t} \right) dt + \frac{\partial V}{\partial \bar{t}} d\bar{t},$$

given that $d\bar{t} = O(dt)$. From (4.1), the small change in option price becomes

$$dV = \begin{cases} \sigma S\dfrac{\partial V}{\partial S}dX + \left(\mu S\dfrac{\partial V}{\partial S} + \dfrac{1}{2}\sigma^2 S^2\dfrac{\partial^2 V}{\partial S^2} + \dfrac{\partial V}{\partial t}\right)dt & \text{if} \quad S(t) < H \\ \sigma S\dfrac{\partial V}{\partial S}dX + \left(\mu S\dfrac{\partial V}{\partial S} + \dfrac{1}{2}\sigma^2 S^2\dfrac{\partial^2 V}{\partial S^2} + \dfrac{\partial V}{\partial t} + \dfrac{\partial V}{\partial \bar{t}}\right)dt & \text{if} \quad S(t) > H \end{cases}, \tag{4.3}$$

here $dt = d\bar{t}$. On the barrier, the value of barrier-clock is reset to zero, so to maintain path continuity the value of the option for all $\bar{t}$ must be equal to the value at of the option when $\bar{t} = 0$. Hence we need only solve $V(H, t, \bar{t}\,)$ for $\bar{t} = 0$. Consequently, for a small change in V when the asset price is at the barrier we also have

$$dV = \sigma S\frac{\partial V}{\partial S}dX + \left(\mu S\frac{\partial V}{\partial S} + \frac{1}{2}\sigma^2 S^2\frac{\partial^2 V}{\partial S^2} + \frac{\partial V}{\partial t}\right)dt \tag{4.4}$$

By constructing a hedging portfolio in the usual way we arrive at the following PDEs, which are valid over different regions of S and $\bar{t}$

$$\frac{\partial V}{\partial t} + \frac{1}{2}\sigma^2 S^2\frac{\partial^2 V}{\partial S^2} + (r-d)S\frac{\partial V}{\partial S} - rV = 0, \qquad S < H, \tag{4.5}$$

$$\frac{\partial V}{\partial \bar{t}} + \frac{\partial V}{\partial t} + \frac{1}{2}\sigma^2 S^2\frac{\partial^2 V}{\partial S^2} + (r-d)S.\frac{\partial V}{\partial S} - rV = 0, \qquad S > H. \tag{4.6}$$

When the asset value is below the barrier, $S < H$, then we must solve (4.5) with $\bar{t} = 0$, since the barrier-clock is always zero below the barrier. If the asset value is at the barrier, the clock is reset to zero. When the asset value is above the barrier, $S > H$, we solve (4.6) for $\bar{t} < \bar{T}$, where the additional $\partial V/\partial \bar{t}$ term indicates that the clock is ticking.

4.2.1 Parisian Options – Boundary Conditions

For a Parisian option, the clock is reset to zero when $S = H$, then we must maintain continuity across paths, which gives rise to

$$V(S = H, t, \bar{t}\,) = V(S = H, t, 0). \tag{4.7}$$

In order to satisfy the BSM equation we must also maintain a continuous hedge across the barrier. Since all paths cross at $\bar{t} = 0$, we require

$$\lim_{S\uparrow H} \frac{\partial V}{\partial S}(S, t, 0) = \lim_{S\downarrow H} \frac{\partial V}{\partial S}(S, t, 0), \tag{4.8}$$

where $\Delta = \partial V/\partial S$ is the usual BSM hedge.

There are many variants of the Parisian option: up/down, in/out on any number of possible payoffs. We specify here that the payoff of the option, when it is knocked-in/out at $\bar{t} = \bar{T}$, is $G(S, \bar{t}\ )$, and the terminal condition, if the option is not knocked-in/out, is $F(S, \bar{t}\ )$. Then we have

$$\begin{aligned} V(S, T, \bar{t}\ ) &= F(S, \bar{t}\ ) \quad \text{for} \quad 0 \le \bar{t} < \bar{T}, \\ V(S, t, \bar{T}\ ) &= G(S, \bar{t}\ ). \end{aligned}$$

For example, on a Parisian up-and-out call, we have $F(S, \bar{t}\ ) = \max[0, S - E]$ and $G(S, \bar{t}\ ) = 0$.

At extremes in the asset value we have to take into account the difference between the time-to-knockout (TTK) and the time-to-maturity (TTM). For example, let us examine the up-and-out call option. If the TTK is less than or equal to the TTM, then as $S \to \infty$ the option is almost certain to be above the barrier until it is knocked out, so

$$V(S \to \infty, t, \bar{t}\ ) \to 0 \qquad \text{if} \qquad (\bar{T} - \bar{t}\ ) \le (T - t).$$

However, if TTK is greater than TTM, then there is no chance that the option can be knocked out, and the option value behaves like a standard call option,

$$V(S \to \infty, t, \bar{t}\ ) \to Se^{-d(T-t)} - Ee^{-r(T-t)} \qquad \text{if} \qquad (\bar{T} - \bar{t}\ ) > (T - t).$$

Hence, there is an apparent discontinuity in the option value above the barrier if $\bar{t}$ is held constant, and we move in t across the point $t = \bar{t}$, or vice versa. However, the discontinuity does not really exist as it is not possible for the option value above the

barrier to move in real time without the barrier-clock advancing at the same rate.

4.2.2 Numerical Method

The scheme adopted here is based on the Crank-Nicolson method, considered in chapter 1. The Crank-Nicolson scheme is second-order accurate and unconditionally stable (at least in the European case). These two factors become especially important when pricing occupational time derivatives. With two time variables to consider, the storage requirements are restricted by the number of timesteps used. At each point in real time, the value of the option for all values of barrier time must to be stored, in addition to all asset values. Consequently, if the number of timesteps is doubled, then so is the storage requirement. Hence, the number of nodes over which we must solve at each timestep will also double, resulting in a (minimum) fourfold increase in computation time. Consequently, the ability to gain accurate results with a small number of timesteps will greatly increase the efficiency of the solution.

Since we solve backwards in time, we define two modified variables τ and $\bar{\tau}$, such that

$$0 < \tau = T - t < T, \quad 0 < \bar{\tau} = \bar{T} - \bar{t} < \bar{T}.$$

Using this change of variables in (4.5) and (4.6) we have the following PDEs,

$$V_\tau + V_{\bar{\tau}} = \frac{1}{2}\sigma^2 S^2 V_{SS} + (r-d)SV_S - rV \tag{4.9}$$

$$V_\tau = \frac{1}{2}\sigma^2 S^2 V_{SS} + (r-d)SV_S - rV. \tag{4.10}$$

The PDE (4.10) can be discretised in the standard fashion. However (4.9) is a little unusual as it has two time derivatives. Discretising according to the Crank-Nicolson method, the left hand side of (4.9) becomes

$$\begin{aligned} V_\tau + V_{\bar{\tau}} \simeq\ & \frac{1}{2}\left\{ \frac{1}{\Delta\tau}(v_i^{k+1,l+1} - v_i^{k,l+1}) + \frac{1}{\Delta\tau}(v_i^{k+1,l} - v_i^{k,l}) \right\} \\ & + \frac{1}{2}\left\{ \frac{1}{\Delta\bar{\tau}}(v_i^{k+1,l+1} - v_i^{k+1,l}) + \frac{1}{\Delta\bar{\tau}}(v_i^{k,l+1} - v_i^{k,l}) \right\}, \end{aligned} \tag{4.11}$$

where $V(i\cdot\Delta S, k\cdot\Delta\tau, l\cdot\Delta\bar{\tau}) = v_i^{k,l}$. The PDE (4.9) is derived from (4.1) with $dt = d\bar{t}$, so we may set $\Delta\tau = \Delta\bar{\tau}$, and then (4.11) becomes

$$V_\tau + V_{\bar{\tau}} = \frac{1}{\Delta\tau}(v_i^{k+1,l+1} - v_i^{k,l}). \tag{4.12}$$

The discretisation of (4.11) uses the four time points at nodes (k,l), $(k,l+1)$, $(k+1,l)$ and $(k+1,l+1)$ and for second-order accuracy, the right hand side should be the average over all four nodes. However, our choice of $\Delta\bar{\tau} = \Delta\tau$ leads to fortuitous cancellations taking place, resulting in a discretisation over just the two nodes (k,l) and $(k+1,l+1)$, and therefore we can maintain second-order accuracy on the right-hand-side averaging over just those two nodes. By using just two nodes storage requirements are reduced; we need only store values at one timestep. It is not required that $\Delta\tau = \Delta\bar{\tau}$ in order to solve the PDE. In fact, if $\Delta\tau \neq \Delta\bar{\tau}$ then the cancellations do not take place and we will need to use all four nodes on the right hand side. Also there will be stability issues (which are discussed later in section 4.4), increased storage and iteration (Parisian option only) in this case.

4.2.3 Two Numerical Schemes

We present two possible schemes using either two or four nodes. Scheme 1 has the restriction $\Delta\bar{\tau} = \Delta\tau$ whereas we are free to choose $\Delta\bar{\tau}$ in Scheme 2. The latter is more flexible, but it comes at a price: the scheme can oscillate violently.

Scheme 1

For an 'up' option we can form the following set of equations,

$$\begin{aligned} \alpha_i v_{i-1}^{k+1,l+1} + (\frac{1}{\Delta\tau} + \beta_i) v_i^{k+1,l+1} + \gamma_i v_{i+1}^{k+1,l+1} &= Z_i^{k,l+1} \quad \text{if} \quad i < h_i, \\ \alpha_i v_{i-1}^{k+1,l+1} + (\frac{1}{\Delta\tau} + \beta_i) v_i^{k+1,l+1} + \gamma_i v_{i+1}^{k+1,l+1} &= Z_i^{k,l} \quad \text{if} \quad i \geq h_i. \end{aligned} \tag{4.13}$$

where the position of the barrier is $h_i = \text{NINT}\left(\frac{H}{\Delta S}\right)$ and

$$Z_i^{k,l} = -\alpha_i v_{i-1}^{k,l} + (\frac{1}{\Delta\tau} - \beta_i)v_i^{k,l} - \gamma_i v_{i+1}^{k,l}.$$

To avoid non-linearity errors in the scheme, it is best to set ΔS such that

$$e_i \cdot \Delta S = E,$$
$$h_i \cdot \Delta S = H,$$

where e_i and h_i are integers, and also $\Delta\tau$ so that

$$t_k \cdot \Delta\tau = T,$$
$$\bar{t}_l \cdot \Delta\tau = \bar{T},$$

where t_k and $\bar{t}_l$ are integers.

Scheme 2

If we discretise with $\Delta\tau \neq \Delta\bar{\tau}$ then,

$$\begin{aligned}
\alpha_i v_{i-1}^{k+1,l+1} + (\frac{1}{\Delta\tau} + \beta_i)v_i^{k+1,l+1} + \gamma_i v_{i+1}^{k+1,l+1} &= Z_i^{k,l+1} \\
&\text{if} \quad i < h_i, \\
\frac{1}{2}\alpha_i v_{i-1}^{k+1,l+1} + \frac{1}{2}\left(\frac{1}{\Delta\tau} + \frac{1}{\Delta\bar{\tau}} + \beta_i\right) v_i^{k+1,l+1} + \frac{1}{2}\gamma_i v_{i+1}^{k+1,l+1} &= W_i^{k,l} \\
&\text{if} \quad i \geq h_i. \qquad (4.14)
\end{aligned}$$

where

$$\begin{aligned}
W_i^{k,l} = &-\frac{1}{2}\alpha_i v_{i-1}^{k,l} + \frac{1}{2}\left(\frac{1}{\Delta\tau} + \frac{1}{\Delta\bar{\tau}} - \beta_i\right) v_i^{k,l} - \frac{1}{2}\gamma_i v_{i+1}^{k,l} \\
&-\frac{1}{2}\alpha_i v_{i-1}^{k,l+1} + \frac{1}{2}\left(\frac{1}{\Delta\tau} - \frac{1}{\Delta\bar{\tau}} - \beta_i\right) v_i^{k,l+1} - \frac{1}{2}\gamma_i v_{i+1}^{k,l+1} \\
&-\frac{1}{2}\alpha_i v_{i-1}^{k+1,l} - \frac{1}{2}\left(\frac{1}{\Delta\tau} - \frac{1}{\Delta\bar{\tau}} + \beta_i\right) v_i^{k+1,l} - \frac{1}{2}\gamma_i v_{i+1}^{k+1,l}. \qquad (4.15) \\
&\qquad (4.16)
\end{aligned}$$

This scheme is also valid when $\Delta\tau = \Delta\bar{\tau}$ but only has the same accuracy as Scheme 1.

4.2.4 Implementing the Schemes on a Parisian Option

When solving for the Parisian option to obtain a consistent solution we must ensure that the continuity of paths condition (4.7) is satisfied. Let us consider Scheme 1 first, for an up-and-out option. To start, we must find the value of the option at the barrier. This is found by solving (4.13) with $l = \bar{t}_l$ for all i. Then we set

$$v_{h_i}^{k+1,l} = v_{h_i}^{k+1,t_l} \qquad \text{for} \qquad 0 < l < \bar{t}_l.$$

For the remaining values of v with $0 < l < \bar{t}_l$, we now solve the second part of (4.13) (with $Z_i^{k,l}$) over the region $h_i < i < n$ with the usual boundary condition for v at $i = n$ and the condition above for v at $i = h_i$, again to reduce the storage requirement we solve from $l = \bar{t}_l - 1$ to $l = 1$.

When using Scheme 2, we see that this is not actually explicit, and we need to iterate in order to find the solution; this is as a result of condition (4.7). In order to solve for v at $l = \bar{t}_l$, we must determine the value at $l = \bar{t}_l - 1$, but this value cannot be calculated without the boundary condition given by (4.7). Consequently, in order to estimate the value at the barrier we solve for v with

$$\alpha_i \left(v_{i-1}^{k+1,t_l}\right)^{q+1} + \left(\frac{1}{\Delta\tau} + \beta_i\right)\left(v_i^{k+1,t_l}\right)^{q+1} + \gamma_i \left(v_{i+1}^{k+1,t_l}\right)^{q+1} = Z_i^{k,t_l} \quad \text{if} \quad i < h_i,$$

$$\frac{1}{2}\alpha_i \left(v_{i-1}^{k+1,t_l}\right)^{q+1} + \frac{1}{2}\left(\frac{1}{\Delta\tau} + \frac{1}{\Delta\bar{\tau}} + \beta_i\right)\left(v_i^{k+1,t_l}\right)^{q+1} + \frac{1}{2}\gamma_i \left(v_{i+1}^{k+1,t_l}\right)^{q+1} = \left(W_i^{k,t_l-1}\right)^q \quad \text{if} \quad i \geq h_i,$$

at the $(q+1)$th iteration. The right-hand side $\left(W_i^{k,t_l-1}\right)^q$ uses the qth iteration

$\left(v^{k+1,t_l}\right)^q$ as a guess for the value at the current time step. Next we solve

$$\frac{1}{2}\alpha_i\left(v_{i-1}^{k+1,l+1}\right)^{q+1}+\frac{1}{2}\left(\frac{1}{\Delta\tau}+\frac{1}{\Delta\bar{\tau}}+\beta_i\right)\left(v_i^{k+1,l+1}\right)^{q+1}+\frac{1}{2}\gamma_i\left(v_{i+1}^{k+1,l+1}\right)^{q+1}=\left(W_i^{k,l}\right)^{q+1},$$

over $h_i < i < n$ moving from $l = 1$ to $l = t_l - 1$, with

$$\left(v_{h_i}^{k+1,l}\right)^{q+1}=\left(v_{h_i}^{k+1,t_l}\right)^{q+1}.$$

We can use the $(q+1)$th estimate for W if we use the most up to date value at $l-1$. The scheme does converge, but significantly slower if the qth estimate is used.

4.3 ParAsian Options

An obvious extension to the Parisian option is the ParAsian option. For a Parisian, if the asset price were to fluctuate above and below the barrier, it is possible that the option would not be knocked-in/out even though it may have spent a considerable time over the barrier. Hence we define the ParAsian option to be the cumulative time spent over the barrier. It turns out that these options can be priced more easily than their Parisian counterparts, because of not having to reset the clock at the barrier.

The formulation of this class of option is essentially the same as for the Parisians, except that we must now solve over all values of $\bar{t}$ even when the asset price is not beyond the barrier, since the clock retains its value even when it is not ticking. The change in barrier-clock is now defined as

$$d\bar{t}=\begin{cases}0 & \text{if} \quad S(t)<H\\ dt & \text{if} \quad S(t)\geq H\end{cases}, \tag{4.17}$$

where the ParAsian option here is of the 'up' variety. The boundary condition (4.7) is not required as the clock is not reset.

Using the BSM framework as above, we arrive at the same two PDEs as before,

(4.5) and (4.6), except they are valid over different regions. For an up (down) option, we must solve (4.5) for $\bar{t} < \bar{T}$ when the asset price is below (above) the barrier, and (4.5) for $\bar{t} < \bar{T}$ when the asset value is at or above (below) the barrier.

4.3.1 ParAsian Options – Boundary Conditions

There is no condition on the value of the ParAsian option at the barrier since the clock is not reset. Nevertheless, we must still maintain the continuity of both V and its first derivative $\frac{\partial V}{\partial S}$ across the barrier, resulting in the following equations

$$\lim_{S\uparrow H} V(S,t,\bar{t}\,) = \lim_{S\downarrow H} V(S,t,\bar{t}\,), \tag{4.18}$$

$$\lim_{S\uparrow H} \frac{\partial V}{\partial S}(S,t,\bar{t}\,) = \lim_{S\downarrow H} \frac{\partial V}{\partial S}(S,t,\bar{t}\,). \tag{4.19}$$

Any solution of the BSM PDE will be at least $\mathcal{C}^1$ continuous so will satisfy both (4.18) and (4.19). However, this condition becomes important, later in chapter 7, when we study the delayed-exercise option, and these conditions are used to derive the position of the barrier. Otherwise, boundary conditions for ParAsian options will be interchangeable with those for Parisian options.

4.3.2 Implementing the schemes on a ParAsian Option

Implementing schemes on a ParAsian option is significantly easier than in the case of a Parisian option, and so we deal with the former case first. First, let us consider scheme 1. At each timestep simply solve (4.13) for $0 < l \leq \bar{t}_l$ in the appropriate regions in S depending on whether the option is 'down' or 'up'. We may also have to solve for the corresponding European (or American) option which the holder receives if the option is an 'in' option. Hence, for the 'in' option

$$v_i^{k,0} = V_E(S,\tau),$$

otherwise if the option is 'out' then

$$v_i^{k,0} = 0.$$

Since $v^{k+1,l+1}$ depends on $v^{k,l+1}$ and $v^{k,l}$, then the scheme can be solved backwards from $l = \bar{t}_l$ to $l = 1$ so that v need only be stored at one time level, namely k.

For Scheme 2, (4.14) is implemented on the appropriate regions. Now $v^{k+1,l+1}$ depends on $v^{k,l+1}$, $v^{k+1,l}$, and $v^{k,l}$, so the scheme must be stored at two time levels k and $k+1$ and solved forwards from $l = 1$ to $l = \bar{t}_l$ so that the updated $v^{k+1,l}$ can be used to solve for $v^{k+1,l+1}$.

4.4 Results

We compare our results to those of Haber et al. (1999) (obtained using an explicit scheme) for the up-and-out call. Scheme 1 with $\Delta\bar{\tau} = \Delta\tau$ is compared to Scheme 2 with varying $\Delta\bar{\tau}$. It is well known that a central-difference scheme such as Crank-Nicolson, while being efficient and accurate for smooth solutions, has difficulty dealing with discontinuous solutions. As described earlier, such a discontinuity propagates along the line $\tau = \bar{\tau}$ (beyond the barrier), where the option value is either almost definitely knocked out ($\tau > \bar{\tau}$), or will definitely reach maturity and gain a payoff ($\tau < \bar{\tau}$). It would be unreasonable to assume that there is not a possibility that the solution may oscillate in this region in the common phenomenon experienced by central-differencing schemes. In figure 4.1, the solution in such a region is investigated. The four diagrams represent four possible cases. The variation of a Parisian option value is shown with $\bar{\tau}$, for an up-and-out call with barrier $H = 12$; the time-to-maturity $\tau = 0.01$. The five plots indicate the value of the option at $S = 12$, though to 12.225 with intervals of 0.025. This region is shown as it is the most sensitive and has greatest influence on the option value below the barrier (the value below the barrier is unconditionally stable since the option cannot be knocked out in this region). The horizontal line in all four figures is the value at $S = 12$; at the barrier the

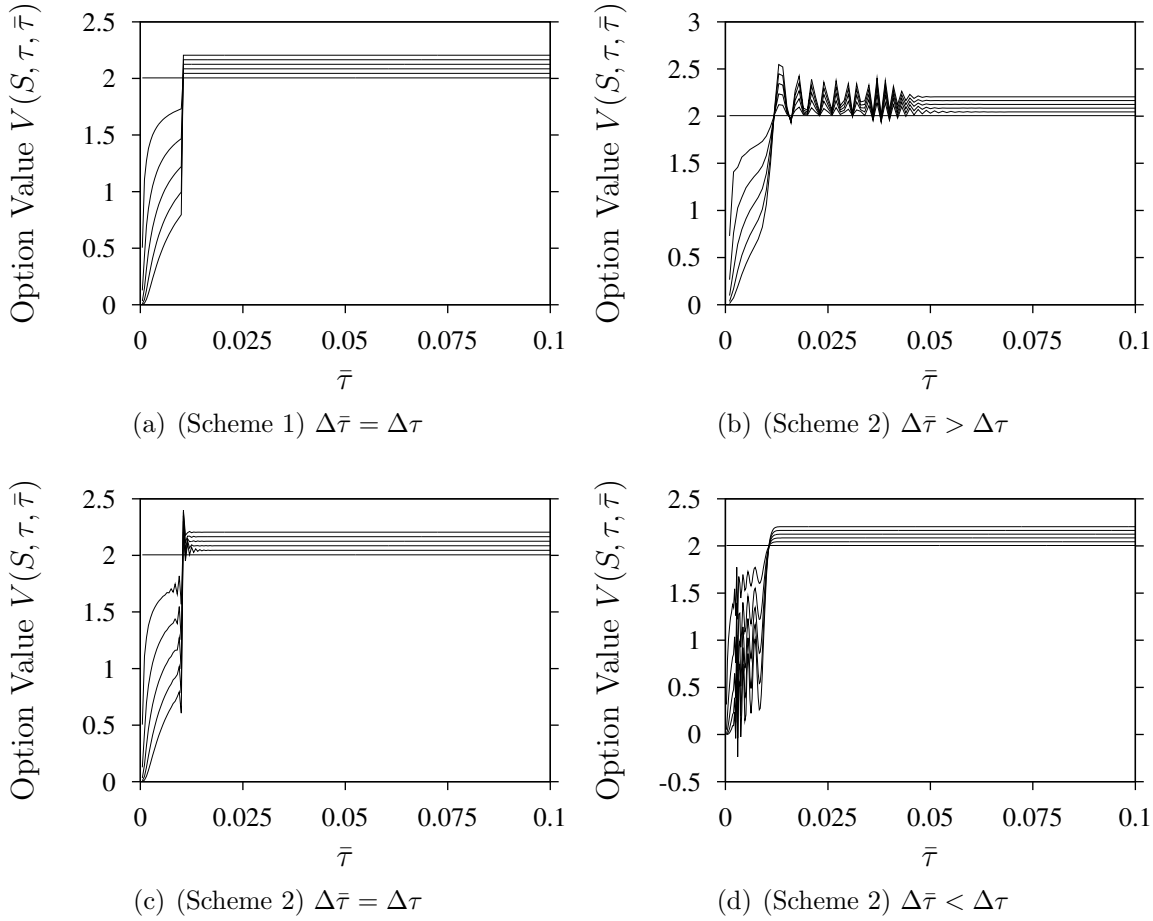

(a) (Scheme 1) $\Delta\bar{\tau} = \Delta\tau$

(b) (Scheme 2) $\Delta\bar{\tau} > \Delta\tau$

(c) (Scheme 2) $\Delta\bar{\tau} = \Delta\tau$

(d) (Scheme 2) $\Delta\bar{\tau} < \Delta\tau$

Figure 4.1
Parisian up-and-out option vs. time-to-knockout close to maturity
The value of a Parisian up-and-out option against time-to-knockout for $S = 12$ through to 12.225 with intervals of 0.025. Here $E = 10$, $H = 12$, $\sigma = 0.2$, $r = 0.05$, and $\tau = 0.1$

value is constant across $\bar{\tau}$ from condition (4.7). As $\bar{\tau} \gg \tau$ then the value approaches the vanilla call option price; the maximum occupation time is $\bar{T} = 0.1$.

The value calculated by Scheme 1 is shown in figure 4.1(a). The value appears smooth and the sharp wave form at $\bar{\tau} = \tau = 0.01$ is maintained. For Scheme 2, however, things deteriorate. When $\Delta\bar{\tau} > \Delta\tau$ (figure 4.1(b)) the solution has oscillations that are both large and move past the point at which $\tau = \bar{\tau}$. When $\Delta\bar{\tau} < \Delta\tau$ the solution seems satisfactory when $\bar{\tau} > \tau$ (there is some smoothing of the discontinuity), but there are large and violent oscillations in the solution when $\bar{\tau} < \tau$ resulting in erroneous negative option values. Even when $\Delta\bar{\tau} = \Delta\tau$ there are still small oscillations either side of $\tau = \bar{\tau}$.

Nonetheless, as τ increases, the oscillations become damped, and the solution at

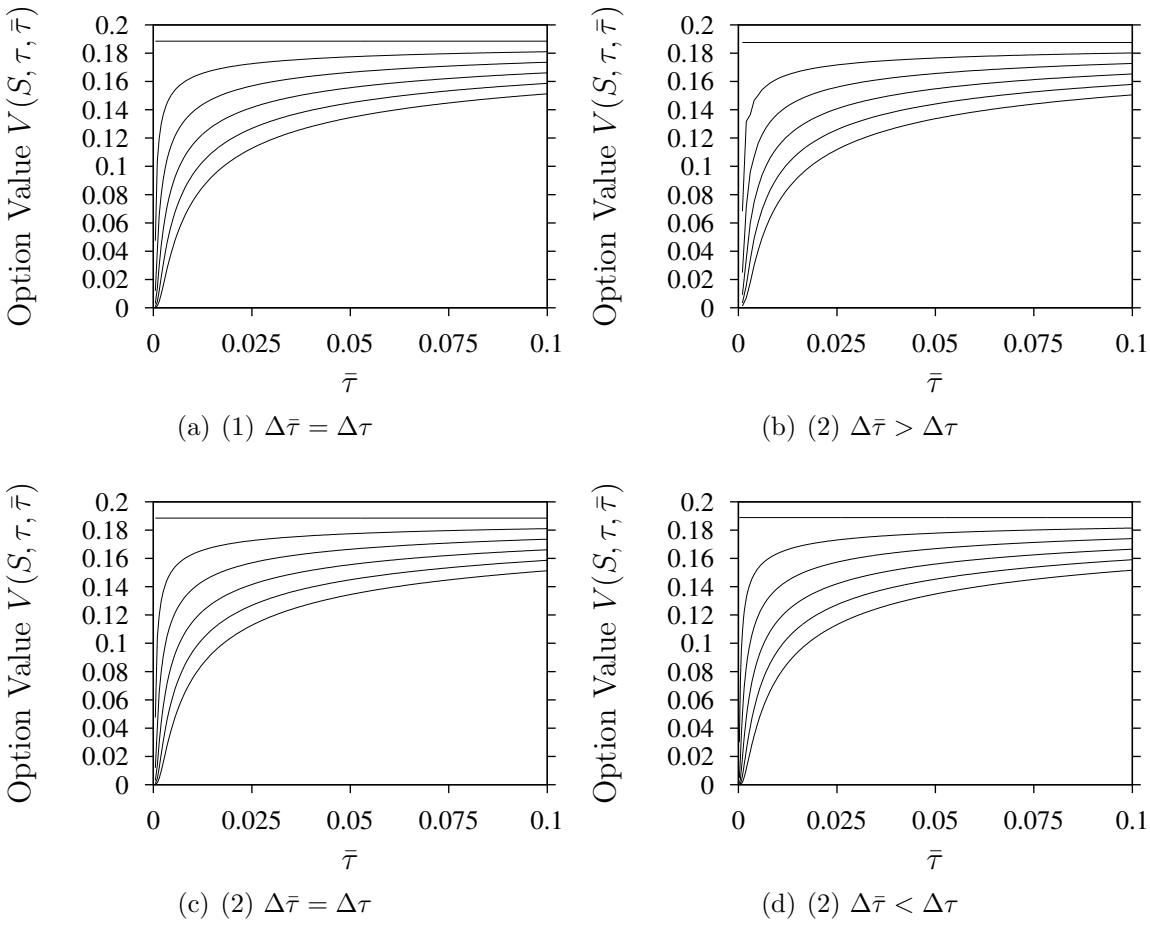

(a) (1) $\Delta\bar{\tau} = \Delta\tau$

(b) (2) $\Delta\bar{\tau} > \Delta\tau$

(c) (2) $\Delta\bar{\tau} = \Delta\tau$

(d) (2) $\Delta\bar{\tau} < \Delta\tau$

Figure 4.2
Parisian up-and-out option value vs. time-to-knockout.
The value of a Parisian up-and-out option against time-to-knockout for $S = 12$ through to 12.225 with intervals of 0.025. Here $E = 10$, $H = 12$, $\sigma = 0.2$, $r = 0.05$, and $\tau = 1$

$\tau = T$ appears to be smooth. Figure 4.2 shows the same option values evaluated with the same schemes at $\tau = 1$ (so that $\tau \gg \bar{\tau}$). The solutions for $\Delta\bar{\tau} > \Delta\tau$ still appear to be slightly oscillatory. It may be possible to damp down these oscillations by reducing $\Delta\bar{\tau}$, however, when $\Delta\bar{\tau} \leq \Delta\tau$ the oscillations become damped and the solutions appear accurate and reliable.

4.4.1 Parisian Options

The following results in figures 4.3–4.5 are comparable to those of Haber et al. (1999). In figure 4.3 the value of a Parisian up-and-out call option is shown. The parameters are: $\sigma = 0.2$, $r = 0.05$, $\bar{\tau} = 0.1$, $T = 1$ and $H = 12$. When S is small and far from the barrier, the option behaves as a vanilla call option. As the asset price approaches the barrier, the value of the option is dragged down as the probability that it will be knocked out at some time during the lifetime of the option is increased. For S greater than H, the option value behaves as a knockout option with a rebate of $V(S = H, \tau, \bar{T})$. The value of the delta is continuous across the barrier at $\bar{\tau} = \bar{T}$, but has a large discontinuity at the barrier for all other values of $\bar{\tau}$; the delta is strictly negative above the barrier.

In figure 4.3(a) the value of the option for very small $\bar{\tau}$ is shown. Above the barrier the option is practically worthless, since the option is almost knocked out. If the asset value is close to the barrier, there may be a slight chance that the asset value will hit the barrier before it is knocked out, and there will be a large positive jump in the value of the option. This results in a large negative value of the delta; this situation is not as prominent as the situation for a barrier option, where small price movements can have a large effect on the hedging strategy (whenever the asset price is close to the barrier). Here, only when the asset has followed a particular path will the situation arise, and hence, the probability of a practitioner having to hedge in such a way is unlikely. It is, however, a problem that can be overcome by taking the cumulative time spent over the barrier rather than the consecutive time.

The convergence of the Crank-Nicolson numerical scheme is shown in table 4.1.

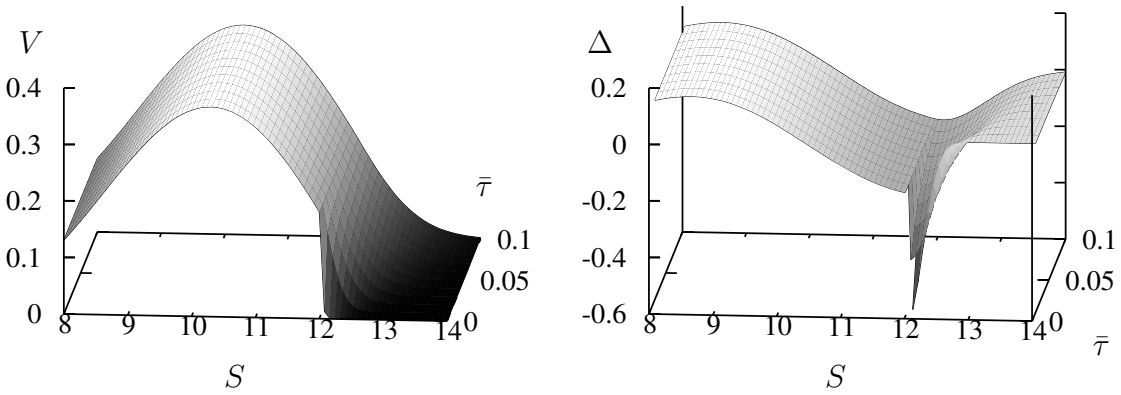

(a) Parisian option value (b) Parisian option delta

Figure 4.3
Parisian option value/delta vs. asset price and time-to-knockout
The parameters are $E = 10$, $H = 12$, $\sigma = 0.2$, $r = 0.05$, and $\tau = 1$.

Table 4.1
Convergence of the Parisian solver

n	S	$V(S,0,0)$	ratio	$V_{RE}(S,0,0)$	ratio	$V_{RE2}(S,0,0)$
201	10.00	0.273459	NA	NA	NA	NA
401	10.00	0.274040	1.76	0.274618	NA	NA
801	10.00	0.274400	1.89	0.274759	4.14	0.274806
1601	10.00	0.274597	1.95	0.274793	4.05	0.274805
3201	10.00	0.274699	1.97	0.274802	4.00	0.274805

The exact value (inverse Laplace) given by Zhu and Stokes (1999) for these parameters is 0.2748, with their finite element scheme giving a value of 0.274975. The option is a down-and-out Parisian with $E = 10$, $H = 8$, $T = 1$, $\bar{T} = 0.1$, $\sigma = 0.2$ and $r = 0.08$. We use n steps in both S and t. The third column is the calculated value while the fifth is a linear Richardson extrapolation, and the seventh a quadratic Richardson extrapolation on the extrapolated results. The ratio gives the ratio of the change in errors for successive grids.

Table 4.2
Comparison of results

	Crank-Nicolson			Explicit		
S	$\bar{t}=0$	$\bar{t}=0.05$	$\bar{t}=0.095$	$\bar{t}=0$	$\bar{t}=0.05$	$\bar{t}=0.095$
11.05	0.3318	0.3318	0.3318	0.2783	0.2783	0.2783
11.24	0.3106	0.3106	0.3106	0.2566	0.2566	0.2566
11.43	0.2851	0.2851	0.2851	0.2314	0.2314	0.2314
11.62	0.2557	0.2557	0.2557	0.2030	0.2030	0.2030
11.81	0.2228	0.2228	0.2228	0.1719	0.1719	0.1719
12.01	0.1870	0.1859	0.1781	0.1387	0.1242	0.0622
12.21	0.1494	0.1315	0.0397	0.1062	0.0814	0.0000
12.42	0.1132	0.0839	0.0027	0.0771	0.0478	0.0000
12.63	0.0811	0.0480	0.0000	0.0529	0.0249	0.0000
12.84	0.0549	0.0244	0.0000	0.0342	0.0113	0.0000
13.06	0.0351	0.0110	0.0000	0.0208	0.0044	0.0000
13.28	0.0211	0.0044	0.0000	0.0118	0.0014	0.0000
13.50	0.0120	0.0016	0.0000	0.0063	0.0004	0.0000
13.73	0.0064	0.0005	0.0000	0.0031	0.0001	0.0000
13.96	0.0032	0.0001	0.0000	0.0014	0.0000	0.0000

Comparison of results between the Crank-Nicolson scheme used here, and the explicit scheme used in Haber et al. (1999). The option being valued is an up-and-out Parisian with $E = 10$, $H = 12$, $T = 1$, $\bar{T} = 0.1$, $\sigma = 0.2$ and $r = 0.05$. The Crank-Nicolson scheme uses extrapolated results from 801, 1601 and 3201 node (both S and t) calculations.

We see that second order convergence from the scheme is lost due to the errors described earlier, with the ratio for the unextrapolated results around 2. However, linear Richardson extrapolation leads to results that show second order convergence (ratio around 4), which can then be extrapolated a further time to yield highly accurate results.

In table 4.2, we compare our results to those of Haber et al. (1999). Our results have been interpolated from a uniform grid in S, to match those from the transformed grid of Haber et al. (1999). Since Haber et al. (1999) do not present any convergence analysis, we can only conclude that the explicit scheme is not even remotely accurate, with large errors contaminating the entire solution. Anyone wishing to solve for a Parisian option with an explicit finite difference scheme must therefore be wary of potentially huge errors.

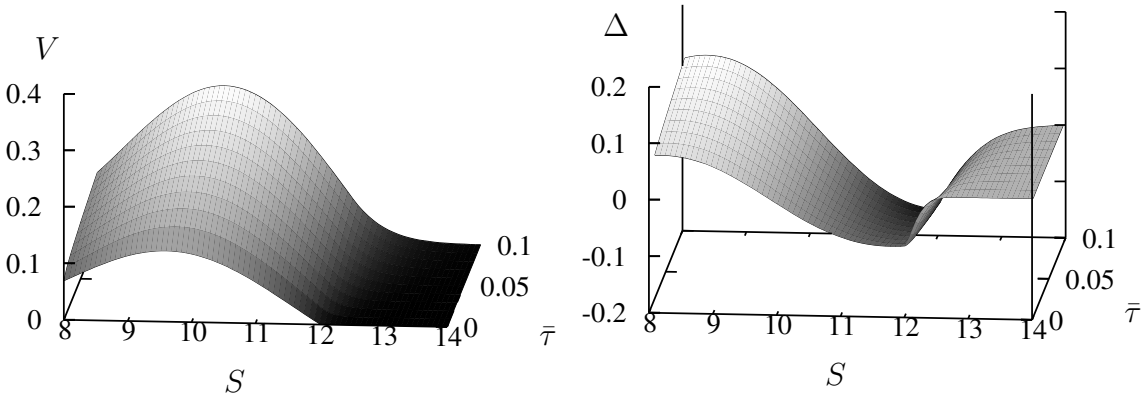

(a) ParAsian Option Value (b) ParAsian Option Delta

Figure 4.4
ParAsian option value/delta vs. asset price and time-to-knockout
The parameters are $E = 10$, $H = 12$, $\sigma = 0.2$, $r = 0.05$, and $\tau = 1$.

4.4.2 ParAsian Options

The ParAsian option exhibits a smoother solution, due to the continuity of the first derivative with respect to asset price S over the solution space. The ParAsian option is more likely to be knocked out than its Parisian counterpart, which causes the price of the option to drop accordingly. Since the ParAsian option is solved over the entire state space, we have a solution at every point even below the barrier and it can be seen that

$$\lim_{\bar{\tau}\to 0} V(S,\tau,\bar{\tau}) = V_B(S,\tau),$$

where $V_B(S,\tau)$ is the value of the corresponding straight barrier option. Again, when $\bar{\tau} \to 0$ and S is close to but not beyond the barrier H, there will be sharp movements in the delta. Figure 4.4 shows the option price and its delta, which is now continuous and of much smaller magnitude than its Parisian counterpart.

Figure 4.5 compares the magnitude of the Parisian price and the ParAsian price. The lower price of the ParAsian would be attractive to purchasers of the option (one of the main reasons for buying the barrier option is because it is cheaper than the corresponding vanilla) and it also appears that it will be easier to hedge than the corresponding Parisian. The large discontinuity in the hedging strategy across the barrier of the Parisian exposes the writer of the option to a large amount of

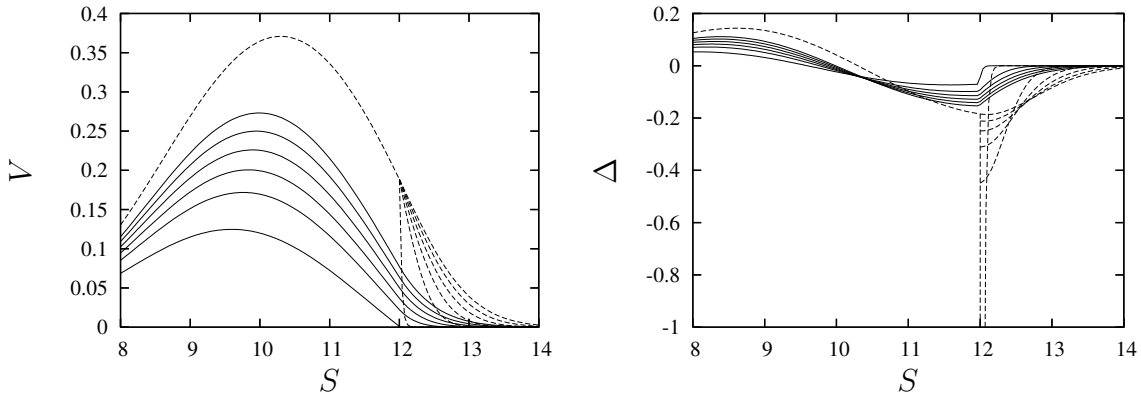

(a) Option Value (b) Option Delta

Figure 4.5
Parisian/ParAsian option value/delta vs. asset price.
The ParAsian option (solid line) and the Parisian option (dashed line), are shown for differing time-to-knockout. Again the parameters are $E = 10$, $H = 12$, $\sigma = 0.2$, $r = 0.05$, and $\tau = 1$

risk, indicated by the delta. The value of the gamma gives some indication into the risk exposure of the delta hedge and is discontinuous across the barrier even for the ParAsian. In the next section, the IT option has a solution which is continuous in both its delta and gamma, and therefore has less risk involved in hedging.

4.5 A New Option – The Integral Time Model

Even though the Parisian options were created to ease hedging around the barrier, some problems still exist, which led Linetsky (1999) to propose the **step** option, in which the payoff at the end is proportional to the time spent under the barrier. By removing large jumps in the payoff the hedging strategy of the option is smoother. For a similar reason, we propose the integral time ParAsian option which has a smoother transition across the barrier than the ParAsian or Parisian. An option of this form has been investigated by Xiao (2007) with regard to foreign exchange options. In the paper by Haber et al. (1999) it is suggested that it would be simple to modify the behaviour of the barrier-clock so that, for instance, more weight could be given according to the size of deviations above (below) the barrier. Let us examine such a model with a cumulative clock, for an up option with barrier H; let the integral I be

defined as

$$I = \int_0^t dI(t),$$

where

$$dI = \begin{cases} 0 & \text{if} \quad S(t) < H \\ \chi(S(t) - H)dt & \text{if} \quad S(t) \geq H \end{cases}. \tag{4.20}$$

Such a situation is shown in figure 4.6. The shaded area indicates the area between the barrier H (here $H = 1.4$) and the asset price. The parameter χ, used to scale the deviations over the barrier, is dimensionless since I has units $[S \times t]$. If S follows the usual geometric Brownian motion in (4.2) then the small change in option price becomes

$$dV = \sigma S \frac{\partial V}{\partial S} dX + \left(\mu S \frac{\partial V}{\partial S} + \frac{1}{2}\sigma^2 S^2 \frac{\partial^2 V}{\partial S^2} + \frac{\partial V}{\partial t} \right) dt + \frac{\partial V}{\partial I} dI,$$

and using the appropriate form for dI we obtain the following

$$dV = \begin{cases} \sigma S \dfrac{\partial V}{\partial S} dX + \left(\mu S \dfrac{\partial V}{\partial S} + \dfrac{1}{2}\sigma^2 S^2 \dfrac{\partial^2 V}{\partial S^2} + \dfrac{\partial V}{\partial t} \right) dt \\ \qquad\qquad\qquad\qquad\qquad\qquad \text{if} \quad S(t) < H \\ \sigma S \dfrac{\partial V}{\partial S} dX + \left(\mu S \dfrac{\partial V}{\partial S} + \dfrac{1}{2}\sigma^2 S^2 \dfrac{\partial^2 V}{\partial S^2} + \dfrac{\partial V}{\partial t} + \chi(S - H)\dfrac{\partial V}{\partial I} \right) dt \\ \qquad\qquad\qquad\qquad\qquad\qquad \text{if} \quad S(t) \geq H \ . \end{cases} \tag{4.21}$$

Then, setting up the BSM hedging portfolio as usual we arrive at the following two PDEs

$$\frac{\partial V}{\partial t} + \frac{1}{2}\sigma^2 S^2 \frac{\partial^2 V}{\partial S^2} + (r - d)S\frac{\partial V}{\partial S} - rV = 0 \quad \text{if} \quad S < H, \tag{4.22}$$

$$\chi(S - H)\frac{\partial V}{\partial I} + \frac{\partial V}{\partial t} + \frac{1}{2}\sigma^2 S^2 \frac{\partial^2 V}{\partial S^2} + (r - d)S\frac{\partial V}{\partial S} - rV = 0 \quad \text{if} \quad S \geq H. \tag{4.23}$$

We call this new class of options Integral Time (IT) options. The option described here is a ParAsian IT option; however, there are many possible variations of the IT option. The option can be up/down, in/out, Parisian/ParAsian, or have a second barrier (step or switch type option). The option may also depend on the time

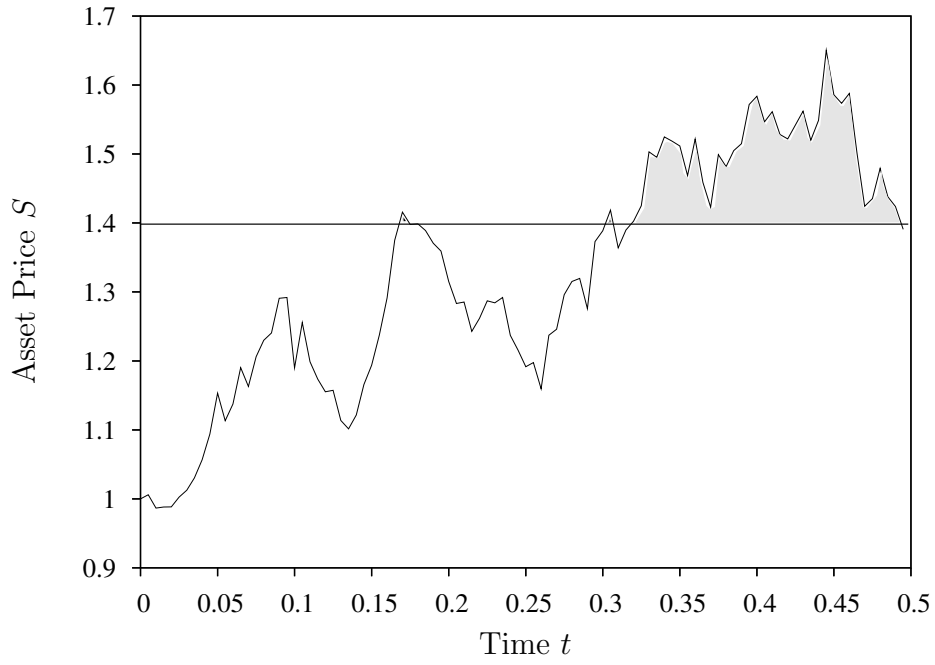

Figure 4.6
A Monte-Carlo simulation of how the area over the barrier is formed.

spent over the barrier as well as the area over the barrier. We concentrate here on the ParAsian IT option and present some interesting findings about the associated Greeks.

4.5.1 Implementing a Crank-Nicolson Scheme on the IT option

Let us reconsider the PDEs (4.22) and (4.23). The only difference between these PDEs and those applicable for the Parisian/ParAsian options is the coefficient of the barrier-clock derivative. It is clear now that if we discretise setting $\Delta\tau = \Delta I$ then terms will not cancel as they do in Scheme 1; hence we follow the methodology developed for Scheme 2. Equation (4.22) will discretise in the usual manner. For (4.23), we use a Crank-Nicolson scheme on the left-hand side;

$$V_\tau + \chi(S-H)V_I \simeq \frac{1}{2}\left\{\frac{1}{\Delta\tau}(v_i^{k+1,l+1} - v_i^{k,l+1}) + \frac{1}{\Delta\tau}(v_i^{k+1,l} - v_i^{k,l})\right\}$$
$$+\zeta_i \frac{1}{2}\left\{\frac{1}{\Delta I}(v_i^{k+1,l+1} - v_i^{k+1,l}) + \frac{1}{\Delta I}(v_i^{k,l+1} - v_i^{k,l})\right\}, \quad (4.24)$$

where

$$\zeta_i = \chi(i \cdot \Delta S - h_i \cdot \Delta S).$$

Then (4.22) and (4.23) become

$$\begin{aligned}
\alpha_i v_{i-1}^{k+1,l+1} + (\frac{1}{\Delta\tau} + \beta_i) v_i^{k+1,l+1} + \gamma_i v_{i+1}^{k+1,l+1} &= Z_i^{k,l+1} \\
&\text{if} \quad i \le h_i, \\
\frac{1}{2}\alpha_i v_{i-1}^{k+1,l+1} + \frac{1}{2}\left(\frac{1}{\Delta\tau} + \zeta_i \frac{1}{\Delta\bar{\tau}} + \beta_i\right) v_i^{k+1,l+1} + \frac{1}{2}\gamma_i v_{i+1}^{k+1,l+1} &= W_i^{k,l} \\
&\text{if} \quad i > h_i. \qquad (4.25)
\end{aligned}$$

where

$$\begin{aligned}
W_i^{k,l} = &-\frac{1}{2}\alpha_i v_{i-1}^{k,l} + \frac{1}{2}\left(\frac{1}{\Delta\tau} + \zeta_i \frac{1}{\Delta\bar{\tau}} - \beta_i\right) v_i^{k,l} - \frac{1}{2}\gamma_i v_{i+1}^{k,l} \\
&-\frac{1}{2}\alpha_i v_{i-1}^{k,l+1} + \frac{1}{2}\left(\frac{1}{\Delta\tau} - \zeta_i \frac{1}{\Delta\bar{\tau}} - \beta_i\right) v_i^{k,l+1} - \frac{1}{2}\gamma_i v_{i+1}^{k,l+1} \\
&-\frac{1}{2}\alpha_i v_{i-1}^{k+1,l} - \frac{1}{2}\left(\frac{1}{\Delta\tau} - \zeta_i \frac{1}{\Delta\bar{\tau}} + \beta_i\right) v_i^{k+1,l} - \frac{1}{2}\gamma_i v_{i+1}^{k+1,l}\ .
\end{aligned}$$

For the integral time model, the movement of V through I space is linked not just to time, but also to its position in S space. When S is above the barrier, but close to H, ζ_I is very small so the movement of V through I space is very slow. Hence, the scheme should be similar to the standard time-dependent scheme. However, in the Crank-Nicolson scheme, information from the solution at l is used to solve for $l+1$, as we solve for $V(S, \tau + \Delta\tau, I + \Delta I)$ using approximations at $V(S, \tau + 1/2\Delta\tau, I + 1/2\Delta I)$. This should be acceptable, so long as the change in V with respect to I is sufficiently small. We have explained earlier (in section 4.4) how there is an apparent discontinuity in the solution for the Parisian/ParAsian around the line $\tau = \bar{\tau}$. There will exist a similar region in (S, I) space, although it is not as simple here and we cannot define such a line, only a region around the line $\tau = \zeta_i I$. In this region the change of V with respect to I is large, so that the Crank-Nicolson scheme in this region may become highly oscillatory. In figure 4.7 the solution at

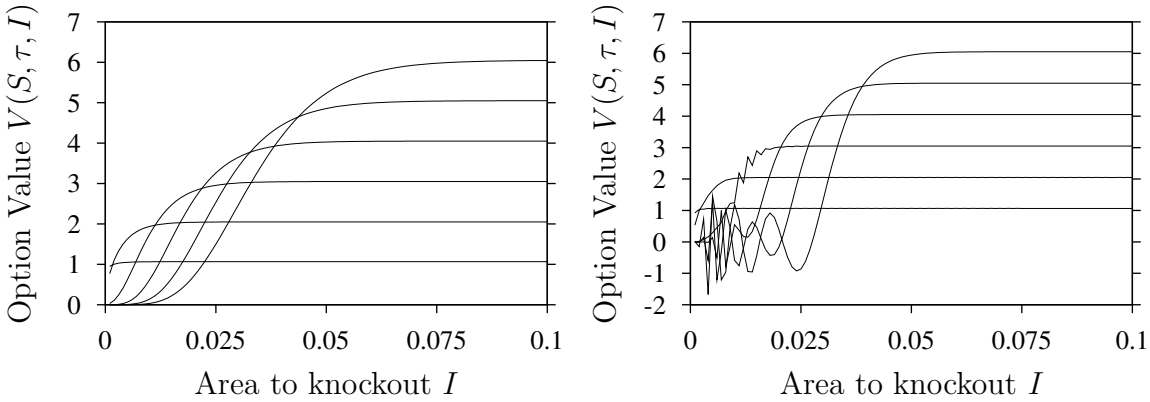

(a) Implicit (b) Crank-Nicolson

Figure 4.7

small τ is shown for both the implicit scheme and the Crank-Nicolson scheme. The plots show the value of the option against I (the *area* left to knockout) for S=11 through to 16. As $I \to \infty$ then the option value is simply a call option. The value of τ is 0.01. The Crank-Nicolson scheme is clearly oscillating in the region where the value of the option changes rapidly with respect to I.

When S is very large, the movement through I space is very rapid and the scheme should be dominated by movement in this direction. Now, the best scheme would be one where we solve for $V(S, \tau + \Delta\tau, I + \Delta I)$ using approximations at $V(S, \tau + \Delta\tau, I + 1/2\Delta I)$. The Crank-Nicolson scheme will be a good approximation to this, so long as the change in V with respect to τ is small. Again, in the region where $\tau = \zeta_i I$, the Crank-Nicolson scheme will become start to oscillate since V can change quickly in time with I held constant.

Considering these observations, we propose that an implicit method should be used, such as the one described in the next section.

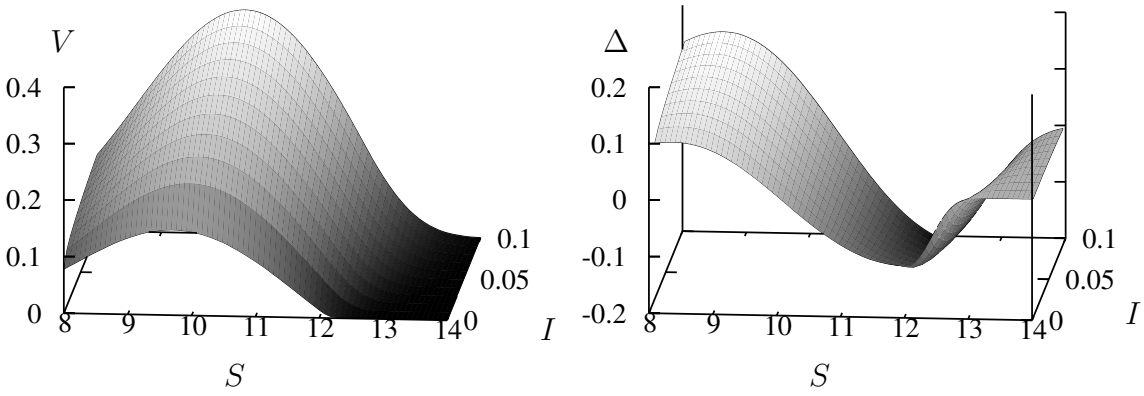

(a) ParAsian IT option value

(b) ParAsian IT option delta

Figure 4.8
ParAsian integral time option value/delta vs. asset price and time-to-knockout.
The parameters are $E = 10$, $H = 12$, $\chi = 1$, $\sigma = 0.2$, $r = 0.05$, $T = 0.1$ and $\bar{I} = 0.1$

4.5.2 An implicit scheme for the IT option

Consider an implicit scheme in time with an 'upwind' difference in I. Then the discretisation over the derivatives in time t and area I are as follows

$$\begin{aligned} V_\tau + \chi(S-H)V_I \;\simeq\; & \frac{1}{\Delta\tau}(v_i^{k+1,l+1} - v_i^{k,l+1}) \\ & + \zeta_i \,\frac{1}{\Delta I}(v_i^{k+1,l+1} - v_i^{k+1,l}). \end{aligned} \tag{4.26}$$

Then we take the other derivatives at the current time (and area level) to arrive at the (first order in $\Delta\tau$ and ΔI) following scheme;

$$\begin{aligned} \alpha_i v_{i-1}^{k+1,l+1} + (\frac{1}{\Delta\tau} + \beta_i) v_i^{k+1,l+1} + \gamma_i v_{i+1}^{k+1,l+1} & \\ = \frac{1}{\Delta\tau} v_i^{k,l+1} \quad \text{if} \quad i < h_i, & \\ \frac{1}{2}\alpha_i v_{i-1}^{k+1,l+1} + \frac{1}{2}\left(\frac{1}{\Delta\tau} + \zeta_i \frac{1}{\Delta\bar{\tau}} + \beta_i\right) v_i^{k+1,l+1} + \frac{1}{2}\gamma_i v_{i+1}^{k+1,l+1} & \\ = \frac{1}{\Delta\tau} v_i^{k,l+1} + \zeta_i \frac{1}{\Delta\bar{\tau}} v_i^{k+1,l} \quad \text{if} \quad i \geq h_i. & \end{aligned} \tag{4.27}$$

4.5.3 Results – ParAsian IT Options

The results presented here have been calculated using the implicit scheme, so as to avoid the violent oscillations caused by the Crank-Nicolson scheme.

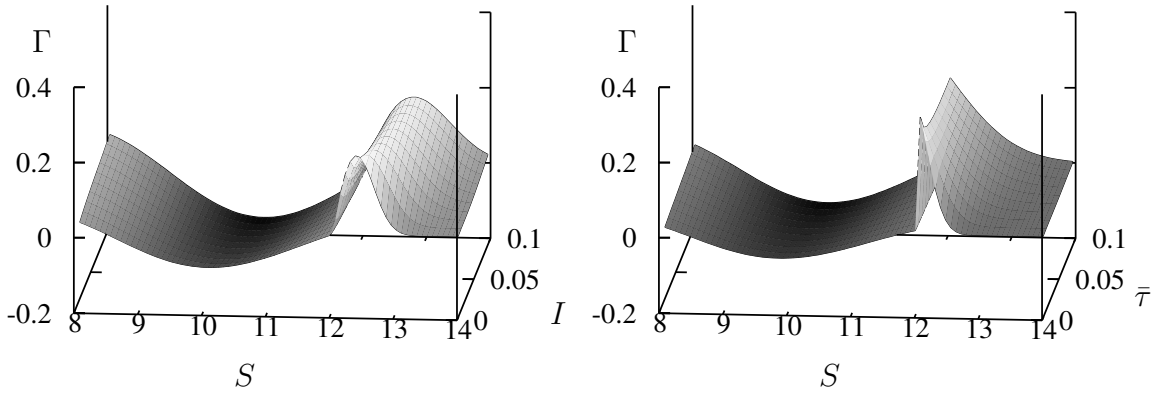

(a) ParAsian IT Option Gamma (b) ParAsian Option Gamma

Figure 4.9
The value of the ParAsian integral time option gamma and the ParAsian option gamma.

The value of the ParAsian IT model is shown in figure 4.8 along with its delta. The option value is similar in magnitude to that of the Parisian option, but is harder to knockout when $S < H + 1$, since the area gained at each timestep is smaller than the time added to the clock in a corresponding ParAsian. When $S > H + 1$ the area gained will be larger than the time added to the clock in a corresponding ParAsian, and the option becomes easier to knockout. In the limit as the area to knockout I tends to zero, the option value will again approach the straight barrier value.

Now, when S is close to the barrier, and the area to knockout I is small, if the asset price moves above the barrier for a short time, whether or not it gets knocked out depends on how far above the barrier the asset price moves. This means that if the asset price only moves a small margin above the barrier, then the area added will be small and the option may not necessarily be knocked out. This has the effect of smoothing the transition toward the vanilla barrier price, as well as smoothing the solution, so it is twice differentiable.

We can see in figure 4.9 that the value of the gamma is now also continuous. Such an option as posed here would have all the benefits of the Parisian and ParAsian option allied with a more stable hedging strategy.

4.6 Conclusions

In this chapter we have examined some of the difficulties of using a Crank-Nicolson scheme to price occupation-time derivatives. One of the main drawbacks, due to the sharp changes in asset price with respect to the barrier time, is the large coefficient of the $O(\Delta t^2)$ errors. When pricing time-dependent barrier options, similar problems can be overcome by reducing the size of the timesteps near the implementation of the barrier. However, we are constrained to keep our timesteps in both directions equal, in order to stop oscillations in the solution. One possible way to circumvent this may be to solve the two coupled PDEs, as suggested in Avellaneda and Wu (1999) with different grids above and below the barrier. A more refined grid could be used beyond the barrier to better capture the fast changing prices in this region. Another method may be to apply singular perturbation analysis, again on the two coupled PDEs; both of these avenues are left for further research.

Chapter 5

Modelling Bankruptcy with ParAsian Options

In this chapter we consider the model developed in collaboration with Yu (2004)[1]. The model uses ParAsian style options discussed in chapter 4. First, we will explain the model, in which some minor modifications have been made by the author since the original work of Yu (2004). Secondly, a description is given of the numerical methods used to solve the problem along with some of the difficulties faced. Finally, a review of results from the modified model will be given (from a mathematical perspective).

In developing the BSM model both Black and Scholes (1973) and Merton (1973) recognised the potential for valuing corporate liabilities under the option pricing framework. Now referred to as Merton-style bond pricing, or a structural model, Merton (1974) values the default risk on a bond as a put option on the value of the firm. The Yu (2004) model of bankruptcy using ParAsian options extends the Merton-style pricing framework to include two important features. First, it can model the accretion of debt by a firm as a constant factor over the life of the contract, by a simple modification of the boundary conditions. Second, the model can include violations of the absolute priority rule (APR) in a two-class debt structure. The APR simply states that the senior creditors claims take precedence over the junior

[1]The model and results here are distinct from the original model by Yu. The chapter is loosely based on Yu et al. (2007) currently in preparation.

creditors, and the junior creditors claims take precedence over the shareholders' claims in the event of default. The ParAsian feature allows the manner in which the creditors are paid to be different at different times in the contract (specifically either before, or at maturity), again just by modifying the boundary conditions. This means that complex capital structure in the firm can now be modelled using Merton-style pricing.

The Yu (2004) model can also be used (by choosing the level of barrier with respect to the total debt level) to mimic internal bargaining between the creditors, and externally between the creditors and the debtors. The level of the barrier may be chosen according to who is monitoring the firm, the senior creditors or their subordinates, which will depend on their relative payoffs when the firm goes into liquidation.

5.1 Literature

Hovakimian et al. (2001) give empirical evidence to suggest that a firm will adhere to a target leverage ratio, taking on new debt as the value of the firm increases, although they also note that the initial target leverage ratio will change over time, dependent on the firm's profitability and stock price. In the usual structural model, where the value of the firm is modelled by a log-normal geometric Brownian motion, the leverage ratio will tend to zero as time tends to infinity. Collin-Dufresne and Goldstein (2001) attempt to overcome this short-coming in Merton's model by allowing the accretion of debt to be a stochastic process in itself. They define a barrier, k_t, at which default occurs, which is the sum of the value of current debt and the debt currently accrued. The process followed by k_t is mean reverting to the target financial policy of the firm. The model presented by Collin-Dufresne and Goldstein (2001) is a reduced form model and requires the value of recovery rate to be specified, whereas the Yu (2004) model has an endogenous recovery rate.

Of the structural models that have been derived from Merton (1974) innovative work on corporate bonds, those such as Black and Cox (1976) and others give only succinct details of the capital structure of the firm. However empirical evidence,

such as that by Eom et al. (2004) suggests that to price bonds with a simple capital structure will discount a large proportion of the bonds on the market. All of the previous structural models assume that the APR is upheld in all instances, even though there is strong evidence to the contrary. Since the APR is upheld, Black and Cox (1976) show that, under their framework, the senior creditors always benefit from the issuance of subordinate bonds as they increase the chances of the firm being liquidated (the barrier for default is increased), while incurring all of the losses of the creditors. Moraux (2003) uses a time-dependent barrier option, the Parisian, to price debt, and shows how a two-class debt structure may be formed under his framework. However the Yu (2004) model is superior in at least two ways. Parisian options are inferior to ParAsian options when modelling bankruptcy, the creditors of the firm will have a memory of the last time that the barrier was crossed, and will not be so forgiving the next time, so the cumulative part of the option models the fact that if the firm has been in distress, it is far more likely to be liquidated in the future. The Parisian feature is included in Moraux (2003) by pricing a down-and-out call on the firm value, where the value of debt is equal to the firm value short the down-and-out-call. The subordinate bond is priced by going long in a down-and-out call with strike price at senior level, and short a down-and-out call with strike price at the total debt level. The barrier is placed at the total level of debt for all of the options. Under Moraux's framework, the fee received by the creditors cannot be altered to include violation of the APR or the firm taking on new debt.

Both of the above structural models (Black and Cox, 1976; Moraux, 2003) assume that the bonds mature at the same time. Geske (1977) was the first to price options on options, or compound options, which can be applied to the Merton framework of corporate bonds to price both coupon bonds, and bond issuances with different maturity dates. To avoid difficulties with APR, Geske (1977), assumes that the senior bond will always mature first, so that when pricing the subordinate debt, the senior debt maturing is viewed as a coupon payment.

Using a reduced-form model, Unal et al. (2003) consider a two-debt structure and allow for violations of the APR. To capture the violations of APR within the

reduced-form framework, they must introduce a new parameter to model the extra payment to the junior creditors when the APR is violated. This results in another parameter which must be prescribed, along with the recovery rates, whereas they are both endogenous to the Yu (2004) model.

Leland (1994) develops a model to find optimal leverage ratio for a firm subject to default risk, tax, interest rate, bond covenants, payout ratio and the bankruptcy costs. Using perpetual options and constant interest rates they can generate closed form solutions. Here the default barrier is determined endogenously in the solution. Later, Leland and Toft (1996) relax the perpetuity of the option to find the optimal maturity of the bond issue. Ju and Ou-Yang (2006) extend the model further to include stochastic interest rates and find that they have a large role to play in the optimisation of capital structure. Broadie et al. (2007) also look to extend the Leland (1994) model this time by including a renegotiation period. Although the probability of default is increased, the probability of liquidation is now decreased implying that the renegotiation period helps the recovery of firm in distress. They use a binomial method outlined in Broadie and Kaya (2007) that can also be used on the Leland (1994) model.

5.2 The Model

In this section we give a brief description of the Yu (2004) model. When there is a two class debt structure, we can allow for earlier maturing debt by altering the boundary conditions. By using similar methods to those outlined by Geske (1977), we could price bonds with different maturities, but this could potentially lead to infinite combinations of the two maturities. In order to produce the term structure for the bonds for comparison, the bonds have the same maturity with one maturing infinitesimally before the other.

Let us consider the Yu (2004) model with a single debt class. In the classic Merton (1974) model, the bond holder is long the principal amount, and short a put on the firm value with strike price equal to the principal amount. Black and Cox

(1976) introduce a safety covenant in the form of a straight knockout barrier (with rebate), and the Yu model takes this barrier and allows the firm value to be below the barrier for a predetermined amount of time, while the firm undergoes chapter 11[2], which in this context, we shall call the *window*. The window attempts to capture the renegotiation of the firm over the lifetime of the bond. Hotchkiss (1995) and Gilson (1997) find that a large proportion of firms that have undergone renegotiation will perform badly and are likely to enter into reorganisation again, meaning that a cumulative time spent in reorganisation is more appropriate than consecutive time: the creditors will be less forgiving if the firm has been recently in distress. The value of the barrier depends on how closely the creditors monitor the firm. There must be some trade-off, between the cost of monitoring the firm, which is an expensive process (Rajan and Winton, 1995), and the potential losses to the creditors. With a ParAsian option, the barrier may be placed at the level of the debt, which has a trivial value for the straight barrier model (if the safety covenant is at the debt level, the creditors instantly default the firm if the bond cannot be repaid, will incur no losses and the bond is risk-free), or even above it without trivial results. If the creditors act optimally (ignoring the cost of monitoring) then they will place the barrier at the level of debt.

When the debt is divided into two classes, Yu (2004) argues that there is an internal bargaining between the creditors that drives the positioning of the barrier. If the junior creditors cooperate with the senior bond holders, then they will take on the monitoring of the firm and the barrier is placed at the total debt level. If they choose not to cooperate, they may leave the monitoring to the senior creditors, in which case the barrier is placed at the senior debt level. In the results section we present the credit spread for a full range of barrier levels.

When firms issue debt, the senior bonds will often have covenants to safeguard the priority of their debt over earlier-maturing debt. Such a covenant is the cross-default provision, whereby the senior debt is automatically defaulted if the subordinate bond defaults, maintaining priority for the senior debt. Defining S as the face value of

[2]Chapter 11 is a form of bankruptcy that allows reorganisation of the companies debt obligations.

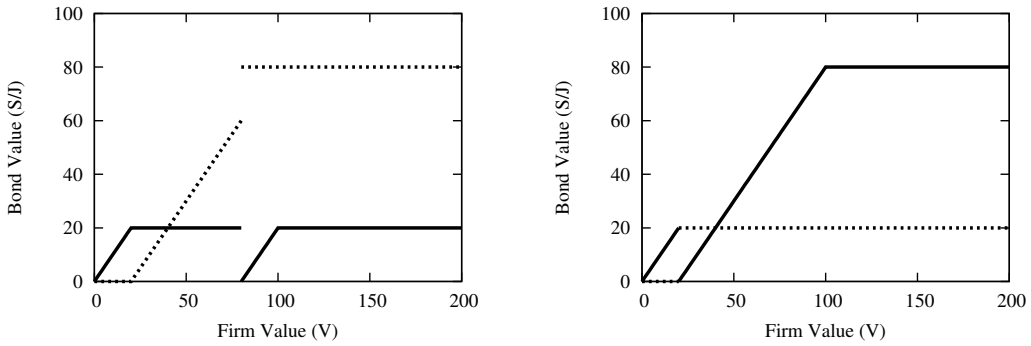

Figure 5.1
Payoffs to Junior and Senior Debt Issues When Junior Debt Matures First.
(a) Junior debt has a higher proportion of the total debt; with $S = 20$ (solid line) and $J = 80$ (dotted line). (b) Senior debt with a higher proportion of total debt; $S = 80$ (solid line) and $J = 20$ (dotted line).

senior debt, and J as the face value of junior debt, figures 5.1(a) and 5.1(b) show the payoff at maturity to the senior and junior debt holders when the junior debt matures first. The senior debt does not always maintain priority even with the cross-default provision. These figures form the basis for our final conditions for the bonds at maturity.

5.3 The Valuation Framework

5.3.1 Assumptions

The cooperative models for the case when senior debt matures earlier and the case when senior debt matures later are labelled as Models Ia and Ib respectively. The non-cooperation model is labelled as Model II, and is applicable to both maturity structures (corresponding to Models Ia and Ib), but with a different bargaining condition; for a single debt issue, we use Model Ia with the face value of junior debt equal to zero, however, the basic assumptions of the models are the same:

Firm value : The dynamics for the asset value, V, follow a geometric Brownian

motion

$$dV = \Bigg[\mu\, V - \delta(t - t_{c_s})\frac{c_s}{2}S_{t_{c_s}^-} - \delta(t - t_{c_j})\frac{c_j}{2}J_{t_{c_j}^-} - \delta(t - t_d)\frac{d}{2}(V - S_{t_d^-} - J_{t_d^-})^+\Bigg]dt + \sigma_V V dZ_V, \quad (5.1)$$

where μ is the instantaneous expected rate of return on the firm, $\delta(\cdot)$ is the Dirac delta function, c_s, c_j and d are coupon rates for senior and junior debt and dividend yield, paid semi-annually at t_{c_s}, t_{c_j} and t_d, respectively, σ_V is the volatility of the asset, dZ_V is a standard Gauss-Wiener process. Here S_{t^-} and J_{t^-} represent the total face value of debt in the firm that is senior and junior respectively (including newly issued debt here). Since the dividend is paid to equity holders, the amount paid is proportional to the firm value minus the face value of debt, or zero if the firm value is below the face value of debt.

Risk-free interest rate : The dynamics of the instantaneous risk-free interest rate, r, follow the Cox et al. (1985) model:

$$dr = \kappa(\theta - r)dt + \sigma_r\sqrt{r}dZ_r, \quad (5.2)$$

where κ is the speed of a mean-reverting process for the short rate; θ is the long-run mean level of interest rate; σ_r is the volatility parameter; dZ_r is also a standard Gauss-Wiener process. The instantaneous correlation coefficient between these two Gauss-Wiener processes is ρ:

$$\mathrm{E}[dZ_V dZ_r] = \rho dt.$$

Recovery :

In contrast to normal structural models where the level of the barrier is in some sense equivalent to the recovery rate, the recovery rate in the ParAsian

framework is endogenous to the model, and so the ParAsian barrier is placed at the total value of the debt. Hence we are not required to give an explicit value for the recovery rate. However at the end of the window, we must decide whether the face value of the bond must be paid in cash, or equivalent securities paying face value at maturity. In most reduced form models such as Longstaff and Schwartz (1995), the recovery rate is defined as the "the fraction of the present value of an otherwise equivalent Treasury bond", and we adopt this approach so that the payout at the end of the window is a security paying face value at maturity. Although there is some evidence to suggest that the recovery rate is best described as "the fraction of the face value of the debt", RFV (Guha, 2002), this could cause some complications. It could be possible for the bond to default even when the firm is not distressed (if interest rates are very high, the value of the firm could be below the face value of the debt, but above the market value), and the bondholders receive more than the bond is worth on the market. This would result in negative credit spreads and possibly negative duration.

Debt level and leverage ratio :

In our model the firm adheres to a constant target leverage ratio. In other words, the firm takes on new debt at the rate at which the total value of the firm increases, in order to keep leverage constant. Under the risk-neutral measure, the rate at which the value of the firm increases is the current interest rate. Then we model the drift of debt level as partly dependent on interest rates (in a risk-neutral environment, the long term mean level of the interest rate θ is the best approximation), and partly dependent on the firm's payout policy. If we let ζ denote the annual payout ratio by the firm, it can be summarised as

$$\zeta V = c_s{}' \cdot \text{Senior Debt} + c_j{}' \cdot \text{Junior Debt} + d' \cdot \text{Equity},$$

where $c_s{}'$, $c_j{}'$ and d' are the coupons and dividends annualised at a continuous

rate. The current total face value of debt at time t can be expressed as:

$$F(t) = F_0\ e^{\phi t},$$

where F_0 is the initial face value of total debt, and $\phi = \theta - \zeta$ is the capital accumulation factor. However, since interest rates are treated as stochastic, the level of the barrier should depend not only on the face value of the debt, but also on the interest rate. Let $L_c(t, r; T)$ be the market value of an equivalent risk-free coupon bond paying 1 dollar at maturity T, with the same coupon payment setting as our corporate bond. This bond can be priced using the CIR equation. Then the default barrier value $K(t, r)$ at time t is set to be:

$$K(t, r) = F_0 \cdot e^{\phi t} \cdot L_c(t, r; T). \tag{5.3}$$

Equation (5.3) is consistent with the definition of recovery rate as the fraction of the equivalent Treasury bond. If we take the recovery rate to be RFV, then the barrier will be:

$$K(t, r) = F_0 \cdot e^{\phi t}. \tag{5.4}$$

ParAsian feature : The trigger of default in the time dimension is the window length of ParAsian options, $\bar{T}$. In addition, when the firm is worthless, it becomes futile in any model for creditors to continue to wait for the emergence of the firm. Zero asset value becomes an absorbing barrier; the window automatically reaches its end for any $\bar{t}$, the measure of the cumulative time below the default barrier. The dynamics of the ParAsian feature follow those set down in chapter 4:

$$d\bar{t} = \begin{cases} 0 & \text{if } V > K(t, r), \\ dt & \text{otherwise.} \end{cases}$$

5.3.2 Partial differential equation - derivation

Pricing the risky debt requires the solution of a four-dimensional problem (in t, $\bar{t}$, V and r). The partial differential equations (PDEs) for both senior and junior debt are the same as for a single issue, in that they are derived from a common process of firm value and interest rates. They differ from one another only through the terminal conditions. Let L denote an otherwise risk-free bond; if we construct a portfolio with long one bond and short a number (D_r/L_r) of risk-free bonds (to eliminate interest-rate risk) and short a number (D_V) of the underlying asset (to eliminate asset risk), then by applying Itô's lemma to equations (5.1) and (5.2), the no-arbitrage condition to the portfolio value (see Yu, 2004 for a full derivation), we obtain the partial differential equation:

$$\begin{aligned} D_t + D_{\bar{t}} + \frac{1}{2}D_{VV}\sigma_V^2 V^2 + \frac{1}{2}D_{rr}\sigma_r^2 r + D_{Vr}\sigma_V V \sigma_r \sqrt{r}\rho \\ + D_r\Big(\kappa(\theta - r) - \lambda\sigma_r\sqrt{r}\Big) + rD_V &= rD, \end{aligned} \tag{5.5}$$

where λ is the market price of risk and D is the general term for debt, which can be senior debt, B, or junior debt, b, or the former definition as the total debt; subscripts on D denote partial derivatives.

At the coupon and dividend dates, the value of the debt must satisfy

$$D(V_+, r, \bar{t}, t_+) = D(V_-, r, \bar{t}, t_-), \tag{5.6}$$

where

$$V_+ = V_- - \frac{c_s}{2}Se^{\phi t} - \frac{c_j}{2}Je^{\phi t} - \frac{d}{2}\max(V_- - Se^{\phi t} - Je^{\phi t}, 0). \tag{5.7}$$

The value of the debt just after a dividend payment is found by interpolation.

5.3.3 Boundary conditions

The ParAsian features are realised in the boundary conditions, which are required to solve the partial differential equation above.

At maturity (terminal condition 1) : When the junior and senior debts mature at different times, the later debt maturity initially appears to be a better choice, but the earlier maturity must be specified and incorporated beforehand, which implies unlimited combinations. The boundary condition at maturity must take into account the issue of new debt, which we assume to be of equal priority to current debt (Smith and Warner, 1979; Fama and Miller, 1972) and issued in such a way so as to maintain the ratio of senior to junior debt. As a result, when the firm defaults, the creditors must share their claim with the new creditors. In the original model proposed by Yu (2004), the debt in its entirety was included at the terminal condition, however the original creditors have no claim on newly issued debt. If we let the face value of the new debt issued be, say, N, and $S = aF_0$, $J = (1-a)F_0$ be the face value of original debt where the parameter a defines the proportion of senior debt in the total debt, then aN is senior debt and $(1-a)N$ is junior debt. Consequently, the senior debt at default will be

$$\begin{aligned} B &= \min[\tfrac{VS}{S+aN}, S] \\ &= \min[\tfrac{VaD}{aD+aN}, S] \\ &= \min[\tfrac{VD}{D+N}, S] \\ &= \min[\tfrac{VD}{De^{\phi T}}, S] \\ &= \min[Ve^{-\phi T}, S]. \end{aligned} \tag{5.8}$$

Therefore, at its expiration for any $\tau \leq \bar{T}$, the payoffs of debt in Model Ia and Ib are:

$$B(T, V, r, \tau) = \text{Min}[V(T) \cdot e^{-\phi T}, S],$$

$$b(T, V, r, \tau) = \text{Min}[\text{Max}[V(T) \cdot e^{-\phi T} - S, 0], J];$$

the payoffs in Model II are:

$$B(T, V, r, \tau) = \begin{cases} \text{Min}[V(T) \cdot e^{-\phi T} - J, S] & \text{if } V(T) \geq J \cdot e^{\phi T} \\ \text{Min}[V(T) \cdot e^{-\phi T}, S] & \text{otherwise} \end{cases},$$

$$b(T,V,r,\tau) = \begin{cases} \text{Min}[V(T)\cdot e^{-\phi T}, J] & \text{if } V(T) \geq J\cdot e^{\phi T} \\ \text{Min}[\text{Max}[V(T)\cdot e^{-\phi T} - S, 0], J] & \text{otherwise} \end{cases}.$$

At the end of the window (terminal condition 2) : Whenever the ParAsian feature is realised, in all models, creditors seize the firm and realise payoffs according to the APR, again $L_c(t,r;T)$ is the market value of an equivalent risk-free coupon bond paying 1 dollar at maturity T:

$$B(t,V,r,\bar{T}) = \text{Min}[V(t)\cdot e^{-\phi t}, S\cdot L_c(t,r;T)],$$

$$b(t,V,r,\bar{T}) = \text{Min}[\text{Max}[V(t)\cdot e^{-\phi t} - S\cdot L_c(t,r;T), 0], J\cdot L_c(t,r;T)].$$

Asset value is zero : When the firm has no value, all its securities are worthless:

$$B(t,0,r,\tau) = b(t,0,r,\tau) = 0.$$

Asset value is infinite : Under these circumstances, creditors are guaranteed their claims without suffering loss:

$$B(t,\infty,r,\tau) = S\cdot L_c(t,r;T),$$

$$b(t,\infty,r,\tau) = J\cdot L_c(t,r;T).$$

Interest rate is zero : When the interest rate is zero, according to the CIR model, the interest rate at the next instant is $\kappa\theta dt$ with certainty (since $\sigma_r\sqrt{r}dZ_r = 0$).

The PDE reduces to

$$D_t + \frac{1}{2} D_{VV} \sigma_V^2 V^2 + D_r \kappa\theta + D_\tau = 0.$$

(d'Halluin et al., 2001 showed that for the CIR model this PDE does not require a boundary condition at $r = 0$, so long as the condition that the Feller, 1951 condition $2\kappa\theta/\sigma_r^2 \geq 1$ is satisfied)

Interest rate is infinite: When the interest rate is infinite, the present value of any asset, becomes zero:

$$B(t, V, \infty, \tau) = b(t, V, \infty, \tau) = 0.$$

5.3.4 Parameter choices

The numerical examples produced in Yu (2004), and here, borrow the "empirically reasonable parameter choices" in Huang and Huang (2003). In contrast, Longstaff et al. (2005) employ the new information available from credit default swap data to determine the default component accounts for the majority of corporate bond spread across all credit ratings (Blanco et al., 2005; Driessen, 2005). The yield spreads generated herein are effectively credit spreads. Our results are not directly comparable with those of Huang and Huang (2003), as recovery rate and default boundary level are important parameter choices. Nevertheless, it is interesting to note that the sizes of credit spreads generated in this chapter match the ideal scenario in Huang and Huang (2003).[3]

Calibrated with the same economic assumptions as those in Huang and Huang (2003), our parameter choices are: the initial value of total debt $F = 100$, (Huang and Huang, 2003 assume that bonds are issued at par), which we arbitrarily decompose into $S = 20$ and $J = 80$ or $S = 80$ and $J = 20$ in pairs to examine the effect

[3]The results in the next section are different, although similar, from those presented in Yu (2004), all computer codes were written and run by the author of this thesis for both sets of results.

Table 5.1
Leverage Ratio and Asset Volatility For Each Rating

	Aaa	Aa	A	Baa	Ba	B	C	D
Leverage ratio (%)	13.1	21.2	32.0	43.3	53.5	65.7	100.0	125.0
Asset Volatility (%)	36.6	34.8	30.0	29.1	34.3	39.3	45.0	50.0

of relative weights of the two classes; the leverage ratio and the volatility of asset value σ_V depend on the firm's specific feature (a proxy here is the credit rating) and are listed in Table 5.1, the credit ratings following Moody's system; the annual coupon rate $c_s = c_j = 8.162\%$; the annual asset payout ratio $\zeta = 6\%$; the initial instantaneous rate $r_0 = 8\%$; mean reverting speed $\kappa = 0.226$; long-term mean level of interest rate $\theta = 0.113$; volatility parameter $\sigma_r = 4.68\%$; the market price of risk $\lambda = 0$; the correlation coefficient between asset return and the change in interest rate $\rho = -0.25$. For the window time, $\bar{T}$, Yu (2004) cites values from Eberhart and Sweeney (1992), that the average time in reorganisation is 25.6 months (2.1 years); and Altman (1993), that the reorganisation experience on average is 21 months, and so we set $\bar{T} = 2$ years.

5.4 Numerical Method

Following the analysis detailed in chapters 3 and 4, for multi-asset options, and time-dependent barrier options, we must now combine the two. We make the usual substitutions, defining τ and $\bar{\tau}$, such that

$$0 < \tau = T - t < T, \quad 0 < \bar{\tau} = \bar{T} - \bar{t} < \bar{T}.$$

Then applying this change of variables to (5.5) we have the following PDE,

$$\begin{aligned} D_\tau + D_{\bar{\tau}} = \frac{1}{2} D_{VV} \sigma_V^2 V^2 + \frac{1}{2} D_{rr} \sigma_r^2 r + D_{Vr} \sigma_V V \sigma_r \sqrt{r} \rho \\ + D_r \Big(\kappa(\theta - r) - \lambda \sigma_r \sqrt{r} \Big) + r D_V - r D. \end{aligned} \tag{5.9}$$

From the analysis on time-dependent barrier options in chapter 4 (see particularly section 4.4) we deduce that the problem must be approached differently depending on the terminal conditions. When pricing within a single debt structure, or in a two class debt structure with APR upheld, the terminal conditions at expiry and knockout are continuous. This means that the most appropriate manner to discretise is with a Crank-Nicolson style scheme setting the timesteps in real time equal to the barrier timesteps. However, when the APR is not upheld in a two-class debt structure, the Crank-Nicolson scheme will be prone to ringing and an implicit scheme must be used.

$$\Delta\bar{\tau} = \begin{cases} \Delta\bar{t} & \text{if} \quad V \leq K_{r,\bar{t}} \\ 0 & \text{if} \quad V > K_{r,\bar{t}} \end{cases}.$$

We next define the value of debt at a particular point to be

$$D(V, r, \bar{t}, \bar{\tau}) = D(i \cdot \Delta V, j \cdot \Delta r, k \cdot \Delta\bar{t}, l \cdot \Delta\bar{\tau}) = D_{i,j}^{k,l}$$

As a result, the left-hand side of (5.9) can now be written

$$D_{\bar{t}} + D_{\bar{\tau}} = \begin{cases} \frac{1}{\Delta t}(D_{i,j}^{k+1,l+1} - D_{i,j}^{k,l}) & \text{if} \quad V \leq K_{r,\bar{t}} \\ \frac{1}{\Delta t}(D_{i,j}^{k+1,l+1} - D_{i,j}^{k,l+1}) & \text{if} \quad V > K_{r,\bar{t}} \end{cases}. \tag{5.10}$$

Since we are now working with an extra dimension (interest rate), the barrier is a line rather than the usual point barrier synonymous with other models. Now the barrier is chosen to be the total face value multiplied by the value of an equivalent Treasury bond, hence we must find the value of the treasury bond L_c *a priori* since it is a function of both time and interest rate. The Treasury bond value can either be found using a finite-difference scheme on the CIR equation, or we may take advantage of the fact that there is an analytical solution[4] available. We choose the latter, then

[4] A closed-form formula for a risk-free bond with initial interest rate r is:

$$P(r, T) = H(T)e^{-G(T)r},$$

with

$$H(T) = \Big[\frac{2\gamma\, e^{(\kappa+\lambda+\gamma)T/2}}{(\kappa+\lambda+\gamma)(e^{\gamma\tau}-1)+2\gamma}\Big]^{2\kappa\theta/\sigma^2},$$

assume that L_c is now a known function, then the barrier value may be expressed as

$$h_j^k = \text{INT}\left(\frac{F\ e^{\phi t_k}\ L_c(t_k, r_j)}{\Delta V}\right) + 1 \tag{5.11}$$

where h_j^k is the integer equivalent to $K_{r,t}$. By definition of the function 'INT', $h_j^k \leq K_{r,t}$, so if $i \leq h_j^k$ then the node (i, j) is below or at the barrier.

Now, after expanding each of the terms in (5.9), a set of equations of the following form is obtained for $D_{i,j}^{k+1,l+1}$,

$$\begin{aligned} \alpha_{i,j} D_{i-1,j}^{k+1,l+1} + \beta_{i,j} D_{i,j}^{k+1,l+1} + \gamma_{i,j} D_{i+1,j}^{k+1,l+1} & \\ +\delta_{i,j} D_{i,j-1}^{k+1,l+1} + \epsilon_{i,j} D_{i,j+1}^{k+1,l+1} & \\ +\mu_{i,j}(D_{i-1,j-1}^{k+1,l+1} - D_{i-1,j+1}^{k+1,l+1} + D_{i+1,j+1}^{k+1,l+1} - D_{i+1,j-1}^{k+1,l+1}) &= Z_{i,j} \end{aligned} \tag{5.12}$$

for $0 < i < n$ and $0 < j < m$, where the right-hand-side of the equation is

$$\begin{aligned} Z_{i,j} = \quad & \alpha_{i,j} D_{i-1,j}^{k,l} + \beta_{i,j} D_{i,j}^{k,l} + \gamma_{i,j} D_{i+1,j}^{k,l} + \delta_{i,j} D_{i,j-1}^{k,l} + \epsilon_{i,j} D_{i,j+1}^{k,l} & \\ & +\mu_{i,j}(D_{i-1,j-1}^{k,l} - D_{i-1,j+1}^{k,l} + D_{i+1,j+1}^{k,l} - D_{i+1,j-1}^{k,l}) & \text{if } i \leq h_j^k \\ Z_{i,j} = \quad & \alpha_{i,j} D_{i-1,j}^{k,l+1} + \beta_{i,j} D_{i,j}^{k,l+1} + \gamma_{i,j} D_{i+1,j}^{k,l+1} + \delta_{i,j} D_{i,j-1}^{k,l+1} + \epsilon_{i,j} D_{i,j+1}^{k,l+1} & \\ & +\mu_{i,j}(D_{i-1,j-1}^{k,l+1} - D_{i-1,j+1}^{k,l+1} + D_{i+1,j+1}^{k,l+1} - D_{i+1,j-1}^{k,l+1}). & \text{if } i > h_j^k \end{aligned}$$

This scheme is implicit and we are presented with a $(m+1).(n+1) \times (m+1).(n+1)$ matrix system to compute.

Next, we must decide how to solve this set of equations in a fast and efficient way. We are presented with two issues. First, at each barrier time step we have to solve a two-dimensional PDE problem. Second, the storage space required is extremely large as we are solving for a three-dimensional array, which is dependent on the number of timesteps. In fact, when we double the timesteps, not only will we double the storage

$$G(T) = \frac{2(e^{\gamma\tau} - 1)}{(\kappa + \lambda + \gamma)(e^{\gamma\tau} - 1) + 2\gamma},$$

and

$$\gamma = \sqrt{(\kappa + \lambda)^2 + 2\sigma^2},$$

where λ is the market price of interest rate risk (Cox et al., 1985).

requirements, but also the number of discretised solutions to be solved.

We decided that the ideal method would be to solve the entire set of equations simultaneously using the (sparse) banded routine in the NAG library. This way, we did not need to consider any stability issues of the method, as we can obtain an 'exact' solution to the above set of equations. However, if were to use this method to solve over the range $\bar{\tau} \in [0, \bar{T}]$ at each timestep, the code is slow and laborious. When solving (for example) a ten year bond, the number of timesteps used becomes very important so as to maintain accuracy in the solution. With this method, doubling the number of timesteps will, in fact, quadruple (at the very least) the computation time.

The direct sparse solver is preferable to schemes based on iteration (e.g. point or line relaxation) in regions where the solution changes rapidly; however, as we solve over the range $\bar{\tau} \in [0, \bar{T}]$, the solution will tend toward a constant European value as $\bar{\tau}$ increases. In fact, if $\bar{\tau} > \bar{t}$ then the solution is European and $D^{l+1} = D^l$. It is obvious that it would be inefficient to use the sparse solver in the region $\bar{\tau} > \bar{t}$ when we have already calculated the solution, but if we inspect figure 5.4 we see that there is a significant region in $[0, \bar{T}]$ over which the solution is approximately constant. Iterating to find the solution in this region should be expected to be quick to converge if we use an iterative scheme with the solution at k as our initial guess. Hence, we use a successive over relaxation scheme in conjunction with the sparse solver. Thus, combining the two schemes is more efficient than using either on its own, because increasing the number of time steps will improve the accuracy of the initial guess for the next solution and, hence, the required number of iterations will decrease. Even though the required number of calculations has increased 4-fold, in practice the computation time only increases by a factor of between 2 and 3.

Table 5.2 documents the convergence of the Crank-Nicolson scheme used for single class debt calculations in this chapter. As in chapter **??**, the solution exhibits linear convergence, and the Richard extrapolated solution shows quadratic convergence, allowing for further extrapolation of the results. We see that the twice extrapolated results give sufficient accuracy to price the credit risk to the nearest basis point.

Table 5.2
Convergence of the bond price

n	m	p	$D(V_0, r_0, 0, 0)$	D_{RE}	D_{RE2}	Credit Spread (bps)
51	5	9	76.8761			
101	9	17	77.0074	77.1387		
201	17	33	77.0704	77.1335	77.1317	505.8
401	33	65	77.1071	77.1437	77.1471	505.4
801	65	129	77.1274	77.1478	77.1492	505.3
1601	129	257	77.1383	77.1491	77.1496	505.2

A table showing the convergence of the Crank-Nicolson method. We price a 5 year B-rated bond in a single debt structure with parameters as defined in section 5.3.4, at the given firm value V_0 and interest rate r_0. n, m and p are the number of points in V, r and $\bar{t}$ respectively. The grid is contained by $V \in [0 : 5F]$, $r \in [0 : 4r_0]$ and $\bar{t} \in [0, 2]$. The value of the straight calculation is shown in the fourth column, with once and then twice extrapolated results (Richardson extrapolation, see chapter 4) in the fifth and sixth columns respectively. The price of the equivalent treasury bond is 95.0388, and the final column shows the credit spread of the twice extrapolated results.

Here, since we are investingating the general shape and qualitative effects of the model, pricing to the nearest basis point is all that is required.

5.5 Results for a Single Class of Debt

We will show first the features arising from our ParAsian model with a single debt class. The window length in the model will be seen to influence both the level and the shape of the term structure of credit spreads. The influence of interest rate, its volatility, and other factors in the model will be discussed.

5.5.1 Credit Spread and Firm Rating

In order to relate results here conveniently to observed shapes and trends in bond data, a proxy is required for the ratings given by the major agencies, such as Moodys, Standard & Poor's, Fitch and others. Clearly, this is an imprecise science; practical bond ratings are not determined by a single, simple factor, but we will follow in the footsteps of Merton (1974), who used the quasi-leverage ratio as a reasonable proxy, to demonstrate general features. Having already used their key data inputs, we again follow Huang and Huang (2003) in relating leverage ratios to Moodys ratings.

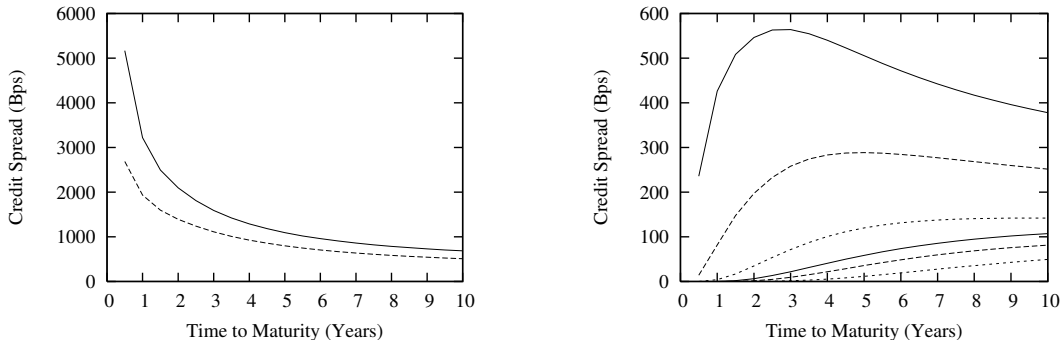

Figure 5.2
Term Structure of Credit Spreads.
(a) Leverage ratios greater than or equal to 1; from the top to the bottom are term structures of credit spreads for defaulted and distressed bonds, respectively. (b) Leverage ratios less than 1; from the top to the bottom are term structures of credit spreads for B, Ba, Baa, A, Aa and Aaa rated bonds in turn.

Figure 5.2 shows the term structure for the eight different ratings and displays the characteristic shapes found by Merton (1974).

5.5.2 Credit Spread and Window length $\bar{T}$

In this section we investigate the effect that the window length $\bar{T}$ has on credit spreads. Figure 5.3 shows the relation between window length and credit spread with a single class of debt. At the short end, the term structures are identical, even if their windows are different, so long as these windows are longer than maturity – the bonds are effectively European, because the options are not alive long enough to be knocked out.

The credit spread increases as the window increases. This corresponds to the value of the debt decreasing, as the likelihood of the bond defaulting decreases. The creditors are better off if they can force default earlier, so as to minimise their potential losses. Yu (2004) refers to this phenomenon as the "window effect". The effect is more prominent for large maturity, especially for the investment grade bond, since the chances of it defaulting before maturity are increased as the length of maturity is increased.

Finally, it is found that the growth rate of credit spread dependency with the

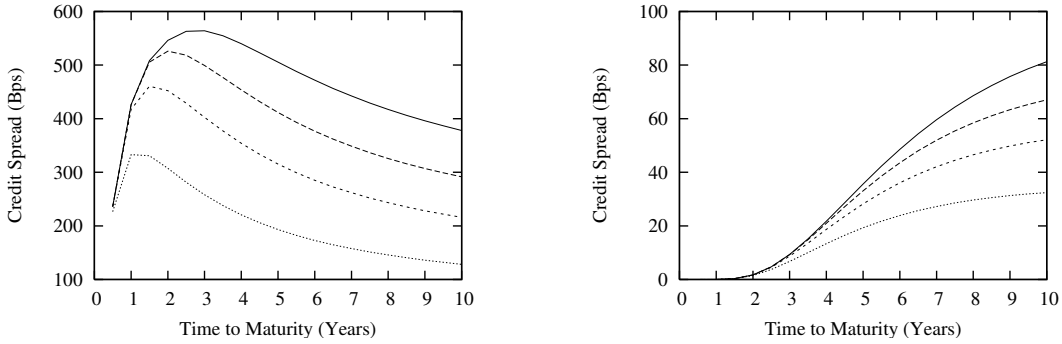

(a) B-rated (b) Aa-rated

Figure 5.3
Term Structure of Credit Spreads and Window Length
From the top to the bottom, the window length is equal to two years, one year, six months and two months respectively.

window length is nonlinear. In figure 5.4, the credit spreads for different window lengths are shown for both Aa rated and B rated bonds with a ten-year maturity. The increment of credit spread exhibits a concave behaviour. If the window length is zero, then we have a standard barrier option. Since the barrier level is equal to the exercise price on the put option, then the value of that option, and hence the credit spread, will be zero. When the window length is equal to the time to maturity, we have in effect a European put option. It is the traits of the firm that determine the window effect, for instance for higher rated bonds, such as an Aa in the figure, when the window period exceeds one year, the underlying ParAsian differs little from a European, which means default can be avoided almost completely. However, for a lower-rated bond, default is inevitable until the window length is much longer.

5.5.3 Interest rate and debt accumulation factor

Changing the capital structure accumulation factor, ϕ, changes the future policy of the firm. This will affect both the level of the default barrier and the recovery rate. As ϕ increases the level of the barrier is increased, which will make the debt safer, since default is more likely to happen at a higher firm value. However, the effect of taking on more debt is known to increase credit spreads (Collin-Dufresne and Goldstein, 2001), and in our model this is incorporated into the recovery rate. As the

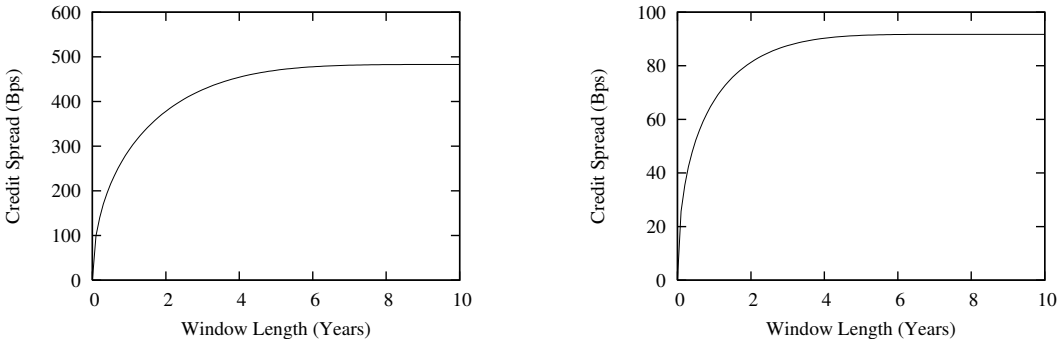

(a) B-rated (b) Aa-rated

Figure 5.4
Credit Spread vs. Window Length
Credit spread for a ten year bond with varying window length. Parameters are as given in the text.

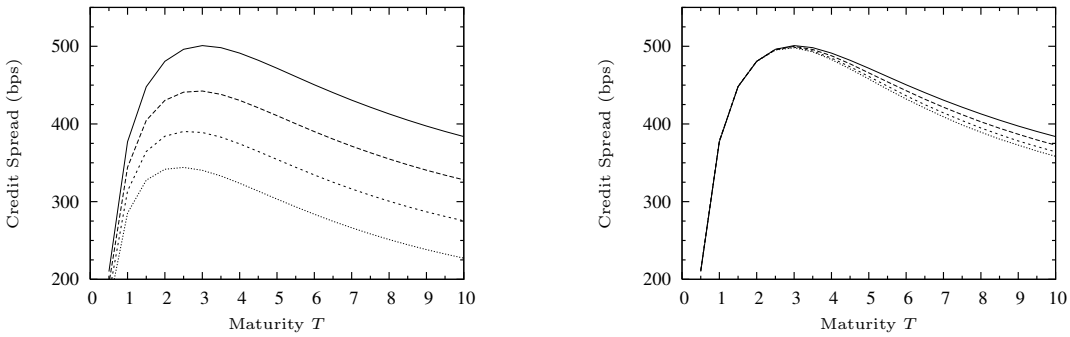

(a) $\phi = 0$ (b) $\phi = r - \zeta$

Figure 5.5
Term structure for varying interest rate in a one-factor model
(a) The rate at which the firm accumulates debt is held constant with $\phi = 0$, and the constant interest rate is varied from $r = 6\%$ (solid) through to $r = 12\%$ (dotted). (b) The rate at which the firm accumulates debt is matched to the interest rate, $\phi = r - \zeta$, and the constant interest rate is varied from $r = 6\%$ (solid) through to $r = 12\%$ (dotted).

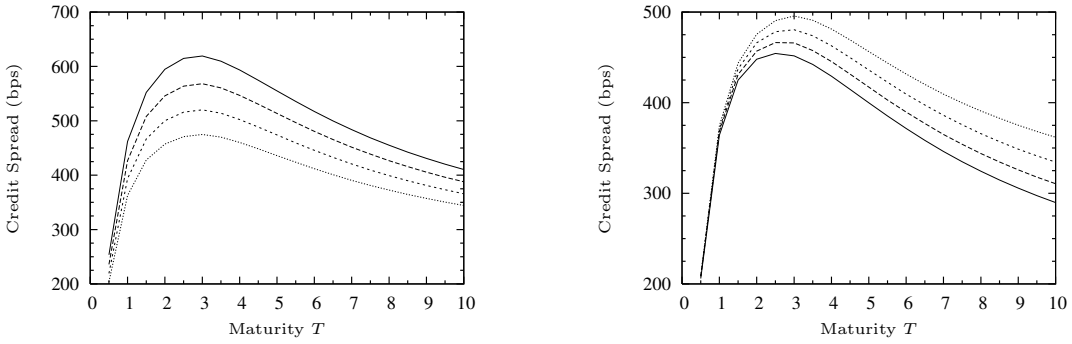

(a) $\phi = \theta - \zeta$ (b) $\phi = r_0 - \zeta$

Figure 5.6
Term structure for varying stochastic interest rate, single issue debt
(a) The rate at which the firm accumulates debt is held constant with $\phi = \theta - \phi$, and the initial interest rate is varied from $r_0 = 6\%$ (solid) through to $r_0 = 12\%$ (dotted). Here θ as in the text is 11.3%. (b) The rate at which the firm accumulates debt is matched to the interest rate, $\phi = r_0 - \zeta$, and the initial interest rate is varied from $r_0 = 6\%$ (solid) through to $r_0 = 12\%$ (dotted).

firm takes on more debt, the proportion of the firm value that the initial debt holders will receive is reduced by a factor $e^{\phi t}$. Figures 5.5 and 5.6 demonstrate the interaction of the rate at which the firm acquires new debt, and the level of interest rate. In figure 5.5(a), non-stochastic interest rates in a one-factor model have a negative effect on the credit spreads, which is a well documented effect in most structural models. However, when the parameter ϕ is matched to the interest rate via $\phi = r - \zeta$ in figure 5.5(b), all four curves are matched in the short term. Thus, the reduction in probability of default when the risk-free rate is increased is offset by the increased probability of default as the rate of debt accumulation is increased. In the long term we do see a return to the negative effect.

In the Yu model we choose to match the parameter ϕ to the long term interest rate θ, but it is instructive to see what happens with a different setup. In figure 5.6(a) we match to the long term rate but in figure 5.6(b), to the initial rate. Figure 5.6(a) also plots the term structure for four different initial starting interest rates, all with the same long term interest rate θ. The curves initially show the classic effect for interest rate in structural models, but do appear to close in on each other in the long term. In contrast, if we choose to match ϕ to the initial rate r_0 then in the short term the curves are identical, but then are flipped compared to the usual result. Interest

rates (combined with ϕ) now have a positive effect on the credit spreads. Hence, the influence of the parameter ϕ outweighs the effects of the interest rate.

In this chapter, to allow comparisons to be made, we choose the parameter ϕ to be constant across all firm ratings. However, it may be better to vary this parameter according to the firm rating, and hence the probability with which it will take on new debt. This implies ϕ will be relatively small for speculative grade bonds, and high for investment grade bonds. We can then reproduce the results of Collin-Dufresne (2001) in which the credit spreads will be less variable across firm ratings.

5.5.4 Duration

It is well documented that defaultable bonds have shorter durations than equivalent risk-free bonds (Chance, 1990; Longstaff and Schwartz, 1995). Here, the most common definition of duration is adopted, namely the negative percentage change in bond price to the change in its own yield (an alternative definition adopted by Acharya and Carpenter, 2002 is a ratio to the change in a corresponding T-bond yield). Figure 5.7(a) illustrates duration decreasing with the increase in default risk. Under the Yu framework, negative durations are not possible, even for very high risk bonds. Longstaff and Schwartz (1995) present a set of parameters (the bond is close to default and the recovery rate is low) for which bond price increases as interest rates are increased, resulting in negative duration, which agrees with the conditions required for negative duration argued by Acharya and Carpenter (2002). Although the default barrier is similar in both the Yu (2004) model and the Longstaff and Schwartz (1995) model, in as much as an increase in interest rates can reduce the probability of hitting the barrier (both barriers are decreasing functions of interest rate), the endogenous nature of recovery in the Yu model means that there is no loss avoided by such a movement: hitting the barrier does not result in a loss. Therefore with endogenous recovery rate, no negative durations are possible.

In figure 5.7(b), the effect of window length on the duration of the bond is shown. The window length gives us an indication of the riskiness of a bond, with short

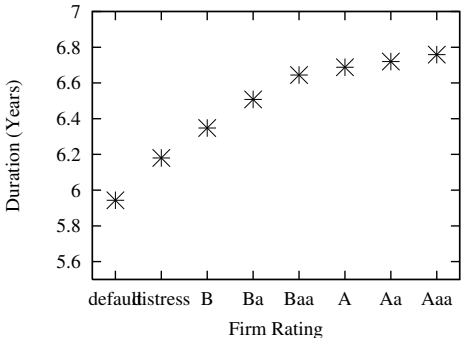

(a) Firm Ratings vs. Duration

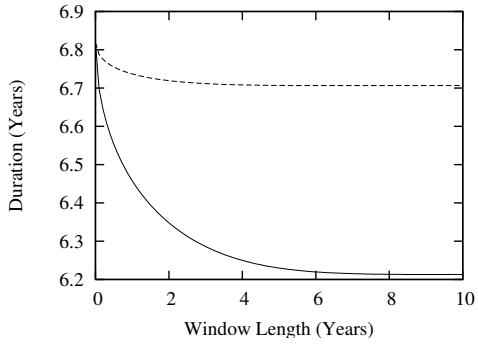

(b) Duration vs. Window Length; an Aa-rated bond (dashed line) and a B-rated bond (solid line).

Figure 5.7
Duration

windows the bond is almost riskless, and the risk increases as the window increases and the creditors become less protected. As the window length tends toward zero, both the speculative and investment grade bonds tend to the same riskfree duration value. As mentioned before, it is well known that duration reduces with increased risk so it is no surprise that duration reduces as the window is increased.

5.6 Results for a Two-Class Debt Structure

The scene has now been set for consideration of a two-class debt structure. In the following examples, only results for B and Aa rated bonds are displayed, as examples of speculative and investment grade bonds.

5.6.1 Credit spread and priority

Figure 5.8 compares the term structures of credit spreads generated in Model Ia and those of two single issues whose face value is equivalent either to the total debt level (i.e. the single debt structure) or to the senior debt level, fixing other parameters in the same rated firm.

The results in figure 5.8 are standard, and are consistent with the findings in Black and Cox (1976), where the senior debt is less risky than, and the junior debt more risky than the combined total debt. Here the APR is upheld, so the junior debt

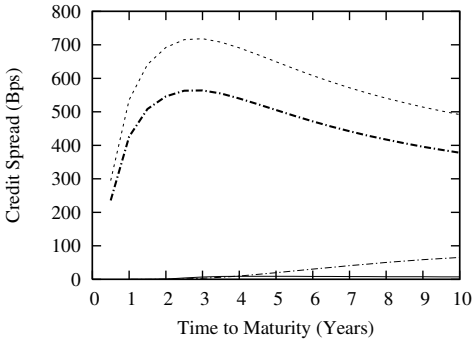

(a) B-rated, senior debt makes up 20%.

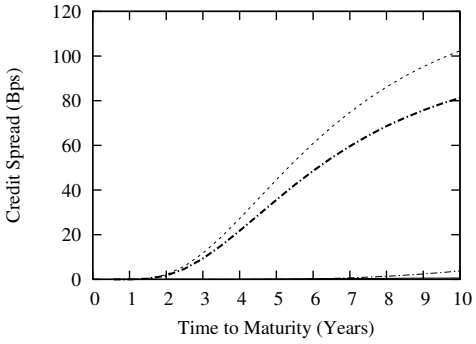

(b) Aa-rated, senior debt makes up 20%.

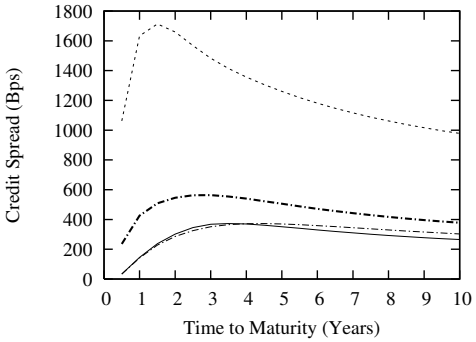

(c) B-rated, senior debt makes up 80%.

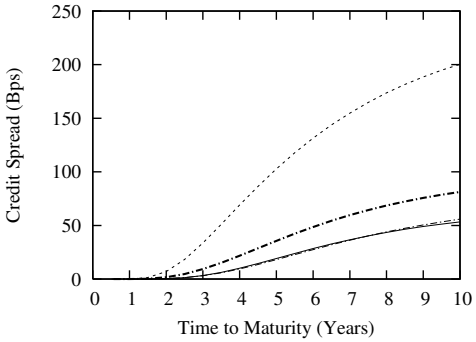

(d) Aa-rated, senior debt makes up 80%.

Figure 5.8
Senior Debt Matures First.
The solid line is senior debt, and dotted line junior. The thick dot-dash line is the single issue, and the thin dot-dash line the equivalent single issue.

acts as a cushion for the senior debt, effectively taking on all the risk. When the majority of the debt is junior (figures 5.8(a) and 5.8(b)), the junior debt has a term structure close to that of the total debt, and the senior debt is effectively risk free. In figures 5.8(c) and 5.8(d), when the majority is reversed, the senior debt is now close to the total debt, and the junior debt has a spread that is similar to a firm in distress for the speculative bond. The effects are much more pronounced in the long term for junior debt, where in figure 5.8(d) the junior is still relatively risk free in the short term. The senior debt is less risky than its equivalent single issue, with the addition of the junior debt increasing the level of the default barrier, which means that the firm is more likely to default and the creditors receive their claims.

Results for Model II, as shown in figure 5.9, provide further interesting insights into the *relative* priority between different classes of creditors. Here the junior debt matures first, and we have assumed that it will violate the APR at maturity. Therefore, the higher the chance that debt survives until maturity, the more likely the junior debt will have higher priority than the senior debt. Consequently, in the short term, the senior debt is more risky than junior debt. However, for longer term bonds, the probability of defaulting before maturity (where the APR will be upheld) becomes much greater than the probability of defaulting at maturity as the time to maturity is increased, so the credit risk will return to approximately those values in figure 5.8 where the senior bond maturing is first.

All three curves must cross at the same point due to the linearity of the problem. At any time, the value of the senior plus the junior debt must equal the total debt package, so when their risk is equal, there market values will be weighted in the same ratio as their face value. When they cross, the maturity at which they cross will be determined by the ratio between the face value of the bonds, and their rating. The curves cross earlier in figure 5.9(a) than figure 5.9(c) due to the cross default provision. When the proportion of junior debt is large the cross default provision is much more likely to come into effect and the APR upheld, so the positions are reversed much sooner. Similarly, the curves cross later for the investment grade bonds, since the chances of the cross default provision being triggered is smaller than

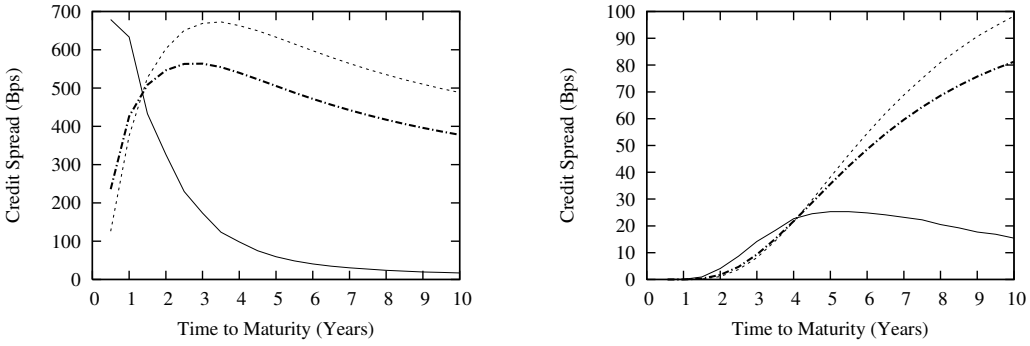

(a) B-rated, senior debt makes up 20%.

(b) Aa-rated, senior debt makes up 20%.

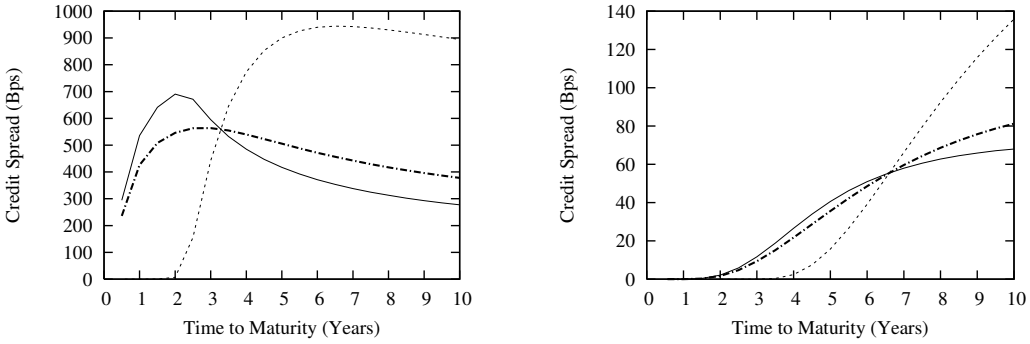

(c) B-rated, senior debt makes up 80%.

(d) Aa-rated, senior debt makes up 80%.

Figure 5.9
Senior Debt Matures Second
The solid line is senior debt, and dotted line junior. The thick dot-dash line is the single issue.

for the speculative grade bonds.

There are some interesting observations to be made regarding the shape of the term structure of credit spreads, in particular for the speculative grade bonds. The normal shape for a speculative bond predicted by a Merton-style model is the humped shape as seen in figure 5.2(b), but in figure 5.8(a), the senior bond has an upward slope, and in figure 5.9(a) the senior bond is downward sloping. There is some disagreement in the empirical evidence as to whether we should see a upward or downward sloping. Sarig and Warga (1989) and Fons (1994) predict downward sloping curves for the B-rated credit yield, whereas Helwege and Turner (1999) document upward sloping curves for B-rated issuers, which, they say, is the practitioners view of the world. The upward sloping curve in figure 5.8(a), would be much more common than the downward sloping curve in figure 5.9(a), due to the firms preference to issue longer term junior debt.

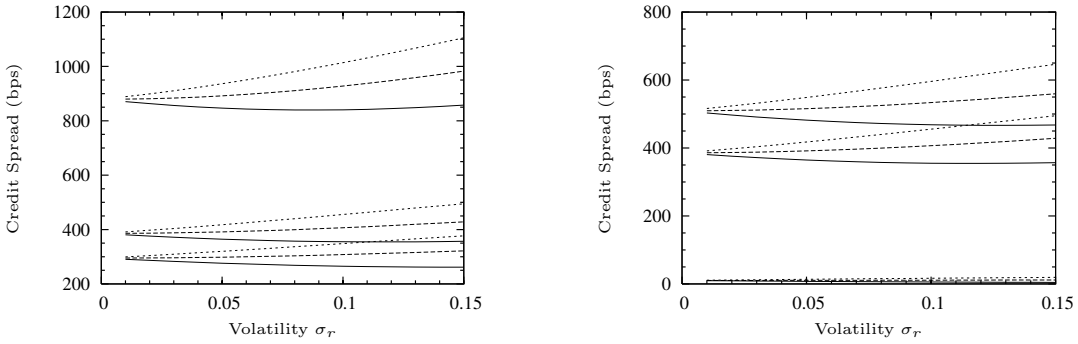

(a) $B = 20$ (b) $B = 80$

Figure 5.10
Credit Spread vs. Volatility of Interest Rate
Credit spreads for the senior, junior and total debt are shown from top to bottom. The correlation parameter ρ is varied from -0.5 (solid), 0 (dashed) and 0.5 (dotted) for each of the three bonds. (a) Top to bottom are the junior, total and senior debt curves with senior debt making up 20% of the total debt. (b) Top to bottom are the junior, total and senior debt curves with senior debt making up 80% of the total debt.

The shape of the credit spread curve appears to be affected not only by the seniority structure, but also the relative weight and maturity structure. For the speculative bond when the junior has a shorter maturity, the senior bond changes from a downward slope in figure 5.9(a) to a humped shape in figure 5.9(c). Then, for the junior bond, in figure 5.9(c) the weighting between the two bonds results in an unusual curve, which is very safe at the short end, then very risky at the long end, while in figure 5.9(a) the junior displays the normal humped shape.

5.6.2 Credit spread and interest rate volatility

In our model we take interest rate parameters from Huang and Huang (2003), and in figure 5.10 we demonstrate the effect of some of those parameters. The model is sensitive to the volatility of interest rates, but equally so to the correlation between the interest rate and the firm value. When the correlation is negative, an increase in interest rate volatility can actually result in the credit spread decreasing (see Acharya and Carpenter, 2002). The effect of the of the correlation is large even for the modest range of interest rate volatility (0-15%) shown.

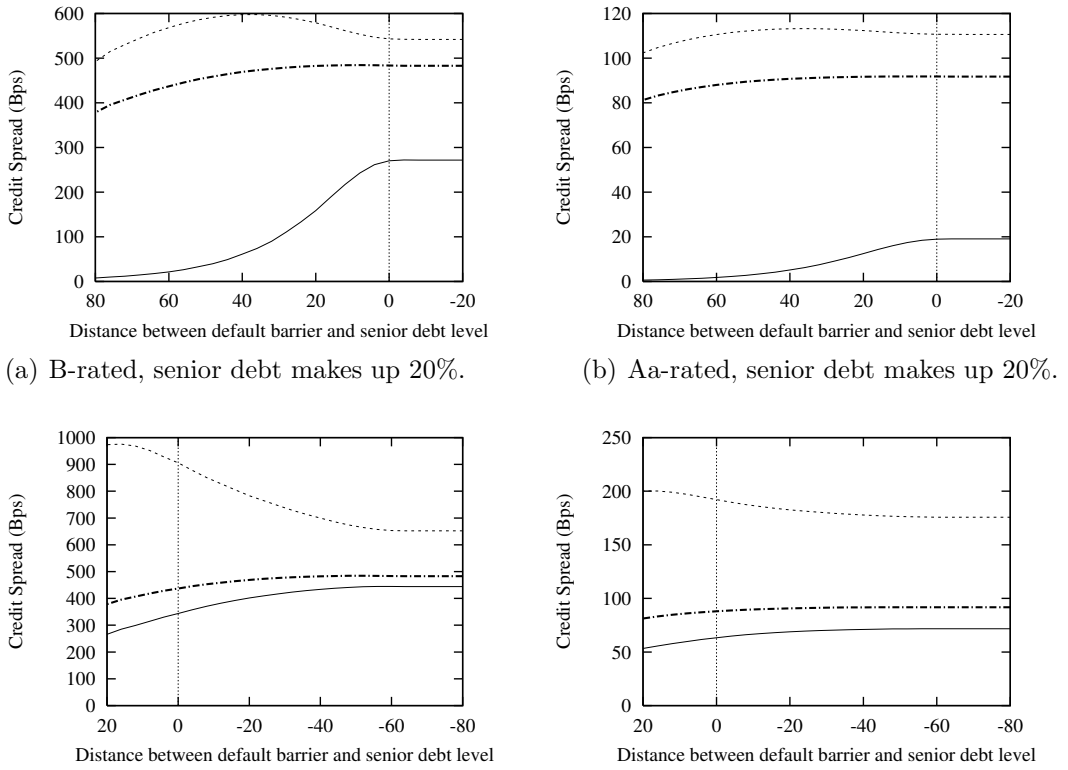

(a) B-rated, senior debt makes up 20%.

(b) Aa-rated, senior debt makes up 20%.

(c) B-rated, senior debt makes up 80%.

(d) Aa-rated, senior debt makes up 80%.

Figure 5.11
Credit Spread vs. Default Barrier Level, with Senior Debt Maturing First
The solid line is senior debt, and dotted line junior. The thick dot-dash line is the single issue.

5.6.3 Credit spread and default barrier

So far, all results have taken the barrier to be at level of total debt, which Yu (2004) assumes is the situation where the junior creditors fully cooperate with the senior creditors. Here in this section we investigate an internal bargaining between the creditors, resulting in a change in the level of the default barrier. Figure 5.11 shows the credit spread of the senior, junior and total debt at a maturity of ten years against the position of the default barrier. The position is given as its distance from the senior debt level, with positive indicating above and negative below. The total debt shows the result of the internal bargain on the debtors.

We know that when the barrier is lowered, the chance that the ParAsian option will be knocked out is reduced, so we expect credit spread to increase. Conversely, as the barrier level is increased, the higher the chance that the ParAsian option is

knocked out and the creditors receive their full claim, so the credit spread should decrease. Consequently we would expect credit spread to be a monotonically decreasing function of the barrier level, however, figure 5.11 shows this is not always the case.

First, we note that as the barrier level approaches zero, the curves plateau. When the barrier is so small, the likelihood of the ParAsian option being knocked out is so small that the option becomes effectively European. The curves displayed by the senior bond are quite easy to explain, given that all curves are monotonically decreasing, with the senior debt curves in figures 5.11(c) and 5.11(d) almost identical to the total debt. Although the senior curves in figures 5.11(a) and 5.11(b) appear to be quite different to the total debt curves, if we were to plot the total debt curves and let the barrier extend out to four or five times the total debt level, we should expect that the curves will look the same. The reason that the decrease in credit spread is so steep around the senior debt level is due to the discontinuity in the boundary condition at the senior debt level. Above this level, the creditors will receive their full claim rather than a portion of it when below the level.

More interesting however, are those results observed for the junior debt. The credit spread is no longer a monotonically decreasing function of the barrier, actually increasing over some range of barrier values, for instance in figure 5.11(a) the credit spread increases between $[-20, 40]$. As the barrier value is increases from zero above the senior value the probability of default gradually increases, but since the junior creditors are likely to end up with nothing if the bond defaults, they are actually worse off. The result is that the curve is initially increasing, before this effect is offset by the increasing recovery value that the junior creditors will receive at default, until they are close to (possibly) receiving their full claim and the curve starts to decrease. The barrier level at which the spread will stop increasing is obviously highly dependent on the weighting of junior to senior. In figures 5.11(a) and 5.11(b) where the senior debt level is low, the junior creditors start to receive a benefit from default much faster than in figures 5.11(c) and 5.11(d) where the senior holds the larger proportion of debt.

When the junior debt matures first, the position of the barrier can play an even

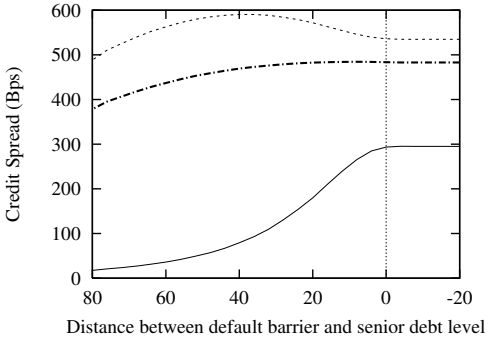

(a) B-rated, senior debt makes up 20%.

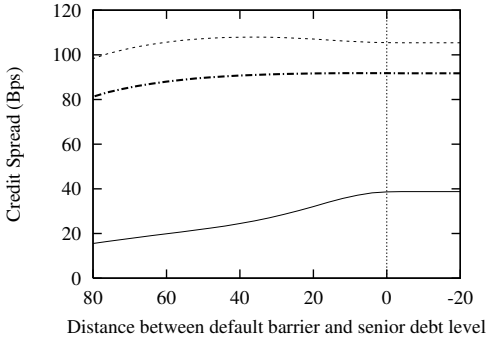

(b) Aa-rated, senior debt makes up 20%.

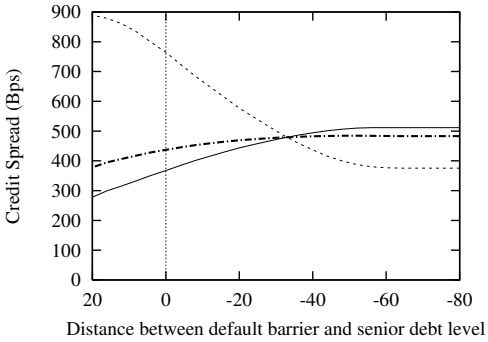

(c) B-rated, senior debt makes up 80%.

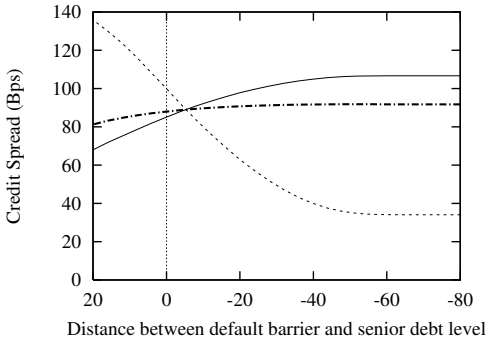

(d) Aa-rated, senior debt makes up 80%.

Figure 5.12
Credit Spread vs. Default Barrier Level, with Senior Debt Maturing Second
The solid line is senior debt, and dotted line junior. The thick dot-dash line is the single issue.

more important role than in the previous case. While figures 5.12(a) and 5.12(b) show similar trends to those observed in figure 5.11, figures 5.12(c) and 5.12(d) show quite different results. By changing the level of the barrier, the junior can become senior, and vi ca versa. This is due to the fact that even at a maturity of ten years, the European option values for the junior and senior bonds are switched, with the senior having a higher credit spread than the junior. Since the ParAsian knockout will have the same effect as before, i.e. that the senior is decreasing and the junior is initially increasing, their positions are eventually returned to normal. This effect is lessened when the junior debt has a high proportion, since the cross-default provision will influence the value of the European.

5.6.4 Credit spread and window length

We have already discussed the effect of the window on a single debt issue in section 5.5.2, and here we compare the single issue results to those of senior and junior bonds. As in the previous section where the default barrier influenced the probability of the ParAsian option being knocked out, so it is with the window length. The shorter the window length, the more likely the ParAsian will be knocked out, and the longer it is the less likely it will be knocked out. This means that figures 5.13 and 5.14 follow very similar trends to those in figures 5.11 and 5.12. In fact, the trends for the window length figures in the region $\bar{T} \in [2, 10]$, are identical to the barrier figures, as this is the region where the option becomes more European.

In the limit as window length tends to zero, credit spreads across all bonds plunge to zero. As mentioned earlier in section 5.5.2, because the barrier is placed at the total debt level, the instant knocked out at the barrier with zero window length means that all creditors receive their full claim. Conversely, as the window length tends to the maturity length the probability of knockout approaches zero and the option becomes European. We note again that in figures 5.14(c) and 5.14(d) the senior debt is more risky than the junior debt when the ParAsian option becomes European.

When analysing the effect of window length for senior bond, the effect is similar

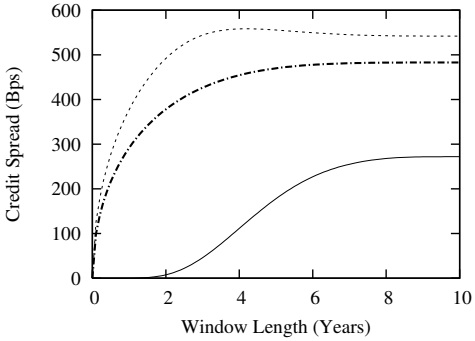

(a) B-rated, senior debt makes up 20%.

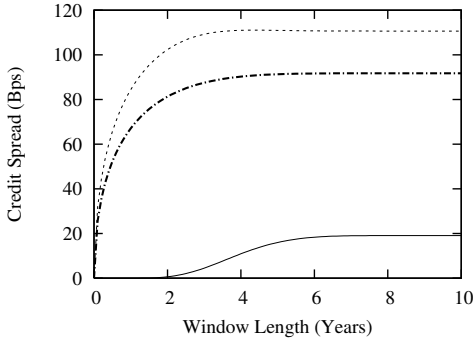

(b) Aa-rated, senior debt makes up 20%.

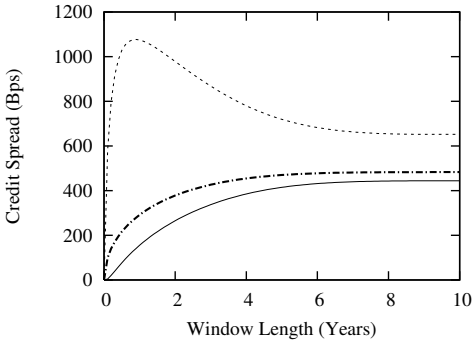

(c) B-rated, senior debt makes up 80%.

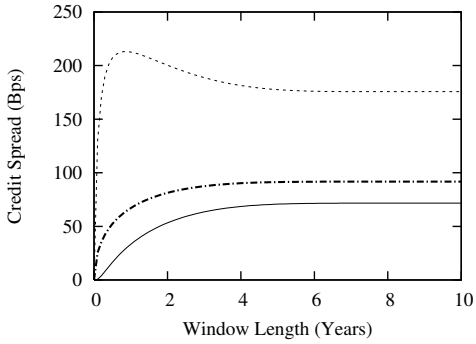

(d) Aa-rated, senior debt makes up 80%.

Figure 5.13
Credit Spread vs. Window Length, with Senior Debt Maturing First
The solid line is senior debt, and dotted line junior. The thick dot-dash line is the single issue.

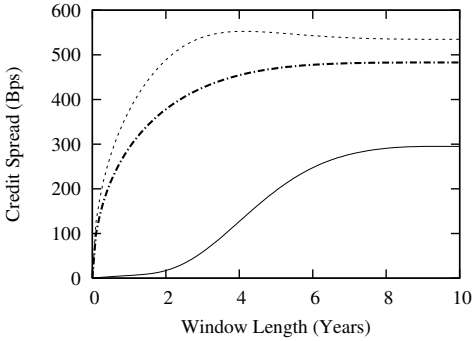

(a) B-rated, senior debt makes up 20%.

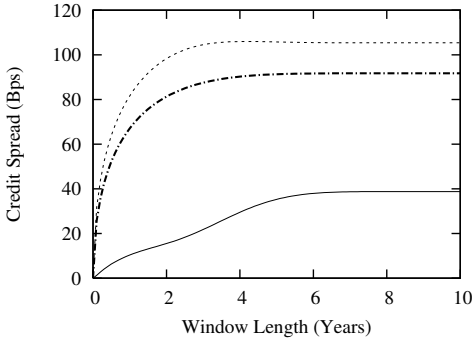

(b) Aa-rated, senior debt makes up 20%.

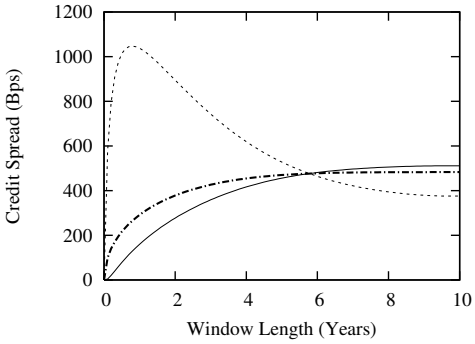

(c) B-rated, senior debt makes up 80%.

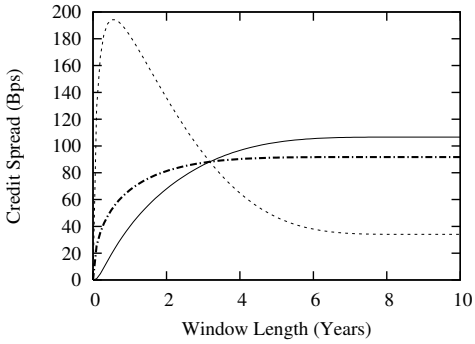

(d) Aa-rated, senior debt makes up 80%.

Figure 5.14
Credit Spread vs. Window Length, with Senior Debt Maturing Second
The solid line is senior debt, and dotted line junior. The thick dot-dash line is the single issue.

to that felt by the total debt, especially when the proportion of senior debt is high. In figures 5.13(a) and 5.13(b) the effect is step-like, with a window length of two or less years not having much effect, and likewise six or more. In between the credit spread rises (relatively) sharply, and the window length we have chosen is just outside of this region, so for the senior debt a decrease in window length will have a small effect as compared to an increase in window length.

For the junior debt, the trends are most interesting when the proportion of junior debt is small. Again as the window length is reduced from the European value at $\bar{T} = 10$ (the chance of knockout increases), the credit spread is initially at least increasing. Then around the one year mark, the credit spread drops dramatically toward zero as not only the probability of knockout increases, but also the recovery rate. The recovery rate increases as the window length decreases as the average distance the process can travel below the barrier is decreased as the window length is decreased.

5.7 Conclusions

In this chapter we systematically model corporate debt, both for a single class of debt and for two debt classes, under a variety of seniority and maturity structures, testing several variants of ParAsian option to model the process prior to possible bankruptcy. Results for the single debt class show the practicality of the ParAsian window which, amongst other effects, increases credit spreads. Different structures present some unique characteristics of corporate bonds in a two-class debt structure. These characteristics include the shapes and magnitudes of the term structures of credit spreads, the sensitivities of credit spreads to the volatility of asset, the initial interest-rate level and the volatility of interest rate, as well as bond durations. The results for the senior debt are consistent with an otherwise identical debt but improved credit status. However, the results for the junior debt can be counterintuitive, owing to its equity trait, the degree of which is governed by its weight in the total debt and the maturity structure.

Importantly, *a propos* each model, we further investigate the bargaining power of the junior creditors and debtors, as well as the interaction between these two, by means of changing the default barrier and the ParAsian window. We find that both make the senior creditors worse off, though to different extents according to their proportions in the total debt as well as the firm's credit status. The story is more complicated in the junior case, in that the junior debt has mixed features of debt and equity. The junior creditors mainly exert their bargaining power when they are more susceptible to credit deterioration or they are able to seize the chronological priority at maturity. They can also benefit from a stronger bargaining power of the debtors, where it is possible that interests become aligned.

Chapter 6

Convertible Bonds

The unique manner in which convertible bonds combine features of both equity and debt has made them an attractive solution to firms wishing to raise capital and, unsurprisingly, a popular investment tool. They are also notoriously difficult to price relative to the underlying stock, with any number of factors from market illiquidity to market psychology giving arbitrage opportunities for fund managers to exploit.

As the name suggests, the convertible bond gives the owner the option to exchange the bond for some prearranged number of stocks in the issuing firm. The conversion policy is usually expressed as either the conversion ratio (the ratio of stocks to bonds that can be exchanged) or the conversion price (the stock price above which the holder may exchange at maturity). The convertible bond is a hybrid security, a combination of both debt and equity. The bond component will provide the holder with interest payments, though these are usually lower than a normal corporate bond, which is offset by the potential gains if the stock price rises and the holder wishes to convert. The bond appears to offer a win-win situation, unless of course the bond defaults in which case the holder will incur losses.

The holder may convert at any time during the contract, making this an American-style contract. There are also two other American options often in the contract; one, the call, will limit the upside potential, and the other, the put, will limit the downside potential. The call gives the issuer the option to make the holder choose, over a short period of time, either to convert the bond or to exchange it for a cash sum equal to

the *call price*. This is usually a function of time, and defined for all future times in the contract. To encourage the purchase of these bonds, there is often a *hard call protection* period during which the firm is prohibited from calling the bond back. During the *soft call protection* period, the company can call the bond back, but only if the stock price is above some trigger price for more than 30 days. The put option on a *premium put convertible* means that the holder may sell back the bond to the issuer at a premium at any time before maturity, during certain periods or on specified dates. Grimwood and Hodges (2002) find that almost all bonds in their sample have an embedded call option, with a significant proportion also having some form of put option also.

We aim to extend the current convertible bond literature in two ways. First, to model the default of the bond, we will adopt the Yu (2004) framework as discussed in chapter 5. Second, we will attempt to price the convertible bond issue in a more complex capital structure framework than is usually attempted. We will see the effect of senior bond issues on the price of the convertible, as well as its effect on the optimal call and conversion policies.

6.1 Literature

There have been two main approaches to the problem of valuing convertible bonds, both of which are structural, but depend on whether the stochastic process is the value of the firm (firm models), or the value of the stock (equity models). There are obvious advantages and disadvantages to both, such as the fact that the firm value cannot be observed, but can model default in a better way, whilst equity models can take data straight from the market, but cannot model default very well.

Ingersoll (1977b) was the first to propose a model for convertible bonds which are modelled as a contingent claim on the firm value. This is a primitive model, though, and assumptions that are now commonly relaxed (default only at maturity, no dividend payments, constant interest rates) are enforced here. These assumptions guarantee that the problem has a closed form solution, which is presented in Ingersoll

(1977b).

Relaxing the assumptions made by Ingersoll (1977b) leads to the problem no longer having a closed form solution. For this reason, Brennan and Schwartz (1977a) propose an implicit numerical scheme to price the convertible bond, which permits the model to include dividend/coupon payments, American style conversion, optimal calling of the bond and the possibility of default before maturity. They later extend the model to include stochastic interest rates (Brennan and Schwartz, 1980) in a two-factor model. One of the main results from the paper is that stochastic interest rates have little effect on the solution, although the argument for abandoning them seems to be for the ease of solution rather than effective pricing. Brennan and Schwartz (1980) also outline how one would go about solving for a convertible bond with a more complicated capital structure, i.e. the firm is made up of a senior issue, the convertible and equity. The results in this paper do not pay attention to the effect of the senior issue on the price of the convertible.

Nyborg (1996) defines how the Brennan and Schwartz (1980) model may incorporate a put option, without actually solving the PDE presented in the paper. Carayannopoulos (1996) tests the Brennan and Schwartz model using the CIR interest rate model (Cox et al., 1985) rather than the Vasicek (1977) style rates used by Brennan and Schwartz. They find that in some circumstances the stochastic interest rate can have a large effect on the accuracy of the pricing model. The barrier at which default occurs is particularly low, bonds only default if the firm value is less than the next coupon payment, which is unrealistic – firms normally default much sooner than this.

McConnell and Schwartz (1986) were the first to deviate from the firm value analysis for convertible bonds, choosing instead to model the option using the firm's stock as the underlying process. The Liquid Yield Option Note (LYON) that they price, is callable, puttable, and convertible, making it rather a complicated problem, and so equity is chosen as the underlying to reduce the complexity of the problem. If the firm has other debt that it is senior to the issued debt, under the firm value analysis this must be valued first in order to value the convertible debt. McConnell

and Schwartz realise they cannot model default with equity as the underlying process, so simply 'gross' up the risk-free interest rate to capture default risk, to compensate for the underpricing of the model. The model they present is easily solved using simple finite-difference methods, and can be extended to include stochastic interest rates. The simplification of the model however, is not always appropriate, since the credit risk is (intuitively) not constant across all share prices.

The first interpretation that the convertible bond with its hybrid nature should have different discount rates for its equity and debt parts is by Goldman Sachs (1994). Using the first derivative $\frac{\partial V}{\partial S}$ (the *delta* hedge) value as an indication of the probability that the debt was to be converted into equity, they form a discount rate in which the risky part is related to this probability of conversion. This achieves something in that the bond is more risky at low share prices, and less so as the share price increases, but it has little financial or economic backing for such a weighting.

Ho and Pfeffer (1996) also propose an idea that the bond should be split into components, some of which are subject to credit risk, and some that are not. The convertible bond is split into the sum of a straight bond (subject to credit risk), a warrant (not subject to credit risk) and a forced conversion option. The bond is split using the argument that the warrant will not be exercised before maturity, so the option is not American as such. American options cannot be split so easily, since they have non-linear boundary conditions, and as a consequence this model will not work if it is optimal for the convertible bond-holders to exercise before maturity, although the model does incorporate the yield curve into the solution, using the Ho and Lee (1986) model of interest rates.

A popular equity model developed by Tsiveriotis and Fernandes (1998) also splits the bond into two parts; however the convertible bond is not the sum of the two parts, but both parts are linked via coupled PDEs. They consider that the 'cash-only' part of the bond should be subject to default risk while the remaining part of the convertible bond is not. The cash-only component is priced as a digital option with a knock-out barrier where the convertible bond is converted. The convertible bond is then priced in the usual fashion, with the discount rate adjusted according to the value

of the cash-only component. The fact that the rate at which the convertible bond is discounted is linked to the conversion strategy of the holder, through boundary conditions for the cash-only part, seems to contradict the notion that the default of the firm, and hence the credit risk, is independent of the strategy taken by the convertible bondholders. Furthermore, the firm does not default (at least no loss is incurred) even if the stock price reaches zero. There are, therefore, some obvious flaws in this model.

A more recent approach, developed by Davis and Lischka (1999), Takahashi et al. (2001) and Ayache et al. (2003) is to follow a reduced form approach to default (Jarrow and Turnbull, 1995; Duffie and Singleton, 1999; Madan and Unal, 2000). In contrast with the structural approach, default is now an exogenous process, which can happen instantaneously at any time. The probability of default is captured in the hazard rate (a function of the stock price that may itself be stochastic) and at default the bond holder is assumed to receive some compensation. The model by Ayache et al. (2003) is the only study which discusses what happens at default, whereas other studies assume either total or zero recovery. The model is also driven by the fundamental principles of the continuous hedge and no-arbitrage, which are somewhat circumvented by Tsiveriotis and Fernandes (1998) with their *ad hoc* splitting of the bond, which Ayache et al. (2003) show to be inconsistent. However, all of the equity models discussed here have problems attributed to the exogenous nature of default, such as predicting unrealistic prices (a risky bond may be worth more than a riskless one); no possibility of a reorganisation period or emergence from bankruptcy; the dilution of the firm share price is not taken into account.

Bermudez and Webber (2004) attempt a cross-over model, part structural, part reduced form in order to endogenise both default and the recovery rate. The recovery rate is endogenised in the sense that there is a reorganisation period during which the creditors must wait to receive compensation, in which time the value of the firm (that they will receive) is allowed to move stochastically. So, in short, they surrender a European put which is exercised at the end of the reorganisation period. This is different from a Parisian or ParAsian option, since the firm cannot emerge from

the reorganisation under the Bermudez and Webber (2004) framework. This greatly simplifies the pricing of the option, which they simplify further by using the Vasicek (1977) interest model, allowing them to value the European put with an explicit formula when the correlation (between asset and interest rate) is zero; in fact they also use the formula even when the correlation is not zero. The firm may default either when payments by the firm cannot be made (endogenous) or at some jump time of a counting process (exogenous), where the firm value is reduced by some proportion of its current value. The probability of the firm defaulting endogenously is slim, however, and exogenous default will still account for the majority of the default risk. The firm only appears to pay coupons, not dividends, which greatly simplifies the computation, since the problem is not American unless dividends are present.

In the next section we develop a model using the Yu (2004) framework under which the default risk of the bond is correctly valued against the equity conversion. The model allows for all possible embedded options to be present, with a simple modification of boundary conditions. The model can also show how the capital structure of the firm can have a large effect on the price, something overlooked in the majority of the literature (which effectively takes the senior priority debt to be risk-free); convertible bonds are often issued by firms with outstanding debt as subordinate bonds. This also introduces an interesting problem in that the price of the senior debt may also be affected by the issue of convertible debt. If the convertible debt matures first (c.f. section 5.2), then the convertible debt holders may be able to violate the APR reducing the senior debt holders claim on the firm. Conversely, the convertible debt provides a cushion to the senior debt that increases its recovery rate, which may be removed if the convertible debt holders convert to shares. There is clearly a complex interplay between the creditors.

6.2 The Model

First we define the convertible bond following the framework of Brennan and Schwartz (1980). We assume that the firm is made up of senior debt holders, the convertible bond issue and the shareholders. Then we may express value of the firm to be

$$V = N_b\ B + N_c\ C + N_s\ S. \tag{6.1}$$

where N_b, N_c, and N_s are the number of senior bonds, convertible bonds and shares respectively. B is the value of a single senior bond, C the value of a convertible bond, and S the value of a share.

Let us examine what happens to the value of the firm at conversion. Now note that before conversion we have

$$V^{BC} = N_b\ B + N_c\ C + N_s\ S^{BC},$$

and after conversion

$$V^{AC} = N_b\ B + (\Delta N + N_s)\ S^{AC},$$

where $\Delta N = q.N_c$. Then the fraction of shares owned by the holder of each of the convertible bonds is

$$Z = q/(\Delta N + N_s),$$

the so called dilution factor.

Next, the conversion value for each of the bonds can be expressed in two ways, using either the share price before conversion or the share price after conversion. We then have

$$\text{Conversion Value}(1) = q.S^{BC} \tag{6.2}$$

$$\text{Conversion Value}(2) = q.S^{AC}, \tag{6.3}$$

and so when equating with previous equations we arrive at two different prices for

the convertible bond at conversion,

$$\text{Conversion Value}(1) = \frac{q}{N_s}.[V - N_b\ B - N_c\ C] \tag{6.4}$$

$$\text{Conversion Value}(2) = Z.[V - N_b\ B]. \tag{6.5}$$

If we assume that $S^{BC} = S^{AC}$ and equate equations (6.2) and (6.3) then

$$\frac{q}{N_s}.[V - N_b\ B - N_c\ C] = \frac{q}{\Delta N + N_s}.[V - N_b\ B],$$

will become

$$(\Delta N + N_s).[V - N_b\ B - N_c\ C] = N_s.[V - N_b\ B]$$

$$(\Delta N + N_s).N_c\ C = \Delta N.[V - N_b\ B]$$

$$C = Z.[V - N_b\ B]. \tag{6.6}$$

Consequently, only if the convertible bond is selling at the conversion price will the two equations be consistent.

6.2.1 The Governing PDE

We aim to price the convertible bond as a contingent claim on the value of the firm. We assume that the value of the firm moves under a geometric Brownian motion

$$\frac{dV}{V} = \mu\ dt + \sigma_v\ dZ_V. \tag{6.7}$$

The instantaneous interest rate, r, is assumed to follow the Cox et al. (1985) model,

$$dr = \kappa(\theta - r)dt + \sigma_r\sqrt{r}dZ_r, \tag{6.8}$$

where r is a mean-reverting process. The two processes are correlated via the parameter ρ,

$$dZ_V\ dZ_r = \rho\ dt. \tag{6.9}$$

Following the analysis in chapters 4 and 5 we model the default of the firm via a ParAsian option. Then defining the time under reorganisation as the barrier time $\bar{t}$, which is characterised by equation 4.17, we arrive at the following PDE to describe the price of the convertible bond:

$$\begin{aligned} C_{\bar{t}} + C_t + \frac{1}{2}C_{VV}\sigma_V^2 V^2 + \frac{1}{2}C_{rr}\sigma_r^2 r + C_{Vr}\sigma_V V \sigma_r \sqrt{r}\rho \\ + C_r\Big(\kappa(\theta - r) - \lambda\sigma_r\sqrt{r}\Big) + rC_V = rC \quad \text{if} \quad V \leq K \end{aligned} \tag{6.10}$$

$$\begin{aligned} C_t + \frac{1}{2}C_{VV}\sigma_V^2 V^2 + \frac{1}{2}C_{rr}\sigma_r^2 r + C_{Vr}\sigma_V V \sigma_r \sqrt{r}\rho \\ + C_r\Big(\kappa(\theta - r) - \lambda\sigma_r\sqrt{r}\Big) + rC_V = rC \quad \text{if} \quad V > K, \end{aligned} \tag{6.11}$$

where K is the default barrier described later.

6.2.2 At Maturity

We assume, as we did previously in chapter 5, that both the senior and convertible bond issues mature at the same time (although it is possible to allow for the convertible issue to mature slightly earlier, which may result in a violation of the APR). Let us assume intially that the APR is upheld, then at maturity each senior bond holder will receive the face value of the bond (and the final coupon payment for a coupon bond) unless the firm cannot afford to pay back all the senior bondholders, and so at maturity they receive

$$B(V, r, T, \bar{t}\,) = \begin{cases} \frac{1}{N_b}V & \text{if} \quad V < N_b\ F_b \\ F_b & \text{if} \quad V \geq N_b\ F_b \end{cases}. \tag{6.12}$$

If the value of the firm is high, then the convertible bondholders may choose to convert. However, if it is low, the convertible bondholders have a claim on the firm

so long as the senior bondholders have already been fully paid.

$$C(V,r,T,\bar{t}\,) = \begin{cases} 0 & \text{if} \quad V < N_b\ F_b \\ \frac{1}{N_c}[V - N_b\ F_b] & \text{if} \quad 0 \le \frac{1}{N_c}[V - N_b\ F_b] < F_c \\ F_c & \text{if} \quad Z \cdot [V - N_b\ F_b] < F_c \le \frac{1}{N_c}[V - N_b\ F_b] \\ Z \cdot [V - N_b\ F_b]. & \text{if} \quad Z \cdot [V - N_b\ F_b] \ge F_c\ . \end{cases} \tag{6.13}$$

6.2.3 Default Barrier

For simplicity, we assume that the firm will not issue any new debt to keep to a target leverage ratio (as in Collin-Dufresne and Goldstein, 2001). Then defining $L(r,t;T,c_l)$ to be the value of an otherwise equivalent risk-free coupon paying bond, F_b and F_{cb} as the face value of a senior and convertible bond respectively, and c_b and c_{cb} their respectivecoupon payments, then we choose c_l such that

$$c_l = \frac{N_b\ F_b}{N_b\ F_b + N_c\ F_{cb}} c_b + \frac{N_c\ F_{cb}}{N_b\ F_b + N_c\ F_{cb}} c_{cb}\ ,$$

which is equivalent to the total coupon paid out by the firm. Then the barrier, K (c.f. section 5.3), is placed at the value of an equivalent riskfree debt to that of the total debt in the firm;

$$K(r,t) = (F_b + F_{cb})\ L(r,t;T,c_l). \tag{6.14}$$

The barrier need not necessarily be placed at the total debt level if bargaining similar to that described in chapter 5 takes place, but it could be placed somewhere between the senior debt level and the total debt level. If the firm cannot undergo a period of reorganisation and instantly defaults, placing the barrier at or above the senior debt levels makes the senior debt riskfree, which is the assumption most models make. Here, as in the previous chapter we allow a reorganisation period of two years, for reasons defined in chapter 5, so that the senior debt is not risk-free and will influence the price of the convertible debt depending on the ratio between the two of them.

6.2.4 Optimal Call and Conversion

If the convertible bondholders act optimally, they will choose to exercise only when the return on dividend payments exceeds the proposed coupon payment. Although, under this framework, we allow the dividend payment to be continuous, in reality the dividend payment will be discontinuous, implying that the convertible bondholders will only convert just before a dividend payment: the option is effectively Bermudan. However, by allowing continuous payments we gain more insight into the dynamics of the problem. At conversion, the bondholders receive $Z\ [V - N_b\ B]$, so the value of the option must be always greater than this value;

$$C(V, r, t, \bar{t}) \geq Z\ (V - N_b\ B). \tag{6.15}$$

We assume that the firm may call back the convertible bond at a predetermined call price. Now under the Brennan and Schwartz (1980) framework, the share price is also viewed as a contingent claim on the firm value. When the firm contains only non-convertible debt, the shareholders hold a (perpetual) call option on the firm's assets with strike price at the face value of debt. If the firm issues convertible debt, the share holders effectively write an (American) call option (on the firm value) to the convertible bond holders, which could (if converted) result in their stake in the firm being reduced[1]. The share price process follows the same PDE as that governing the convertible bond, with appropriate boundary conditions. Of interest here is that under the firm value model, the movement of the share price reacts to the impending conversion. The process that the share price undergoes is different, depending on whether the convertible debt is acting like debt or equity, in this way the process for the share price is nonlinear, it is the process of the total firm that stays log-normal. In equity models, the share price is assumed to follow the same process, regardless of whether the convertible bonds are acting like debt or equity, but impending conversion has been shown to affect the share price.

If the firm is acting optimally, then the management will choose to maximise the

[1]Some convertible bond issue have covenants protecting the shareholder from dilution.

value of the shares, which, from (6.1) means they must minimise the value of the convertible bonds. Therefore, they will exercise the right to call back the bonds the first instant that the value of the bonds exceed the call price, hence

$$C(V, r, t, \bar{t}) \leq C_p. \tag{6.16}$$

There is empirical evidence to suggest that firms do not always act optimally and call the bonds back after they have exceeded the call price by on average 43% (Ingersoll, 1977a). A framework for modelling the delay in exercising an option, is explored later, in chapter 7. If the call has the soft-call constraint (where the share price must be above some barrier for a predetermined amount of time, modelled by Avellaneda et al., 1999 as a Parisian option) this will present a problem since, as mentioned above, the value of the shares is a function of the firm value and not of the underlying asset, and therefore cannot be modelled as a simple Parisian type option. The delayed exercise framework in chapter 7 makes it possible to value such an option in the firm value model.

6.3 Numerical methods

The technique used to solve this problem must be quick and efficient to solve what is essentially a four dimensional free boundary problem. We choose to adapt the boundary-updating solver from chapter 3. The method is flexible and is around ten-times faster than the equivalent PSOR method. In order to adopt this method, we must abandon the Crank-Nicolson scheme in favour of an implicit scheme. The Crank-Nicolson scheme is prone to ringing in ParAsian/Parisian options due to discontinuities in option price at zero barrier time, which are fully explained in chapter 4. Any such errors in the scheme (such as negative option prices for small V) may be amplified through from the senior bond solution to the convertible bond, possibly causing the boundary-updating solver not to work. We do not choose an explicit scheme since time step restrictions for the ParAsian option result in a hefty increase

Table 6.1
Convergence of the convertible bond price

n	m	p	$C(V_0, r_0, 0, 0)$	C_{RE}	C_{RE2}
41	5	9	1012.9		
81	9	17	1009.3	1005.7	
161	17	33	1009.2	1009.0	1010.1
321	33	65	1009.2	1009.3	1009.4
641	65	129	1009.3	1009.4	1009.4
1281	129	257	1009.3	1009.4	1009.4

A table showing the convergence of the implicit method used in this chapter. We price a B-rated bond convertible bond in a two-tier debt structure with parameters as defined in table 6.2, at the given firm value V_0 and interest rate r_0. n, m and p are the number of points in V, r and $\bar{t}$ respectively. The grid is contained by $V \in [0 : 8F_t]$, $r \in [0 : 4r_0]$ and $\bar{t} \in [0, 2]$ The value of the straight calculation is shown in the fourth column, with once and then twice extrapolated results (Richardson extrapolation, see chapter 4) in the fifth and sixth columns respectively.

in calculations since we require $\Delta t = \Delta\bar{t}$, therefore halving the time steps increases computation time four-fold.

In table 6.1 we show the convergence of the convertible bond price. The implicit scheme adopted here is not as effective as the Crank-Nicolson scheme adopted in previous chapters, and the convergence is not quite as smooth as that seen by the straight bond (see section 5.4, table 5.2), which may be due to any one of a number of factors, such as non-linearity from the free boundary, or contaminating errors from the senior bond calculations. As a result of non-smooth convergence the Richardson extrapolation is not as effective as seen previously. We must solve here over a larger grid ($V \in [0 : 8F_t]$) than the straight bond ($V \in [0 : 8F_t]$) in order to take both the debt and equity of the convertible bond into account. Therefore, the values of dV are twice as large as those in the corresponding entries in table 5.2, so we should not expect similar accuracy to those results. Note here that, if we set dV to be the same as before, the greater grid size results in a calculation over so many nodes that even a top range computer with 8Gbs of RAM could not handle the calculation. We do however have a price for the bond that is accurate to the nearest 10¢ on bond with a \$1000 face value, which is adequate enough.

Table 6.2
Parameters

Parameter	Value	Parameter	Value
σ_v	0.2	σ_r	0.0468
r_0	0.08	θ	0.113
λ	0.	κ	0.225
c_b	0.08	c_{cb}	0.04
ϕ	0.	ρ	-0.25
F_b	1000	F_{cb}	1000
N_b	250	N_{cb}	250
S_{cp}	12 .5	S_0	10
$\bar{T}$	2	d	0.05

The value of the base parameters. σ_v is the volatility of the firm, σ_r is the volatility of interest rate, r_0 is the initial value of interest rate, θ is the long-term interest rate, λ is the market price of risk, κ the mean reversion rate, c_b the senior debt coupon, c_{cb} the convertible debt coupon, ϕ the accretion of new debt, ρ the correlation, F_b the face value of senior debt, F_{cb} the face value of convertible debt, N_b the number of senior bonds, N_{cb} the number of convertible bonds, S_{cp} is the conversion price, S_0 is the initial share price, $\bar{T}$ is the window length and d the continuous dividend rate.

6.4 Results

In this section we present convertible bond values across a wide range of possible capital structures. In table 6.2 we give a set of base parameters which define the parameters used in the calculations unless otherwise stated. In the first subsection, we present results for three different bond ratings defined by the leverage ratio and volatility in table 5.1, to give an idea of the effect of leverage. For the remainder of the results we concentrate on the Baa rated bond, since it exhibits a good mix of equity and bond features.

Firm ratings

In figures 6.1 and 6.2 we show the value of the convertible bond and its optimum conversion price for three different bond ratings. They are five-year bonds without any put or call features, with parameters as in table 6.2 and table 5.1. The results are plotted against firm value, with points of interest at V_0, the initial value of the firm given by the leverage ratio corresponding to $S_0 = 10$, and F_T the total face value of debt for all bond issues. Firstly we note that over five years, the B rated bond

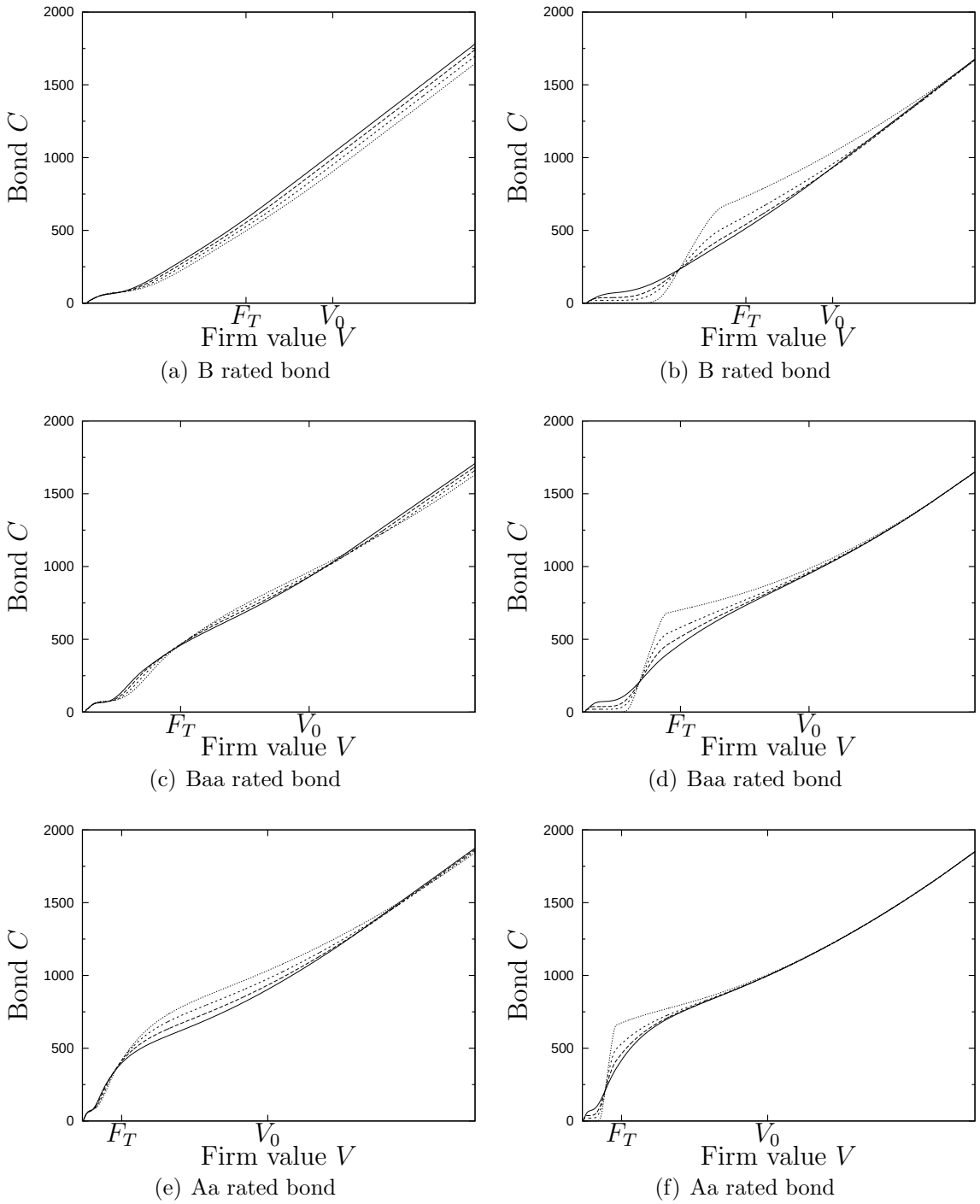

(a) B rated bond (b) B rated bond

(c) Baa rated bond (d) Baa rated bond

(e) Aa rated bond (f) Aa rated bond

Figure 6.1
Convertible bond value for different ratings
Parameters as in table 6.2 and 5.1. F_T is the total face value of debt and $V_0 = F_T/l$. For (a), (c), and (e), $r_0 = 0.05$ (dot), 0.1 (shortdash), 0.15 (longdash), 0.2 (solid). For (b), (d), and (f), $\bar{T}$ =0.0833 (dot), 0.5 (shortdash), 1 (longdash), 2 (solid).

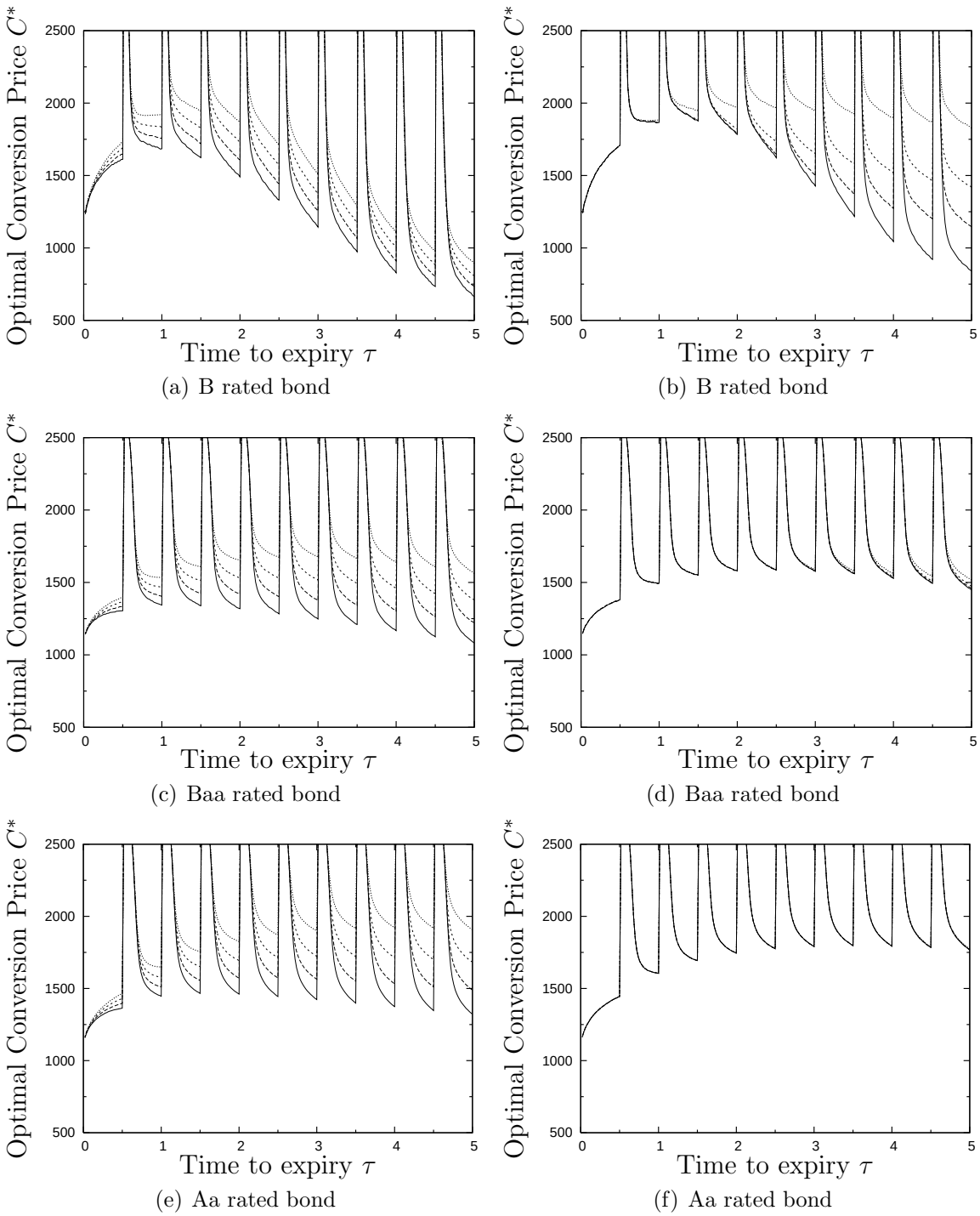

(a) B rated bond (b) B rated bond

(c) Baa rated bond (d) Baa rated bond

(e) Aa rated bond (f) Aa rated bond

Figure 6.2
Optimum conversion price for different ratings
Parameters as in tables 6.2 and 5.1. For (a), (c), and (e), $r_0 = 0.05$ (dot), 0.1 (shortdash), 0.15 (longdash), 0.2 (solid). For (b), (d), and (f), $\bar{T}$ =0.0833 (dot), 0.5 (shortdash), 1 (longdash), 2 (solid).

(figure 6.1(a)) is sufficiently risky and the conversion price ($S_{cp} = 12.5$) sufficiently small so that the convertible debt simply becomes a call on the stock, with the bond part contributing practically nothing to the value. Alternatively, for the Aa rated bond, even after five years the bond is safe enough so as to retain value in the bond part of the convertible price.

Figures 6.1(a), 6.1(c) and 6.1(e) show the effect of the interest rate on the price. The interest rate has a negative effect on the bond part of the convertible debt, most notably in figure 6.1(e), but a positive effect on the equity part, most notable in figure 6.1(a). The negative effect is obvious, and the positive effect comes from the change in conversion price, caused by the negative effect of interest rates on the senior bond. Then in figure 6.1(c) we can see that the value twists under these contrasting effects.

Figures 6.1(b), 6.1(d) and 6.1(f) show the effect of window length on the price. The window length gives an indication of the credit risk on the bond, with a window length of zero equating to a credit risk of zero. The effect of the window length is positive, except where V is small. This is because the convertible debt holders can receive coupons while the firm is in distress, hence the convertible bond holders will lose out if the firm defaults and they forfeit those coupon payments. Due to the leverage ratio of the B rated bond, it is no surprise that the credit risk has most influence on this bond.

In figure 6.2 we show the optimal conversion price for the the convertible. The value of the free boundary from the solver is calculated in terms of the firm value V, but the conversion price in terms of C^* allows for easier comparison between the different rated bonds. The effect of interest rate on the conversion price is shown in figures 6.2(a), 6.2(c) and 6.2(e). Although the interest rates have a positive effect on the price when the convertible is equity like, this only exaggerates the need for early conversion since a higher price for conversion is available. Consequently the interest rate has a negative effect on the optimum conversion price for the bond. The higher rated bonds again show more sensitivity to the interest rate since they are more bond-like than equity-like. Also in this figure, 6.2(b), 6.2(d) and 6.2(f) demonstrate

the effect of window length on optimal conversion. For the B rated bond, the window length has a huge effect on the conversion price, with a shorter window (less risky) implying that the optimal conversion price should be higher. There is not much sensitivity in the Baa rated bond, and the effect is diminished further for the Aa rated bond.

Interest rate and other parameters

Brennan and Schwartz (1980) find the value of a convertible bond to be relatively insensitive to the volatility of interest rate. We find, as did Carayannopoulos (1996), that the sensitivity to interest rate risk is parameter dependent. Figure 6.3(a) suggests that bonds with lower firm value volatility will be more sensitive to interest rate risk. Interestingly there is a maximum in the convertible value (dependent on correlation) for $\sigma_V \approx 0.275$. This is caused by the effect of the volatility on the two options, the default option and the conversion option. Obviously, for this value of V, the increase in value of the default option begins to outweigh the increase in the value of conversion, so the price begins to drop, and a maximum achieved.

In figure 6.3(b) we see the effects of correlation and interest rate risk, which is similar to the effects discussed in the previous chapter for figure 5.10. In this model the effect of the long term interest rate is the most important parameter, since it feeds into the model not only directly through when pricing the convertible bond, but also indirectly through the senior bond issue. Figure 6.4 suggests that the assigning of these two parameters for the interest rate will have a much larger effect than that of the interest rate volatility and correlation.

Capital structure

In chapter 5 we demonstrated how the capital structure of debt was an important factor in determining the price of a corporate bond. From figure 6.5 we see that under this framework the capital structure of the debt together with the leverage ratio of the firm play a huge role in determining the price. The figure 6.5(a), the value of the firm is relatively low, so as the window length is reduced (and hence risk) the structure of

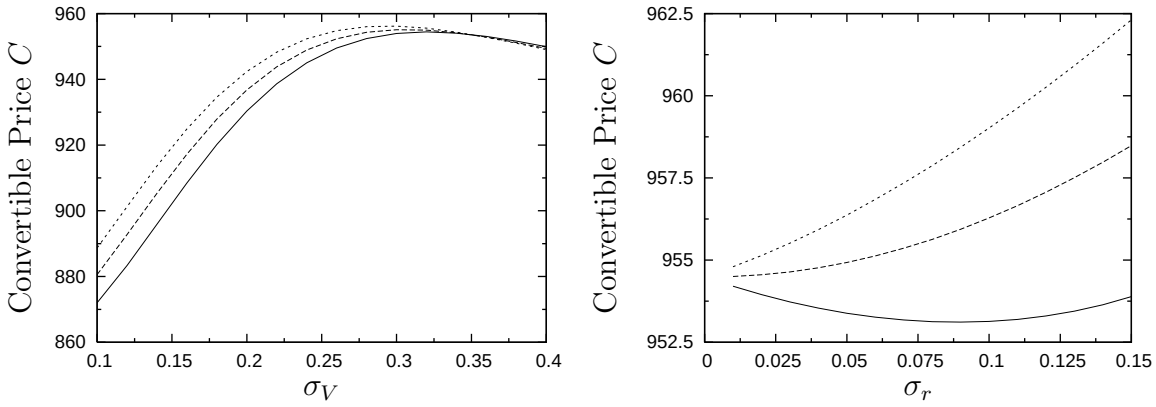

(a) Firm volatility (b) Interest rate volatility

Figure 6.3
Convertible bond price against volatility.
Parameters as in tables 6.2 and 5.1. The bond value $C(V_0, r_0, \bar{T}, T)$ is shown for different volatilities and correlation factors, ρ =-0.5 (solid), 0 (longdash) and 0.5 (shortdash).

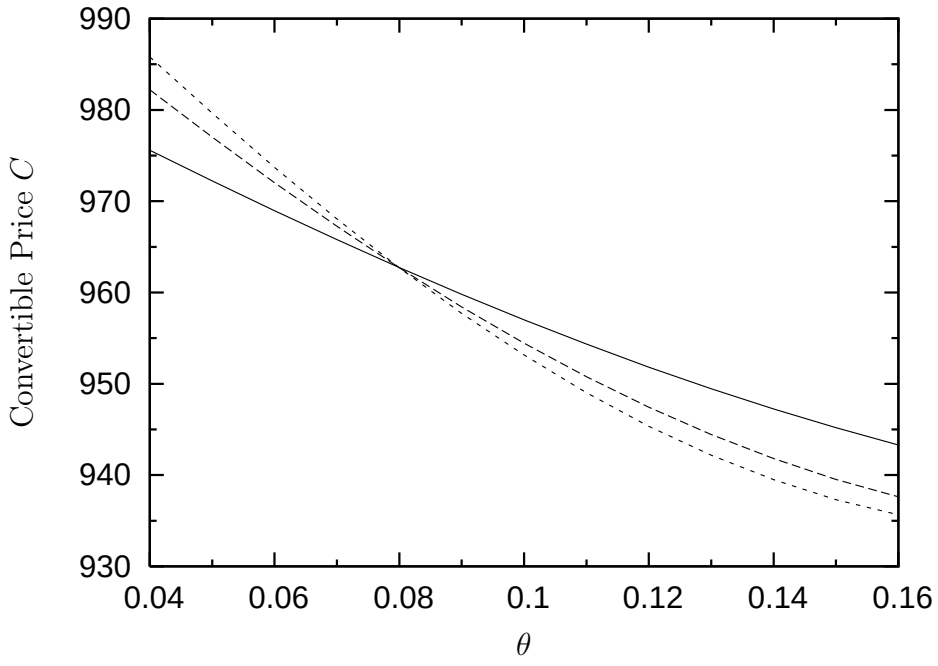

Figure 6.4
Convertible bond price against long term interest rate.
Parameters as in tables 6.2 and 5.1. The bond value $C(V_0, r_0, \bar{T}, T)$ for varying long term mean and mean-reversion rate, κ =0.25 (solid), 0.5 (longdash) and 0.75 (shortdash).

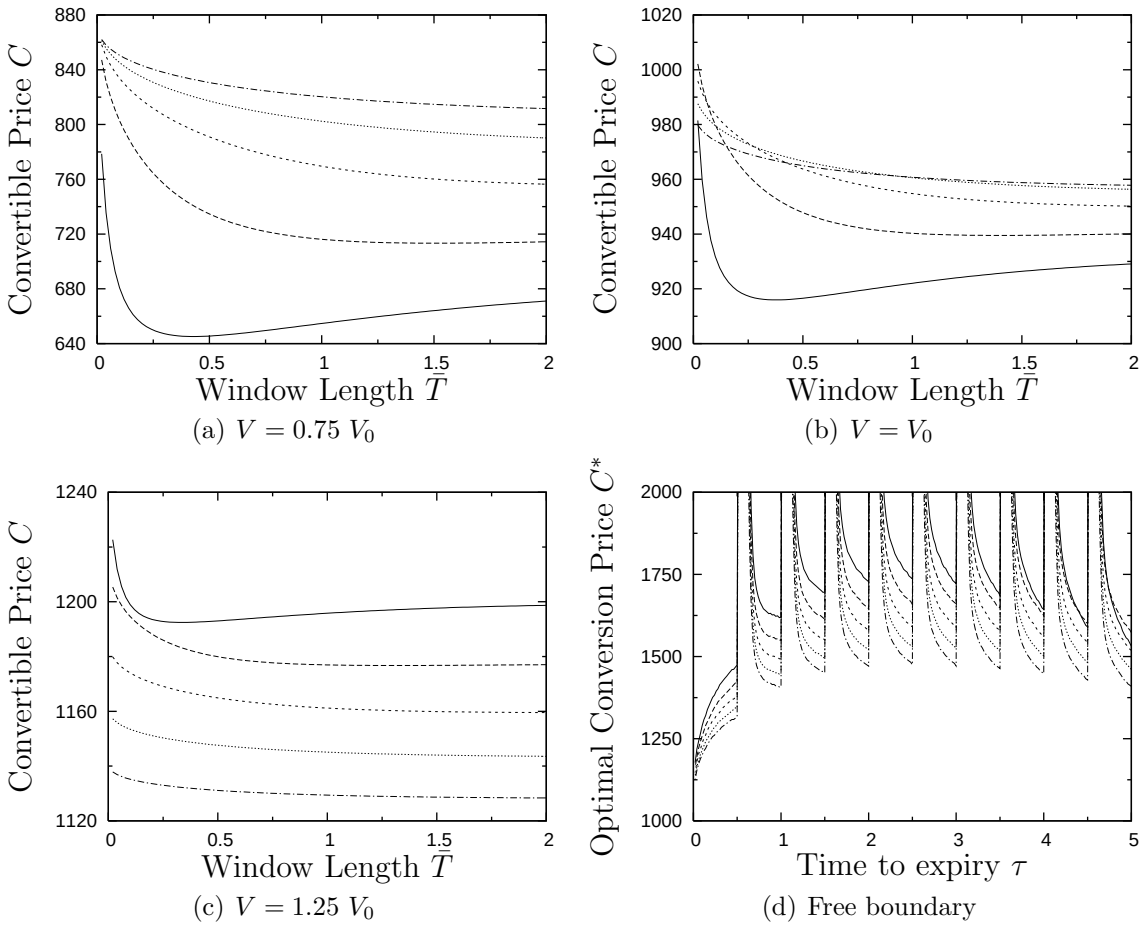

Figure 6.5
Capital structure of the firm's debt
Parameters as in tables 6.2 and 5.1. Total debt $F_T = 500$, with F_{cb} =50 (solid), 150 (longdash), 250 (shortdash) , 350 (dot), and 450 (dashdot). Again $V_0 = F_T/l$

the firm becomes less and less important, all five curves converge towards the same point. As window length is increased, the order of the firms is maintained so that the smallest issue is the cheapest and the largest is most expensive. In figure 6.5(c), when the firm value is relatively high, the order of the bonds has completely reversed. Here the dilution of the firm comes into play, as the smaller issues dilute the firm less, the conversion option on such bonds is worth more. The relative value of the default option for these bonds is negligible at this value of the firm. However, in figure 6.5(b), this region is a more complicated transition region as the conversion option on the firms stock increases in price, and the probability of default decreases. Here we see that for shorter window lengths, some of the smaller issues become more expensive than the large issues, although the trend is eventually reversed as $\bar{T} \to 2$.

The structure of the firm would not necessarily have a large effect on the optimal conversion of the bond since the value of the default option is usually so small for the values of V for which we would convert. We can show that if the issue is small enough, then the reduced dilution of the firm can lead to options where default is still likely even for V close to conversion, since the firm value at which we convert is now so much smaller. Figure 6.5(d) illustrates this as the small issue represented by the solid line (F_{cb}=50) shows optimal conversion at smaller values than the corresponding larger issues, for longer maturities.

Call option

The call option on a convertible bond has been extensively studied, and the results here are standard and complement those from other studies. We present the value of a convertible bond with a call option at facevalue. This is an extreme case although it does present a nice boundary problem, for which the results are given in figure 6.6(b). There are two American options now present, conversion, which attempts to maximise the value, and a call, which attempts to minimise the value. As time tends to expiry, the bond may be called when the interest rate is sufficiently low, or forced to convert when the firm value is sufficiently high (so triggering the call). In the limit as time tends to expiry, this can be expressed as when $r < c_{cb}$ and $V > F_T$, or $V > F_T + N_S S_{cp}$.

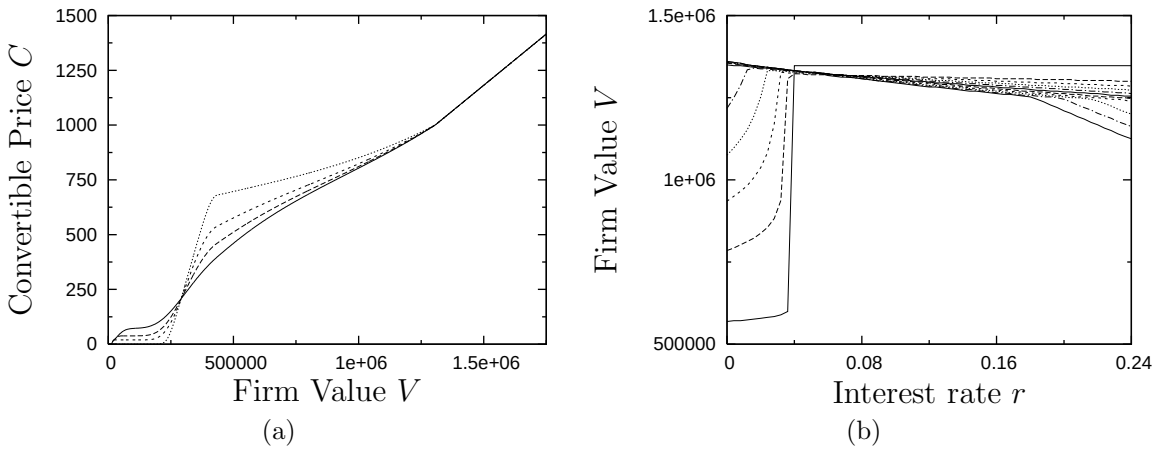

Figure 6.6
Convertible bond with call option.
Parameters as in tables 6.2 and 5.1. The bond is callable at face value. (a) The convertible price at the given value of the firm with $\bar{T}$ =0.0833 (dot), 0.5 (shortdash), 1 (longdash), 2 (solid). (b) The exercise boundary in r and V shown semi-annually over a 5 year maturity, as well as close to expiry (solid).

The boundary as a function of V and r is shown semi-annually over a five year maturity. We can see that for small r, for longer than around two years to maturity the bond is no longer called. For large r, with around four years to maturity and above the bond price is sufficiently small so that conversion is no longer forced (the bottom three lines on the right hand side).

6.5 Conclusions

In this chapter we develop a two-factor model for convertible debt in which the capital structure of debt in the firm is two-tier, and default is a ParAsian option. We investigate the importance of the interest rate and its parameters on the solution, as well as the effect of the window length of the ParAsian option on both the convertible price and optimal conversion, over a range of leverage ratios and debt structures. The ratio of senior debt to convertible debt is found to be important as the senior debt not only affects the default risk of the convertible, but also conversion, since the value at conversion is a function of the senior debt price. Varying the window length gives us an indication of the effect of credit risk on the price. We find that the credit risk can have a significant effect on the price, especially if the convertible debt has a smaller

portion of total debt. We surmise that convertible bond prices need to take these factors into account when either the firm has a low rating, or if the convertible issue is small.

Chapter 7

A New Class of Option – The Delayed-Exercise Option

In this chapter we propose a new type of option, motivated by a practical desire to find an alternative to "ruthless prepayment" used in Real Estate options work. In that area a common assumption in the valuation of mortgages that householders perfectly time their remortgaging activity, prepaying the moment this becomes optimal. Here, in contrast, we model an option that requires the holder to wait a specified period of time during which the option price is beyond a threshold before action can occur. In order to act optimally, the holder initiates this period of waiting earlier than would be optimal if exercise were instantaneous. This presents itself as a free boundary problem, similar to but more complicated than the usual American option. We study this option and those properties that give insight into the dynamics of the American option. First, we discuss the American value process as the limiting case in which the waiting time is zero, before discussing at length the dynamics of the delayed-exercise option. Results are presented for a terminal as well as a perpetual option (for which some approximations may be made), and then finally conclusions are drawn.

7.1 The American Option as a Barrier Option

As is well known, the American option has an early exercise feature, such that the holder of the option may exercise the option at any time during the life of the contract. For an American put, we have that

$$V(S,t) \geq \max[E-S,0] \tag{7.1}$$

Now, let the asset price follow a risk neutral lognormal random walk,

$$\frac{dS}{S} = r\ dt + \sigma\ dW,$$

where dW is the risk neutral measure. Then consider the stochastic process of the option value itself, from Itô's lemma the process followed by V is governed by the following equation.[1]

$$dV = \left[rS\frac{\partial V}{\partial S} + \frac{1}{2}\sigma^2 S^2 \frac{\partial^2 V}{\partial S^2} + \frac{\partial V}{\partial t}\right] dt + \sigma S \frac{\partial V}{\partial S}\ dW. \tag{7.2}$$

Now, the holder of the American option chooses to exercise the option when the value of the option is at or below the exercise price, so the payoff function can be thought to form a barrier in the option value process, at which the option itself is knocked out. However, the exercise strategy has an effect on both the expected rate of return on the option, (the dt term in (7.2)) and the random component, so we cannot specify the process as such without first knowing the exercise strategy.

We also know that there exists a corresponding barrier in the asset price, the optimal exercise boundary $S_f(t)$, at which it is optimal to exercise below (above) and not so above (below). This is a moving barrier, which, if hit by the asset price, knocks out the option and the holder receives $E-S$. So there exists a relationship between the option value process and its barrier, and the underlying process and its

[1] If the option were European, all of the partial derivatives have explicit formulae from which they may be calculated, so the process followed by the European option is a known function of time.

barrier, which can be expressed as

$$V(S,t) = \max[E - S, 0] \qquad \text{if} \quad S < S_f(t)$$
$$V(S,t) \geq \max[E - S, 0] \qquad \text{if} \quad S \geq S_f(t).$$

In this chapter a new framework is set down for an option where the one-touch feature of the American option is relaxed somewhat, such that the option value has to be below the payoff function for a prescribed amount of time before the option can be exercised. We call this option the **delayed-exercise** option.

7.2 The Delayed-Exercise Option

Here we present a model where the holder of the option must initiate a 'waiting' period before the option can be exercised. We assume that the holder of the option initiates this period when the value of the option is above or below the current exercise price of the option. The option can only be exercised when the cumulative time spent by the option value over the 'barrier' reaches some pre-agreed time. The Parisian type version of the option has more financial possibilities, but mathematically is less interesting. In this chapter, we concentrate on the nuances of the cumulative variation, as both options have similar derivations.

Usually a barrier is crossed by the underlying asset but here we think of it as being crossed by the option value itself. Section 7.1 described how the American option can be regarded as a barrier option on either the option value process, or the underlying process, as both are inextricably linked. From a framework in which the barrier is declared in terms of the option value, we will need to find the corresponding barrier in terms of the asset value in order to price the option

We refer back to section 4.3 for the formulation of the ParAsian option, and we use the same notation here. In (4.17) we gave the change in barrier clock time to be dependent on whether the asset value was above (below) some barrier H, for this

new option (of the 'down' variant), let

$$d\bar{t} = \begin{cases} dt & \text{if} \quad V(S,t,\bar{t}\,) \leq G(S,t) \\ 0 & \text{if} \quad V(S,t,\bar{t}\,) > G(S,t) \end{cases}, \tag{7.3}$$

where $G(S,t)$ is the barrier on the option value process. As before, we wish now to interpret this in terms of the underlying asset. So we will require the existence of some function in the underlying asset, $H(t,\bar{t}\,)$ for which

$$\begin{aligned} V(S,t,\bar{t}\,) &< G(S,t) \qquad \text{if} \quad S < H(t,\bar{t}\,) \\ V(S,t,\bar{t}\,) &\geq G(S,t) \qquad \text{if} \quad S \geq H(t,\bar{t}\,). \end{aligned} \tag{7.4}$$

Then it follows that we can write (7.3) as

$$d\bar{t} = \begin{cases} dt & \text{if} \quad S \leq H(t,\bar{t}\,) \\ 0 & \text{if} \quad S > H(t,\bar{t}\,) \end{cases}, \tag{7.5}$$

where the $H(t,\bar{t}\,)$ is a function to be determined. We define the function $H(t,\bar{t}\,)$ to be the *implied* barrier since it depends on the value of the function $V(S,t,\bar{t}\,)$ by (7.4), which itself depends on the value of $H(t,\bar{t}\,)$ through (7.5.) Therefore the function $H(t,\bar{t}\,)$ cannot be determined until $V(S,t,\bar{t}\,)$ has been determined, so the implied barrier creates a free boundary which needs to be determined as part of the solution. Hence, we can reduce the problem to a 'free' barrier ParAsian problem, in which the position of the implied barrier has to be found as part of the solution.

The delaying of exercise, is, in essence, a sub-optimal option, so the question is to reason why anyone would need to model such an option. There are two main motivations for studying such options. First, the early exercise feature is not always the preserve of the holder. Notable exceptions are the call features in bond contracts, in which the writer of the bond has the option to buy back the bond at a predetermined amount, and also similar features on mortgage-backed securities. In

collaboration with the author, Sharp et al. (2007) have introduced the Parisian variant of the option into mortgage-backed securities framework, where the writer of the option, the borrower (the holder is the bank), often chooses to delay prepayment. It is well known that the writers of convertible bonds do not always act 'optimally' and delay the calling of the bond until the stock price is above the conversion price for some time, or alternatively, the bond value is above the call price. Gauthier (2000) also concludes that real options are often exercised sub-optimally, or that exercise is delayed. Second, the option can provide a fluid link between the European option and the American option. This will be of especial interest later, when a new method will be suggested for extrapolating from European to American values.

7.2.1 Rational Pricing

Following rational option pricing, such as that used by Merton (1990), some bounds can be imposed on the value of the delayed-exercise option. Let $V_E(S,t)$ be the European Option, $V_A(S,t)$ be the American equivalent, and $V(S,t,\bar{t}\,)$ be the delayed-exercise option. Given the European option and the American option with the same parameters, it follows that

$$V_A(S,T-t) \geq V_E(S,T-t), \tag{7.6}$$

and that

$$V_A(S,T-t_1) \geq V_A(S,T-t_2) \quad \text{if} \quad t_2 \geq t_1. \tag{7.7}$$

These two inequalities follow from the principle that the option to exercise, like all options, intrinsically has positive value. For (7.6), if the holder has the right to exercise, then he must pay for this right, since he can choose to exercise, or not to exercise, optimally. At worst, if he never exercises, the two options are equivalent, since he will only choose to exercise if it is optimal to do so; the value of the option must increase if he chooses to exercise. Similarly, for (7.7) the holder of the option with longer maturity has more time during which to exercise. If the holder of the

option with longer maturity, adopts an approach to convert optimally up until the maturity date of the shorter option, at which time he unconditionally exercises, the two options would be worth the same amount. Since the holder of the option with longer maturity does not have to convert at the shorter ones maturity date, and acting optimally would not necessarily do so, the longer option has more value.

For the delayed-exercise option, if the time to knock-out, $\bar{T} - \bar{t}$ is longer than the time to maturity then the option value is simply that of the corresponding European,

$$V(S, T-t, \bar{T}-\bar{t}\,) = V_E(S, T-t) \quad \text{if} \quad \bar{T}-\bar{t} > T-t.$$

At the other extreme, analogous to the manner in which the ParAsian option asymptotes to the vanilla barrier option as the time to knock-out reaches zero, the delayed-exercise becomes American:

$$\lim_{\bar{T}-\bar{t}\to 0} V(S, T-t, \bar{T}-\bar{t}\,) = V_A(S, T-t).$$

Section 7.1 has already explained how an American option can be viewed as a knock-out barrier option.

The delayed-exercise option must also satisfy

$$V(S, T-t, \bar{T}-\bar{t}_1) \geq V(S, T-t, \bar{T}-\bar{t}_2) \quad \text{if} \quad \bar{T}-\bar{t}_1 \leq \bar{T}-\bar{t}_2.$$

When the time-to-knock-out is closer, the option is worth more, because it is more likely to be exercised (much in the same way as the American is always worth more than the European). Hence the following inequalities between the three options can be stated,

$$V_E(S, T-t) \leq V(S, T-t, \bar{T}-\bar{t}\,) \leq V_A(S, T-t).$$

If we assume that the value of the delayed-exercise option is continuous across $\bar{t}$, the knock-out time, then the delayed option will form a continuous function linking the European option to its American counterpart.

7.2.2 Pricing the delayed-exercise option

Now let us study delayed-exercise on a put option. Let the option be defined such that

$$V(S,T,\bar{t}) = \max[E-S,0] \qquad \forall \quad \bar{t}, \tag{7.8}$$

$$V(S,t,\bar{T}\,) = \max[E-S,0] \qquad \forall \quad t, \tag{7.9}$$

noting that at knock-out the exchange is not for an option expiring at T, but the exercise value. Then the condition on the barrier clock is

$$d\bar{t} = \begin{cases} dt & \text{if} \quad S \le H(t,\bar{t}\,) \\ 0 & \text{if} \quad S > H(t,\bar{t}\,) \end{cases}, \tag{7.10}$$

where $H(t,\bar{t}\,)$ is the implied barrier. Since we must solve the option as if it were a ParAsian option with a moving barrier, then referring to section 4.3, we must solve (4.6) for $S \le H(t,\bar{t}\,)$, and (4.5) for $S > H(t,\bar{t}\,)$. Now from (7.4), we know that the value of the option at the barrier is given by

$$V(H(t,\bar{t}\,),t,\bar{t}) = E - H(t,\bar{t}\,), \tag{7.11}$$

since the option value must be below the payoff when the asset price is below the barrier, and above the payoff when the asset price is above the barrier. We also need a second condition on the barrier in order to determine the position of the barrier, namely continuity of the first derivative across the barrier,

$$\left.\frac{\partial V}{\partial \hat{S}}\right|_{S=H(\bar{t},t)_-} = \left.\frac{\partial V}{\partial \hat{S}}\right|_{S=H(\bar{t},t)_+}. \tag{7.12}$$

Let us refer back to section 7.2.1, where we have that

$$V_E(S,T-t) \le V(S,T-t,\bar{T}-\bar{t}\,) \le V_A(S,T-t).$$

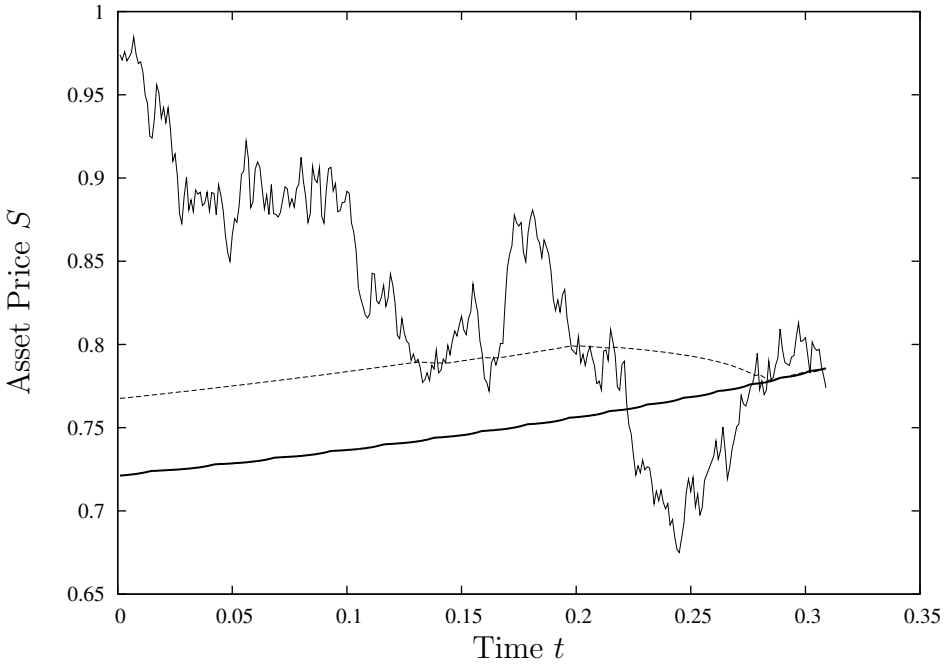

Figure 7.1
Monte Carlo simulation.
A Monte Carlo simulation showing how the option is highly path dependent. The thin solid line shows a random walk with $S_0 = 1$, the thick solid line is the optimal stopping barrier S_f for an American put, the dashed is the implied barrier H for the random walk shown. S_f is calculated using methods from chapter 2, H is calculated by methods discussed later, with $\sigma = 0.4$, $r = 0.1$, $T = 0.5$ and $\bar{T} = 0.1$.

It then follows that for a put option, where it optimal to exercise at or below the exercise boundary

$$H_E(T-t) \geq H(T-t, \bar{T}-\bar{t}\,) \geq S_f(T-t).$$

We also have that

$$V(S, T-t, \bar{T}-\bar{t}_1) \leq V(S, T-t, \bar{T}-\bar{t}_2) \quad \text{if} \quad \bar{T}-\bar{t}_1 \geq \bar{T}-\bar{t}_2,$$

from which it follows that

$$H(T-t, \bar{T}-\bar{t}_1) \leq H(T-t, \bar{T}-\bar{t}_2) \quad \text{if} \quad \bar{T}-\bar{t}_1 \geq \bar{T}-\bar{t}_2.$$

In figure 7.1, a single Monte-Carlo simulation was used to produce a risk-neutral random-walk by the asset (solid line). Then using numerical methods described later in this chapter, the value of option and its implied barrier were calculated. The dashed line shows the implied barrier $H(t, \bar{t}\,)$, for the given path. As the asset value moves below the barrier, $\bar{t}$ increases, and the option is more likely to be knocked out. This has the effect of decreasing H, therefore making it less likely to be knocked out. For the walk shown, the delayed-exercise option from which we derive H has a knock-out time of 0.1, the thick solid line shows $S_f(T-t)$ for the corresponding American option. This American option would have been knocked-out around $t = 0.22$, when the asset path crosses the thick solid line. Here, exercise is delayed until $t = 0.31$, when the option value has been cumulatively below the exercise price for 0.1 years. Notice that $H(t, \bar{t}\,) \to S_f(t)$, as knock-out becomes more and more likely.

7.2.3 The Existence of the Implied Barrier

Now we can use the bounds imposed from section 7.2.1 to guarantee that there exists a unique point, $\hat{S}$ such that

$$V(\hat{S}, t, \bar{t}\,) = G(\hat{S}, t). \tag{7.13}$$

Let us consider a put option, as described above, with $G(S,t) = E - S$. The fact that the solution is bounded above and below by V_A and V_E (by definition there exists a point both on V_E and V_A for which (7.13) holds) implies that we can guarantee that there exists at least one point such that (7.13) is satisfied, and that $\hat{S} \in (\ S_f(t), H_E(t)\ )$. It can be shown that for there to exist two or more points such that (7.13) holds, we would require that

$$\frac{\partial V}{\partial S} \leq -1,$$

for $S \in (\ S_f(t), H_E(t)\ )$. However, by rational pricing theory, the minimum value Δ can take for a put option is -1. When hedging, the writer of the option would never need to go long in more than one share, since that is the maximum number of shares the writer is liable to deliver. If $\Delta = -1$ over some range $[S^*_{min}, S^*_{max}] \in (\ S_f(t), H_E(t)\ )$ such that $V(S^*, t, \bar{t}\ ) = E - S^*$, then $V(S, t, \bar{t}\ )$ is an American option with optimal exercise boundary $S^*_{max} > S_f(t)$. So by the uniqueness of $V_A(S,t)$ such a solution cannot exist. Similarly this type of argument can be extended to more general options, such as a call on a stock, where $\Delta \leq 1$, or a call on a bond where $\Delta \geq 0$.

For the implied barrier to exist, we require that when we impose the barrier $H(t, \bar{t}\ )$, there exists a barrier such that

$$H(t, \bar{t}\ ) = \hat{S} \tag{7.14}$$

$$V(\hat{S}, t, \bar{t}\ ) = E - \hat{S}. \tag{7.15}$$

This can be achieved by trapping the barrier. Let us apply an arbitrary barrier, $H' \in [\ S_f(t), H_E(t)\ ]$, at time t, $\bar{t}$, and assume that $V(S, t, \bar{t}; H')$ is a continuous function with respect to the parameter H'. Then for a given H', there exists a point in S, say S', such that

$$V(S', t, \bar{t}; H') = E - S'.$$

So we have that either $S' \in (S_f(t), H')$, $S' \in (H', H_E(t)\ )$ or $S' = H'$ in which case

$H' = H(t, \bar{t}\ )$.

Assume that $S' \in (S_f(t), H')$ is now a function of the choice of barrier,[2] H', then by the continuity of $V(S, t, \bar{t}\ ; H')$ w.r.t. the barrier H', the function $S'(H')$ is also continuous. Therefore we can always choose a value H'_{min} such that

$$S'(H) < H \qquad \forall \qquad H \in (H'_{min}, H'). \tag{7.16}$$

Then at the minimum value of H'_{min} for which (7.16) is satisfied, $H' = S'$, which determines the location of the implied barrier.

7.3 Numerical Analysis

In this section we outline a fixed grid method with which to solve the delayed-exercise option. Unfortunately, the formulation of the problem does not lead to variational inequalities, and then a linear complementarity problem (such as the one outlined in chapter 2 for the American option), for which it would be simple to solve using a Projected SOR algorithm. To develop a numerical scheme to price such an option is a lot less straightforward than for the simple American option. We use Newton iteration to find the position at which V crosses the payoff function, S', as a function of H so that we can iterate until $S' = H$. The convergence of this scheme relies on our ability to position the barrier continuously over the domain. In modelling the ParAsian feature we follow the numerical techniques outlined in section 4.2.2.

We can then form the following set of equations for nodes not on the barrier,

$$\begin{aligned} \alpha_i v_{i-1}^{k+1,l+1} + (\frac{1}{\Delta\tau} + \beta_i) v_i^{k+1,l+1} + \gamma_i v_{i+1}^{k+1,l+1} &= Z_i^{k,l} \quad \text{if} \quad i \le h_i^{k+1,l+1}, \\ \alpha_i v_{i-1}^{k+1,l+1} + (\frac{1}{\Delta\tau} + \beta_i) v_i^{k+1,l+1} + \gamma_i v_{i+1}^{k+1,l+1} &= Z_i^{k,l+1} \quad \text{if} \quad i > h_i^{k+1,l+1}. \end{aligned} \tag{7.17}$$

[2]The argument is the same if $S' \in (H', H_E(t)\ )$

where the position of the barrier is $h_i^{k+1,l+1} = \text{INT}\left(\frac{H(\tau,\bar{\tau})}{\Delta S}\right)$ and

$$Z_i^{k,l} = -\alpha_i v_{i-1}^{k,l} + (\frac{1}{\Delta\tau} - \beta_i)v_i^{k,l} - \gamma_i v_{i+1}^{k,l}.$$

The function INT takes the integer part of a real number, so the true position of the barrier is somewhere in-between, $h_i^{k+1,l+1} \cdot \Delta S \leq H(\tau,\bar{\tau}) < h_{i+1}^{k+1,l+1} \cdot \Delta S$. In (7.17) the position of the barrier is under-estimated, since $h_i^{k+1,l+1} \cdot \Delta S \leq H(\tau,\bar{\tau})$. Let us examine a scheme where the barrier is *over*-estimated, such as

$$\begin{aligned}
\alpha_i v_{i-1}^{k+1,l+1} + (\frac{1}{\Delta\tau} + \beta_i)v_i^{k+1,l+1} + \gamma_i v_{i+1}^{k+1,l+1} &= Z_i^{k,l} \quad \text{if} \quad i \leq h_i^{k+1,l+1} + 1, \\
\alpha_i v_{i-1}^{k+1,l+1} + (\frac{1}{\Delta\tau} + \beta_i)v_i^{k+1,l+1} + \gamma_i v_{i+1}^{k+1,l+1} &= Z_i^{k,l+1} \quad \text{if} \quad i > h_i^{k+1,l+1} + 1. \quad (7.18)
\end{aligned}$$

Next, we define a parameter $\theta \in [0,1)$ such that

$$H(\tau,\bar{\tau}) = h_i^{k+1,l+1} \cdot \Delta S + \theta \cdot \Delta S.$$

Then to make a first order approximation to the solution with a barrier at $H(\tau,\bar{\tau})$, we simply take the weighted average of the two schemes, (7.17) and (7.18). Then the following scheme, which can have a barrier in between nodes, is obtained

$$\begin{aligned}
&\alpha_i v_{i-1}^{k+1,l+1} + (\frac{1}{\Delta\tau} + \beta_i)v_i^{k+1,l+1} + \gamma_i v_{i+1}^{k+1,l+1} \\
&\qquad = Z_i^{k,l} \quad \text{if} \quad i < h_i^{k+1,l+1} + 1, \\
&\alpha_i v_{i-1}^{k+1,l+1} + (\frac{1}{\Delta\tau} + \beta_i)v_i^{k+1,l+1} + \gamma_i v_{i+1}^{k+1,l+1} \\
&\qquad = \theta Z_i^{k,l} + (1-\theta)Z_i^{k,l+1} \quad \text{if} \quad i = h_i^{k+1,l+1} + 1. \\
&\alpha_i v_{i-1}^{k+1,l+1} + (\frac{1}{\Delta\tau} + \beta_i)v_i^{k+1,l+1} + \gamma_i v_{i+1}^{k+1,l+1} \\
&\qquad = Z_i^{k,l+1} \quad \text{if} \quad i > h_i^{k+1,l+1} + 1. \qquad (7.19)
\end{aligned}$$

If $\theta = 0$, then (7.19) is identical to (7.17), and when $\theta \to 1$, (7.19) $\to$ (7.18). The scheme can be solved using a numerical solver, such as LU decomposition or Gaussian elimination, provided H is given. Therefore, an algorithm must be devised in order

```
GRID SEARCH(barrier, v, g)
 1  theta = 0
 2  while error > tol
 3  do
 4      ComputeScheme(alpha, beta, gamma, z, v, barrier, theta)
 5      TridiagonalSolver(alpha, beta, gamma, z, v)
 6      FindNewBarrier(newbarrier, barrier, newtheta, theta, v, g)
 7      error ← (barrier − newbarrier)^2 + (theta − newtheta)^2
 8      theta ← newtheta
 9      barrier ← newbarrier
10  return NIL
```

Figure 7.2
Grid search algorithm – pseudo code

to iterate and find the barrier H. This updated scheme ensures that the solution $v^{k+1,l+1}$ is continuous with respect to the choice of the barrier.

7.3.1 The Delayed-Exercise Option Algorithm

Figure 7.2 shows the algorithm used to solve for the delayed-exercise option. The algorithm is used to solve for each barrier timestep in turn. The inputs to the algorithm are: the integer value $h_i^{k+1,l}$ from the previous calculation, '*barrier*'; the value of the option at each of the four nodes needed to calculate $v^{k+1,l+1}$, 'v'; and the constraint or exercise value $G(S) = E - S$, 'g'. The function '*ComputeScheme*' sets up the numerical scheme as in (7.19). Then the system is solved using a tridiagonal solver. Then we can find the position S^*, at which the solution v crosses the constraint g. We can then calculate '*newbarrier*' and '*newtheta*' from

$$S^* = newbarrier \star \Delta S + newtheta \star \Delta S$$

where '*newbarrier*' is an integer and '*newtheta*' is a real number in $[0, 1)$. Then, when the difference between the old position of the barrier and the barrier position *implied* by that barrier is sufficiently small we exit the loop.

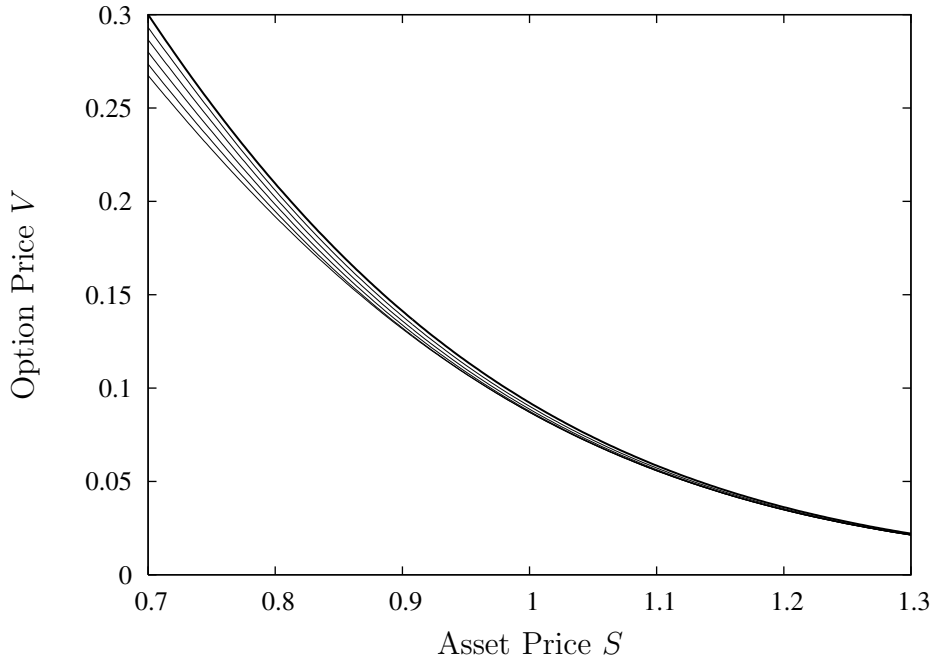

Figure 7.3
The delayed-exercise put option
The delayed-exercise put option (solid) and the corresponding American (thick solid). Top to bottom $\bar{T} = 0$ (American), 0.1, 0.2, 0.3, 0.4, and 0.5 (European)

7.4 Results

Unless otherwise specified, all of the subsequent results are for a delayed-exercise Put option with $\sigma = 0.4$, $r = 0.1$, a maturity of six months ($T = 0.5$), a strike price of $E = 1$, and no dividend payments. Figures 7.3 - 7.5 show that the delayed-exercise option upholds all of the criteria set down in subsection 7.2.1. It is shown that the value of the option is increasing as the time-to-knockout decreases, the value of the option is continuous, and that the free-barrier is both continuous, and tends to the American free-boundary as the time-to-knockout decreases.

In figure 7.4 the value of the exercise premium, which we denote as $\varepsilon(S, t, \bar{t}\ )$, is shown.[3] This was calculated by taking the difference between the delayed-exercise option and the European option. As the value of the asset tends to zero, the exercise

[3]It was Barone-Adesi and Whaley (1987) that used an approximation to the value of the exercise premium to get a quadratic approximation to the American option value.

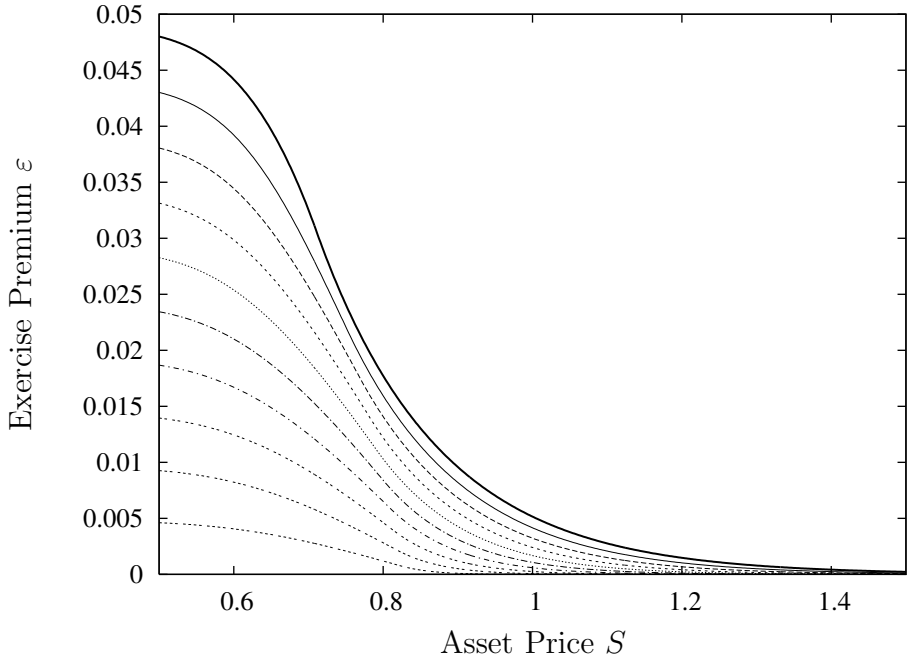

Figure 7.4
The exercise premium.
The value of the option to exercise $(V(S,0,0) - V_E(S,0))$ against the asset price S. The thick solid line is the value of the American option to exercise $(V_A - V_E)$. Top to bottom time-to-knockout $\bar{T}$ is increased in steps of 0.05, from 0 (American) to 0.5 (European).

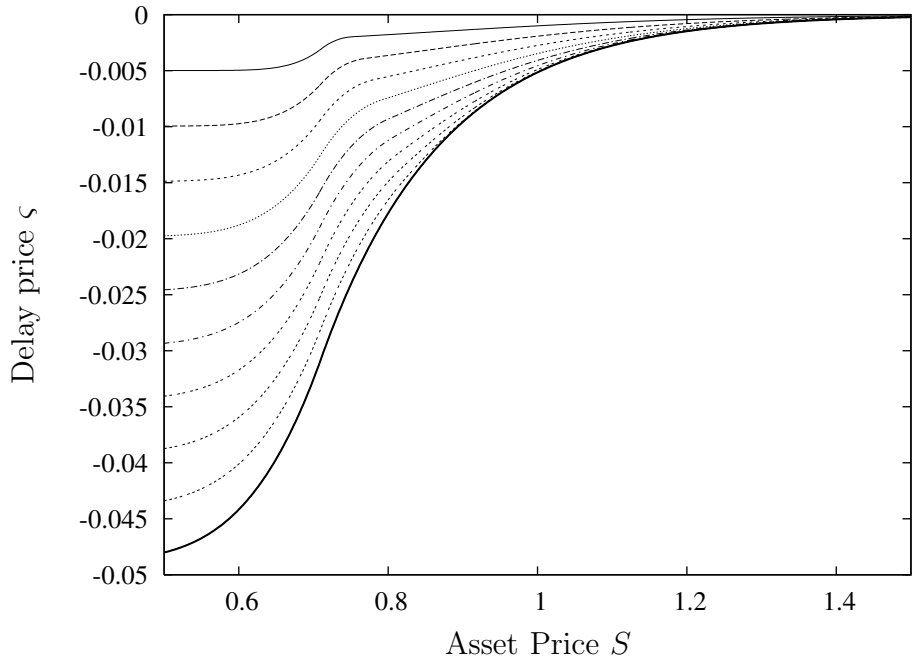

Figure 7.5
The delay option.
The value of the option to delay ($V(S,0,0) - V_A(S,t)$) against the asset price S. The thick solid line is the value of the option to wait till expiry ($V_E - V_A$). Top to bottom time-to-knockout $\bar{T}$ is increased in steps of 0.05 from 0 (American) to 0.5 (European).

premium is given by

$$\varepsilon(0,t,\bar{t}\,) = E \cdot \left(\min[e^{-r(\bar{T}-\bar{t}\,)},1] - e^{-r(T-t)}\right).$$

This is because when $S = 0$ the asset price will definitely be below the implied asset barrier, and will either be exercised at maturity, or after $\bar{T}-\bar{t}$ if $\bar{T}-\bar{t} < T-t$. As the asset value grows without bound, the value of the option to exercise is reduced as the probability that it will ever be under the implied barrier for $\bar{T}-\bar{t}$ approaches zero. Hence, the American, and all delayed-exercise option values approach that of the European. Around the strike price $E = 1$ we can see that when the time-to-knockout is small the growth in value of the option appears linear in $\bar{t}$.

In figure 7.5 the option to *delay* exercise, denoted $\varsigma(S,t,\bar{t}\,)$ is shown. This is calculated by taking the difference between the delayed-exercise option and the American option. The option value is negative because it is to the option writer's advantage to

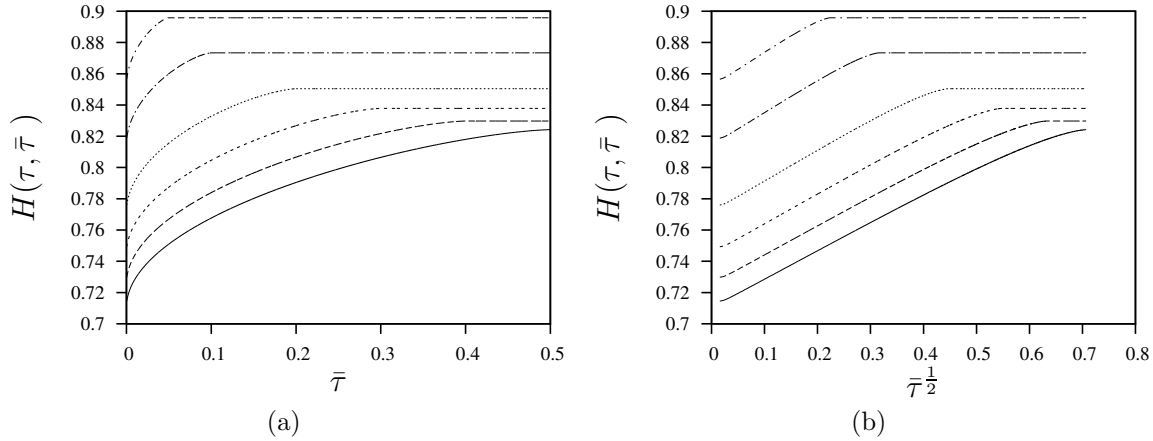

Figure 7.6
Barrier H vs. time to knockout and root time to knockout.
The free "barrier" for the delayed-exercise option against time-to-knockout, for varying time-to-maturity. Top to bottom, $\tau = 0.05$, 0.1, 0.2, 0.3, 0.4 and 0.5.

delay exercise. When the time-to-knockout is small, the period of time that exercise is delayed is small, and hence the option to delay value is small. In this region, there is a sharp increase in the gradient of the option around $S = 0.7$. This relates to the position of the barrier, where the clock ticks below but not above. Obviously, if the value of the asset is below the barrier, the probability of the option being exercised is greatly increased as opposed to it being even just slightly above.

In figure 7.6 the free barrier location $H(\tau, \bar{\tau}\ )$ is shown. When $\tau \leq \bar{\tau}$ the curve is flat and $H(\tau, \bar{\tau}\ ) = H_E(\tau)$. As $\bar{\tau} \to 0$ and the option becomes almost like the American, then $H(\tau, \bar{\tau}\ ) \to S_f(\tau)$. Figure 7.6(b) plots $H(\tau, \bar{\tau}\ )$ against $\tau^{1/2}$, and since all the curves appear straight (also appear to have the same gradient) the suggestion is that the asymptotic behaviour of H is

$$H(\tau, \bar{\tau}) \approx S_f(\tau) + A \cdot \bar{\tau}^{\frac{1}{2}} \quad \text{if} \quad \bar{\tau} \ll \tau.$$

However, this could only be confirmed by rigorous asymptotic analysis. A possible explanation, of this nature is given later in the chapter, when the perpetual case is investigated.

Figures 7.7 and 7.8 show the variation of $H(\tau, \bar{\tau}\ )$ with τ for varying $\bar{\tau}$. For a given $\bar{\tau}$, $H(\tau, \bar{\tau}\ )$ will follow the European barrier for $\tau < \bar{\tau}$, then deviate toward the

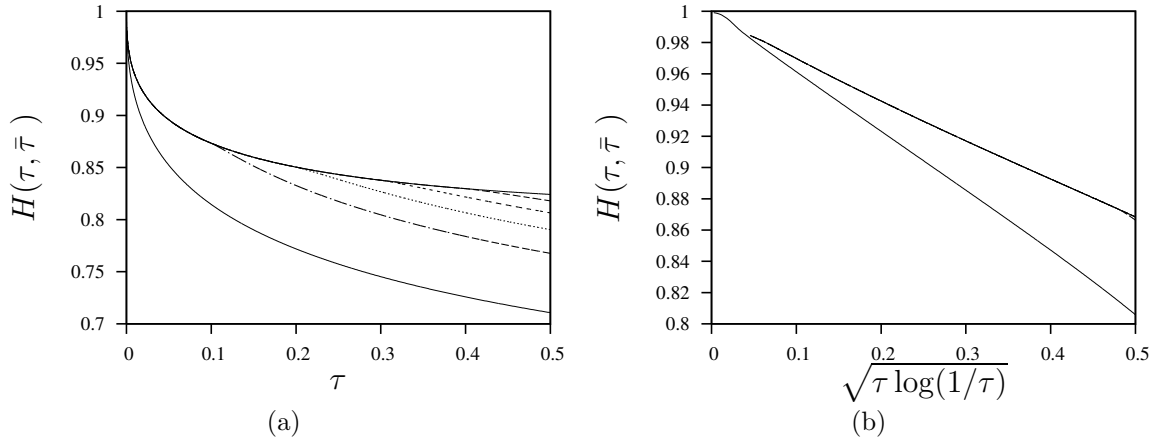

Figure 7.7
Barrier H vs. time to maturity and log time.
The free "barrier" for the delayed-exercise option against time, for large time-to-knockout. Top to bottom, $\bar{\tau} = 0.5$, 0.4, 0.3, 0.2,0.1 and 0.

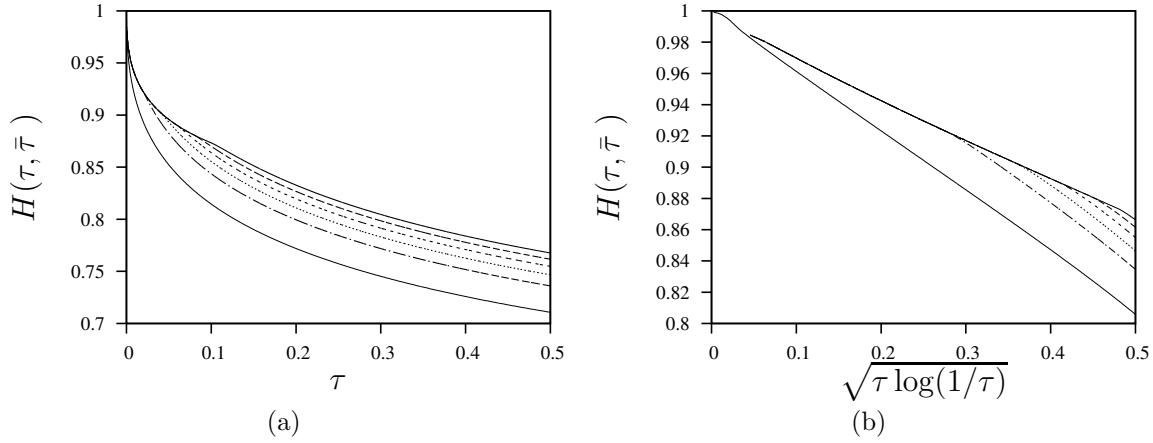

Figure 7.8
Barrier H vs time to maturity and log time
The free "barrier" for the delayed-exercise option against time, for small time-to-knockout. Top to bottom, $\bar{\tau} = 0.1$, 0.08, 0.06, 0.04,0.02 and 0.01. The dashed line shows the free boundary for the American.

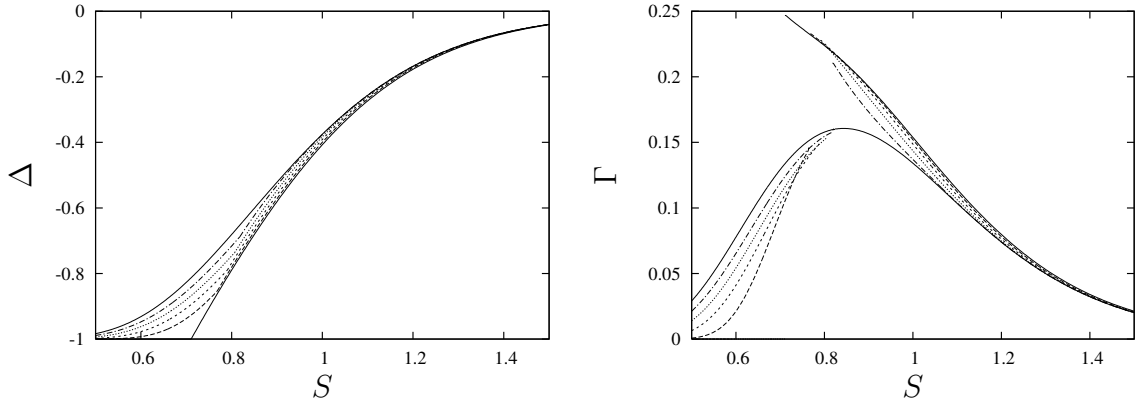

(a) Δ (b) Γ

Figure 7.9
The Greeks.
The value of Δ and Γ against the asset price S for varying values of time-to-knockout for a six month option. Top to bottom $\bar{\tau} = 0.5$ (European), 0.4, 0.3, 0.2, 0.1 and 0 (American).

American free boundary, and then seems to stay parallel to it. It has been shown earlier (section 2.3) that for small τ the free boundary of the American put will be of order $\sqrt{\tau \log(1/\tau)}$. Then in figures 7.7(b) and 7.8(b) the free barrier is plotted against $\sqrt{\tau \log(1/\tau)}$. The American free boundary forms a straight line, as does the European barrier. When $\bar{\tau}$ is small H also forms a straight line parallel to the American free boundary. This suggests that H is of order $\sqrt{\tau \log(1/\tau)}$ in τ when $\tau \gg \bar{\tau}$. Again though, these graphs cannot confirm these trends, and future work could involve investigating the asymptotic analysis of such a problem.

Figures 7.9 and 7.10 plot the Greeks Δ and Γ for various $\bar{\tau}$. Figure 7.10(a) shows how the Δ for the European option converges as $\bar{\tau} \to 0$ to the Δ for the American. The Δ for the American is undefined for $S < S_f(t)$ since the option has been exercised, but we take it to be -1 here. This causes an apparent discontinuity in Γ, but the option is undefined in this region so it does not really exist. The discontinuity is transferred to the delayed-exercise Γ, at the barrier level $H(\tau, \bar{\tau}\ )$. Δ is continuous across the barrier though, and in figure 7.10(a) it can be seen how Δ follows the hedging strategy for the American when $S > H$ and one that resembles a European (with time-to-maturity equal to the time-to-knockout) when $S < H$. It is this change in strategy across the barrier that causes the discontinuity in Γ.

In fact, we can use the continuity across the barrier to give us a smooth pasting

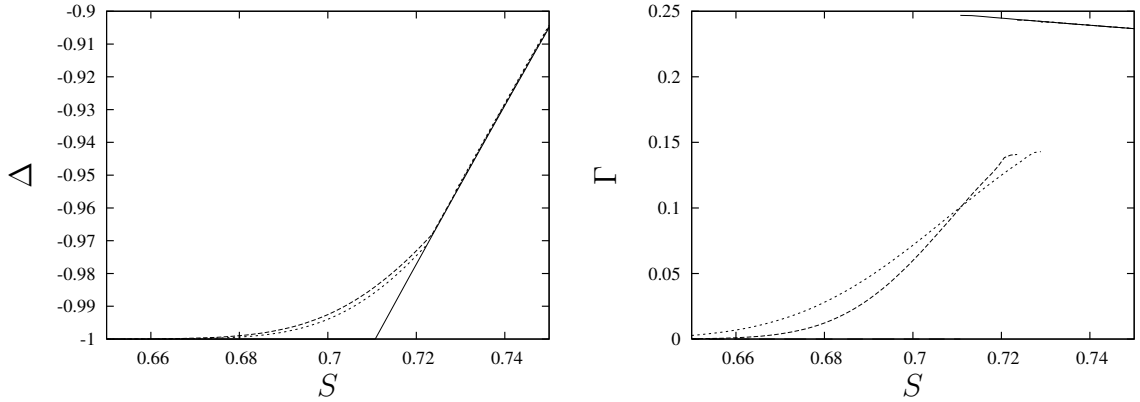

(a) Δ (b) Γ

Figure 7.10
The Greeks, zoomed region.
The value of Δ and Γ against the asset price S for varying small values of time-to-knockout for a six month option. Top to bottom $\bar{\tau} = 0.01$, 0.005 and 0 (American).

condition, just as we have for the standard American option. The continuity of Δ ensures that a solution is consistent and satisfies the BSM equation. For the American option, the constraint says that the value of the option must always be greater than or equal to the exercise price. However, when the problem is formulated using the free-boundary condition, the constraint is hidden inside the smooth pasting condition:

$$V(S,t) > G(S) \quad \Longleftrightarrow \quad V(S_f,t) = G(S_f) \quad \text{and} \quad V_S(S_f,t) = G_S(S_f).$$

Similarly, we can formulate the delayed-exercise option using a smooth pasting condition:

$$\begin{aligned} V(S,t,\bar{t}\,) &< E - H(t,\bar{t}) \quad \text{if} \quad S < H(t,\bar{t}) \\ \text{and} \quad V(S,t,\bar{t}\,) &> E - H(t,\bar{t}) \quad \text{if} \quad S > H(t,\bar{t}), \\ \Longleftrightarrow \quad & V(H(t,\bar{t}\,),t,\bar{t}\,) = E - H(t,\bar{t}) \\ \text{and} \quad V_S(H(t,\bar{t}\,)_-,t,\bar{t}\,) &= V_S(H(t,\bar{t}\,)_+,t,\bar{t}\,). \end{aligned} \tag{7.20}$$

When studying the option value it has been previously commented that the option value appears to tend toward the American option value in a linear fashion. If this is the case, this may lead to a means of extrapolating from the European value to the

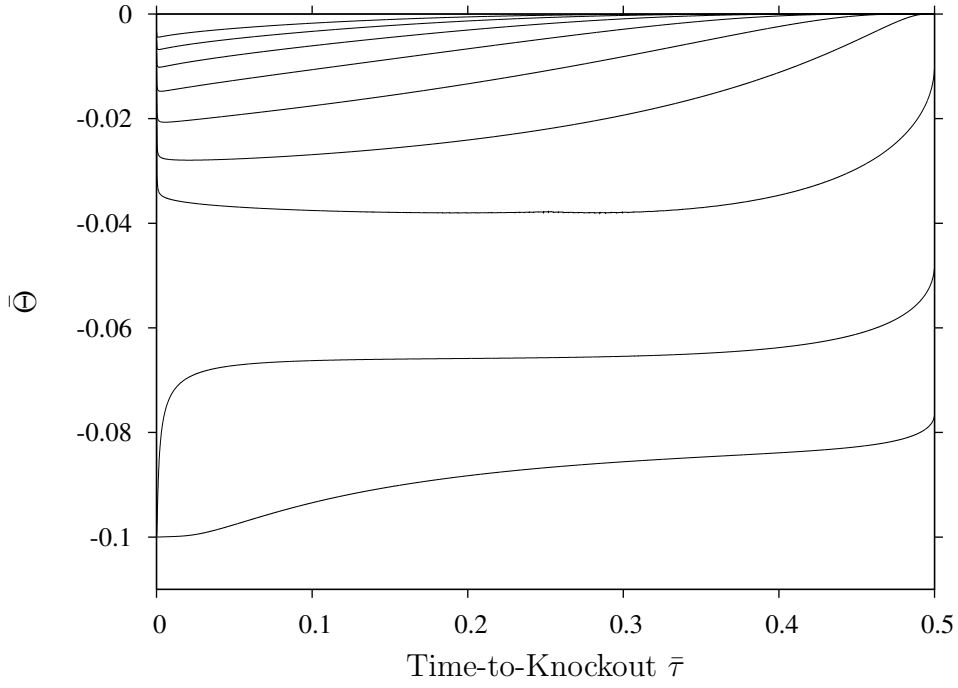

Figure 7.11
The value of $\bar{\theta} = \partial V/\partial\bar{\tau}$.

American. For this reason, in figure 7.11 we examine a new Greek, $\bar{\Theta}$, the effect of decay in barrier time,

$$\bar{\Theta} = \partial V/\partial\bar{\tau}.$$

Not surprisingly the behaviour of the option with respect to barrier time is not simple. The lower bound in figure 7.11 is $-rE$. This is because the value of the option decreases fastest when the option is in-the-money and $V \approx Ee^{-r\bar{\tau}} - S$.

7.5 The Perpetual Case

It is well-known that the American option has a steady-state solution. This can be shown since there exists a maximum bound on the value, and also that the value of the American option is a monotonically increasing function in time-to-expiry. It can also be shown, therefore, that there exists a steady-state solution for the delayed-exercise

option. From the rational pricing discussed earlier,

$$V(S,\tau_1,\bar{\tau}) > V(S,\tau_2,\bar{\tau}) \quad \text{if} \quad \tau_1 > \tau_2 \quad \text{and} \quad \tau_2 \geq \bar{\tau},$$

shows the function is monotonically increasing in τ for $\tau > \bar{\tau}$, and we have the upper bound

$$V(S,\tau,\bar{\tau}) < V_A(S,\tau) \quad \text{if} \quad \bar{\tau} > 0.$$

Then there must exist a steady state solution. So let us set $\partial/\partial\tau = 0$ in (4.6) and (4.5) to obtain

$$V_{\bar{\tau}} = \frac{1}{2}\sigma^2 S^2 V_{SS} + rSV_S - rV \quad \text{for} \quad S < H(\bar{\tau}) \tag{7.21}$$

$$0 = \frac{1}{2}\sigma^2 S^2 V_{SS} + rSV_S - rV \quad \text{for} \quad S > H(\bar{\tau}), \tag{7.22}$$

subject to the following boundary conditions;

$$V(S,0) = \max[E - S, 0], \tag{7.23}$$

$$V(0,\bar{\tau}) = E \cdot e^{-r\bar{\tau}}, \tag{7.24}$$

$$V(H(\bar{\tau}),\bar{\tau}) = E - H(\bar{\tau}), \tag{7.25}$$

$$\left.\frac{\partial V}{\partial \hat{S}}\right|_{S=H(\bar{\tau})_-} = \left.\frac{\partial V}{\partial \hat{S}}\right|_{S=H(\bar{\tau})_+}, \tag{7.26}$$

$$V(\infty,\bar{\tau}) = 0. \tag{7.27}$$

Let us examine (7.22), which can be solved analytically using a solution of the Euler type. Assume a solution of the Euler type, then

$$V(S,\bar{\tau}) = A\ S^{\alpha},$$

and on substituting into (7.22) we obtain

$$\frac{1}{2}\sigma^2\alpha(\alpha-1) + r\alpha - r,$$

from which

$$\alpha = -\frac{2r}{\sigma^2} \quad \text{or} \quad \alpha = 1.$$

From (7.27) we deduce that $\alpha = -\frac{2r}{\sigma^2}$ is the correct root, and apply the boundary condition (7.25) to obtain

$$V(S, \bar{\tau}) = \frac{E - H(\bar{\tau})}{H(\bar{\tau})^{\alpha}} \, S^{\alpha} \tag{7.28}$$

This solution, for a given value of $H(\bar{\tau})$, will have a value for the first derivative, which will feed into (7.21) via the boundary condition (7.26). Hence, (7.21) must be solved numerically, subject to the boundary conditions

$$V(S, 0) = \max[E - S, 0] \tag{7.29}$$

$$V(0, \bar{\tau}) = E \cdot e^{-r\bar{\tau}} \tag{7.30}$$

$$V(H, \bar{\tau}) = E - H \tag{7.31}$$

$$\left.\frac{\partial V}{\partial \hat{S}}\right|_{S=H} = \alpha \frac{E - H}{H}. \tag{7.32}$$

This is similar to the free-boundary formulation for a American option, and just as in that case an extra condition for the initial value of the free boundary is required. It has already been shown that the free-barrier H tends toward the free-boundary S_f when $\bar{\tau} \to 0$, so

$$H(0) = \frac{\alpha E}{\alpha - 1}. \tag{7.33}$$

7.5.1 Asymptotic analysis – in the limit as time-to-knockout tends to zero

Making the substitutions $S = Ee^x$, $\bar{\tau} = \hat{\tau}/\frac{1}{2}\sigma^2$, and $V(S, \bar{\tau}) = E - S + Ee^{-\rho\tau}v(x, \hat{\tau})$ into (7.21), the result is

$$\frac{\partial v}{\partial \hat{\tau}} = \frac{\partial^2 v}{\partial x^2} + (\rho - 1)\frac{\partial v}{\partial x} - \rho e^{\rho\hat{\tau}} \tag{7.34}$$

subject to the boundary conditions

$$\begin{aligned} v(x,0) &= 0, \\ v(-\infty,\hat{\tau}) &= 1 - e^{\rho\hat{\tau}}, \\ v(x_f,\hat{\tau}) &= 0, \\ \left.\frac{\partial v}{\partial x}\right|_{x=x_f} &= \rho e^{\rho\hat{\tau}}(e^{x_f}-1) + e^{x_f+\rho\hat{\tau}}, \\ x_0 &= \log\left(\frac{\rho}{\rho+1}\right), \end{aligned}$$

where $H(0) = Ee^{x_0}$.

Let us study the behaviour of the solution in the knockout limit. Let $\hat{\tau} = \epsilon\hat{T}$ where $\hat{T} = O(1)$ and ϵ is a small parameter. Then we have the following PDE,

$$\frac{\partial v}{\partial \hat{T}} = \epsilon\left[\frac{\partial^2 v}{\partial x^2} + (\rho-1)\frac{\partial v}{\partial x} - \rho e^{\epsilon\rho\hat{T}}\right] \tag{7.35}$$

So let us look for an asymptotic solution of the form

$$v(x,\hat{\tau}) = V_0(x,\hat{T}) + \epsilon V_1(x,\hat{T}) + O(\epsilon^2) \tag{7.36}$$

Then the $O(1)$ approximation is just zero, and to $O(\epsilon)$ we have

$$\frac{\partial V_1}{\partial \hat{T}}(x,\hat{T}) = 0, \tag{7.37}$$

then subject to the transformed boundary condition we have the following expansion for v in the region $x < x_0$.

$$v(x,\hat{\tau}) = -\rho\hat{\tau} + O(\epsilon^2).$$

This solution matches neither of the boundary conditions at x_0, so we need to introduce a new scaling to the problem.

Let us define a separate region close to the free boundary, and introduce the

following scalings

$$x = x_0 + \epsilon^{\frac{1}{2}} X, \qquad V = \epsilon \hat{V} \qquad x_f = x_0 + \epsilon^{\frac{1}{2}} L_0.$$

Then

$$\frac{\partial \hat{V}}{\partial \hat{T}} = \frac{\partial^2 \hat{V}}{\partial X^2} + \epsilon^{\frac{1}{2}}(\rho - 1)\frac{\partial \hat{V}}{\partial X} - \rho(1 + \epsilon\rho\hat{T}) + O(\epsilon^{\frac{3}{2}}), \tag{7.38}$$

and to first order we obtain

$$\frac{\partial \hat{V}}{\partial \hat{T}} = \frac{\partial^2 \hat{V}}{\partial X^2} - \rho, \tag{7.39}$$

with boundary conditions

$$\hat{V}(L_0, \hat{T}) = 0, \tag{7.40}$$

$$\frac{\partial \hat{V}}{\partial X}(L_0, \hat{T}) = \rho L_0, \tag{7.41}$$

$$\hat{V} \to -\rho\hat{T} \quad \text{as} \quad x \to -\infty, \tag{7.42}$$

where the last condition is a matching condition for the expansion. Then seek a similarity solution of the form $\hat{V} = \hat{\tau} g(\xi)$ where $\xi = X/\sqrt{\hat{T}}$, and $L_0 = \xi_0\sqrt{\hat{T}}$, to arrive at the following ODE;

$$g'' + \frac{1}{2}\xi g' - g = \rho, \tag{7.43}$$

with boundary conditions

$$g(\xi_0) = 0, \tag{7.44}$$

$$g'(\xi_0) = -\rho\xi_0, \tag{7.45}$$

$$g \sim -\rho \quad \text{as} \quad \xi \to -\infty. \tag{7.46}$$

This ODE matches both of the boundary conditions at the free boundary.

7.5.2 Solution to the ODE

First, we start by seeking a simple polynomial solution to the homogeneous equation. Try a solution of the form

$$g(\xi) = a + b\xi + c\xi^2 + d\xi^3, \tag{7.47}$$

which on substitution into (7.43) and equating coefficients gives $a = 1$, $b = 0$, $c = \frac{1}{2}$, and $d = 0$. Then a solution to the homogeneous equation is

$$g(\xi) = B\left(1 + \frac{1}{2}\xi^2.\right)$$

To find the general solution to the homogeneous equation we apply the method of reduction of order to our solution. After some laborious algebra we arrive at

$$g = A.\left\{\left(1 + \frac{1}{2}\xi^2\right)\int_{-\infty}^{\xi} e^{-\frac{1}{4}s^2}ds + \xi e^{-\frac{1}{4}\xi^2}\right\} + B\left\{1 + \frac{1}{2}\xi^2\right\}, \tag{7.48}$$

which is the general solution to the homogeneous ODE. The general solution to (7.43) is the general solution of the homogeneous plus the particular solution, which fortunately is easy to spot ($g_p = -\rho$). Then the general solution is

$$g = A.\left\{\left(1 + \frac{1}{2}\xi^2\right)\int_{-\infty}^{\xi} e^{-\frac{1}{4}s^2}ds + \xi e^{-\frac{1}{4}\xi^2}\right\} + B\left\{1 + \frac{1}{2}\xi^2\right\} - \rho\ . \tag{7.49}$$

Now we must apply the boundary conditions. From (7.46) it is obvious that $B = 0$. That leaves us with two equations to find ξ_0 and A. The first boundary condition (7.44) implies that

$$A.\left\{\left(1 + \frac{1}{2}\xi_0^2\right)\int_{-\infty}^{\xi_0} e^{-\frac{1}{4}s^2}ds + \xi_0 e^{-\frac{1}{4}\xi_0^2}\right\} = \rho,$$

and (7.45) that

$$A\left(\xi_0\int_{-\infty}^{\xi_0} e^{-\frac{1}{4}s^2}ds + 2e^{-\frac{1}{4}\xi_0^2}\right) = \rho\xi_0.$$

Using simple algebra we find that the transcendental equation for the free boundary

is

$$\xi_0^3 e^{\frac{1}{4}\xi_0^2} \int_{-\infty}^{\xi_0} e^{-\frac{1}{4}s^2} ds = 2(2 - \xi_0^2), \tag{7.50}$$

and the constant A is found via

$$A = \frac{\rho(1 - 1/2\xi_0^2)}{\int_{-\infty}^{\xi_0} e^{-\frac{1}{4}s^2} ds} .$$

This is the same transcendental equation as that arrived at by Wilmott et al. (1995) for the case of the American call with $d < r$. This is quite interesting since both the ODE and the boundary conditions differ from that case. However, it does mean that the solution has already been found for ξ_0, Wilmott et al. (1995) state the value to be

$$\xi_0 = 0.9034\ldots.$$

Using Newton iteration a more accurate value can be found,

$$\xi_0 = 0.9034466\ldots.$$

Hence we have found an approximation to the perpetual delayed-exercise option close to knockout.

In the original variables we can express the free barrier to be

$$H(\bar{\tau}) = E\frac{\alpha}{\alpha - 1}\left(1 + \xi_0\sqrt{\frac{1}{2}\sigma^2\bar{\tau}} + \ldots\right)$$

In figure 7.12 the asymptotic results are shown against the numerical results. Since we are only interested in the premium that the option to delay exercise from instantaneous, we look at the price difference between the American option and the delayed-exercise option. Figure 7.12(b) plots the value of the option to delay exercise, and figure 7.12(a) the corresponding barrier. It is clear that even a small miscalculation of the barrier can lead to large errors in the pricing of the option. Above the barrier, the value is analytic, so no numerical errors are present and the only error comes from the placement of the barrier. So even though the asymptotic

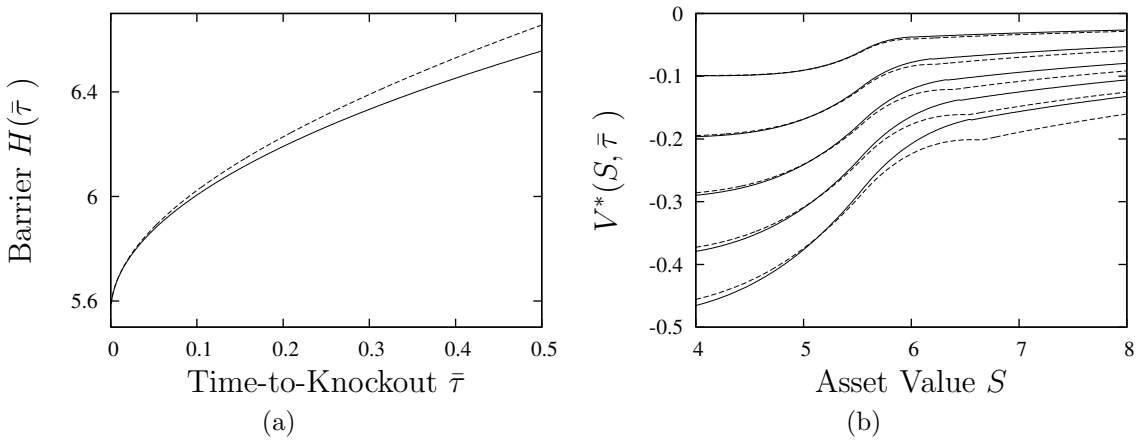

Figure 7.12
Asymptotic approximation to the perpetual case
Parameters are $r = 0.1$, $\sigma = 0.4$ and $E = 10$. (a) The free barrier $H(\bar{\tau})$ vs. time to knockout, with the numerical value given by the dashed line, the approximation by the solid line. (b) $V^*(S,\bar{\tau}\ ) = V(S,\bar{\tau}\ ) - V_A(S)$ is the value of the option to delay. From top to bottom, $\bar{\tau} = 0$ through to 0.5, with increments of 0.1.

approximation is very good below the barrier, the resulting errors on the right hand side are large (due to the misplacement of the free barrier). The derivative around the barrier is fast changing so the second order approximation we have taken is not accurate enough to keep down the errors to the right of the barrier. It is to be noted that the pricing of the option for $S > H$ is more important since this is the region where most if not all of these options would be sold.

7.6 Advanced Body-Fitted Solver for the Delayed-Exercise Option

The scheme outlined earlier in section 7.3 is at best a crude attempt at a solution to the delayed-exercise option. When reviewing the results, the extra smooth-pasting condition at the free-barrier came to light, with which we can formulate the problem as a pair of coupled PDEs linked by the continuity of both the option value and its Δ. The region $S > H(\tau,\bar{\tau}\ )$ can be solved in the same way as an American put, using the advanced body-fitted coordinate scheme with an appropriate upper boundary as explained in Chapter 2.

Let W define the solution above to barrier, for which the barrier clock does not tick. In the same manner as before, the upper boundary U, is chosen to be a function of time so that the value of W is approximately zero. Then we choose $U = Ee^{\xi\sigma\sqrt{\tau}}$. The PDE (4.6) becomes

$$W_\tau - \frac{1}{G}(\hat{S}G_\tau + F_\tau)W_{\hat{S}} = \frac{1}{2}\sigma^2\left(\hat{S} + \frac{F}{G}\right)^2 W_{\hat{S}\hat{S}} + r\left(\hat{S} + \frac{F}{G}\right)W_{\hat{S}} - rW. \qquad (7.51)$$

where $\hat{S} = \frac{S-F}{G}$.

For $S < H(\tau, \bar{\tau}\,)$, the boundary conditions suggest an American style call option, and it can be solved in the same way. We assume that V defines the solution below the barrier, resulting in the following PDE to solve for V,

$$V_\tau + V_{\bar{\tau}} - \frac{F_\tau + F_{\bar{\tau}}}{F}\hat{S}V_{\hat{S}} = \frac{1}{2}\sigma^2\hat{S}^2V_{\hat{S}\hat{S}} + r\hat{S}V_{\hat{S}} - rV, \qquad (7.52)$$

where $\hat{S} = \frac{S}{F}$.

The boundary conditions ensure the continuity of the option value and its first derivative. Similarly, just as the perpetual option required a boundary condition for F at knockout, so does the non-perpetual option. It has been shown that this is the American free boundary, the limit of H as time-to-knockout tends to zero, which means that the American option will need to be calculated in order to obtain S_f, before we can calculate the value of the delay-exercise option. This is where the highly accurate ABFC solver is required, in order to position the American free boundary accurately even near expiry. Incorrect positioning could cause errors that may contaminate the entire solution. The option value above and below the barrier

must be solved simultaneously subject to the following boundary conditions;

$$F(0,\bar{\tau}) = \min\left[\frac{rE}{d}, E\right], \tag{7.53}$$

$$F(\tau,0) = S_f(\tau), \tag{7.54}$$

$$V(\hat{S},\tau,0) = E - (\hat{S}F), \tag{7.55}$$

$$W(\hat{S},\tau,0) = \max[E - (\hat{S}G + F), 0], \tag{7.56}$$

$$V_\tau + V_{\bar{\tau}} + rV = 0 \qquad \text{for} \qquad S = 0, \tag{7.57}$$

$$V(1,\tau,\bar{\tau}) = W(0,\tau,\bar{\tau}) = E - F(\bar{\tau}), \tag{7.58}$$

$$\frac{1}{F}\frac{\partial V}{\partial \hat{S}}\bigg|_{\hat{S}=1} = \frac{1}{G}\frac{\partial W}{\partial \hat{S}}\bigg|_{\hat{S}=0}, \tag{7.59}$$

$$W(1,\tau,\bar{\tau}) = 0, \tag{7.60}$$

$$G(\tau,\bar{\tau}) + F(\tau,\bar{\tau}) = U(\tau). \tag{7.61}$$

If we have n nodes below the barrier, and m nodes above, we have $n+m+2$ equations. The two extra equations are required to find F and G and to ensure that the solutions match at the boundary. When we are above the barrier, we can discretise the problem and linearise using the Newton method (c.f. section 2.5) to arrive at

$$\alpha_{j,2}(\delta W_{j-1}) + \beta_{j,2}(\delta W_j) + \gamma_{j,2}(\delta W_{j+1}) + \theta_{n+1+j}(\delta F) + \phi_j(\delta G) = \epsilon_{n+1+j}, \tag{7.62}$$

where $1 < j < m$. There are terms present for both F and G. The counter for θ starts at $n+1$ since there are N equations for V and one equation linking V and W.

When below the barrier, we discretise setting $\Delta\bar{\tau} = \Delta\tau$ for reasons outlined in Chapter 4. Then

$$\begin{aligned} V_\tau(\hat{S},\tau+1/2\Delta\tau,\bar{\tau}+1/2\Delta\bar{\tau}) + \quad & V_{\bar{\tau}}(\hat{S},\tau+1/2\Delta\tau,\bar{\tau}+1/2\Delta\bar{\tau}) \\ = \quad & \tfrac{1}{\Delta\tau}(v_i^{k+1,l+1} - v_i^{k,l}), \end{aligned} \tag{7.63}$$

and

$$F_\tau(\hat{S}, \tau + 1/2\Delta\tau, \bar{\tau} + 1/2\Delta\bar{\tau}) + \quad F_{\bar{\tau}}(\hat{S}, \tau + 1/2\Delta\tau, \bar{\tau} + 1/2\Delta\bar{\tau}) = \quad \frac{1}{\Delta\tau}(f^{k+1,l+1} - f^{k,l}). \tag{7.64}$$

So after using the Newton method to linearise we obtain the following scheme

$$\alpha_{i,1}(\delta V_{i-1}) + \beta_{i,1}(\delta V_i) + \gamma_{i,1}(\delta V_{i+1}) + \theta_i(\delta F) = \epsilon_i, \tag{7.65}$$

for $1 < i < n$.

Now, combining these two schemes along with the boundary conditions we arrive at the following matrix, $\mathbf{A} =$:

$$\begin{pmatrix}
\alpha_{1,1} & \beta_{1,1} & \gamma_{1,1} & & & & & & & & & \theta_1 & 0 \\
\alpha_{2,1} & \beta_{2,1} & \gamma_{2,1} & & & & & & & & & \theta_2 & 0 \\
 & \alpha_{3,1} & \beta_{3,1} & \gamma_{3,1} & & & & & & & & \theta_3 & 0 \\
 & & \ddots & \ddots & \ddots & & & & & & & \vdots & \vdots \\
 & & & \alpha_{n-1,1} & \beta_{n-1,1} & \gamma_{n-1,1} & & & & & & \theta_{n-1} & 0 \\
 & & & \alpha_{n,1} & \beta_{n,1} & \gamma_{n,1} & & & & & & \theta_n & 0 \\
 & & & \alpha_{n+1,1} & \beta_{n+1,1} & \gamma_{n+1,1} & \alpha_{0,2} & \beta_{0,2} & \gamma_{0,2} & & & \theta_{n+1} & \phi_0 \\
 & & & & & & \alpha_{1,2} & \beta_{1,2} & \gamma_{1,2} & & & \theta_{n+2} & \phi_1 \\
 & & & & & & \alpha_{2,2} & \beta_{2,2} & \gamma_{2,2} & & & \theta_{n+3} & \phi_2 \\
 & & & & & & & \ddots & \ddots & \ddots & & \vdots & \vdots \\
 & & & & & & & & \alpha_{m-1,2} & \beta_{m-1,2} & \gamma_{m-1,2} & \theta_{n+m} & \phi_{m-1} \\
 & & & & & & & & \alpha_{m,2} & \beta_{m,2} & \gamma_{m,2} & \theta_{n+m+1} & \phi_m \\
 & & & & & & & & & & & \theta_{n+m+2} & \phi_{m+1}
\end{pmatrix}.$$

Then the system $\mathbf{A}\boldsymbol{x} = \boldsymbol{b}$ can be solved using Gaussian elimination and back-substitution, where

$$\boldsymbol{x} = \begin{pmatrix} \delta V_1 \\ \delta V_2 \\ \vdots \\ \delta V_i \\ \vdots \\ \delta V_n \\ \delta W_1 \\ \vdots \\ \delta W_m \\ \delta F \\ \delta G \end{pmatrix} \qquad \boldsymbol{b} = \begin{pmatrix} \epsilon_1 \\ \vdots \\ \epsilon_i \\ \vdots \\ \epsilon_{n+m+2} \end{pmatrix}. \tag{7.66}$$

Table 7.1 compares the convergence of the two methods for solving the delayed-exercise option in this chapter. Not only is the BFC method far more accurate, but the scheme is more stable, and the extra computational expense is only small compared to the increased accuracy. In fact the scheme is second-order accurate in both time and asset space, allowing for efficient extrapolation. The grid-search scheme suffers from a large nonlinearity error exaggerated by the fast movement of the barrier (figures 7.6 and 7.7). The BFC addresses the nonlinearity error and does not have a discontinuity in the payoff to contend with, which caused problems with the Crank-Nicolson scheme on the vanilla ParAsian option (chapter 4).

A more accurate tracking of the free barrier enables us to investigate the dynamics of the barrier more closely. In the perpetual option the rate of change in option price with respect to the barrier time is far larger than the rate of change with respect to real time (it is zero for the perpetual). But if we look at the limit as barrier time tends to zero, the value of the option still changes far more rapidly with respect to barrier time. In fact, if we look at figure 7.13 then it becomes apparent that the

Table 7.1
Relative RMS errors for delayed-exercise put options

n	Grid-search (time)	BFC (time)
200	0.002556 (0.2)	0.000061535 (0.4)
400	0.000425 (1.4)	0.000013032 (3.2)
600	0.000391 (4.9)	0.000007195 (10.3)
800	0.000363 (11.6)	0.000004733 (23.8)
1000	0.000326 (22.9)	0.00000327 (45.3)
1200	0.000292 (39.6)	0.00000237 (76.7)
1400	0.000263 (63.1)	0.00000175 (119.8)
1600	0.000239 (94.3)	0.00000131 (175.5)
1800	0.000218 (134.)	0.00000097 (245.3)
2000	0.000201 (183.2)	0.00000072 (331.9)

The relative errors for the two methods described in this chapter. The relative RMS errors are calculated against exact values of close to 100 different put options with $T = 0.5/1$, $S_0 \in [0.8E, 1.2E]$, $\sigma = 0.4/0.2$. For all options $r = 0.06$ and $E = 10$. The exact values are calculated by allowing $n \to \infty$ until successive solutions are sufficiently close to one another (1.E-8). We use n nodes in S, results are extrapolated once using n and $n/2$, and the number of timesteps is n and $n/2$ respectively. We set $\Delta\bar{\tau} = \Delta\tau$ as usual.

behaviour of the barrier with small time to knockout mirrors the behaviour of the perpetual barrier with small time to knockout.

In fact, from this we can make an estimate of the free boundary for the American. By taking the point at which the European option crosses the exercise price, H_E, then we can form an approximation to the free boundary for the American option S_f^*, simply as

$$S_f^*(\tau) = H_E(\tau)(1 + \xi_0\sqrt{\frac{1}{2}\sigma^2\tau}) \tag{7.67}$$

The approximation, as shown in figure 7.14 is not as accurate as was hoped for,

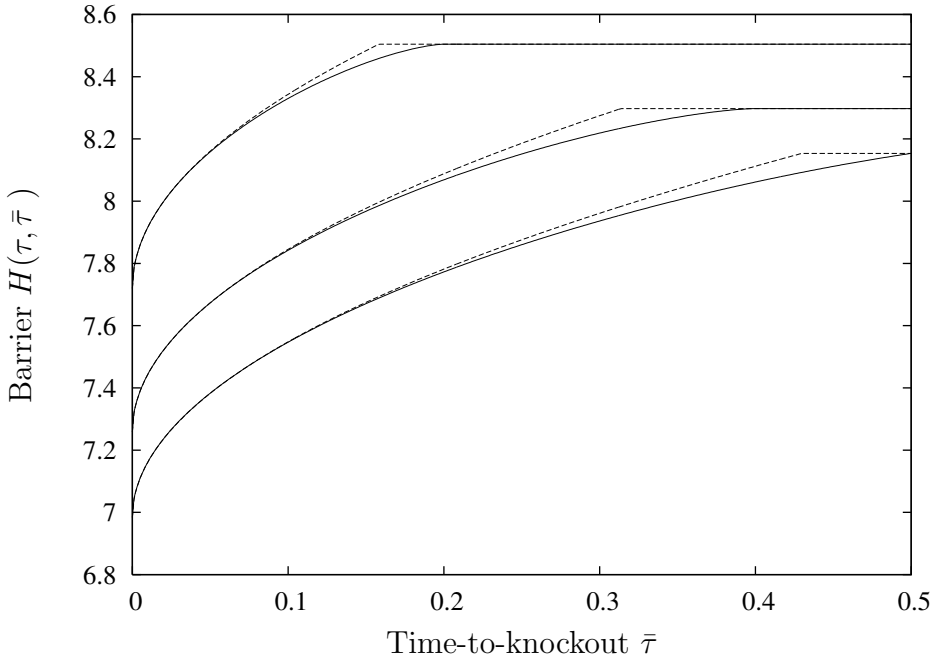

Figure 7.13
Asymptotic $H(\tau, \bar{\tau}\ )$ vs. time to knockout
A guess at the asymptotic form of $H(\tau, \bar{\tau}\ )$ for small barrier time. The straight line is the numerical result form the body-fitted solver and the dashed line the analytical approx from the perpetual case.

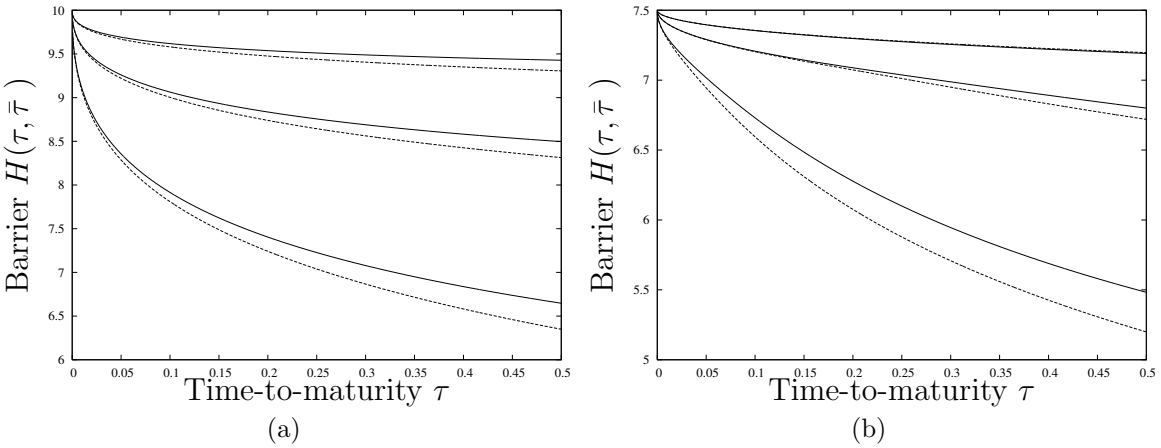

Figure 7.14
Free boundary approximation $S_f^*(\tau)$ vs. time to maturity
The approximation to the free boundary (dashed) along with the exact value calculated numerically (solid). (a) $E = 10$, $r = 0.06$, $d = 0$ and top to bottom $\sigma = 0.1, 0.2, 0.4$ (b) $E = 10$, $r = 0.06$, $d = 0.08$ and top to bottom $\sigma = 0.1, 0.2, 0.4$

although further accuracy may be possible if the expansion for the perpetual option is taken to the next term. Now this does seem rather hand wavy as an approximation, but it does agree to some extent with Evans et al. (2002) and Widdicks et al. 2005. Both find that there is a region of order $O(\tau^{\frac{1}{2}})$ around the free boundary. In effect, under the framework of the delayed option, we have inadvertently set up an equation to solve this region.

7.7 Conclusions

The delayed-exercise option proposed in this chapter is interesting as a mathematical problem providing a fluid link between the European and American options. Studying the perpetual option we can make some approximation to both the free barrier and the option value. Two new methods are created to deal with an option which is highly path (and strategy) dependent. It is not immediately obvious how one could solve such a problem with any other method other than finite difference. For a useful modeling tool however, we must look to the Parisian style delayed-exercise option. The analysis and implementation of such an option is left to further research.

Chapter 8

Conclusions

Under the assumptions of the BSM framework, early-exercise and occupation-time options are investigated in detail. Exploiting the asymptotic behaviour of early-exercise options, we are able to enhance current numerical techniques with improved convergence and efficiency. The resulting scheme is more than 2000 times as accurate as the benchmark finite-difference scheme (PSOR), for same order computation times.

An investigation of finite-difference methods for occupation-time derivatives rules out the use of certain methods under certain conditions. Noting some of the problems caused by the smoothness of the solution, a new occupation time derivative, the integral time Parisian/ParAsian option, is proposed which is at least $\mathcal{C}^2$ continuous. This option has implications for the hedging of occupation-time derivatives.

These advanced techniques are then applied to corporate bonds in a complex capital structure, where the firm issues subordinate bonds. Under the Yu (2004) model, default under chapter 11 is modelled as a ParAsian option, the firm is allowed to issue new debt while the APR may also be violated. A parameter analysis is carried out over a range of maturity and debt structures to present a comprehensive term structure of credit spreads. The model is then further advanced so that the subordinate issue may now be convertible. The effect of the size senior issue present is analysed.

The unique shapes that the term structure of credit spreads exhibit when the firm issues subordinate bonds has important implications for the modelling of corporate

bonds. The relative weight of senior to junior debt is found to be important in determining the positioning of the default barrier, and also the effect that APR violations have on the results. The weighting of senior to junior debt is also found to be important when modelling convertible debt, as it effects both the credit spread of the bond and dilution of shares in the firm.

The Yu (2004) model may be extended further to include the leverage ratio as a state variable, allowing the accretion of debt to be dependent on the position in the state space rather than a constant as given in this thesis. It may also be possible to include the barrier as a state variable, or at least solve to find the optimum barrier level, although this would require the inclusion of taxes and other modelling assumptions. A vital test for the Yu (2004) model would be to test it empirically against other models, allowing the inclusion of firms with multiple debt issues. Similarly the convertible bond model must also be tested against other models to validate the findings.

The early-exercise and occupation-time derivatives are combined to propose the delayed-exercise option. The problem presents itself as a complex free boundary problem, which requires the highly accurate numerical techniques developed earlier in the thesis to be solved comprehensively, by the efficient use of finite-difference techniques, but would be difficult to solve via other methods, due to the complex feedback of the option value on to the solution. The solution to the simple delayed-exercise put also sheds light on some of the intricacies of the American put option.

The delayed-exercise option has a range of interesting modelling applications, such mortgage-backed securities, convertible bonds or real options. All of these areas require further research on their application.

Appendix A

Numerical Schemes

A.1 BFC and ABFC coefficients

The ABFC PDE is more general, and can be reduced to the BFC PDE by appropriate settings of the functions F and G, so we present the coefficients for that only. The equation is:

$$V_\tau - \frac{1}{G}(\hat{S}G_\tau + F_\tau)V_{\hat{S}} = \frac{1}{2}\sigma^2\left(\hat{S} + \frac{F}{G}\right)^2 V_{\hat{S}\hat{S}} + r\left(\hat{S} + \frac{F}{G}\right)V_{\hat{S}} - rV, \qquad \text{(A.1)}$$

with either three or four boundary conditions, depending on whether F and G are known, resulting in $n+1$ or $n+2$ equations. The problem is discretised so that:

$$\Delta\hat{S} = \frac{1}{n}, \qquad \Delta\tau = \frac{1}{m},$$

and

$$u_i^k = V(i\Delta\hat{S}, k\Delta\tau),$$
$$f^k = F(k\Delta\tau), \qquad g^k = G(k\Delta\tau).$$

The coefficients when neither F nor G are known, corresponding to (2.98), are

$$\alpha_i = (gt\hat{S}_i + ft)\frac{1}{4gg\Delta\hat{S}} - \sigma^2\frac{ss_i^2}{4\Delta\hat{S}^2} + (r-d)\frac{ss_i}{4\Delta\hat{S}} \tag{A.2}$$

$$\beta_i = \frac{1}{\Delta\tau} + \sigma^2\frac{ss_i^2}{2\Delta\hat{S}^2} + \frac{1}{2}r \tag{A.3}$$

$$\gamma_i = -(gt\hat{S}_i + ft)\frac{1}{4gg\Delta\hat{S}} - \sigma^2\frac{ss_i^2}{4\Delta\hat{S}^2} - (r-d)\frac{ss_i}{4\Delta\hat{S}} \tag{A.4}$$

$$\theta_i = -\frac{1}{\Delta\tau}\frac{vs_i}{gg} - \sigma^2\frac{ss_i}{gg}vss_i - (r-d)\frac{vs_i}{gg} \tag{A.5}$$

$$\phi_i = ((gt\hat{S}_i + ft)\frac{1}{2gg} - \frac{\hat{S}_i}{\Delta\tau})\frac{vs_i}{gg} + \sigma^2 ff\frac{ss_i}{2gg^2}vss_i + (r-d)ff\frac{vs_i}{2gg} \tag{A.6}$$

$$\epsilon_i = -vt_i + (gt\hat{S}_i + ft)vs_i/gg + \frac{1}{2}\sigma^2 ss_i^2 vss_i + (r-d)ss_i vs_i - rv_i \ , \tag{A.7}$$

where

$$\frac{\partial F}{\partial\tau} = ft = (f^{k+1} - f^k)\frac{1}{\Delta\tau} \tag{A.8}$$

$$F(\tau + 1/2\Delta\tau) = ff = \frac{1}{2}(f^k + f^{k+1}) \tag{A.9}$$

$$\frac{\partial G}{\partial\tau} = gt = (g^{k+1} - g^k)\frac{1}{\Delta\tau} \tag{A.10}$$

$$G(\tau + 1/2\Delta\tau) = gg = \frac{1}{2}(g^k + g^{k+1}), \tag{A.11}$$

and

$$\frac{S_i}{G(\tau + 1/2\Delta\tau)} = ss_i = \hat{S}_i + \frac{ff}{gg} \tag{A.12}$$

$$\frac{\partial V}{\partial\tau} = vt_i = (u_i^{k+1} - u_i^k)\frac{1}{\Delta\tau} \tag{A.13}$$

$$V(S, \tau + 1/2\Delta\tau) = vv_i = \frac{1}{2}(u_i^k + u_i^{k+1}) \tag{A.14}$$

$$\frac{\partial V}{\partial\hat{S}}(S, \tau + 1/2\Delta\tau) = vs_i = (u_{i+1}^k + u_{i+1}^{k+1} - u_{i-1}^k - u_{i-1}^{k+1})\frac{1}{4\Delta\hat{S}} \tag{A.15}$$

$$\frac{\partial^2 V}{\partial\hat{S}^2}(S, \tau + 1/2\Delta\tau) = vss_i = (u_{i+1}^k + u_{i+1}^{k+1} - 2u_i^k - 2u_i^{k+1} + u_{i-1}^k + u_{i-1}^{k+1})\frac{1}{2\Delta\hat{S}^2} \ . \tag{A.16}$$

If either F or G are known, we simple set θ_i or ϕ_i to zero and all other terms remain the same. Hence the BFC for the put is a special case of the ABFC where

$$G = F + aE$$

where a is a constant and E is the strike price.

References

Acharya, V. V. and Carpenter, J. N. (2002). Corporate Bond Valuation and Hedging with Stochastic Interest Rates and Endogenous Bankruptcy, *Review of Financial Studies* **15**(5): 1355–1383.

Altman, E. I. (1993). Evaluating the Chapter 11 Bankruptcy-Reorganization Process, *in* E. I. Altman (ed.), *Bankruptcy, Credit Risk, and High Yield Junk Bonds*, Blackwells. 2002.

Amin, K. I. (1991). On the Computation of Continuous Time Option Prices Using Discrete Approximations, *The Journal of Financial and Quantitative Analysis* **26**(4): 477–495.

Anderluh, J. and van der Weide, H. (2004). Parisian Options – The Implied Barrier Concept. International Conference of Computer Science.

Andersen, L. and Broadie, M. (2004). Primal-Dual Simulation Algorithm for Pricing Multidimensional American Options, *Management Science* **50**(9): 1222–1234.

Andricopoulos, A. D., Widdicks, M., Duck, P. W. and Newton, D. P. (2003). Universal Option Valuation using Quadrature Methods, *Journal of Financial Economics* **67**: 447–471.

Andricopoulos, A., Widdicks, M., Duck, P. W. and Newton, D. (2004). Curtailing the Range for Lattice and Grid Methods, *The Journal of Derivatives* **11**(4): 55–61.

Andricopoulos, A., Widdicks, M., Newton, D. P. and Duck, P. (2007). Extending

Quadrature Methods to Value Multi-Asset and Complex Path Dependent Options, *Journal of Financial Economics* **83**(2): 471– 499.

Avellaneda, M. and Wu, L. (1999). Pricing Parisian-Style Options with a Lattice Method, *International Journal of Theoretical and Applied Finance* **2**: 1–16.

Ayache, E., Forsyth, P. and Vetzal, K. (2003). The Valuation of Convertible Bonds with Credit Risk, *Journal of Derivatives* **11**(1): 9–29.

Barone-Adesi, G. and Whaley, R. E. (1987). Efficient Analytical Approximation of American Option Values, *The Journal of Finance* **42**(2): 301–320.

Bensoussan, A. (1984). On the Theory of Option Pricing, *Acta Applicandae Mathematicae* **2**(2): 139–158.

Bermudez, A. and Webber, N. (2004). An Asset Based Model of Defaultable Convertible Bonds with Endogenised Recovery. *Working paper*, City University, Cass Business School, London.

Bernard, C., Le Courtois, O. and Quittard-Pinon, F. (2005). A New Procedure for Pricing Parisian Options, *The Journal of Derivatives* **12**(4): 45–53.

Black, F. and Cox, J. (1976). On the Pricing of Corporate Debt: The Risk Structure of Interest Rates, *The Journal of Finance* **29**: 449–470.

Black, F. and Scholes, M. (1973). The Pricing of Options and Corporate Liabilities, *The Journal of Political Economy* **81**(3): 637–654.

Blanco, R., Brennan, S. and Marsh, I. W. (2005). An Empirical Analysis of the Dynamic Relation between Investment-Grade Bonds and Credit-Default Swaps, *The Journal of Finance* **60**: 2255–2281.

Boyle, P. P. (1977). Options: A Monte Carlo Approach, *Journal of Financial Economics* **4**(3): 323–338.

Boyle, P. P. (1986). Option Valuation using a Three-Jump Process, *International Options Journal* **3**: 7–12.

Boyle, P. P. (1988). A Lattice Framework for Option Pricing with Two State Variables, *The Journal of Financial and Quantitative Analysis* **23**(1): 1–12.

Boyle, P. P., Evnine, J. and Gibbs, S. (1989). Numerical Evaluation of Multivariate Contingent Claims, *The Review of Financial Studies* **2**(2): 241–250.

Boyle, P. P. and Lau, S. (1994). Bumping Up Against the Barrier with the Binomial Method, *Journal of Derivatives* **1**(4): 6–14.

Boyle, P. P. and Tse, Y. K. (1990). An Algorithm for Computing Values of Options on the Maximum or Minimum of Several Assets, *The Journal of Financial and Quantitative Analysis* **25**(2): 215–227.

Brennan, M. J. and Schwartz, E. S. (1977a). Convertible Bonds: Valuation and Optimal Strategies for Call and Conversion, *The Journal of Finance* **32**(5): 1699–1715.

Brennan, M. J. and Schwartz, E. S. (1977b). The Valuation of American Put Options, *The Journal of Finance* **32**(2): 449–462.

Brennan, M. J. and Schwartz, E. S. (1978). Finite Difference Methods and Jump Processes Arising in the Pricing of Contingent Claims: A Synthesis, *The Journal of Financial and Quantitative Analysis* **13**(3): 461–474.

Brennan, M. J. and Schwartz, E. S. (1980). Analyzing Convertible Bonds, *The Journal of Financial and Quantitative Analysis* **15**(4): 907–929.

Broadie, M., Chernov, M. and Sundaresan, S. (2007). Optimal Debt and Equity Values in the Presence of Chapter 7 and Chapter 11, *The Journal of Finance* **62**(3): 1341–1377.

Broadie, M. and Detemple, J. (1996). American Option Valuation: New Bounds, Approximations, and a Comparison of Existing Methods, *The Review Financial Studies* **9**(4): 1211–1250.

Broadie, M. and Detemple, J. (1997). The Valuation of American Options on Multiple Assets, *Mathematical Finance* **7**(3): 241–286.

Broadie, M. and Glasserman, P. (1997). Pricing American-Style Securities Using Simulation, *Journal of Economic Dynamics and Control* **21**(8-9): 1323–1352.

Broadie, M. and Kaya, O. (2007). A Binomial Lattice Method for Pricing Corporate Debt and Modeling Chapter 11 Proceedings, *Journal of Financial and Quantitative Analysis* **42**.

Bunch, D. and Johnson, H. (1992). A Simple and Numerically Efficient Valuation Method for American Puts using a Modified Geske-Johnson Approach, *The Journal of Finance* **47**: 809–816.

Carayannopoulos, P. (1996). Valuing Convertible Bonds under the Assumption of Stochastic Interest Rates: An Empirical Investigation., *Quarterly Journal of Business and Economics* **35**(3): 17–31.

Carr, P. (1988). The Valuation of Sequential Exchange Opportunities, *The Journal of Finance* **43**(5): 1235–1256.

Chance, D. M. (1990). Default Risk and the Duration of Zero-coupon Bonds, *The Journal of Finance* **45**: 265–274.

Chesney, M. and Gauthier, L. (2006). American Parisian Options, *Finance and Stochastics* **10**(4): 475–506.

Chesney, M., Jeanblanc, M. and Yor, M. (1997). Brownian Excursions and Parisian Barrier Options, *Advances in Applied Probability* **29**: 165–184.

Christopherson, D. G. and Southwell, R. V. (1938). Relaxation Methods Applied to Engineering Problems. III. Problems Involving Two Independent Variables, Vol. 168, pp. 317–350. Proceedings of the Royal Society of London. Series A, Mathematical and Physical Sciences.

Clark, C. (1961). The Greatest of a Finite Set of Random Variables, *Operations Research* **9**: 145–162.

Collin-Dufresne, P. and Goldstein, R. S. (2001). Do Credit Spreads Reflect Stationary Leverage Ratios?, *The Journal of Finance* **56**(5): 1929–1958.

Costabile, M. (2002). A Combinatorial Approach for Pricing Parisian Options, *Decision in Economics and Finance* **25**: 111–125.

Cox, J. C., Ingersoll, J. E. and Ross, S. A. (1985). A Theory of the Term Structure of Interest Rates, *Econometrica* **53**: 385–407.

Cox, J. C., Ross, S. A. and Rubinstein, M. (1979). Option Pricing: a Simplified Approach, *Journal of Financial Economics* **7**: 229–263.

Crank, J. (1957). Two Methods for the Numerical Solution of Moving-Boundary Problems in Diffusion and Heat Flow, *Q J Mechanics Appl Math* **10**(2): 220–231.

Crank, J. (1984). *Free and Moving Boundary Problems*, Oxford: Clarendon Press.

Crank, J. and Nicolson, P. (1947). A Practical Method for Numerical Evaluation of Solutions of Partial Differential Equations of the Heat-Conduction Type, *Proc. Cambridge Philos. Soc* **43**: 50–67.

Cryer, C. W. (1971). The Solution of a Quadratic Programming Problem using Systematic Overrelaxation, *SIAM Journal of Control* **9**(3): 385–392.

Davis, M. and Lischka, F. (1999). Convertible Bonds with Market and Credit Risk. *Working paper*, Tokio-Mitsubishi International PLC.

d'Halluin, Y., Forsyth, P., Vetzal, K. and Labahn, G. (2001). A Numerical PDE Approach For Pricing Callable Bonds, *Applied Mathematical Finance* **8**: 49–77.

Driessen, J. (2005). Is Default Event Risk Priced in Corporate Bonds?, *The Review of Financial Studies* **18**(1): 165–195.

Duck, P. W., Newton, D. P., Widdicks, M. and Leung, Y. (2005). Enhancing the Accuracy of Pricing American and Bermudan Options, *Journal of Derivatives* **12**(4): 34–44.

Duffie, D. and Singleton, K. (1999). Modeling Term Structures of Defaultable Bonds, *Review Financial Studies* **12**(4): 687–720.

Dupire, B. (1994). Pricing with a Smile, *Risk Magazine* **7**(1): 18–20.

Eberhart, A. C. and Sweeney, R. J. (1992). Does the Bond Market Predict Bankruptcy Settlements?, *The Journal of Finance* **47**: 943–980.

Elliot, C. M. and Ockendon, J. R. (1982). *Weak and Variational Methods for Moving Boundary Problems*, Pitman, London.

Eom, Y. H., Helwege, J. and Huang, J.-Z. (2004). Structural Models of Corporate Bond Pricing: An Empirical Analysis, *The Review of Financial Studies* **17**: 499–544.

Evans, J., Kuske, R. and Keller, J. (2002). American Options on Assets with Dividends Near Expiry, *Mathematical Finance* **12**(3): 219–237.

Fama, E. and Miller, M. (1972). *The Theory of Finance*, Holt, Rinehart and Winston, New York.

Feller, W. (1951). Two Singular Diffusion Problems, *The Annals of Mathematics* **54**(1): 173–182.

Figlewski, S. and Gao, B. (1999). The Adaptive Mesh Model: A New Approach to Efficient Option Pricing - New Bounds, Approximations, and a Comparison of Existing Methods, *Journal of Financial Economics* **53**(3): 313–351.

Fons, J. S. (1994). Using Default Rates to Model the Term Structure of Credit Risk, *Financial Analysts Journal* **50**: 25–32.

Francois, P. and Morellec, E. (2004). Capital Structure and Asset Prices: Some Effects of Bankruptcy Procedures, *The Journal of Business* **77**: 387–412.

Friedman, A. (1988). *Variational Principles and Free Boundary Problems*, Robert E. Krieger Publishing.

Gauthier, L. (2000). *Options Réelles et Options Exotiques, une Approche Probabiliste*, Thèse de mathématiques, Université Paris 1 Panthéon-Sorbonne.

Geske, R. (1977). The Valuation of Corporate Liabilities as Compound Options, *Journal of Financial and Quantitative Analysis* **12**(4): 541–552.

Geske, R. (1979). A Note on an Analytical Valuation Formula for Unprotected American Call Options on Stocks with Known Dividends, *Journal of Financial Economics* **7**: 375–380.

Geske, R. and Johnson, H. (1984). The American Put Option Valued Analytically, *The Journal of Finance* **39**(5): 1511–1524.

Gilson, S. C. (1997). Transactions Costs and Capital Structure Choice: Evidence From Financially Distressed Firms, *The Journal of Finance* **52**: 161–196.

Goldman Sachs (1994). Valuing Convertible Bonds as Derivatives, *Quantitative Strategies Research Notes, Goldman Sachs* pp. 1–27.

Grimwood, R. and Hodges, S. (2002). The Valuation of Convertible Bonds: A Study of Alternative Pricing Models. *Working paper*, Warwick University.

Guha, R. (2002). Recovery of Face Value at Default: Theory and Empirical Evidence. *Working paper*, London Business School.

Haber, R. J., Schönbucher, P. J. and Wilmott, P. (1999). Pricing Parisian Options, *Journal of Derivatives* **6**(3): 71–79.

Haugh, M. B. and Kogan, L. (2004). Pricing American Options: A Duality Approach, *Operations Research* **52**(2): 258–270.

Helwege, J. and Turner, C. M. (1999). The Slope of the Credit Yield Curve for Speculative-Grade Issuers, *The Journal of Finance* **54**(5): 1869–1884.

Heston, S. (1993). A Closed-Form Solution for Options with Stochastic Volatility, *The Review of Financial Studies* **6**: 327–343.

Heston, S. and Zhou, G. (2000). On the Rate of Convergence of Discrete-Time Contingent Claims, *Mathematical Finance* **10**(1): 53–75.

Ho, T. S. and Lee, S.-B. (1986). Term Structure Movements and Pricing Interest Rate Contingent Claims, *The Journal of Finance* **41**(5): 1011–1029.

Ho, T. S. and Pfeffer, D. (1996). Convertible Bonds: Model, Value, Attribution and Analytics, *Financial Analysts Journal* **52**: 35–44.

Ho, T. S., Stapleton, R. C. and Subrahmanyam, M. G. (1995). Multivariate Binomial Approximations for Asset Prices with Nonstationary Variance and Covariance Characteristics, *The Review of Financial Studies* **8**(4): 1125–1152.

Ho, T. S., Stapleton, R. C. and Subrahmanyam, M. G. (1997). The Valuation of American Options with Stochastic Interest Rates: A Generalization of the Geske-Johnson Technique, *The Journal of Finance* **52**(2): 827–840.

Hotchkiss, E. S. (1995). Postbankruptcy Performance and Management Turnover, *The Journal of Finance* **50**: 3–21.

Hovakimian, A., Opler, T. and Titman, S. (2001). The Debt-Equity Choice, *The Journal of Financial and Quantitative Analysis* **36**(1): 1–24.

Huang, J., Subrahmanyam, M. and Yu, G. (1996). Pricing and Hedging American Options: A Recursive Integration Approach, *The Review of Financial Studies* **9**: 277–300.

Huang, J.-Z. and Huang, M. (2003). How Much of the Corporate-Treasury Yield Spread is Due to Credit Risk? *Working paper*, Stanford University.

Hugonnier, J. (1999). The Feynman-Kac Formula and Pricing Occupation Time Derivatives, *International Journal of Theoretical and Applied Finance* **2**: 153–178.

Hull, J. and White, A. (1990). Valuing Derivative Securities Using the Explicit Finite Difference Method, *The Journal of Financial and Quantitative Analysis* **25**(1): 87–100.

Hull, J. and White, A. (1993). Efficient Procedures for Valuing European and American Path-Dependent Options, *The Journal of Derivatives* **1**: 21–31.

Ingersoll, J. (1977a). An Examination of Corporate Call Policies on Convertible Securities, *The Journal of Finance* **32**(2): 463–478.

Ingersoll, Jr., J. E. (1977b). A Contingent-Claims Valuation of Convertible Securities, *Journal of Financial Economics* **4**(3): 289– 321.

Jaillet, P., Lamberton, D. and Lapeyre, B. (1990). Variational Inequalities and the Pricing of American Options, *Acta Applicandae Mathematicae* **21**(3): 263–289.

Jarrow, R. and Turnbull, S. (1995). Pricing Derivatives on Financial Securities Subject to Credit Risk, *The Journal of Finance* **50**(1): 53–85.

Johnson, H. (1983). An Analytic Approximation for the American Put Price, *The Journal of Financial and Quantitative Analysis* **18**(1): 141–148.

Johnson, H. (1987). Options on the Maximum or the Minimum of Several Assets, *The Journal of Financial and Quantitative Analysis* **22**(3): 277–283.

Johnson, P. (2003). *Using CFD Methods on Problems in Mathematical Finance*, MSc Thesis, University of Manchester.

Joubert, A. and Rogers, L. (1995). Fast, Accurate and Inelegant Valuation of American Options, *in* L. Rogers and D. Talay (eds), *Numerical Methods in Finance*, Cambridge University Press, pp. 88–92. 1997.

Ju, N. and Ou-Yang, H. (2006). Capital Structure, Debt Maturity, and Stochastic Interest Rates, *Journal of Business* **79**(5): 2469 – 2503.

Kamrad, B. and Ritchken, P. (1991). Multinomial Approximating Models for Options with k State Variables, *Management Science* **37**(12): 1640–1652.

Karatzas, I. (1988). On the Pricing of American Options, *Applied Mathematics and Optimization* **17**(1): 37–60.

Kim, I. J. (1990). The Analytic Valuation of American Options, *The Review financial Studies* **3**(4): 547–572.

Kinderlehrer, D. and Stampacchia, G. (1980). *An Introduction to Variational Inequalities and their Applications*, Academic Press.

Kuske, R. and Keller, J. (1998). Optimal Exercise Boundary for an American Put Option, *Applied Mathematical Finance* **5**: 107 – 116.

Kwok, Y. K. and Lau, K. W. (2001). Pricing Algorithms for Options with Exotic Path-Dependence, *Journal of Derivatives* **9**(1): 1–11.

Landau, H. G. (1950). Heat Conduction in a Melting Solid, *Quarterly of Applied Mathematics* **8**: 81–94.

Leisen, D. (1998). Pricing the American put option: A detailed convergence analysis for binomial models, *Journal of Economic Dynamics and Control* **22**: 1419–1444.

Leland, H. (1994). Corporate Debt Value, Bond Covenants, and Optimal Capital Structure, *The Journal of Finance* **49**(4): 1213–1252.

Leland, H. and Toft, K. (1996). Optimal Capital Structure, Endogenous Bankruptcy, and the Term Structure of Credit Spreads, *The Journal of Finance* **51**(3): 987–1019.

Linetsky, V. (1999). Step Options, *Mathematical Finance* **9**(1): 55–96.

Longstaff, F. A., Mithal, S. and Neis, E. (2005). Corporate yield spreads: Default Risk or Liquidity? New evidence from the Credit Default Swap Market, *The Journal of Finance* **60**: 2213–2253.

Longstaff, F. A. and Schwartz, E. S. (1995). A Simple Approach to Valuing Risky Fixed and Floating Rate Debt, *The Journal of Finance* **50**: 789–819.

Longstaff, F. A. and Schwartz, E. S. (2001). Valuing American Options by Simulation: A Simple Least-Squares Approach, *The Review of Financial Studies* **14**(1): 113–147.

MacMillan, L. W. (1986). Analytic Approximation for the American Put Option, *Advances in Futures and Options Research* **1**(1): 119–139.

Madan, D. and Unal, H. (2000). A Two-Factor Hazard Rate Model for Pricing Risky Debt and the Term Structure of Credit Spreads, *The Journal of Financial and Quantitative Analysis* **35**(1): 43–65.

Margrabe, W. (1978). The Value of an Option to Exchange One Asset for Another, *The Journal of Finance* **33**(1): 177–186.

McConnell, J. J. and Schwartz, E. S. (1986). LYON Taming, *The Journal of Finance* **41**(3): 561–576.

McKean Jr, H. (1965). Appendix: A Free Boundary Problem for the Heat Equation Arising from a Problem in Mathematical Economics, *Industrial Management Review* **6**(2): 32–39.

Merton, R. C. (1973). Theory of Rational Option Pricing, *The Bell Journal of Economics and Management Science* **4**(1): 141–183.

Merton, R. C. (1974). On the Pricing of Corporate Debt: The Risk Structure of Interest Rates, *The Journal of Finance* **29**: 449–470.

Merton, R. C. (1976). Option Pricing When Underlying Asset Returns are Discontinuous, *Journal of Financial Economics* **3**: 125–144.

Merton, R. C. (1990). *Continuous-Time Finance*, Basil Blackwell.

Moraux, F. (2002). On Cumulative Parisian Options, *Finance* **23**: 127–132. (Special Issue in Financial Mathematics).

Moraux, F. (2003). Valuing Corporate Liabilities When the Default Threshold is not an Absorbing Barrier. *Working paper*, The Université de Rennes.

Nyborg, K. G. (1996). The Use and Pricing of Convertible Bonds, *Applied Mathematical Finance* **3**: 167–190.

Parkinson, M. (1977). Option Pricing: The American Put, *Journal of Business* **50**: 21–36.

Rajan, R. and Winton, A. (1995). Covenants and Collateral as Incentives to Monitor, *The Journal of Finance* **50**(4): 1113–1146.

Reisinger, C. and Wittum, G. (2004). On Multigrid for Anisotropic Equations and Variational Inequalities: Pricing Multi-Dimensional European and American Options, *Computing and Visualization in Science* **7**(3): 189–197.

Revuz, D. and Yor, M. (1999). *Continuous Martingales and Brownian Motion*, Springer, chapter 12.

Ritchken, P. (1995). On Pricing Barrier Options, *Journal of Derivatives* **3**(2): 19–28.

Rogers, L. and Zane, O. (1997). Valuing Moving Barrier Options, *Journal of Computational Finance* **1**(1): 5–11.

Roll, R. (1977). An Analytic Valuation Formula for Unprotected American Call Options on Stocks with Known Dividends, *Journal of Financial Economics* **5**(2): 251–258.

Sarig, O. and Warga, A. (1989). Some Empirical Estimates of the Risk Structure of Interest Rates, *The Journal of Finance* **44**: 1351–1360.

Sharp, N. J., Newton, D. P. and Duck, P. W. (2007). A New Prepayment Model: An Occupation-Time Derivative. *Working paper*, Nottingham University Business School.

Smith, C. W. and Warner, J. B. (1979). On Financial Contracting: An Analysis of Bond Covenants, *Journal of Financial Economics* **7**(2): 117–161.

Smith, G. D. (1985). *Numerical Solution of Partial Differential Equations: Finite Difference Method*, Oxford University Press.

Snyder, G. L. (1969). Alternative Forms of Options, *Fiancial Analysts Journal* **25**: 93–99.

Stapleton, R. C. and Subrahmanyam, M. G. (1984). The Valuation of Multivariate Contingent Claims in Discrete Time Models, *The Journal of Finance* **39**(1): 207–228.

Stulz, R. M. (1982). Options on the Minimum or the Maximum of Two Risky Assets: Analysis and Applications, *Journal of Financial Economics* **10**(2): 161–185.

Sullivan, M. (2000). Valuing American Put Options using Gaussian Quadrature, *The Review of Financial Studies* **13**(1): 75–94.

Takahashi, A., Kobayashi, T. and Nakagawa, N. (2001). Pricing Convertible Bonds with Default Risk: A Duffie-Singleton Approach, *Journal of Fixed Income* **11**(3): 20–29.

Tian, Y. (1999). A Flexible Binomial Option Pricing Model, *Journal of Futures Markets* **19**(7): 817–843.

Tsiveriotis, K. and Fernandes, C. (1998). Valuing Convertible Bonds with Credit Risk, *Journal of Fixed Income* **8**(2): 95–102.

Unal, H., Madan, D. and Levent, G. (2003). Pricing the Risk of Recovery in Default with APR Violation, *Journal of Banking and Finance* **27**(6): 1001–1025.

Vasicek, O. (1977). An Equilibrium Characterization of the Term Structure, *Journal of Financial Economics* **5**(2): 177–188.

Villeneuve, S. (1999). Exercise Regions of American Options on Several Assets, *Finance and Stochastics* **3**(3): 295–322.

Villeneuve, S. and Zanette, A. (2002). Parabolic ADI Methods for Pricing American Options on Two Stocks, *Mathematics of Operations Research* **27**: 121–149.

Whaley, R. (1981). On the Valuation of American Call Options on Stocks with Known Dividends, *Journal of Financial Economics* **9**(2): 207–211.

Widdicks, M. (2002). *Examination, Extension and Creation of Methods for Pricing Options with Early Exercise Features* , PhD Thesis, University of Manchester.

Widdicks, M., Andricopoulos, A. D., Newton, D. P. and Duck, P. W. (2002). On the Enhanced Convergence of Standard Lattice Methods for Option Pricing, *Journal of Futures Markets* **22**(4): 315–338.

Widdicks, M., Duck, P. W., Andricopoulos, A. D. and Newton, D. P. (2005). The Black-Scholes Equation Revisited: Asymptotic Expansions and Singular Pertubations, *Mathematical Finance* **15**(2): 373–391.

Wilmott, P. (2001). *Paul Wilmott Introduces Quantitative Finance*, John Wiley & sons Ltd, Chichester.

Wilmott, P., Howison, S. and Dewynne, J. (1993). *Option Pricing: Mathematical Models and Computation*, Oxford Financial Press.

Wilmott, P., Howison, S. and Dewynne, J. (1995). *The Mathematics of Financial Derivatives*, Cambridge University Press.

Xiao, X. (2007). *Advanced Monte Carlo Techniques: An Approach for Foreign Exchange Derivative Pricing*, PhD Thesis, University of Manchester.

Yu, L. (2004). *Corporate Bond Valuation via ParAsian Options with Endogenous Recovery Rate*, PhD Thesis, Manchester Business School.

Yu, L., Newton, D. P., Johnson, P. V. and Duck, P. W. (2007). Pricing Credit Risk in a Two-Class Debt Structure. *Working paper*, Manchester Business School.

Zhang, P. G. (1995). Correlation Digital Options, *Journal of Financial Engineering* **4**(1).

Zhu, Z. and Stokes, N. (1999). A Finite Element Platform for Pricing Path-Dependent Exotic Options. Proceedings of the Quantitative Methods in Finance Conference, Australia.